BASIC DISCONTINUITY ANALYSIS

of Multishell Axisymmetric Junctions

by Andrew C. Whyte

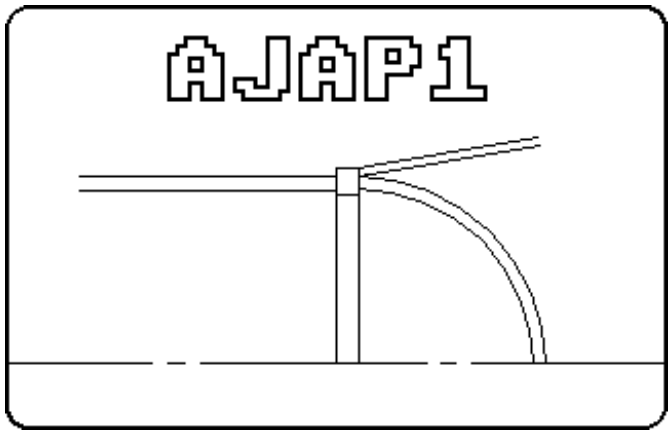

BASIC DISCONTINUITY ANALYSIS
of Multishell Axisymmetric Junctions

by

Andrew C. Whyte, CEng, MIMechE
Senior Design Engineer
Babcock Energy Limited
Renfrew, Scotland

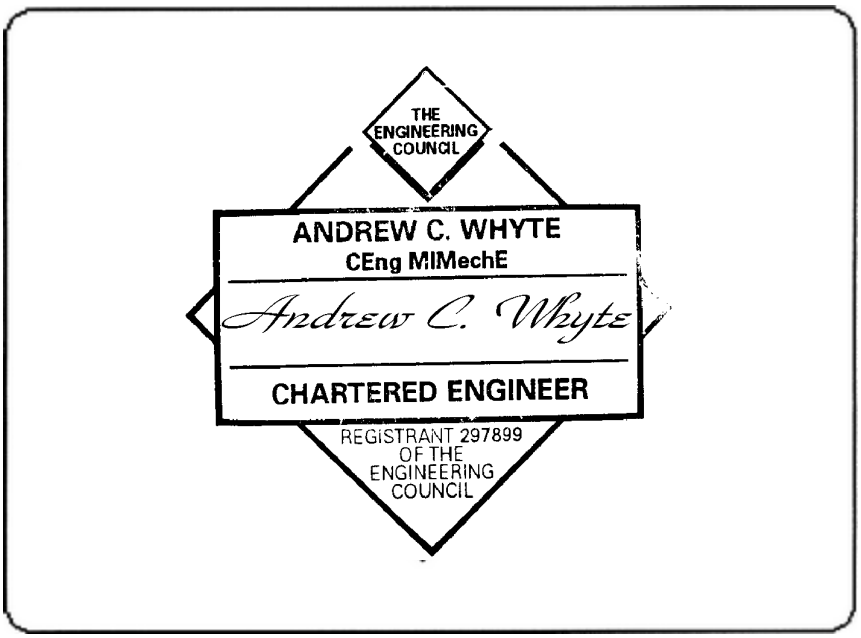

Copyright ©Andrew C. Whyte, 1994, 2010, 2015, 2017, 2019

Published by: Andrew C. Whyte
Web Site: www.acwhyte.droppages.com

This revision of the book is a reduced file size pdf so as to go onto my web site. Some typographical, grammar and spelling errors have been corrected. Some additions to the notation and other short additions for clarification have been made. None of these affect the computer program results. The author has now retired but still takes an interest in engineering matters.

All rights reserved. No part of this publication may be reproduced, stored in a retrieval system, or transmitted in any form or by any means electronic, mechanical, photocopying, or otherwise, without the prior permission of the copyright holder. The only exception is the option of entering the programs provided into a computer for the sole use of the purchaser of this book. The purchaser may make one back up copy of the program for security purposes only. It is essential that program users should read and understand the sections on input data, limitations and defaults before proceeding with practical problems.

Reference has been made to several pressure vessel codes in the text. New editions of these codes are re-issued every three years and there are amendments (addenda) issued between editions. Users should always refer to the latest issue of the code as the governing document.

Limitation of liability. The computer programs supplied with this book are supplied "as is". The author does not guarantee that the programs will function correctly in every hardware or software environment. The programs have been carefully tested but the author can accept no responsibility for any loss or damage, however caused, as a result of the user's use of the programs.

Trademark Acknowledgements

IBM PC, XT, AT, Proprinter: International Business Machines Corporation.
GW BASIC: Microsoft Corporation.
QBasic: Microsoft Corporation.
Atari ST: Atari Corporation.
ST BASIC: Atari Corporation.
GEM: Digital Research Inc.
FirST BASIC: HiSoft.
Olivetti: Ing. C. Olivetti & C., S.p.A.
EPSON: EPSON Corporation.
HP Laserjet: Hewlett Packard Company.

To my wife Elizabeth and my mother Mrs. Margaret Lillian Whyte.

Errata, etc. The following corrections to the text have been made. None of these affect the computer program results.

Page 10, EX = $\alpha(1-\mu)dT/T$ should be EX = $\alpha(1+\mu)dT/T$

Pages 10 to 15, Notation, various symbols added.

Page 39 [Originally Page 45], $\theta r_1 = (\theta r_1 - \theta r_2)$ should be $\theta r_1 = (\theta f_1 - \theta f_2)$

Page 40 [Originally Page 46], FIGURE 2.9, θj should be θr

Page 42 [Originally Page 48], $\Sigma C9 = \Sigma C9 + Mo = \Sigma C9 = 0 = -753355.44$ Nmm/mm circumference should be $\Sigma C9 = \Sigma C9 + Mo = \Sigma C9 + 0 = -753355.44$ Nmm/mm circumference

Page 66 [Originally Page 80] equation C9 added.

Page 79 [Originally Page 96] Figure 3.17 (d), Results for case 2. M1=-2402.175 should be M2=-2402.175

Page 91 [Originally Page 113] Table 3.6, example 3.1 should be example 3.3

Page 100 [Originally Page 128], equation (3.29), h_E should be h_L

Page 121 [Originally Page 158], Figure 3.28(c) results for component No. 2, sign of V should be negative. i.e. V=-99.36525 N/mm

Page 124 [Originally Page 163], Figure 3.29(c) results for component No. 2, sign of SV should be negative. i.e. SV=-1.231324

Page 147 [Originally Page 198], Figure 3.36(g) simply supported tubesheet should be clamped tubesheet.

Page 150 [Originally Page 203], H_T is applied as a point load W2 to component No. 3 not No. 2.

Pages 151, 158, 164, 170 and 177 [Originally Pages 205, 216, 229, 237 and 251], bolting-up condition reference to W_{M1} removed. See clarification below.

Pages 151 and 178 [Originally Pages 205 and 251], bolted flanges, example 3.18, the bolt material B7 should be B7A.

Pages 157, 163, 169 and 175 [Originally Pages 215, 226, 237 and 248], flange face should just be flange.

Pages 158, 164, 170 and 177 [Originally Pages 217, 229, 239 and 251], point load W1 = -3637.752 should be W2.

Pages 163 and 169 [Originally Pages 226 and 237], H_T is applied as a point load W4 not W2.

Page 169 [Originally Page 237], H_D is applied over the outside diameter of the flange not the inside.

Page 206 [Originally Page 289], Table 4.1, point B3, point C3 and point D3 the first reference to shear stress f_{ZY} should be f_{XZ}.

Page 215 [Originally Page 301], Appendix 1, Table A1.1, Section D – D point D3, component stress difference for f_Y and principal stress f_2 should be +ve not –ve.

Pages 151, 158, 164, 170 and 177 [Originally Pages, 205, 216, 229, 237 and 251]. Clarification:
Bolted flanges example 3.18. The flange design bolt load W, for the bolting-up condition, has been calculated using BS5500 code rules where $W = 0.5(A_m + A_b)S_a$. The load is applied at the bolt pitch circle (in a similar manner to W_{M1}) and at the gasket reaction diameter (in a similar manner to H_G).

Figure 2.1, Page 30 [Originally Page 34], i <= n was i < n.

Equation (2.82), Page 52 [Originally Page 62], $-Rs*\alpha*Gj*SIN\ \phi$ should be $-Rs*\alpha*Gj$

Page 12, Notation, symbol SL added.

CONTENTS

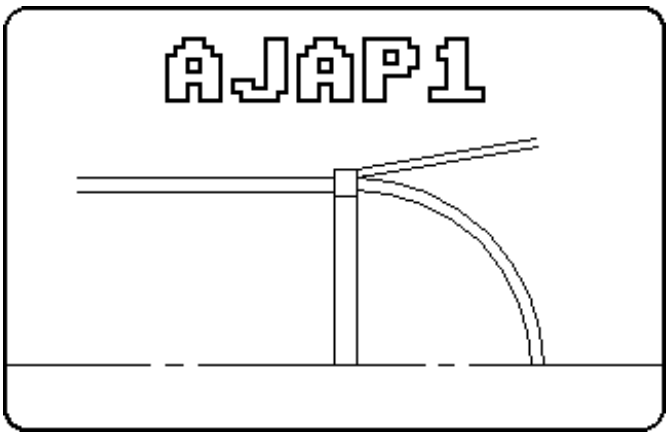

AJAP1 stands for Axisymmetric Junction Analysis Program version 1

One hundred years have past since A.E.H. LOVE first published his paper *On the Small Free Vibrations and Deformation of a Thin Elastic Shell* (reference 1). A centenary lecture has taken place (ref. 23) and this discusses LOVE's background, his relationship with RAYLEIGH and others, and assesses the historical significance of the work. In 1992 it was the centenary of the publication of LOVE's famous *Treatise on the Mathematical Theory of Elasticity* (ref. 27). Although the original paper by LOVE was 'an attempt to construct a theory of the vibration of bells' the deformations and the resulting stresses in thin elastic shells are of great interest to engineers working in the mechanical, civil and aircraft industries. This is borne out by LOVE's *Treatise* which, although highly academic, went on to four editions between 1892/3 and 1927.

The design and safe working of many items of industrial plant such as: pressure vessels, boilers, storage tanks, pumps and piping, aircraft and missiles, submarines, turbines and heat exchangers etc. depend upon the correct evaluation and assessment of stresses induced in these items of plant as a result of applied loading. It is normal practice to manufacture industrial plant from components such as cylinders, cones, spheres, flat plates, rings etc. The connection point or junction of these components when subjected to loading can produce a situation where the stress field at (or near) the junction is significantly higher than that remote from the junction. These discontinuity stresses, as they are called, are of particular interest to engineers because the higher stresses at the junction can result in catastrophic failure of the plant especially when fatigue, brittle fracture or creep conditions are present.

The analysis of discontinuity stresses in shell structures has interested engineers for many years and references (2) to (11) are just a few sources of reference from the last forty years. While the analysis can be done by hand calculation, the use of a digital computer makes the analysis much more convenient and allows the effects of altering the input parameters to be investigated in a reasonable time scale. As far as the author is aware there has been no published reference which combines a discussion on the analysis and assessment of discontinuity stresses together with a computer program. The author has therefore attempted to fill this gap by presenting a discussion together with a computer program in BASIC. This program will enable engineers to analyse practical problems likely to be encountered in multishell axisymmetric junctions commonly found in the items of industrial plant mentioned above.

The BASIC programs included with this book will run on an IBM PC compatible microcomputer or an Atari ST microcomputer. The program will calculate the discontinuity stresses and deformations both at and away from the junction, as well as analysing single components. It is possible to analyse many geometries under a combination of loads such as pressure, temperature, applied external forces and moments and centrifugal loading. For example the multishell junction shown opposite comprising of: a cylinder, flat plate, hemisphere, cone, and compact ring can be analysed for pressure and temperature loading.

Two graphic subroutines are included in the program to enhance the presentation of the results. Detailed input data instructions are given in section 3.4. The input has been error trapped for most of the common errors likely to occur. An error trap listing is given in appendix 3 for information. The program makes extensive use of subroutines so that future developments to include more specialised geometries and loadings should be possible.

The book will be of use to engineers and stress analysts in the pressure vessel, boiler, civil engineering and aircraft industries as well as students and research engineers who require an understanding of discontinuity analysis and a means of analysing the stresses on a microcomputer. Design engineers and stress analysts should find the program a useful supplement to their sophisticated finite element analysis.

The program is written with the pressure vessel engineer in mind. Certain defaults are present in the program which may not be applicable in every case. The user should read section 3.3 before deciding to accept or reject these defaults.

Where compression stresses are present the structure may fail by buckling. The program will *not* predict this type of failure. It is also important to remember that deformation and stiffness are often the criteria as well as strength, e.g. bolted flanges can leak if they are not stiff enough, even though they meet strength criteria.

Section 3.6 presents eighteen examples chosen to show the working of the program and to give the input data sets and solutions to practical problems likely to be encountered by engineers and students working in industry. The examples can also be used as benchmarks for programmers.

Once the stresses in a structure have been obtained it is necessary to assess these stresses against a recognised set of rules or specification. The final chapter therefore provides guidance notes and a discussion on the assessment of pressure vessels that are "Designed by Analysis". Since it requires experience and specialist knowledge to assess a pressure vessel, a worked example is included so that the main principles of assessment can be understood. The assessment rules for fatigue are brought up to date with BS5500 Enquiry Case 79. A discussion and example of the application of this important enquiry case is given in appendix 1.

Appendix 2 briefly discusses some aspects of the strain energy of stretching and bending of plates and shells that can easily be visualised by utilising the graph plotting routine included in the program. A statement on program verification is given in appendix 4. Finally appendix 5 summarises the notation used

in the analysis of conical shells. This notation will be of use to readers who wish to study the analysis of conical shells in detail.

Andrew C. Whyte
Renfrew, Scotland
1994

ACKNOWLEDGEMENTS

In the course of compiling the program reference has been made to many sources of information. These are referenced in the text.

The author would like to thank the directors of Babcock Energy Limited for their permission to publish this book. Thanks are also due to the following persons: Mr R. Houston formerly of Babcock Energy Limited and member of the IMechE Pressure Systems Group for his advice and encouragement throughout the preparation of the typescript. Professor C.E. Taylor for his permission to use his conical shell theory.

The following is a comprehensive list of the symbols used in the text and in the program. In most cases the symbol used in the text is the same as that used within the program (but in upper case), e.g. F_{AX}, Fax and FAX all have the same meaning. The units and sign convention are indicated where applicable. The program variables are given as an aid to program development. In most cases each variable has a single meaning but in some cases the variable has been overlayed to save on computer memory. Note that within mathematical expressions the asterisk* has been used to represent multiplication where necessary. Additional notation for conical shells is given in appendix 5.

A constant used in design fatigue curves. Refer to section 4.5 and appendix 1. [Added]
Ab actual total cross-sectional area of bolts at least diameter under load. [Added]
AL coefficient of thermal expansion, see α
ALG sets the left margin for some well known printer types.
Am total required cross-sectional area of bolts. [Added]
ANG15, ANG3, ANG7 angle of the faces of the compact ring from the datum.
AR cross section area of the compact ring.
A(i) array, holds the coefficient of thermal expansion for each component i.
A$ title string.

BE see β
BETAA see β_A
B(MNL, i) array holding the loading data for each component i.
B(1,i) = pressure difference, P
B(2,i) = axial end load, F_{AX} (if component is a shell)
= external pressure, qo (if component is a flat plate)
B(3,i) = ambient temperature, Ta
B(4,i) = mean temperature, Tm
B(5,i) = thermal gradient, Gj (if component is a shell)
= radial temperature difference, dTr (if a flat plate)
B(6,i) = temperature difference across the thickness, dT
B(7,i) = internal pressure on the inside radius of the flat plate, qi.
B$ load case string.

C distance to the extreme fibre of compact ring from the centroid.
+ve to the right of the axis, -ve to the left.
CH = 2 is output to the screen, = 3 is output to the printer.
Cm, Cv integration constants for spherical shells.
c_P connection point number on compact ring.
C1 to C12 variables used in main calculation, cylinder and flat plate analysis and face stresses on the compact ring.
C(i) array, holds the component type numbers for each component i.
C$(MCT, 30) string array holding the component and menu titles.

D $=E*T^3/(12(1 - \mu^2))$ flexural rigidity for cylinders and flat plates.
$=I_{NA}/|C|$ the section modulus for the compact ring.
DEL attitude angle of the compact ring from horizontal datum, see δ
DELF face angle of the compact ring, see δ_F
dT linear temperature difference across the thickness, +ve if the inside (right) surface is at a higher temperature than the outside (left) surface.
dTr radial temperature difference across the flat plate, +ve if the inside radius is at a higher temperature than the outside radius.
DX result plot, distance (or angle in degrees) between points.
D(i) array, holds parameter D for each component i.
D$ string, degrees.

E Young's modulus (modulus of elasticity), units of stress.
E_C Young's modulus value used to plot the design fatigue curve.
E_A actual value of Young's modulus.
E' Modified equivalent Young's modulus for a perforated plate.
ER error variable used to alter the input data.
ERI component i being altered in the error routine.
ETA integration constant § used in the spherical shell analysis.

EX = $\alpha(1+\mu)dT/T$ expansion factor used in the flat plate analysis. [Corrected, was = $\alpha(1-\mu)dT/T$]
E(i) array, holds Young's modulus E for each component i.

F, FA series terms used in the cone analysis
F_{AX} axial end load per unit circumference at the junction, +ve if it tends to produce tension in the component.
Fc a factor used in altering the handing of the junction,
+1 for a junction at the right end of a component. -1 for a junction at the left end of a component.
F_O meridional membrane force per unit circumference at the junction, +ve tension, -ve compression.
Fp, F_P axial pressure end load (hydrostatic end load) per unit circumference at the junction,
+ve tension, -ve compression.
F1, etc., variables used in the flat plate analysis.
F(i) array holding: half arc angle PHI ϕ degrees for a spherical shell.
half apex angle PHI ϕ degrees for a conical shell.
inside radius Ri for a flat plate.
f material design strength value.
f_B primary bending stress intensity.
f_E material nominal design strength for short-term tensile strength characteristics. [Added]
f_F material nominal design strength for creep characteristics. [Added]
f_G secondary stress intensity.
f_L local primary membrane stress intensity.
f_M general primary membrane stress intensity.
f_P peak stress intensity.
f_R total stress intensity range.
f_X, f_Y, f_Z normal component stresses in x, y and z directions.
f_{XZ}, f_{YX}, f_{ZY} shear component stresses.
f_1, f_2, f_3, f_N principal stresses.
f_{12}, f_{23}, f_{31} principal stress differences.
[*f*1] to [*f*8] functions used in flat plate analysis. [Added]
F$ string, force units.

G results plot, tick mark number.
G2, etc., variables used in the flat plate analysis.
GNT results plot, Y-axis scale value at the tick marks.
G(9) array, holds the distances of the 9 points on the compact ring from the centroid axis of the ring.
Gj thermal gradient at the junction, units temperature/length,
+ve if the heat flows away from the junction.
G$ string, mass units.

h_E height of domed end.
h_L height of liquid.
H distance between points 1 and 5 on the compact ring.
H_D total hydrostatic end force applied via the shell to the flange. [Added]
H_G total compression load (reaction load) on the gasket to ensure a tight joint. [Added]
H_T total hydrostatic end force due to pressure on the flange face. [Added]
H_1 position of the ring centroid along distance H from point 1.
H(i) array, holds the connection point numbers on the compact ring.

i, I component number under consideration.
I_{NA} second moment of area of compact ring about the centroid axis.
IND indicator 0 or 1 used throughout the program.
Ix 2nd moment of area about the X principal axis of the compact ring.
Iy 2nd moment of area about the Y principal axis of the compact ring.
I(i) array, holds an indicator 0 or 1 for each component. 0=default,
1 indicates that the default free displacements are overwritten.

J loop counter used throughout the program.
J(2*MPL,i) array holding the point loads on the flat plate and radius of the point load.
JP junction position for the flat plate, for -1=< JP <=+1.

K = Ri/Ro for flat plates.

K_t stress concentration or fatigue strength reduction factor.
K1, K2, variables used in the spherical shell and flat plate analysis.
K1 =1-(1-2μ)/(2βTAN(ϕ-Ω)) (if component is a spherical shell), =Ro^2-Ri^2 (if component is a flat plate)
K2 =1-(1+2μ)/(2βTAN(ϕ-Ω)) (if component is a spherical shell), =Ro^2+Ri^2 (if component is a flat plate)
K10 =K1 for spherical shell analysis at Ω=0
K(4,n) array holding the component stiffness coefficients.
K$ string holding variable being plotted.

L axial length between points 1 and 5 on the compact ring = H*cos(δ).
L1 variable used in the compact ring and series term in cone analysis.
L1, etc., variables used in the flat plate analysis.
LA series term used in the cone analysis.
LAMBDA variable used in cone analysis, see appendix 5.
Le length of the thermal gradient.
Ln natural logarithm.
Lo offset distance on compact ring as shown on FIGURE 3.33(c) [Added]
LP length parameter for conical shells = $| XI_A - XI |/2^{1/2}$
LS results plot, length of the Y-axis string.
Lx axial distance from the centroid axis to a point on the compact ring +ve to the right, -ve to the left.
L(i) array holding β for cylindrical and spherical shells.
L$ string, length units.

M bending moment per unit circumference acting at the centroid of the compact ring, +ve clockwise.
M, MA series terms used in the cone analysis.
m exponent index used in design fatigue curves. Refer to section 4.5 and appendix 1. [Added]
MAX and MIN values used in results plot.
MC moment at centre of the flat plate.
MCF =Md*$(2\pi RPS)^2$
MCT maximum number of component types (=11).
Md mass density.
MFACE thermal moment at the face of a compact ring.
Mj discontinuity bending moment per unit circumference at the junction,
refer to FIGURE 2.2 for the sign direction.
Mj_i discontinuity bending moment of the i_{th} component. [Added]
MNL maximum number of component loads (=7), sets the size of array B( ).
Mo applied external bending moment per unit circumference at the junction (or at the centroid of the compact ring), +ve clockwise.
MPL maximum number of point loads applied to a flat plate (default=12).
Mr applied bending moment per unit circumference at the centroid of the compact ring, +ve clockwise.
MU function used in the cone analysis, see appendix 5.
M1 meridional bending moment per unit circumference, +ve if it produces compression on the outside surface (left surface if the component is a flat plate).
M2 hoop (circumferential) bending moment per unit circumference, +ve direction as for M1.
M(i) array, stores the junction discontinuity moments Mj for each component i.
M$ string, units of moment/unit circumference.

n, N number of components analysed, also the number of fatigue cycles.
n_n specified number of fatigue cycles of type $_n$. Refer to assessment example, section 4.6. [Added]
N_n allowable number of fatigue cycles of type $_n$. Refer to assessment example, section 4.6. [Added]
N1 meridional membrane force per unit circumference, +ve tensile.
N2 hoop (circumferential) membrane force per unit circumference, +ve tensile.
NP number of points being plotted on the result plot.
NT result plot, distance between the Y-axis tick marks.
N$ string, units of force/unit circumference.

OM angle OMEGA see Ω.
O(i) array, holds the junction position for flat plates.

P pressure difference across the thickness, +ve outward (internal) for shells,
+ve acting to the right for flat plates.

Notation

PI π=3.141593
PHI shell angle see ϕ
PHI1 to PHI17 functions used in the cone analysis, see appendix 5.
PL number of point loads on the flat plate.
POSX position of MAX along X axis on the result plot.
POSX position of MAX along X axis on the result plot.
PR Poisson's ratio μ.
P(i) array, holds Poisson's ratio for each component i.
P$ string holding variable in the result plot.

qi radial pressure on inside radius of the flat plate, +ve internal.
qo radial pressure on outside radius of the flat plate, +ve external.
Q(4,i) array, holds indicator 0 or 1 for each stiffness coefficient, 0=default, 1=default stiffness overwritten.

R radius of the component.
= mean radius of a cylindrical shell.
= mean spherical radius of a spherical shell (=Rs).
= mean junction radius of a conical shell (=Rj).
= outside radius of a flat plate (=Ro).
= centroid radius of the compact ring (=Rc).
RA range of values used in the result plot to scale Y axis.
RATIOb, ratio of strain energy of bending action Ub/(Um+Ub).
RATIOm, ratio of strain energy of membrane action Um/(Um+Ub).
Rc centroid radius of the compact ring.
R_E material minimum yield strength at room temperature. [Added]
$R_{E(T)}$ material minimum proof stress at temperature $_{(T)}$. [Added]
RHO nozzle shell parameter. [Added]
Ri inside radius of the flat plate.
Rj mean radius of the cone at the junction.
R_L, Rl left mean radius of the compact ring.
R_M material minimum tensile strength at room temperature. [Added]
RN radius R of the last component.
Ro outside radius of the flat plate.
RPS revolutions per second.
Rr right mean radius of the compact ring.
Rs mean spherical radius of a spherical shell.
Rw radius of point load on the flat plate.
RX radius at distance X along the cone =(Z $\pm$ X)SIN ϕ
R(i) array, holds the radius R for each component i.
R$ string, radians.

S stress amplitude in fatigue analysis. [Added]
S,SA series terms used in the cone analysis.
S_A allowable stress amplitude.
Sa bolt nominal design stress at atmospheric temperature. [Added]
S_{ALT} alternating stress intensity.
SBH hoop bending stress at the surface.
SBL meridional bending stress at the surface.
SC geometry plot scale factor.
SCF nozzle stress concentration factor. [Added]
SCY result plot, Y-axis scale factor.
SH hoop membrane stress.
Sh calculated longitudinal stress in the flange hub. [Added]
SHi, SHI hoop membrane + bending stress at the inside surface of shell.
SHl, SHO hoop membrane + bending stress, at the left surface of flat plate.
SHo, SHO hoop membrane + bending stress at the outside surface of shell.
SHr, SHI hoop membrane + bending stress, at the right surface of flat plate.
SH1 to SH9 hoop membrane + bending stresses at the compact ring.
SL meridional membrane stress. [Added]
SLi, SLI meridional membrane + bending stress at the shell inside surface.
SLl, SLO meridional membrane + bending stress, left surface of flat plate.
SLo, SLO meridional membrane + bending stress at the shell outside surface

SLr, SLI meridional membrane + bending stress, right surface of flat plate.
SL1 to SL8 meridional membrane + bending stresses on the faces of the compact ring.
Sm material design strength value (ASME VIII). [Added]
S_R stress range used in enquiry case 5500/79 fatigue analysis.
Sr calculated radial stress in the flange. [Added]
S_{Rt} material mean stress to rupture at time t at a specified temperature. [Added]
ST variable = 0.5*SIN(δ) used in the compact ring analysis.
St calculated tangential stress in the flange. [Added]
STIF1,2,3,4 the four stiffness coefficients at the edge of the component.
SV average shear stress, +ve if shear force V is +ve.
Sy material yield strength. [Added]
SV1,SV3,SV5,SV7 average shear stresses on faces 1, 3, 5 and 7 of the compact ring.
SX graph plot, overall scale factor in the X(horizontal) direction
SY graph plot, overall scale factor in the Y(vertical) direction.
SXY geometry plot, sets the pixel aspect ratio.
S(9) array, holds the hoop bending stresses at the 9 points on the compact ring.
S$ string, stress units.

T thickness of the shell or flat plate.
Ta ambient temperature of surrounds. [Added]
TC thickness at the centroid of the compact ring.
TH rotation THETA, see θ.
THB rotation at the inside radius of the flat plate.
THF free rotation, see θf.
THGJ free rotation due to the thermal gradient along the shell.
THJ final rotation, see θj.
THR free rotation, see θr.
Ti Temperature at inside surface of shell. [Added]
TICY result plot, position of the Y-axis tick marks.
T_L, TI left thickness of the compact ring.
Tm mean temperature of component. [Added]
To Temperature at outside surface of shell. [Added]
Tr right thickness of the compact ring.
T(i) array, holds the thickness T for each component i.
T$ string, temperature units.
T_1, T_2 Different shell thicknesses or temperature difference or thermal gradient ($T_2 - T_1$). [Added]

U current component type being considered.
Also cumulative usage factor in fatigue analysis. Refer to assessment example, section 4.6. [Added]
U_n ratio n_n/N_n for each fatigue cycle type $_n$. Refer to assessment example, section 4.6. [Added]
U2,U4 variables used in the cone analysis
Ub linear elastic strain energy of bending moments at a section.
Um linear elastic strain energy of membrane forces at a section.
Ut Sum total of Um and Ub.

V shear force per unit circumference, +ve outward (+ve to the right for a flat plate).
= Transverse shear force in a shell or flat plate.
= radial shear force acting at the centroid of the compact ring.
VB transverse shear force at the inside radius of a flat plate.
VFACE radial or shear force at the face of a compact ring.
Vj discontinuity radial force per unit circumference at the junction, +ve inward.
Vj_i discontinuity radial force of the i_{th} component. [Added]
Vo applied external radial force per unit circumference at the junction (or at the centroid of the compact ring), +ve inward.
Vr applied radial force per unit circumference at centroid of compact ring, +ve inward.
V(i) array, stores the discontinuity radial forces for each component i.

W applied point load per unit circumference acting at radius Rw on a flat plate, +ve to right. Twelve loads (W1 to W12) max. per plate.
Also the flange design bolt load = 0.5(A_m + A_b)S_a. [Added]
Wd weight density.

Notation

W_{M1} total minimum required bolt load for operating conditions. [Added]

X = distance from the junction (or end) along the cylinder or cone.
= radius Rx on flat plate.
XA length check for a cone = R/SIN ϕ
XMAX geometry plot, maximum overall length in the X direction.
XP variable used to plot the results.
XX geometry plot, positions the junction. Result plot, positions the Y-axis.
xi, xi_1, XI, XI_A, XIA cone shell parameter, refer to appendix 5.
X1 to X5 variables used in the geometry plot.

Y radial deflection, +ve outwards.
YB transverse deflection at the inside radius of a flat plate.
YC transverse deflection at the centre of a flat plate.
YCF $=Md*(2\pi RPS)^2/E$
Yd radial deflection (= Yj - Yr) due to the discontinuity loads Vj and Mj.
Yd_i radial deflection due to the discontinuity loads Vj_i and Mj_i for the i_{th} component. [Added]
Y_{DIFF} difference in the radial deflection between a hub and shaft.
YL transverse deflection of a flat plate, +ve to the right.
Yf free radial deflection of a component at the junction, +ve outwards.
Yf_i free radial deflection of the i_{th} component. [Added]
Yf_n free radial deflection of the n_{th} (the last) component. [Added]
Yj final radial deflection at the junction (=Yr + Yd).
YMAX geometry plot, maximum overall radius in the Y direction.
YP variable used to plot the results.
Yr free radial deflection relative to the last component.
Yr_i free radial deflection of the i_{th} component relative to the last (the n_{th}) component. [Added]
YY geometry plot, position of centre line. Result plot, position of the X-axis.
Y1 to Y8 variables used in the geometry plot.

Z = βX for a cylinder.
= $\beta\Omega$ for a spherical shell.
= Rj/SIN ϕ = distance along the cone from apex to the junction.
Z(2i) array, stores the free displacements of each component i. Z(2i) = Yf, Z(2i - 1) = θf
ZETA function used in the cone analysis, see appendix 5.

α, AL coefficient of thermal expansion, ALPHA.
α_F for ferritic steel.
α_A for austenitic stainless steel.

β, BE $= [3(1-\mu^2)/(R^2T^2)]^{1/4}$ (shell characteristic for a cylinder)
$= [3(1-\mu^2)(R/T)^2]^{1/4}$ (shell characteristic for a spherical shell)
β_A, BETAA variable used in the cone analysis, see appendix 5.

ΔT uniform temperature change. [Added]
δ, DEL attitude angle, DELTA, of the compact ring from horizontal datum.
δ_F, DELF angle of faces 3 and 7 on the compact ring relative to the ring attitude angle δ.
§, ETA = TAN^{-1}(-K10) integration constant used in the spherical shell analysis.

θ, TH rotation of the tangent to a meridian, THETA in radians, +ve anti-clockwise.
Also weld profile overfill angle. See appendix 1 FIGURE A1.2. [Added]
θd rotation due to discontinuity loads Vj and Mj (θd = θj - θr)
θd_i rotation due to the discontinuity loads Vj_i and Mj_i for the i_{th} component. [Added]
θf, THF free rotation at the junction, radians +ve anti-clockwise.
θf_i free rotation of the i_{th} component. [Added]
θf_n free rotation of the n_{th} (the last) component. [Added]
θj, THJ final rotation at the junction (θj = θr + θd).
θr, THR free rotation relative to the last component.

θr_i free rotation of the i_{th} component relative to the last (the n_{th}) component. [Added]

μ, PR Poisson's ratio. Also ligament efficiency in BS5500 analysis of tubesheets.
μ' modified equivalent Poisson's ratio for a perforated plate.

π, PI =3.141593

ϕ, Phi, PHI = half arc angle for spherical shells.
= half apex angle for conical shells.
ϕ_{min}, ϕ_{max} = range of half arc angle for spherical shells. Refer to FIGURE 3.2. [Added]
ϕ_1 to ϕ_{17} functions used in the cone analysis, see appendix 5.

Ω, OM distance OMEGA in degrees from the junction (or end) along a spherical shell. Also a stress factor used in BS5500 analysis of tubesheets.

$\wedge$ exponent

Σ summation

|x| absolute value of x

1.0 INTRODUCTION, Structural Discontinuities

A computer program has been written in BASIC which will calculate the discontinuity stresses at thin shell axisymmetric junctions subjected to: pressure, temperature, applied external loads and centrifugal forces. Axisymmetric junctions are commonly found in items of industrial plant such as pressure vessels, boilers, storage tanks, pumps and piping, aircraft and missiles, submarines, turbines and heat exchangers etc. A typical axisymmetric structure, like the pressure vessel shown in FIGURE 1.1, may have several junctions at which discontinuities can occur. TABLE 1.1 lists some typical junctions that can be analysed by the program presented with this book.

In the past such junctions were analysed by hand calculation by completing a discontinuity analysis similar to that described by HARVEY (ref. 9) or ASME SECTION VIII (ref. 10). Closed form solutions have also been obtained, typical of these is the WEIL and MURPHY solution for a three-cylinder intersection (ref. 5) and the 6th edition of ROARK (ref. 11) has tabulated results for several two component junctions.

The solution of a discontinuity is not particularly difficult, provided the component stiffness coefficients can be obtained, but it is a time consuming exercise and great care has to be taken with the sign directions. It is very easy to make errors in the formulation especially when more than two components are involved. The discussion and program presented here should resolve some of these difficulties for many of the common types of component encountered in industry. Note that although the discontinuity analysis is not particularly difficult the theory of shell structures is a complex and mathematical subject. For a modern text on this subject the reader is referred to CALLADINE, reference (24), and in particular his approach to the stretching and bending of shells.

There are limitations in the scope of the program and in the assumptions of the shell theory used in the analysis. These limitations are discussed in detail in section 3.2 but it is best to make it clear now that this text and program is concerned only with solving the most basic problems, i.e. axisymmetric shells of revolution subjected to axisymmetric loadings and isotropic materials with a linear elastic stress-strain law. The program could however be developed to include more specialised geometries and loadings.

1.1 WHAT ARE STRUCTURAL DISCONTINUITIES?

Although it is possible to consider a shell structure in which only membrane forces are transmitted in the plane of the shell, in general, curved shells such as cylinders, spheres, cones etc. and flat plates are capable of transmitting bending moments and shear forces through the thickness as well as membrane forces. Shell structures like the pressure vessel shown in FIGURE 1.1 are far from being simple membrane shapes. There are many reasons for deviating from the ideal membrane shapes and TABLE 1.2 lists some of the important factors that need to be considered.

Regions of discontinuity occur in structures where there are changes in: geometry, material properties, or loading over short distances. At the discontinuity the free displacements (deflections and rotations) are constrained by the adjacent parts of the structure or by the self-constraint of the structure. This constraint, results in additional loads and hence stresses being induced in the structure. The effects can best be illustrated by a few examples.

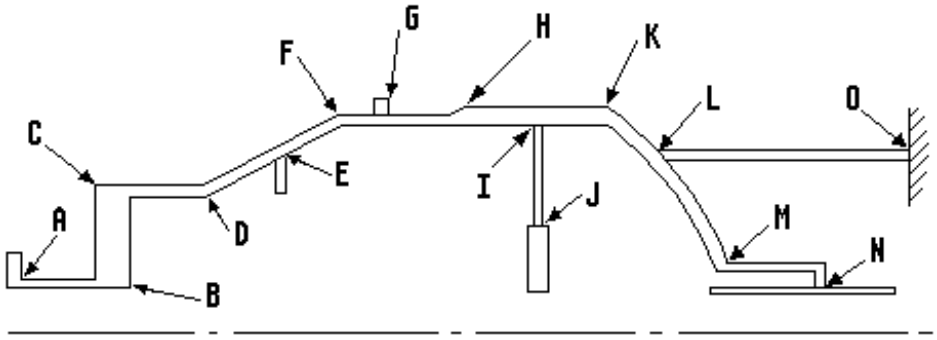

FIGURE 1.1 A typical pressure vessel with regions of axisymmetric discontinuity

A Flange to nozzle junction
B Nozzle to flat end (head)
C Flat end to cylindrical shell
D Cylinder to small end of conical shell
E Stiffener to conical shell
F Cylinder to large end of conical shell
G Compact ring to cylinder
H Cylinder to cylinder junction
I Internal baffle to cylinder
J Flat plate to flat plate junction
K Cylinder to domed end
L Support skirt to domed end
M Nozzle to spherical end
N Thermal sleeve (3-cylinder junction)
O Support skirt fixed to ground

TABLE 1.1 Some typical axisymmetric junctions that can be analysed

(1) Supports and means of lifting have to be provided.
(2) Openings are necessary for services, safety devices, and access manways. Internals are often required for functional requirements.
(3) Loading may not be uniform and transient conditions may be experienced during test, shipping and operating conditions. Certain geometry details may not be suitable under conditions where fatigue or brittle fracture or creep are present.
(4) Client will require a particular vessel orientation and size for functional reasons or site space requirements.
(5) Works manufacturing and heat treatment capability may limit sizes of components or complete shells that can be fabricated.
(6) Lifting and dimensional restrictions in works, at site or transportation may limit the overall size of vessels.
(7) Availability and cost may dictate the size of material to be used.
(8) Special grades or types of materials may be required for strength, operational or environmental reasons.
(9) Access for non-destructive examination and in-service inspection may be required.
(10) Design code requirements have to be met plus client's own specifications.

TABLE 1.2 Some factors that influence pressure vessel design

Example 1.1 GEOMETRIC DISCONTINUITY

Shell structures are often manufactured from components with different thicknesses. If we consider a two-cylinder junction subjected to a uniform internal pressure, as shown in FIGURE 1.2. Assuming that the cylinders are long, i.e. the ends are sufficiently far apart so that the boundary conditions at the ends do not have any influence at the junction. If we imagine the cylinders to be separated at the junction into two components, each component would then be free to resist the applied pressure loading by stretching in the hoop and longitudinal directions (refer to section 1.3 for a discussion on directions). For an isotropic, linear elastic material, the free displacements for the cylinders with capped ends can be calculated from simple theory.

Radial deflection, component 1; $Yf_1 = P*R^2(1-\mu/2)/(E*T_1)$

Radial deflection, component 2; $Yf_2 = P*R^2(1-\mu/2)/(E*T_2)$

Rotation, components 1 and 2; $\theta f_1 = \theta f_2 = 0$

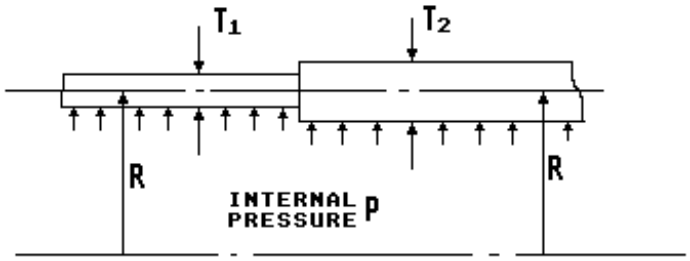

FIGURE 1.2 Cylinders subjected to uniform internal pressure

The thinner cylinder will have a radial growth greater than that of the thicker cylinder and so there will be a difference in radial deflection relative to component 2 of $Yr = Yf_1 – Yf_2$. This is best seen by sketching the displacements (to an exaggerated scale) on a diagram known as a free body diagram like that shown in FIGURE 1.3.

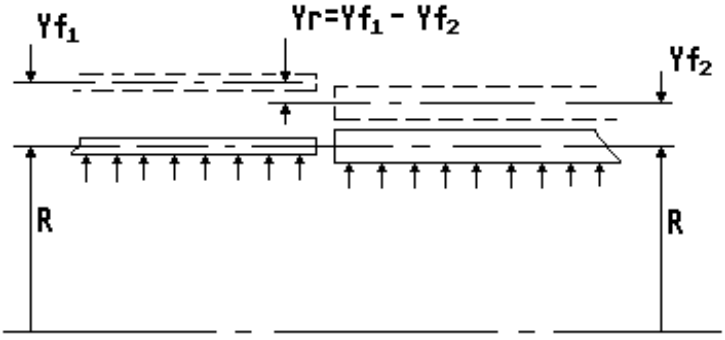

FIGURE 1.3 Free body diagram for cylinders subjected to internal pressure

Since there must be physical connection between the two components this is achieved by bending of the components local to the junction so that continuity of displacements is maintained at the junction. This effect is shown (again to an exaggerated scale) in FIGURE 1.4. The continuity of displacements at the junction is brought about by radial shearing forces Vj and meridional bending moments Mj being set up circumferentially around the junction as shown in FIGURE 1.5.

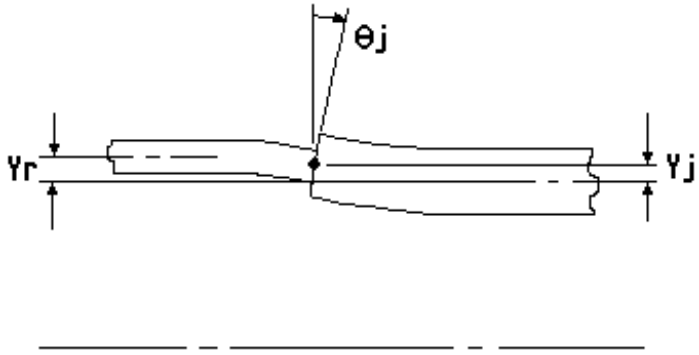

FIGURE 1.4 Connected cylinders subjected to internal pressure

These discontinuity forces and moments, as they are called, produce discontinuity stresses at the junction and for a short distance away from the junction. The discontinuity stresses can be written simply by four equations (1.1).

$$\text{Average Shear Stress, } SV = V/T$$

$$\text{Hoop (Circumferential) Membrane Stress, } SH = E*Y/R \qquad (1.1)$$

$$\text{Meridional Bending Stress, } SBL = \pm 6*M1/T^2$$

$$\text{Hoop Bending Stress, } SBH = \pm 6*M2/T^2$$

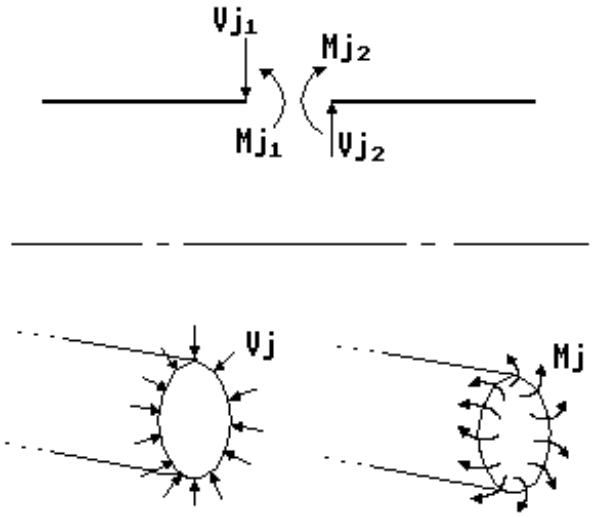

FIGURE 1.5 Discontinuity loads (forces and moments) at a junction

At the junction V = Vj, Y = Yj -Yr, M1 = Mj and M2 = μ*Mj (for a cylinder). E and μ are the material properties, Young's modulus and Poisson's ratio. R and T are the component radius and thickness respectively. Hence we can say that the calculation of discontinuity stresses will require consideration of the loading, of the material properties and the geometry of the structure. There is a fourth influence, that of the boundary conditions, but in this text we are only considering components with ends sufficiently far apart so that the effects of one end of the component do not significantly influence the other end. In general, at a junction the discontinuity loads Mj and Vj are indeterminate. The main purpose of a discontinuity analysis is to obtain these loads and deflections so that equations (1.1) can be solved.

Note that the formulation of the analysis can be arranged to consider the units of the loading in any of three ways: (1) as total loads of the whole circumference, (2) as loads per unit circumference and (3) as loads per radian of the circumference. In this text the loading is formulated as *loads per unit circumference*. If referring to other text it is necessary to study the notation carefully to establish the applicable units that are used.

Example 1.2 MATERIAL DISCONTINUITY

Operating and environmental conditions often require parts of a vessel to be constructed of different materials. If we consider two connected cylinders of equal thickness, FIGURE 1.6. One cylinder is manufactured from a ferritic steel and the other from an austenitic stainless steel. If the cylinders are subjected to a uniform temperature change ΔT there will be a difference in radial thermal expansion of $Yr = R*\Delta T*(\alpha_A - \alpha_F)$ as the coefficient of thermal expansion of the austenitic steel is significantly higher than that of the ferritic steel. As with Example 1.1, in order to maintain continuity of displacements, there will be discontinuity loads and stresses induced at the junction of the two cylinders simply due to a change in metal temperature.

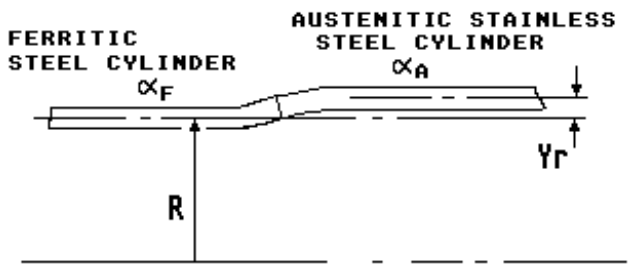

FIGURE 1.6 Material discontinuity, cylinders with different coefficients of thermal expansion

Example 1.3 LOADING DISCONTINUITY

Sudden changes in loading can also produce a discontinuity. If we consider a cylinder of uniform thickness but subjected to an internal pressure on one side of the cylinder only, FIGURE 1.7. The loaded side of the cylinder will tend to deflect relative to the unloaded side by the amount $Yr = P*R^2(1-\mu/2)/(E*T)$. Hence like Example 1.1, discontinuity loads and stresses will be induced in the cylinder in a region close to the change of loading.

Although the above three examples are for discontinuities resulting from differences in radial deflection, the discontinuity can just as easily result from differences in rotation as shown in Example 1.4.

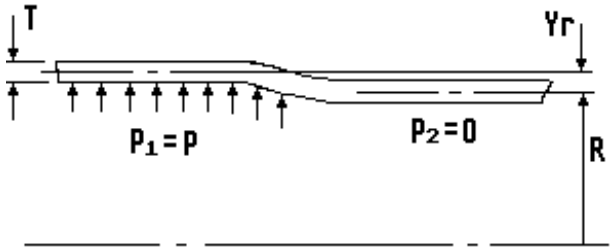

FIGURE 1.7 Loading discontinuity, a cylinder subjected to a step loading

Example 1.4 LOADING DISCONTINUITY (Thermal Gradient)

If we consider a cylinder of uniform thickness, FIGURE 1.8. One side of the cylinder is at a uniform temperature the other side has a linear rise in temperature (axial thermal gradient) over a specified length, FIGURE 1.8(a). The thermal gradient is given by the temperature rise (or fall) over a specified length, i.e.
$G j = (Tm - Ta)/Le$.

The free body diagram, FIGURE 1.8(b), shows that an angle (or slope) of discontinuity would be present at the point where the temperature changes from a uniform to a linear gradient. The angle, in radians, is given by $\theta r = \alpha*R*(Tm - Ta)/Le$. Since the cylinder is continuous, the angle of discontinuity has to be absorbed by rotation of the cylinder so that there is continuity of displacements at the point where there is a change in the thermal gradient. The rotation of the cylinder is brought about by discontinuity loads at the point where the change of loading occurs.

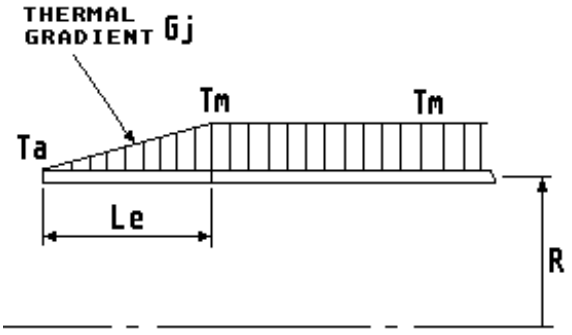

FIGURE 1.8(a) Loading discontinuity, cylinder with an axial thermal gradient

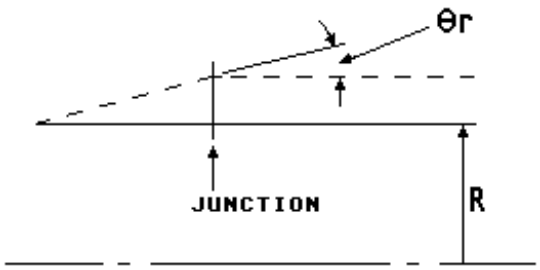

FIGURE 1.8(b) Free body diagram for a cylinder with an axial thermal gradient

In general, combinations of geometric, material and loading discontinuity may occur simultaneously and can result in differences in displacements which are sometimes difficult to predict without experience. Where there is doubt, it is good practice to follow a general step by step procedure and try to identify the possibility of a potential discontinuity. A typical procedure is listed in TABLE 1.3.

STEP 1 Imagine each component to be separated at the junction, or at the point where the change of loading or change in material properties occur.
STEP 2 Load each component separately for a given time point. Take care with the direction and sign of the loading.
STEP 3 Calculate the free deflections and rotations at the junction end of each component. Use simple theory or text such as ROARK (ref. 11) or BAKER (ref. 8). Again take care with the directions and sign of the displacements.
STEP 4 Sketch a free body diagram of the displacements to help visualise how the structure will deform.
STEP 5 Choose one of the components as a datum and subtract (algebraically) the free displacements of the datum component from each of the other components.
STEP 6 If there are non zero radial deflections or rotations resulting from step 5 then there is a discontinuity at the junction.

TABLE 1.3 Procedure list for investigating the possibility of a potential discontinuity

1.2 WHY ARE STRUCTURAL DISCONTINUITIES IMPORTANT?

Regions of discontinuity are important because the stresses resulting from the discontinuity can be significantly higher than in regions (membrane regions) remote from the discontinuity. How much higher the stresses are can best be illustrated by a few examples.

Example 1.5 REINFORCED CYLINDER

If we consider a long cylinder with a rigid reinforcing ring subjected to internal pressure, FIGURE 1.9. The ring acts like a concentrated load applied circumferentially around the cylinder. The hoop membrane stress in the cylinder, remote from the ring, is given by simple theory as:

$$SH = P*R/T \qquad (1.2a)$$

If the cylinder has end caps, so that the pressure end load is taken by the cylinder, there will be a meridional (longitudinal) membrane stress in the cylinder amounting to:

$$SL = 0.5*P*R/T \qquad (1.2b)$$

At the rigid ring the radial deflection of the cylinder is suppressed by a radial force Vo. This causes shear and bending stresses to be induced in the cylinder at the ring. It can be shown by a discontinuity analysis that the shear force and the meridional bending moment are given by:

$$V = E*T*Yr/(R^2\beta) \qquad (1.3a)$$

$$M1 = E*T*Yr/(2*R*\beta^2) \qquad (1.3b)$$

Where Yr is the free radial deflection of the cylinder relative to the ring and β is the shell characteristic. For a material with a Poisson's ratio of μ=0.3 (a typical value for a metal) the shell characteristic for a cylinder becomes $\beta=1.285/(R*T)^{1/2}$. If the ends of the cylinder are *not* capped, the free radial deflection due to the internal pressure is given by $Yf = P*R^2/E*T$. Relative to the rigid ring the deflection Yr = Yf. Substituting for β and Yr in equation (1.3) gives $V=0.778*P(R*T)^{1/2}$ and M1=0.303*P*R*T.

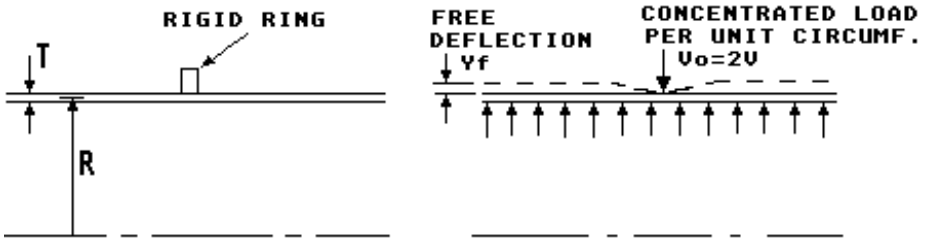

FIGURE 1.9 Reinforced cylinder subjected to internal pressure

Substituting V and M1 into equations (1.1) we get the following equations for the discontinuity stresses, in the cylinder, adjacent to the ring:

$$SV = 0.778*P(R/T)^{1/2}$$

$$SH = 0$$

$$SBL = \pm 1.818*P*R/T \qquad (1.4)$$

$$SBH = \pm 0.545*P*R/T$$

The hoop membrane stress in the cylinder is zero at the ring (since the radial deflection is suppressed) but the meridional bending stress is approximately 82% higher than the hoop membrane stress remote from the ring.

Equation (1.4) is applicable for the case where the ends of the cylinders are *not* capped. The more usual case is for the ends to be capped, so that the pressure end load is taken by the cylinder. In this case the free radial deflection $Yr = P*R^2(1-\mu/2)/(E*T)$. This reduces to $Yr = 0.85*P*R^2/(E*T)$, for a material with a Poisson's ratio of 0.3.

Substituting for β and Yr in equation (1.3) gives $V = 0.66*P(R*T)^{1/2}$ and M1 = 0.257*P*R*T. Finally substituting for V and M1 in equation (1.1), gives the resulting discontinuity stresses, equation (1.5).

$$SV = 0.66*P(R/T)^{1/2}$$

$$SH = 0.15*P*R/T$$

$$SBL = \pm 1.55*P*R/T \qquad (1.5)$$

$$SBH = \pm 0.465*P*R/T$$

Adding the meridional membrane stress from equation (1.2b) to the meridional bending stress of equation (1.5) gives the maximum stress at the inside surface as:

$$SLi = 2.05*P*R/T \qquad (1.6)$$

i.e. 105% higher than the hoop membrane stress remote from the ring. Note that the hoop membrane stress does not reduce to zero in this case. The reason for this is that the radial deflection to be suppressed, by load Vo, is only 85% of that required for the case with no end caps. As the hoop membrane stress, given by equation (1.2a), represents 100% in both cases there must be 15% of the total hoop stress remaining in the case with end caps.

The ratio R/T is typically >= 10 for thin shells. It can be seen that the shear stress will be low compared to the bending stresses and hence the shear stress is often ignored in thin shell analysis.

Example 1.6 FIXED END CYLINDER SUBJECTED TO INTERNAL PRESSURE

If we consider a cylinder fixed (built-in) at one end subjected to an internal pressure, FIGURE 1.10. This condition is very similar to that described in Example 1.5 and discontinuity stresses of the same magnitude as equations (1.4) or (1.5) are present in the cylinder adjacent to the fixed end.

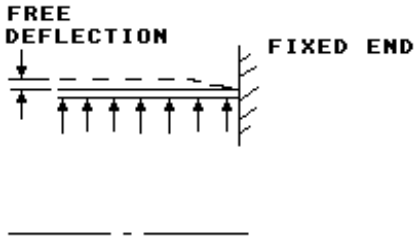

FIGURE 1.10 Cylinder with a fixed end subjected to internal pressure

Example 1.7 FIXED END CYLINDER SUBJECTED TO A UNIFORM TEMPERATURE

If we again consider the cylinder with a fixed end as shown in FIGURE 1.10, but this time subjected to a uniform temperature rise ΔT relative to the fixed end. The free radial expansion of the cylinder relative to the fixed end is given by $Yr = R*\alpha*\Delta T$. In its free state there would be no stress in the cylinder. However, if the end is constrained, like Examples 1.5 and 1.6, there will be shear and bending stresses induced in the cylinder at the fixed end. Following the same procedure as described in Example 1.5 it can be shown that the discontinuity stresses, in the cylinder, adjacent to the fixed end are:

$$\begin{aligned} SV &= 0.778*E*\alpha*\Delta T(T/R)^{1/2} \\ SH &= -E*\alpha*\Delta T \\ SBL &= \pm 1.818*E*\alpha*\Delta T \\ SBH &= \pm 0.545*E*\alpha*\Delta T \end{aligned} \qquad (1.7)$$

The maximum stress is the meridional bending stress. This stress is approximately 82% higher than the hoop membrane stress (calculated from equation (1.1) by putting Y= -Yr) due to the complete suppression of the free radial expansion at the fixed end. The maximum hoop stress, at the outside surface, becomes:

$$SHo = -1.545*E*\alpha*\Delta T \qquad (1.8)$$

Example 1.8 CYLINDER WITH A MATERIAL DISCONTINUITY

If the cylinder of FIGURE 1.10 is made of an austenitic stainless steel and the fixed end made of a ferritic steel. If the whole structure is then subjected to a uniform temperature change, there will be discontinuity stresses induced in the cylinder, due to the austenitic steel having a higher coefficient of thermal expansion than the ferritic steel.

The results of equations (1.7) and (1.8) will apply except that α is replaced by $(\alpha_A - \alpha_F)$.

Example 1.9 CYLINDER WITH FREE END

The previous examples were for cases where the fixed end induced an increase in the stress. However, increases in stress can also occur at free ends. If we consider a semi infinite cylinder subjected to a temperature difference dT across the thickness. For a thin shell, the resulting temperature distribution is essentially linear. At distances remote from the end, the bending stresses are given by:

$$SBH = SBL = \pm 0.5*E*\alpha*dT/(1 - \mu) \qquad (1.9)$$

For $\mu = 0.3$ equation (1.9) reduces to:

$$SBH = SBL = \pm 0.714*E*\alpha*dT \qquad (1.10)$$

It can be shown by analysis that, at the free end, the hoop bending moment is given by $M2 = E*\alpha*dT*T^2/12$ and there is a hoop membrane force of $N2 = E*Y*T/R$. The radial deflection $Y = E*\alpha*dT*T^2/(24(1-\mu)D*\beta^2)$. The shear force and meridional bending moment are zero at the free end.

Substituting for M2 and Y in equation (1.1) gives the discontinuity stresses, for $\mu = 0.3$, at the free end, equation (1.11).

$$\begin{aligned} SV &= 0 \\ SH &= 0.393*E*\alpha*dT \\ SBL &= 0 \\ SBH &= \pm 0.5*E*\alpha*dT \end{aligned} \qquad (1.11)$$

Adding the hoop bending stress to the hoop membrane stress gives the maximum stress at the outside surface of the free edge as:

$$SHo = 0.893*E*\alpha*dT \qquad (1.12)$$

i.e. 25% higher than the bending stress remote from the free end.

The above examples show that there is potential for increased stress levels at discontinuities but it cannot be assumed that the increase in stress will only be some percentage higher than a membrane stress value.

Examples of fixed junctions do not often occur and flexibility at the junction may even reduce the stress level, especially where thermal loading is involved. However in practice, unfavourable combinations of geometry, loading and material discontinuities may be present and these can produce significant increase in the stress levels leading to fatigue, brittle fracture or creep failure.

An example of what can occur is discussed in detail in Chapter 3 Example 3.5, where a cylinder is connected to a flat end closure and subjected to internal pressure. The hoop membrane stress remote from the cylinder to end junction is only 16.66 N/mm^2 but the maximum stress at the junction is 239.27 N/mm^2, i.e. an almost fifteen times increase in stress. An assessment of the strength and fatigue life of this junction is discussed by example in section 4.6.

1.3 WHAT STRESS TERMINOLOGY IS USED?

Since the main purpose is to calculate stresses it is necessary to have an understanding of the terminology used by stress analysts. This section briefly discusses stress directions, stress distributions and classifies the structural discontinuity as there can be confusion over what is required to be included in the analysis. Stresses in thin axisymmetric shells are normally calculated in three directions:

(1) Meridional direction
(2) Hoop (or Circumferential) direction
(3) Transverse direction

All loadings can be resolved into these three directions and they are convenient for reasons of symmetry. For a general axisymmetric shell of revolution the three directions at a point on the shell are as shown in FIGURE 1.11. In some text the meridional and hoop directions are called the tangential directions, i.e. a tangent to the meridian and a tangent to the circumference. In some cases the circumference is referred to as the parallel circle.

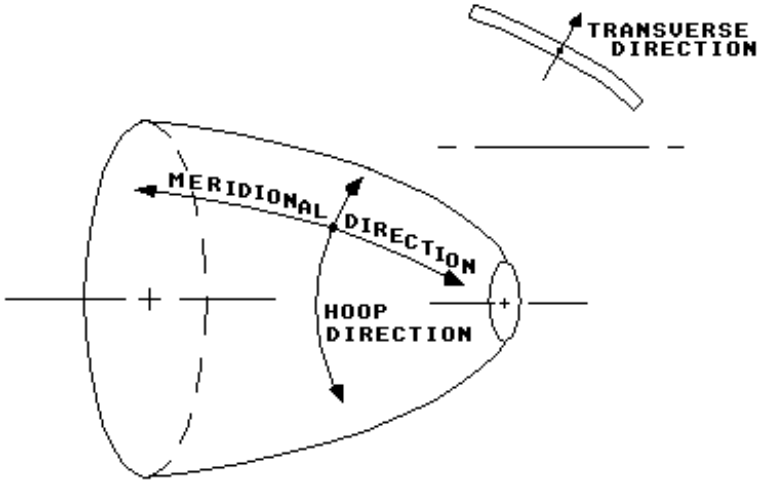

FIGURE 1.11 General axisymmetric shell showing hoop (circumferential), meridional and transverse directions

Two special cases are Cylinders and Flat Plates. For the cylinder the meridional direction is in the longitudinal or axial direction and the transverse direction is radial as shown in FIGURE 1.12. For the flat plate the meridional direction is in the radial direction and the transverse direction is axial as shown in FIGURE 1.13.

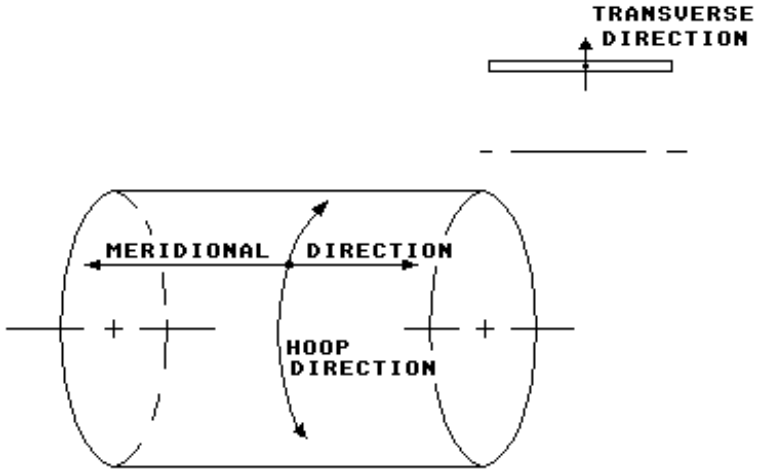

FIGURE 1.12 Cylindrical shell showing hoop, meridional and transverse directions

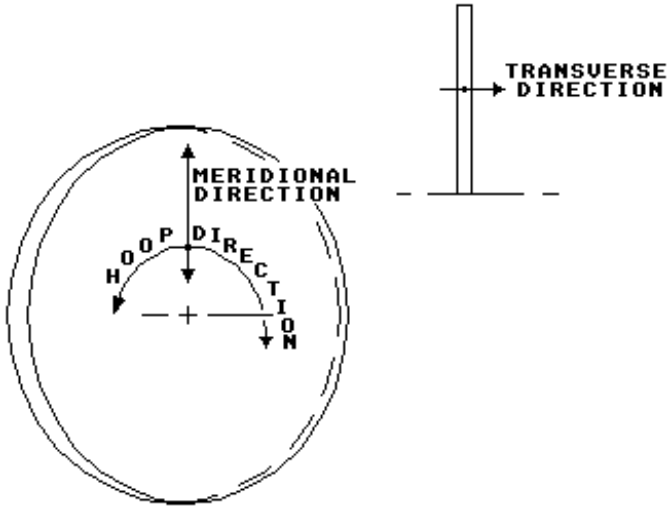

FIGURE 1.13 Flat plate showing hoop, meridional and transverse directions

Introduction

For a discontinuity analysis it is necessary to calculate three types of stress:

(1) Membrane stress
(2) Bending stress
(3) Transverse shear stress

These stresses are calculated for a specified section across the thickness of the shell. Note that where the loading is not symmetric there will be additional shear stresses due to shear forces and twisting moments. These additional stresses are not considered in this text but they may be significant in vessels subjected to torsion or lateral (sideways) loading.

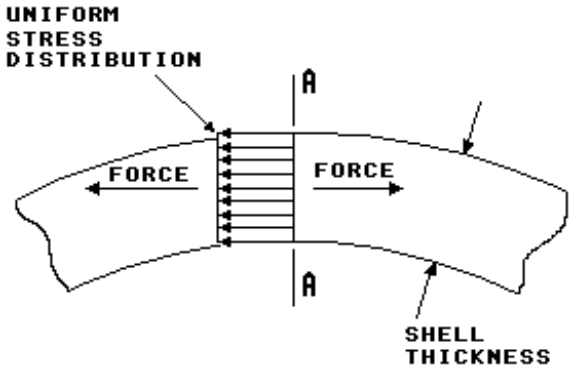

FIGURE 1.14 Membrane stress distribution across a shell section A - A

The membrane stress is the uniform or average stress normal to the section under consideration, FIGURE 1.14. The stress is due to hoop or meridional forces acting at the section. The stress sign is +ve tensile, -ve compression.

The bending stress is the linear variation in stress normal to the section, FIGURE 1.15. This stress is due to a hoop or meridional bending moment. The program calculates the stress at the surface and the sign of the stress indicates +ve tensile and -ve compression. The sign of the moment is +ve if it produces compression on the outside surface (the left surface if a flat plate) this is an arbitrary choice.

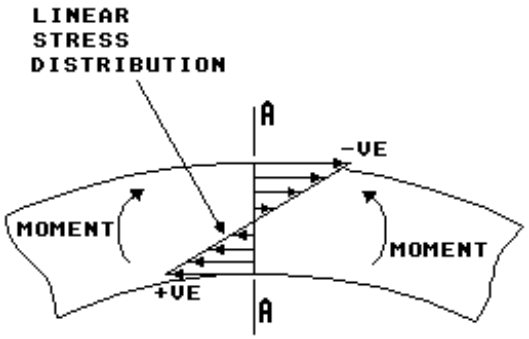

FIGURE 1.15 Bending stress distribution across a shell section A – A

The transverse shear stress is the average stress parallel to the section, FIGURE 1.16. It is due to the transverse shear force. The sign is +ve outward (to the right if a flat plate) this being an arbitrary choice. Note that the actual stress distribution is likely to be parabolic in shape, the maximum stress is at the centre of the shell wall and is 50% higher than the average value.

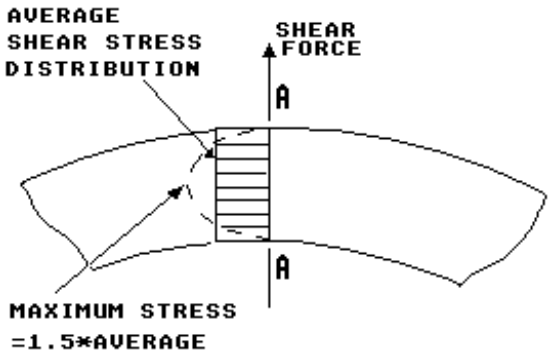

FIGURE 1.16 Transverse shear stress distribution across a shell section A - A

Engineers are normally interested in two main regions of a shell structure, these are: *Membrane* regions and *Discontinuity* regions. The membrane regions are of interest as they essentially govern the overall response of the structure to the applied loading, i.e. if say a pressure vessel is not thick enough to withstand the pressure loading then we could expect it to suffer catastrophic failure, or at least gross plastic deformation, in a single application of the loading. The discontinuity regions on the other hand are local regions of high stresses associated with the geometric features, material properties and loadings necessary for the operation and functioning of the structure. The high stresses present in these discontinuity regions are a potential source of failure due to brittle fracture (possibly in a single application of load) or fatigue due to cyclic loading or creep rupture due to extended operation at elevated temperatures. The two regions are now best discussed with reference to FIGURE 1.17.

1.3.1 Membrane Regions

The membrane regions refer to points on the shell that are remote from regions of discontinuity. Unfortunately there is no clear definition as to what is meant by remote. One "rule of thumb" is to consider points further apart than about $2.5(R*T)^{1/2}$ as remote from each other. This derives from the generally accepted observation that the effects of a discontinuity along a cylindrical shell is a highly damped wave which rapidly diffuses away to membrane behaviour over a short distance of π/β in the meridional direction. Where β is the shell characteristic sometimes called the damping factor.

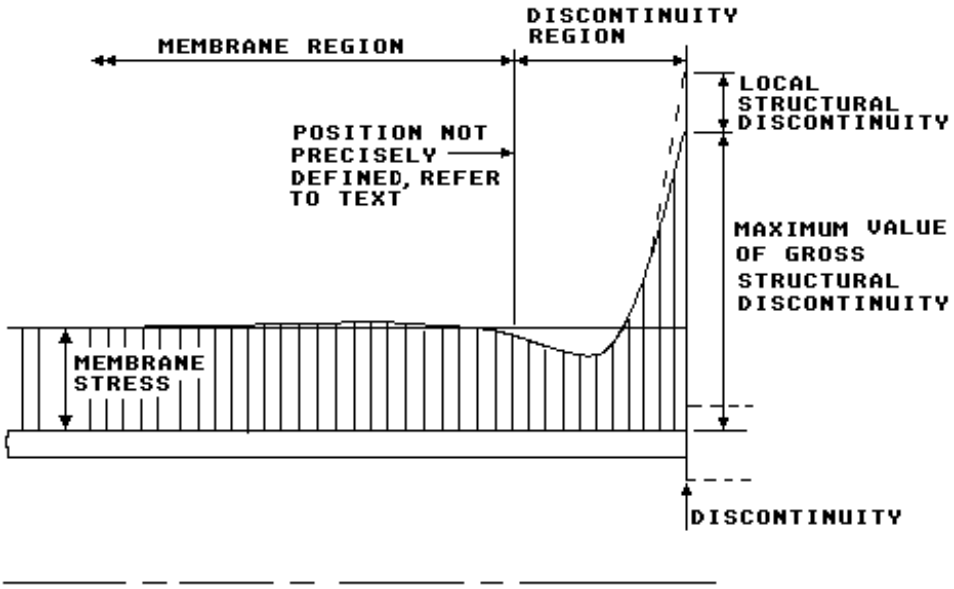

FIGURE 1.17 Typical stress field at a discontinuity

For a cylindrical shell $\beta = [3(1 - \mu^2)/(R^2T^2)]^{1/4}$

and a typical value of Poisson's ratio for metals is $\mu = 0.3$

Therefore the shell characteristic reduces to: $\beta = 1.285/(R*T)^{1/2}$

and hence distance π/β is approximately $2.5(R*T)^{1/2}$

The important feature of membrane regions is that the stress field along the shell is not changing rapidly. Although membrane implies that the stress across the section is essentially uniform with little or no bending, this definition requires some qualification when considering flat plates which resist pressure and point loading by bending and for shells and plates subjected to temperature difference across the thickness. In both cases bending stresses will predominate but if the stress field along the shell surface is not changing rapidly then the region can be considered a membrane region for the purpose of the discontinuity analysis. Stresses in membrane regions can usually be calculated by hand from simple theory found in textbooks. For convenience the program will calculate stresses in the membrane regions for the loadings specified.

1.3.2 Discontinuity Regions

Discontinuity regions are those points on the shell close to a discontinuity feature such as that discussed in section 1.1.

As the discontinuity is approached, additional shear, membrane and bending loads cause the stress field to alter rapidly in a wave form similar to that shown in FIGURE 1.17, i.e. there is a slight fluctuation in the stress field followed by a rapid increase to a maximum value at (or near to) the discontinuity junction. Note that there are cases where the maximum of the individual stress types may be slightly away from the junction (refer to Examples 3.5 and 3.13).

Although the stress field is only affected close to the discontinuity it is generally considered that a relatively large portion of the structure has been affected and because of this the discontinuity is called a *gross* structural discontinuity. The program calculates the stresses due to this gross structural discontinuity.

In cases where there is a geometric discontinuity, the actual stress is usually higher than that predicted by a discontinuity analysis. This is due to the geometric stress concentration factor (K_t) at fillet radii etc., locally raising the stress level. Only a small portion of the structure is affected and the overall stress field is not significantly altered. This additional discontinuity is known as a *local* structural discontinuity. The program does *not* calculate the stresses due to this discontinuity. Some types of analysis, e.g. a fatigue analysis, requires the local structural discontinuity to be evaluated and added to the gross structural discontinuity. This is best done by the use of fatigue strength reduction factors or stress concentration factors given in published text such as PETERSON (ref. 16). Note that some care is required when using the factors as in some cases the gross as well as the local structural discontinuity may be included in the data.

2.0 METHOD OF ANALYSIS

2.1 WHAT COMPONENTS CAN BE ANALYSED?

In principle any axisymmetric component whose governing equations can be defined should be capable of being analysed. The program analyses the seven most common types of component found in shell structures.

TABLE 2.1 lists the components that are considered. These components can all be computed within the memory and accuracy of a microcomputer. The main omissions are torispherical and ellipsoidal shells, these have to be simulated as an equivalent spherical shell.

TABLE 2.1(a) below lists the menu available for the analysis of *single* components. For a *junction* analysis the extended menu, TABLE 2.1(b) is used to specify the position of the junction as indicated in FIGURE 2.2.

COMPONENT TYPE No.	DESCRIPTION
1	Cylinder
2	Spherical shell
3	Cone with a large end
4	Cone with a small end
5	Flat plate with support at the outside diameter
6	Flat plate with support at the inside diameter
7	Compact ring

TABLE 2.1(a) Menu for single components

COMPONENT TYPE No.	DESCRIPTION
1	Cylinder, junction at the right end
2	Cylinder, junction at the left end
3	Spherical shell, junction at the right end
4	Spherical shell, junction at the left end
5	Cone, junction at the large right end
6	Cone, junction at the large left end
7	Cone, junction at the small right end
8	Cone, junction at the small left end
9	Flat plate, junction at the outside diameter
10	Flat plate, junction at the inside diameter
11	Compact ring at the junction

TABLE 2.1(b) Menu for a junction analysis

2.2 THE JUNCTION ANALYSIS

The analysis is based on the displacement method, i.e. the unknown junction displacements are resolved first and then the discontinuity loads are calculated by substituting the displacements into the appropriate equations.

Since only one junction is considered there is no need to store a large stiffness matrix. The analysis proceeds by considering each component in turn. The main steps involved are summarised in FIGURE 2.1. For cross reference the program line numbers are given in brackets [ ]. A listing of the main calculation routine is given in TABLE 2.3. The whole program can be listed out from BASIC using the standard LIST or LLIST commands. The program is large, it will take about 25 - A4 sheets to list the complete program.

The analysis will now be discussed in detail. There are four aspects to be discussed: the sign convention to be used, the formulation of the displacement equations, the loading equations and how to deal with rigid offsets.

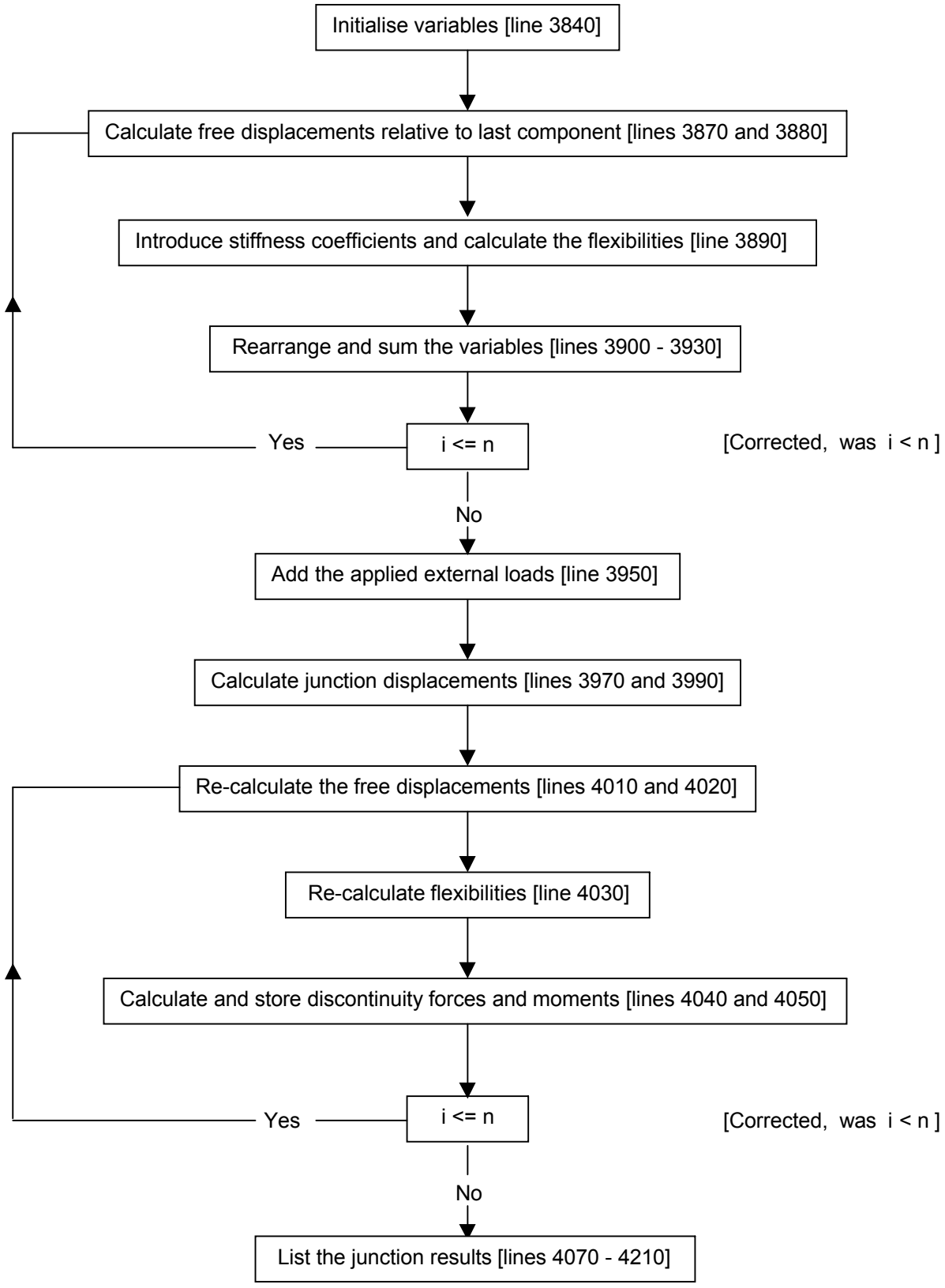

FIGURE 2.1 Summary of main calculation steps for a junction analysis [lines 3840 - 4230]

```
3840  CLS:PRINT "JUNCTION ANALYSIS":IND=0:C1=0:C2=0:C3=0:C4=0:C5=0:C6=0:
C7=0:C8=0:C9=0:C10=0:C11=0:C12=0
3850  FOR I=1 TO N
3860  U=C(I):GOSUB 2920
3870  YR=Z(2*I)-Z(2*N):THR=Z(2*I-1)-Z(2*N-1)
3880  LX=0:IF C(N)=11 AND I<N THEN LX=G(H(I)):YR=YR-Z(2*N-1)*LX
3890  C1=-1/K(1,I):C2=1/K(2,I):C3=-FC/K(3,I):C4=FC/K(4,I)
3900  C5=C2/C1-C4/C3
3910  C6=C1/C2-C3/C4
3920  C7=C7-FC/(C1*C5):C8=C8+FC/(C3*C5):C9=C9-FC*YR/(C1*C5)+FC*THR/(C3*C5)
:C10=C10+1/(C2*C6):C11=C11-1/(C4*C6):C12=C12+YR/(C2*C6)-THR/(C4*C6)
3930  IF C(N)=11 THEN C7=C7+LX/(C2*C6):C8=C8-FC*LX/(C1*C5)-LX/(C4*C6)+
LX*LX/(C2*C6):C9=C9+YR*LX/(C2*C6)-THR*LX/(C4*C6):C11=C11+LX/(C2*C6)
3940  NEXT I
3950  C9=C9+MO:C12=C12+VO
3960  IF C7=0 THEN C7=1E-15
3970  THJ=(C9/C7-C12/C10)/(C8/C7-C11/C10)
3980  IF C11=0 THEN C11=1E-15
3990  YJ=(C9/C8-C12/C11)/(C7/C8-C10/C11)
4000  FOR I=1 TO N:U=C(I):GOSUB 2920
4010  YR=Z(2*I)-Z(2*N):THR=Z(2*I-1)-Z(2*N-1)
4020  LX=0:IF C(N)=11 AND I<N THEN LX=G(H(I)):YR=YR-Z(2*N-1)*LX
4030  C1=-1/K(1,I):C2=1/K(2,I):C3=-FC/K(3,I):C4=FC/K(4,I):C5=C2/C1-C4/C3:
C6=C1/C2-C3/C4
4040  M(I)=(YJ-YR)/(C1*C5)+(THR-THJ)/(C3*C5)+THJ*LX/(C1*C5)
4050  V(I)=(YJ-YR)/(C2*C6)+(THR-THJ)/(C4*C6)+THJ*LX/(C2*C6)
4060  NEXT I
4070  CLS:PRINT "JUNCTION RESULTS":PRINT "DISCONTINUITY FORCES & MOMENTS"
:PRINT A$:PRINT B$:IF CH=3 THEN LPRINT:LPRINT "JUNCTION RESULTS":LPRINT "
DISCONTINUITY FORCES & MOMENTS":LPRINT A$:LPRINT B$
4080  FOR I=1 TO N
4090  U=C(I):GOSUB 2920
4100  IF C(N)=11 AND I=N THEN PRINT:PRINT "at centroid";:IF CH=3 THEN
LPRINT:LPRINT "at centroid";
4110  PRINT:PRINT "Mj";I;"=";M(I);M$;:IF CH=3 THEN LPRINT:LPRINT
 "Mj";I;"=";M(I);M$;
4120  IF M(I)=0 THEN PRINT "":IF CH=3 THEN LPRINT ""
4130  IF FC=1 AND M(I)>0 THEN PRINT " anti-clockwise":IF CH=3 THEN LPRINT-
" anti-clockwise"
4140  IF FC=1 AND M(I)<0 THEN PRINT " clockwise":IF CH=3 THEN LPRINT
" clockwise"
4150  IF FC=-1 AND M(I)>0 THEN PRINT " clockwise":IF CH=3 THEN LPRINT
" clockwise"
4160  IF FC=-1 AND M(I)<0 THEN PRINT " anti-clockwise":IF CH=3 THEN
LPRINT " anti-clockwise"
4170  PRINT "Vj";I;"=";V(I);N$;:IF CH=3 THEN LPRINT "Vj";I;"=";V(I);N$;
4180  IF V(I)>0 THEN PRINT " inward":IF CH=3 THEN LPRINT " inward"
4190  IF V(I)=0 THEN PRINT "":IF CH=3 THEN LPRINT ""
4200  IF V(I)<0 THEN PRINT " outward":IF CH=3 THEN LPRINT " outward"
4210  NEXT I:CH=2
4220  PRINT:PRINT "COPY?":INPUT Y$:IF Y$="Y" OR Y$="y" THEN CH=3:GOTO 4070
4230  RETURN
```

TABLE 2.3 BASIC listing of the main calculation routine

2.2.1 Sign Convention

Before proceeding with the analysis it is necessary to specify a sign convention for the forces, moments and displacements at the junction. The sign direction chosen can be arbitrary but once decided upon must be maintained throughout the analysis.

The positive directions chosen for the discontinuity forces and moments at cylindrical, conical and spherical shells are as shown in FIGURE 2.2(a). Flat plates and compact rings have been formulated as left end components, their positive directions are shown in FIGURE 2.2(b).

Junction analysis

Positive directions for the displacements of all components are shown in FIGURE 2.3 and for the applied external force and moment FIGURE 2.4.

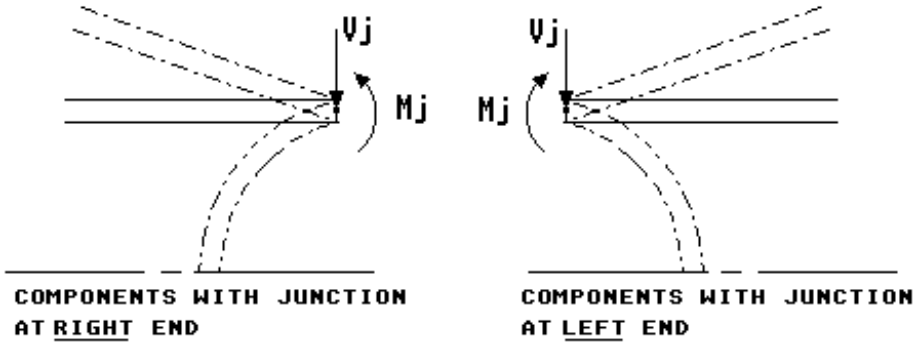

Radial force Vj is +ve inwards
Meridional moment Mj is +ve anti-clockwise on *right* end junction
Meridional moment Mj is +ve clockwise on *left* end junction

FIGURE 2.2(a) Junction discontinuity forces and moments.
Positive directions for cylinders, cones, and spherical shells.

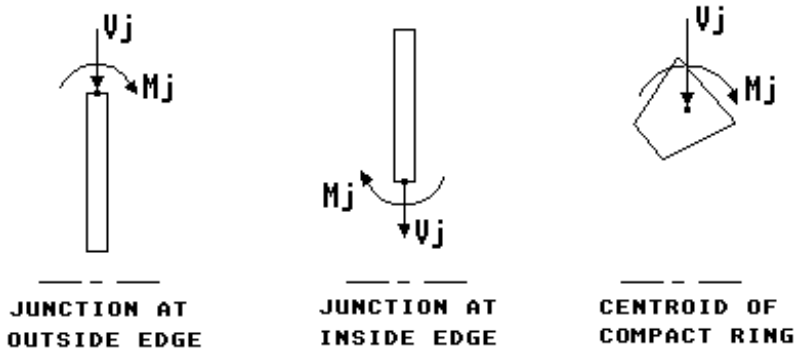

FIGURE 2.2(b) Junction discontinuity forces and moments.
Positive directions for flat plates and the compact ring

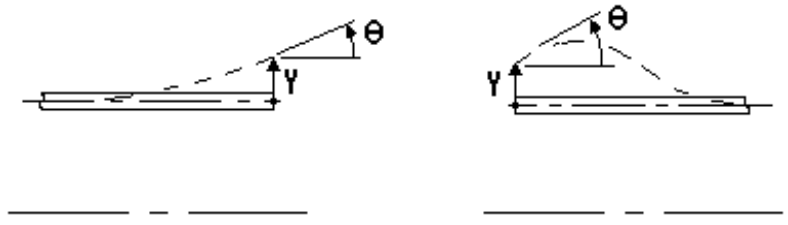

Radial deflection of the circumference, Y is +ve outward
Rotation of a tangent to a meridian THETA, θ is +ve anti-clockwise

FIGURE 2.3 Junction displacements. Positive directions for *all* components

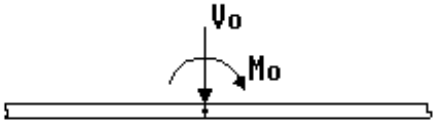

Radial force Vo is +ve inward
Moment Mo is +ve clockwise

FIGURE 2.4 Positive directions of applied external force and moment

2.2.2 Displacement Equations

For continuity the final displacements of the junction must equal the sum of the relative free displacements and the displacements due to the discontinuity loads. We can write:

$$\text{Radial deflection, } Yj = Yr + Yd$$
$$\text{Rotation, } \theta j = \theta r + \theta d \qquad (2.1)$$

Where: Yj and θj are the final displacements of the junction.

Yr and θr are the free displacements relative to the last component specified (an arbitrary choice).

Yd and θd are the displacements due to the discontinuity loads Vj and Mj.

Positive directions for the displacements are as shown in FIGURE 2.3. The relative free displacements are obtained by subtracting the free displacements of the last (the n_{th}) component from the other (the i_{th}) components [line 3870].

$$Yr_i = Yf_i - Yf_n$$
$$\theta r_i = \theta f_i - \theta f_n \qquad (2.2)$$

The relative free displacements of the last component are of course zero.

If we now consider the two components, shown in FIGURE 2.5, subjected to the action of positive discontinuity loads Vj and Mj.

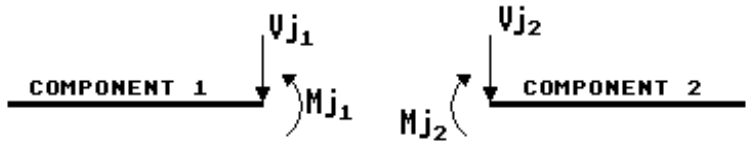

FIGURE 2.5 Components subjected to discontinuity forces and moments

The displacements due to Vj and Mj can be written as:

for junction at RIGHT end (Component 1):

$$Yd_1 = -Vj_1/K(1,1) + Mj_1/K(2,1)$$
$$\theta d_1 = -Vj_1/K(3,1) + Mj_1/K(4,1) \qquad (2.3)$$

Junction analysis

$$\left.\begin{array}{r}\text{for junction}\\ \text{at LEFT end}\\ \text{(Component 2)}\end{array}\right| \quad \begin{array}{l} Yd_2 = -Vj_2/K(1,2) + Mj_2/K(2,2) \\ \\ \theta d_2 = +Vj_2/K(3,2) - Mj_2/K(4,2) \end{array} \qquad (2.4)$$

Where the K( ) terms are structural stiffnesses called stiffness coefficients and are fully discussed later in section 2.3.

Inspection of equations (2.3) and (2.4) show that the form is the same but the sign of θd_2 terms are altered by the handing of the junction end. Therefore for any i_{th} component we can write:

$$\begin{array}{l} Yd_i = -Vj_i/K(1,i) + Mj_i/K(2,i) \\ \\ \theta d_i = -Fc*Vj_i/K(3,i) + Fc*Mj_i/K(4,i) \end{array} \qquad (2.5)$$

Where the term Fc is a factor = 1 for a junction at the *right* end or = -1 for a junction at the *left* end [line 2970].

It is convenient to let [line 3890]:

$$\begin{array}{ll} C1 = -1/K(1,i) & C2 = 1/K(2,i) \\ \\ C3 = -Fc/K(3,i) & C4 = Fc/K(4,i) \end{array} \qquad (2.6)$$

Where C1, C2, C3, and C4 are flexibilities, i.e. the inverse of the stiffness coefficients. We can now drop the subscript and simply write for each component:

$$\begin{array}{l} Yd = C1*Vj + C2*Mj \\ \\ \theta d = C3*Vj + C4*Mj \end{array} \qquad (2.7)$$

Substituting equation (2.1) in (2.7) we have:

$$\begin{array}{l} (Yj - Yr) = C1*Vj + C2*Mj \\ \\ (\theta j - \theta r) = C3*Vj + C4*Mj \end{array} \qquad (2.8)$$

Rearranging equation (2.8) gives:

$$(Yj - Yr)/C1 = Vj + C2*Mj/C1 \qquad (2.9)$$

$$(\theta j - \theta r)/C3 = Vj + C4*Mj/C3 \qquad (2.10)$$

Subtracting equation (2.10) from (2.9) gives:

$$(Yj - Yr)/C1 - (\theta j - \theta r)/C3 = (C2/C1 - C4/C3)*Mj \qquad (2.11)$$

Let [line 3900]:
$$C5 = (C2/C1 - C4/C3) \qquad (2.12)$$

Rearranging gives the junction moment in terms of the displacements.

$$Mj = (Yj - Yr)/(C1*C5) - (\theta j - \theta r)/(C3*C5) \qquad (2.13)$$

Rearranging equation (2.8) again gives:

$$(Yj - Yr)/C2 = C1*Vj/C2 + Mj \qquad (2.14)$$

$$(\theta j - \theta r)/C4 = C3*Vj/C4 + Mj \qquad (2.15)$$

Subtracting equation (2.15) from (2.14) gives:

$$(Yj - Yr)/C2 - (\theta j - \theta r)/C4 = (C1/C2 - C3/C4)*Vj \qquad (2.16)$$

Let [line 3910]: $C6 = (C1/C2 - C3/C4)$ (2.17)

Rearranging gives the junction radial force in terms of displacements.

$$Vj = (Yj - Yr)/(C2*C6) - (\theta j - \theta r)/(C4*C6) \quad (2.18)$$

Equations (2.13) and (2.18) are the junction discontinuity loads in terms of the displacements. In general, Vj and Mj have different values for each component and the displacements (Yj - Yr) and (θj - θr) are unknown. In order to solve equations (2.13) and (2.18), we need to consider the loading acting at the junction.

2.2.3 Loading Equations

For equilibrium, the summation of the discontinuity loads Vj and Mj must equal the applied external loads Vo and Mo acting on the junction, equations (2.19) and (2.20). The positive directions of Vo and Mo are as shown in FIGURE 2.4.

$$\sum_{i=1}^{i=n} -Fc*Mj = Mo \quad (2.19)$$

$$\sum_{i=1}^{i=n} Vj = Vo \quad (2.20)$$

Substituting equation (2.13) in (2.19) gives:

$$-Fc*(Yj - Yr)/(C1*C5) + Fc*(\theta j - \theta r)/(C3*C5) = Mo \quad (2.21)$$

Rearranging gives:

$$-Fc*Yj/(C1*C5) + Fc*\theta j/(C3*C5) = Mo - Fc*Yr/(C1*C5) + Fc*\theta r/(C3*C5) \quad (2.22)$$

Let [line 3920]: $C7 = -Fc/(C1*C5)$ $C8 = Fc/(C3*C5)$

$C9 = -Fc*Yr/(C1*C5) + Fc*\theta r/(C3*C5)$ (2.23)

Substituting equation (2.18) in (2.20) gives:

$$(Yj - Yr)/(C2*C6) - (\theta j - \theta r)/(C4*C6) = Vo \quad (2.24)$$

Rearranging gives:

$$Yj/(C2*C6) - \theta j/(C4*C6) = Vo + Yr/(C2*C6) - \theta r/(C4*C6) \quad (2.25)$$

Let [line 3920] $C10 = 1/(C2*C6)$ $C11 = -1/(C4*C6)$

$C12 = Yr/(C2*C6) - \theta r/(C4*C6)$ (2.26)

Terms C7 to C12 are calculated for each component and summed [line 3920]. The external loads Mo and Vo are added to C9 and C12 respectively, [line 3950], to give the following simultaneous equations with two unknown displacements Yj and θj.

$$C7*Yj + C8*\theta j = C9 \quad (2.27)$$

$$C10*Yj + C11*\theta j = C12 \quad (2.28)$$

Junction analysis

Dividing equation (2.27) by C7 gives:

$$Yj + C8*\theta j/C7 = C9/C7 \quad (2.29)$$

Dividing equation (2.28) by C10 gives:

$$Yj + C11*\theta j/C10 = C12/C10 \quad (2.30)$$

Subtract equation (2.30) from (2.29) gives:

$$(C8/C7 - C11/C10)*\theta j = (C9/C7 - C12/C10) \quad (2.31)$$

Rearranging gives the junction rotation θj [line 3970]:

$$\theta j = (C9/C7 - C12/C10)/(C8/C7 - C11/C10) \quad (2.32)$$

A similar elimination of θj in equations (2.27) and (2.28) gives the junction deflection Yj [line 3990].

$$Yj = (C9/C8 - C12/C11)/(C7/C8 - C10/C11) \quad (2.33)$$

With θj and Yj known, the junction discontinuity loads Vj and Mj for each component can be calculated by substituting θj and Yj back into equations (2.13) and (2.18) [lines 4040 and 4050].

2.2.4 Rigid Offsets

The analysis given in sections 2.2.2 and 2.2.3 is for components connected directly at a point (or nearly at a point). However, a common case requiring analysis is one where the junction is not at a point but is offset. This case can be simulated by allowing a compact ring to be placed at the junction so as to simulate the effects of the offset, FIGURE 2.6. The ring has two degrees of freedom, a radial deflection and a rotation about its centroid, FIGURE 2.7. The freedoms are functions of the ring geometry and the material stiffness, i.e. Young's Modulus. In all other aspects the ring behaves as a rigid ring.

It is possible to connect the components to different points on the ring, as the offset distance Lx from the ring centroid is stored for each component. Offset Lx is positive to the right of the centroid and negative to the left, FIGURE 2.6. For components connected to the surface of a flat plate the offset is included directly in the stiffness coefficients, refer to section 2.3.4.

The junction rotation is the same for the ring and the connected components.

$$\text{i.e. the rotation of the centroid} = \theta j = \theta j_1 = \theta j_2 = \text{- - -} \quad \theta j_n \quad (2.34)$$

The radial deflection of any point on the ring, FIGURE 2.7, is given by:

$$Y = \text{deflection at centroid} + \theta j*Lx$$

The ring is the last component at the junction so we can simply write:

$$Y = Yj + \theta j*Lx \quad (2.35)$$

Equation (2.8) can be rewritten as:

$$\begin{aligned} (Yj + \theta j*Lx - Yr) &= C1*Vj + C2*Mj \\ (\theta j - \theta r) &= C3*Vj + C4*Mj \end{aligned} \quad (2.36)$$

Solving equation (2.36), as described before for equations (2.8) to (2.18), we obtain Mj and Vj in terms of displacements and offset distance Lx.

$$Mj = (Yj + \theta j*Lx - Yr)/(C1*C5) - (\theta j - \theta r)/(C3*C5) \quad (2.37)$$

$$Vj = (Yj + \theta j*Lx - Yr)/(C2*C6) - (\theta j - \theta r)/(C4*C6) \quad (2.38)$$

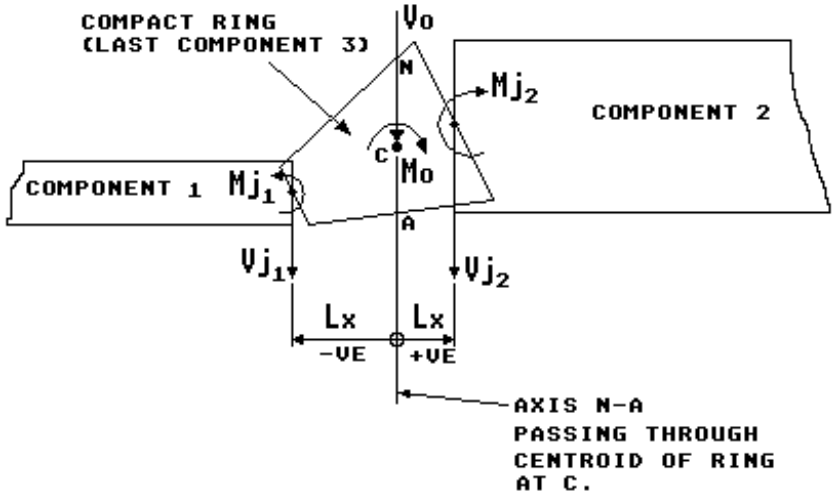

FIGURE 2.6 Rigid offsets simulated by a compact ring

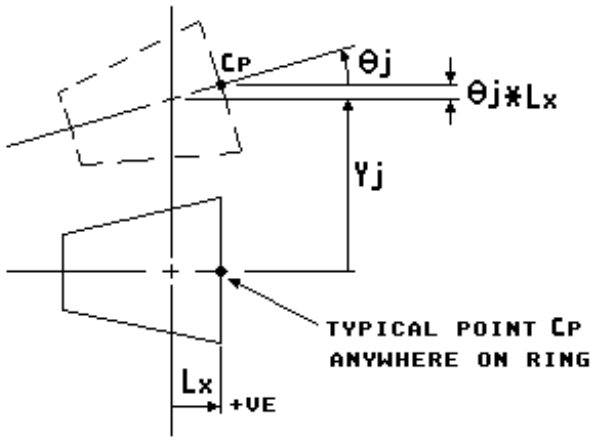

FIGURE 2.7 Displacements of a compact ring

To calculate the unknown displacements Yj and θj at the centroid of the ring we proceed as before, equations (2.19) to (2.33). The loads Mj and Vj are summed for each component about the centroid of the ring and these must equal the applied external loads Mo and Vo, FIGURE 2.6. The equations (2.39) and (2.40) are similar to (2.19) and (2.20) except that equation (2.39) has the added moment Vj times the offset distance Lx.

$$\sum_{i=1}^{i=n} (-Fc*Mj + Vj*Lx) = Mo \qquad (2.39)$$

$$\sum_{i=1}^{i=n} Vj = Vo \qquad (2.40)$$

Junction analysis

Equations (2.37) and (2.38) are substituted in (2.39) to give:

$$-Fc*(Yj + \theta j*Lx - Yr)/(C1*C5) + Fc*(\theta j - \theta r)/(C3*C5) + (Yj + \theta j*Lx - Yr)*Lx/(C2*C6) - (\theta j - \theta r)*Lx/(C4*C6) = Mo \quad (2.41)$$

Rearranging gives:

$$-Yj\{Fc/(C1*C5) - Lx/(C2*C6)\} + \theta j\{Fc/(C3*C5) - Fc*Lx/(C1*C5) - Lx/(C4*C6) + Lx*Lx/(C2*C6)\} = Mo - Yr\{Fc/(C1*C5) - Lx/(C2*C6)\} + \theta r\{Fc/(C3*C5) - Lx/(C4*C6)\} \quad (2.42)$$

Let [lines 3920 and 3930]:

$$C7 = \{-Fc/(C1*C5) + Lx/(C2*C6)\}$$

$$C8 = \{Fc/(C3*C5) - Fc*Lx/(C1*C5) - Lx/(C4*C6) + Lx*Lx/(C2*C6)\} \quad (2.43)$$

$$C9 = Yr\{-Fc/(C1*C5) + Lx/(C2*C6)\} + \theta r\{Fc/(C3*C5) - Lx/(C4*C6)\}$$

equations (2.37) and (2.38) are substituted in (2.40) to give:

$$(Yj + \theta j*Lx - Yr)/(C2*C6) - (\theta j - \theta r)/(C4*C6) = Vo \quad (2.44)$$

Rearranging gives:

$$Yj/(C2*C6) - \theta j\{1/(C4*C6) - Lx/(C2*C6)\} = Vo + Yr/(C2*C6) - \theta r/(C4*C6) \quad (2.45)$$

Let [lines 3920 and 3930]:

$$C10 = 1/(C2*C6) \qquad C11 = -1/(C4*C6) + Lx/(C2*C6)$$

$$C12 = Yr/(C2*C6) - \theta r/(C4*C6) \quad (2.46)$$

Inspection of equations (2.18), (2.21), (2.37) and (2.39) show that C7, C8, C9, and C11 have additional terms with offset Lx. These are calculated for each component and summed [line 3930]. The external loads Mo and Vo are added to C9 and C12 respectively, [line 3950], and the resulting simultaneous equations are solved as before, equations (2.27) and (2.28). The junction displacements θj and Yj, at the ring centroid, are calculated by equations (2.32) and (2.33), [lines 3970 and 3990]. The discontinuity loads Vj and Mj are calculated by equations (2.37) and (2.38), [lines 4040 and 4050].

2.2.5 Worked Example

To show the working of the junction analysis, a hand calculation example is now presented in detail. FIGURE 2.8 shows a cylinder 500mm radius and 15mm thick connected to a compact ring 30mm by 30mm square. The cylinder is subjected to an internal pressure of 3 N/mm^2 and is at a mean temperature 50°C higher than ambient. The ring is at ambient temperature of 0°C and is subjected to a radial force of 250 N/mm circumference inwards and a moment of 15000 Nmm/mm circumference clockwise. The material properties are Young's modulus 200000 N/mm^2, Poisson's ratio 0.3 and the coefficient of thermal expansion is 0.000012mm/mm°C.

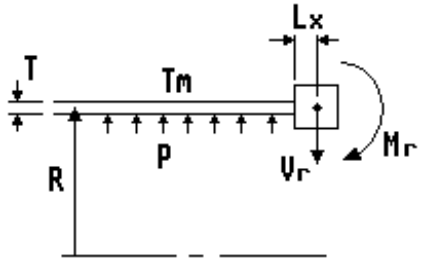

FIGURE 2.8 Worked example, cylinder and compact ring subjected to loading

(1) The component numbering is now defined. There are only two components involved. The cylinder is made component No.1 and the ring, being the last component, is made component No.2. The actual junction between the cylinder and ring is offset from the centroid of the ring by Lx = -15mm.

(2) The free displacements of each component, at the junction, is now calculated. The sign convention of FIGURE 2.3 is followed.

For the cylinder (component 1) with a pressure end load:

Yf_1 due to internal pressure = $P*R^2(1 - \mu/2)/(E*T)$ = 0.2125 mm outward

θf_1 due to internal pressure the meridional rotation is zero.

Yf_1 due to thermal expansion = $R*\alpha*Tm$ = 0.3 mm outward

θf_1 due to thermal expansion the meridional rotation is zero.

The total displacements for the cylinder become:

Yf_1 due to pressure and expansion = 0.5125mm

$\theta f_1 = 0$

For the ring (component 2), the loads Vr = 250 N/mm and Mr = 15000 Nmm/mm could be applied as external loads Vo and Mo. However in order to show the method of working the loads will be introduced at this stage by calculating the free displacements.

The centroid radius, Rc = 500 mm
The cross section area, $AR = 30^2 = 900$ mm^2
The second moment of area, $I_{NA} = 30*30^3/12 = 67500$ mm^4
The distance to the extreme fibre, C = 15 mm
The section modulus, $D = I_{NA}/|C| = 4500$ mm^3

The displacements at the ring centroid become:

$Yf_2 = -Vr*Rc^2/(E*AR) = -0.3472$ mm inwards

$\theta f_2 = -Mr*Rc^2/(E*D*|C|) = -0.27778$ radians clockwise

As the junction is offset from the ring centroid, we need to allow for the rotation of the ring when calculating the deflection at the junction.

Yf at the junction = Yf at the centroid + $\theta f*Lx$

$Yf_2 = -0.3472 + (-0.27778*(-15)) = 3.8195$ mm outward

(3) The free displacements relative to the last component are now calculated by equation (2.2).

For the cylinder (component 1):

$Yr_1 = (Yf_1 – Yf_2) = 0.5125 - 3.8195 = -3.307$ mm inwards relative to the last component (the ring).

$\theta r_1 = (\theta f_1 - \theta f_2) = 0 - (-0.27778) = 0.27778$ radians anti-clockwise [Corrected, was $\theta r_1 = (\theta r_1 - \theta r_2)$] relative to the last component (the ring).

For the ring (component 2) the relative free displacements are zero as the ring is the last component.

$$Yr_2 = \theta r_2 = 0$$

Junction analysis

FIGURE 2.9 diagrammatically shows the free displacements relative to the ring, i.e. if we imagine ourselves to be on the ring at the junction with the cylinder, we would see the cylinder move inward by 3.307mm and rotate by 0.27778 radians anti-clockwise. The fact that there are non-zero displacements relative to the ring indicates that there is a discontinuity at the junction.

Yr = -3.307 mm inward
θr = 0.27778 radians anti-clockwise [Corrected, was θj]

FIGURE 2.9 Free displacements of the cylinder relative to the ring

(4) The stiffness coefficients are now calculated. These coefficients are loads per unit circumference per unit displacement and are discussed in more detail in section 2.3.

For the cylinder (component 1) at the junction end:

The shell characteristic, $\beta = [3(1- \mu^2)/(R^2T^2)]^{1/4} = 0.0148426$ /mm
The flexural rigidity, $D = E*T^3/(12(1 - \mu^2)) = 61813187.0$ Nmm

$K(1,1) = 2*D*\beta^3 = 404.242$ (N/mm circumf.)/mm radial deflection

$K(2,1) = 2*D*\beta^2 = 27235.23$ (Nmm/mm circumf.)/mm radial deflection

$K(3,1) = 2*D*\beta^2 = 27235.23$ (N/mm circumf.)/radian

$K(4,1) = D*\beta = 917468.41$ (Nmm/mm circumf.)/radian

For the ring (comp. 2) at its centroid: AR=900 mm^2, D=4500 mm^3, |C|=15 mm

$K(1,2) = E*AR/Rc^2 = 720.0$ (N/mm circumf.)/mm radial deflection

K(2,2) = 1E15 (Nmm/mm circumf.)/mm radial deflection

K(3,2) = 1E15 (N/mm circumf.)/radian

$K(4,1) = E*D*|C|/Rc^2 = 54000$ (Nmm/mm circumf.)/radian

(5) The flexibilities, equation (2.6), are now calculated. It is at this point that the handing of the junction is introduced. The cylinder has the junction at its right end therefore factor Fc=+1. The compact ring has a factor Fc = -1 as the ring (and flat plates) have all been formulated as left end junctions in the program.

For the cylinder (component 1):

C1 = -1/K(1,1) = -0.002473766 mm/(N/mm circumf.)

C2 = 1/K(2,1) = 0.000036717 mm/(Nmm/mm circumf.)

C3 = -Fc/K(3,1) = -0.000036717 radians/(N/mm circumf.)

C4 = Fc/K(4,1) = 1.0899558E-6 radians/(Nmm/mm circumf.)

For the ring (component 2):

C1 = -1/K(1,2) = -0.00138889 mm/(N/mm circumf.)

C2 = 1/K(2,2) = 1E-15 mm/(Nmm/mm circumf.)

C3 = -Fc/K(3,2) = 1E-15 radians/(N/mm circumf.)

C4 = Fc/K(4,2) = -0.000018519 radians/(Nmm/mm circumf.)

(6) The terms C5 and C6 are calculated by equations (2.12) and (2.17).

For the cylinder (component 1):

C5 = (C2/C1 - C4/C3) = 0.0148428 N/Nmm

C6 = (C1/C2 - C3/C4) = -33.68717 Nmm/N

For the ring (component 2):

C5 = (C2/C1 - C4/C3) = 1.8519E10 N/Nmm

C6 = (C1/C2 - C3/C4) = -1.38889E12 Nmm/mm

(7) The terms C7 to C12 are now calculated by equations (2.43) and (2.46). At this point the free displacements and any offset distance Lx, from the ring centroid to the junction with the shell, is introduced.

For the cylinder (component 1). The offset distance Lx = -15 mm and free displacements are Yr = -3.307 mm and θr = 0.27778 radians.

C7 = {-Fc/(C1*C5) + Lx/(C2*C6)} = 39362.11 (Nmm/mm)/mm radial deflection

C8 = {Fc/(C3*C5) - Fc*Lx/(C1*C5) - Lx/(C4*C6) + Lx*Lx/(C2*C6)} = -2833879.53 (Nmm/mm)/radian

C9 = Yr{-Fc/(C1*C5) + Lx/(C2*C6)} + θr{Fc/(C3*C5) - Lx/(C4*C6)} = -753355.44 Nmm/mm circumf.

C10 = 1/(C2*C6) = -808.47 (N/mm)/mm radial deflection

C11 = -1/(C4*C6) + Lx/(C2*C6) = 39362.11 (N/mm circumference)/radian

C12 = Yr/(C2*C6) - θr/(C4*C6) = 10238.96 N/mm circumference

For the ring (component 2) the relative free displacements Yr and θr are zero as the ring is the last component. The offset distance Lx is always set to zero for the ring.

C7 = -Fc/(C1*C5) = -3.8879E-8 (Nmm/mm circumf.)/mm radial deflection

C8 = Fc/(C3*C5) = -53998.59 (Nmm/mm circumf.)/radian

C9 = 0 Nmm/mm circumference

C10 = 1/(C2*C6) = -720.0 (N/mm circumf.)/mm radial deflection

C11 = -1/(C4*C6) = -3.8879E-8 (N/mm circumf.)/radian

C12 = 0 N/mm circumference

(8) The terms C7 to C12 calculated for each component are now summed.

ΣC7 = 39362.11 + (-3.8879E-8) = 39362.11 (Nmm/mm)/mm radial deflection

Junction analysis

$\Sigma C8 = -2833879.53 + (-53998.59) = -2887878.12$ (Nmm/mm)/radian

$\Sigma C9 = -753355.44 + 0 = -753355.44$ Nmm/mm circumference

$\Sigma C10 = -808.47 + (-720.0) = -1528.47$ (N/mm)/mm radial deflection

$\Sigma C11 = 39362.11 + (-3.8879E-8) = 39362.11$ (N/mm)/radian

$\Sigma C12 = 10238.96 + 0 = 10238.96$ N/mm circumference

(9) Any applied external loads Mo and Vo are now added to the $\Sigma C9$ and $\Sigma C12$ respectively. Note that terms C7 to C12 are loads per unit circumference. In this example Mo and Vo are both zero as we chose to apply the moment Mr and radial force Vr directly to the ring and hence calculate the free displacements of the ring.

$\Sigma C9 = \Sigma C9 + Mo = \Sigma C9 + 0 = -753355.44$ Nmm/mm circumference
[Corrected, was $\Sigma C9 = \Sigma C9 + Mo = \Sigma C9 = 0 = -753355.44$ Nmm/mm circumference]

$\Sigma C12 = \Sigma C12 + Vo = \Sigma C12 + 0 = 10238.96$ N/mm circumference

(10) The final junction displacements (at the ring centroid) are now calculated by substituting the summation terms C7 to C12 into equations (2.32) and (2.33).

$\theta j = (C9/C7 - C12/C10)/(C8/C7 - C11/C10) = 0.26127$ radians anti-clockwise

$Yj = (C9/C8 - C12/C11)/(C7/C8 - C10/C11) = 0.0296$ mm outward

Note that these junction displacements are the sum of the free displacements relative to the last component and the displacements due to the discontinuity loads, refer to equation (2.1). They are *not* the actual component displacements these are calculated later by the component analysis, once the junction analysis is complete. Since the relative free displacements of the last component are zero, the junction displacements θj and Yj are the displacements due to the discontinuity loads acting on the last component. If the last component is a compact ring then the junction displacements refer to the centroid of the ring.

(11) The junction discontinuity moments and forces are now calculated from equations (2.37) and (2.38) for each component. Values of Yj and θj are the junction displacements just calculated above. The values of C1 to C6, Yr, θr and Lx are applicable only for the component under consideration.

$$Mj = (Yj + \theta j*Lx - Yr)/(C1*C5) - (\theta j - \theta r)/(C3*C5)$$

$$Vj = (Yj + \theta j*Lx - Yr)/(C2*C6) - (\theta j - \theta r)/(C4*C6)$$

For the cylinder (component 1): Yr = -3.307 mm, $\theta r = 0.27778$ radians and Lx = -15 mm.
At the junction with the ring.

meridional moment, $Mj_1 = -14427.98$ Nmm/mm circumf. clockwise
radial force, $Vj_1 = 21.31$ N/mm circumf. inward

For the ring (component 2): Yr = 0, $\theta r = 0$ and Lx = 0. At the ring centroid.

moment, $Mj_2 = -14108.21$ Nmm/mm circumf. anti-clockwise
radial force, $Vj_2 = -21.31$ N/mm circumf. outward

FIGURE 2.10 shows the loads applied to their respective components.

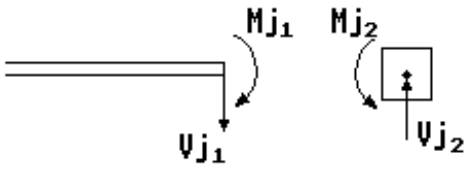

Mj_1 = -14427.98 Nmm/mm circumference at the cylinder junction end
Vj_1 = 21.31 N/mm circumference at the cylinder junction end
Mj_2 = -14108.21 Mmm/mm circumference at the ring centroid
Vj_2 = -21.31 N/mm circumference at the ring centroid

FIGURE 2.10 Discontinuity loads acting at each component

The above calculations took several hours to prepare and check on a hand calculator. Readers who want to save some time can run the example on AJAP1. The input data set and junction results are given in FIGURE 2.11. The slight difference in the results is due to the difference in calculator and computer accuracy. In the days before electronic computers and calculators it was normal practice to carry out the above analysis with the aid of a slide rule.

INPUT DATA, PROGRAM AJAP1

Worked example
Various loads

COMPONENT No. 1
CYLINDER, JUNCTION AT RIGHT END
R= 500 mm
T= 15 mm
E= 200000 N/mm2
PR= .3
ALPHA= .000012 /degC
BETA= .0148426 /mm
D= 6.181319E+07 Nmm
P= 3 N/mm2
Fp= 750 N/mm
Fo= 750 N/mm
Tm= 50 degC

COMPONENT No. 2
COMPACT RING AT JUNCTION
Rl= 500 mm
Tl= 30 mm
Rr= 500 mm
Tr= 30 mm
L= 30 mm
Rc= 500 mm
AREA= 899.9999 mm2
Ina/C= 4499.997 mm3
C= 15 mm
Lx 1 = -15 mm
Lx 2 = -15 mm
Lx 3 = 0 mm
Lx 4 = 15 mm
Lx 5 = 15 mm
Lx 6 = 15 mm
Lx 7 = 0 mm
Lx 8 = -15 mm
Lx 9 = 0 mm
CONNECTION 1,
E= 200000 N/mm2
PR= .3
ALPHA= .000012 /degC
Mr= 15000 Nmm/mm
Vr= 250 N/mm

Mj 1 = -14428.29 Nmm/mm clockwise
Vj 1 = 21.31226 N/mm inward

at centroid
Mj 2 = -14108.53 Nmm/mm anti-clockwise
Vj 2 = -21.31477 N/mm outward

FIGURE 2.11 Input data set and results for the worked example discussed in section 2.2.5

2.3 THE STIFFNESS COEFFICIENTS

The junction analysis discussed in section 2.2 requires that four structural stiffness coefficients, K(1,i), K(2,i), K(3,i) and K(4,i), be calculated for each component. These stiffness coefficients are the "key" to the junction analysis and are the most convenient way to relate the load on a component to a displacement of the component.

The stiffness coefficients are loads per unit displacement, of the mean radius, at the junction end of the component (or of the centroid radius if the component is a compact ring). In some other text the coefficients are given as the inverse of the stiffness coefficient, i.e. a flexibility coefficient representing displacements per unit load. In general terms, whichever way the coefficients are presented they represent the *influence* in terms of a load (or a displacement) of a point on the component due to a *unit* displacement (or *unit* load) at some specified point on the component. Hence the coefficients are sometimes referred to as influence coefficients. In some cases (but not in this text) coefficients per unit pressure are also considered.

At this stage it is necessary to consider the units of the loading to be applied. As explained in the introduction the loading in this text is formulated as loads per unit circumference, this is an arbitrary choice. The physical representation of the stiffness coefficients, at the edge of a shell, are best seen by reference to FIGURE 2.12. If we imagine the shell edge to be loaded by each of the stiffness coefficients in turn, then the four coefficients can be defined as follows:

K(1,i) is the radial force per unit circumference that is required to move the junction end by a unit radial deflection of the circumference.

K(2,i) is the meridional moment per unit circumference that is required to move the junction end by a unit radial deflection of the circumference.

K(3,i) is the radial force per unit circumference that is required to rotate the tangent to a meridian, at the junction end, by one radian.

K(4,i) is the meridional moment per unit circumference that is required to rotate the tangent to a meridian, at the junction end, by one radian.

Where i is the component number (1 to n) under consideration.

For a flat plate the coefficients refer to the outer or the inner edge as shown in FIGURE 2.13. For a compact ring the coefficients refer to the centroid radius as shown in FIGURE 2.14.

The coefficients are calculated for the components listed in TABLE 2.1. It is not intended to derive the coefficients from first principles as they can be obtained from several references. Within the program the coefficients are held in a two dimensional array K(4,n), [lines 3640 - 3670]. The values calculated can be overwritten, [lines 3770 - 3790], so that other geometries outside the scope of the current text may be allowed for.

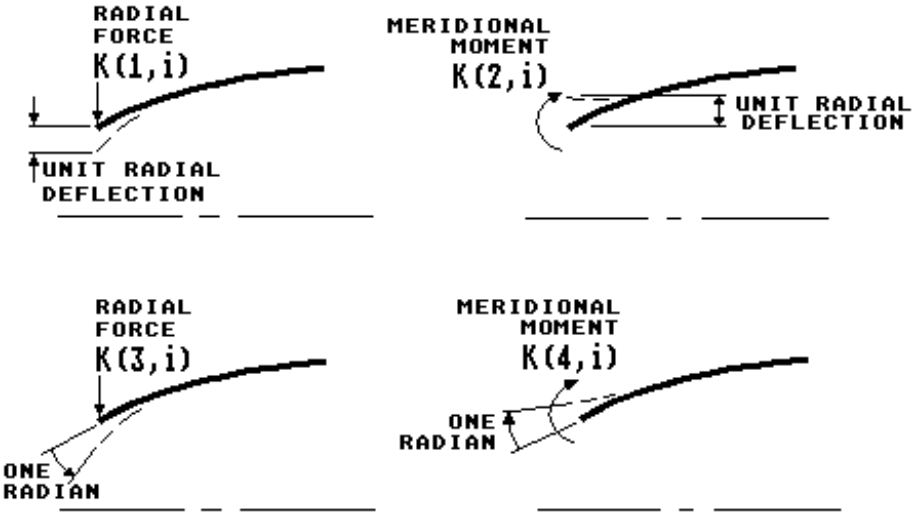

FIGURE 2.12 Stiffness coefficients, loads per unit circumference per unit displacement of a shell

Stiffness coefficients

The coefficients depend upon the component geometry, the material properties and the loading and are now quoted for the particular component type being considered.

2.3.1 Cylinder Coefficients [line 4830]

These are based on well known relationships found in several textbooks:

$$K(1,i) = 2*D*\beta^3$$
$$K(2,i) = 2*D*\beta^2$$
$$K(3,i) = 2*D*\beta^2 \qquad (2.47)$$
$$K(4,i) = D*\beta$$

where [line 2010] $D = E*T^3/(12(1 - \mu^2))$ (2.48)

and [line 2010] $\beta = [3(1-\mu^2)/(R^2T^2)]^{1/4}$ (2.49)

The flexural rigidity (or plate stiffness) D has units of force*length and is similar to the flexural stiffness EI well known in beam theory. This derives from the second moment of area for a rectangular beam, where $I = bd^3/12$. For a unit circumference of a cylinder b = 1 and d = the thickness T, therefore $I = T^3/12$. The stiffness of plates and shells is stiffer than a beam by the ratio $1/(1 - \mu^2)$. Hence the flexural rigidity for plates and shells becomes $EI = D = E*T^3/(12(1 - \mu^2))$.

For cylindrical shells β is known as the shell characteristic and has units of length^{-1}, for other shells it has no units. It derives from the theory of beams on elastic foundation where $\beta = (k/(4EI))^{1/4}$. For a cylindrical shell, k is the foundation modulus = $E*T/R^2$ and EI is the flexural rigidity D. Therefore by substitution $\beta = [3(1 - \mu^2)/(R^2T^2)]^{1/4}$.

The shell characteristic is useful for establishing if the cylinder is long or short and is used in the "rule of thumb", discussed in section 1.3.1 in deciding if points on the shell are remote from each other.

2.3.2 Spherical Shell Coefficients [line 4980]

The coefficients are based on HETÉNYI'S approximation II (ref. 12).

$$K(1,i) = E*T*K1/(Rs*\beta*(1+K1*K2)*SIN^2\phi)$$
$$K(2,i) = E*T*K1/(2*\beta^2 SIN\ \phi)$$
$$K(3,i) = E*T*K1/(2*\beta^2 SIN\ \phi) \qquad (2.50)$$
$$K(4,i) = E*T*Rs*K1/(4*\beta^3)$$

where [line 2020] $\beta = [3(1 - \mu^2)*(Rs/T)^2]^{1/4}$ (note no units) (2.51)

and [line 4970] $K1 = 1 - (1 - 2*\mu)/(2*\beta*TAN\ \phi)$ (2.52)

$$K2 = 1 - (1 + 2*\mu)/(2*\beta*TAN\ \phi)$$

2.3.3 Cone Coefficients [lines 5260 - 5430]

The coefficients are based on the work by C.E. TAYLOR (ref. 28).

$$K(1,i) = E*T*\phi_1/[Rj*(U2*\phi_{16}*COS(\phi)/(T*\beta_A) - \mu*\phi_8*SIN(\phi))]$$
$$K(2,i) = E*T^2\phi_1/(Rj*U2*\phi_{14})$$
$$K(3,i) = E*T^2\phi_1/(Rj*U2*\phi_9) \qquad (2.53)$$
$$K(4,i) = E*T^3XI_A*SIN(\phi)*\phi_1/(2*2^{1/2}U4*Rj*\phi_7)$$

where [line 5260] $U4 = 12(1 - \mu^2)$ and $U2 = (U4)^{1/2}$ (2.54)

and the cone shell parameter at the edge (R = Rj) is [line 5270]: $XI_A = 2*LAMBDA*(Rj/SIN\ \phi)^{1/2}$ (2.55)

where [line 5260] $LAMBDA = [U4/(T^2*TAN^2\phi)]^{1/4}$ (2.56)

The other terms are defined in appendix 5 with reference to the notation used by TAYLOR in reference (28).

2.3.4 Flat Plate Coefficients

The coefficients refer to the inside and outside edge of the plate as shown in FIGURE 2.13. The coefficients are based on the well known theory of circular plates given in several texts. For a junction on the centre line of the plate, FIGURE 2.13(a) and (b), the coefficients are as follows:

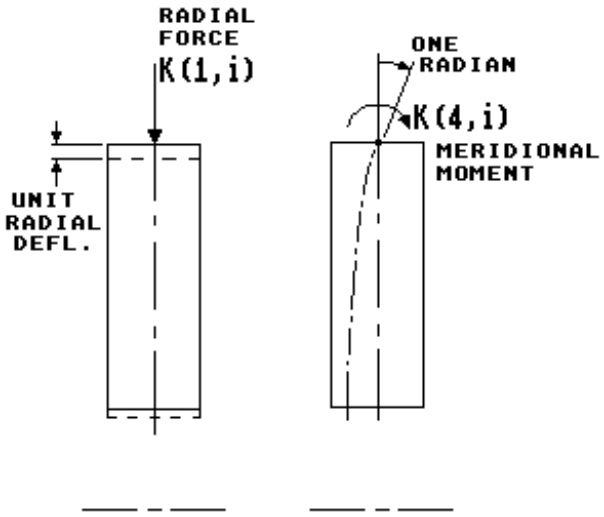

FIGURE 2.13(a) Stiffness coefficients, loads per unit circumference per unit displacement at the outside edge of a flat plate

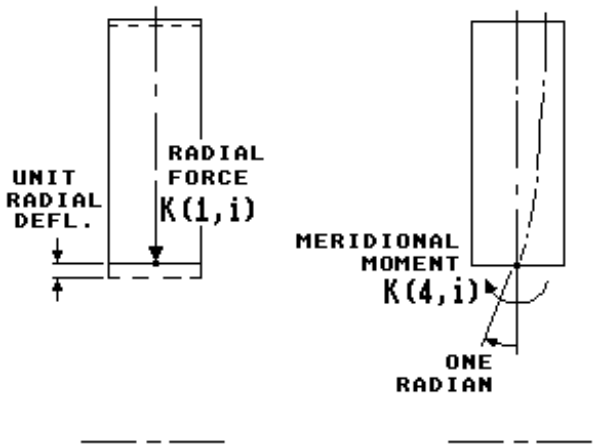

FIGURE 2.13(b) Stiffness coefficients, loads per unit circumference per unit displacement at the inside edge of a flat plate

(1) For a junction at the *outside* radius

If the inside radius is zero, then Ri = 0 and the coefficients become [line 5920]:

$$K(1,i) = E*T/(Ro(1 - \mu))$$
$$K(4,i) = D(1 + \mu)/Ro \quad (2.57)$$

Stiffness coefficients

If the inside radius, Ri is > 0 the coefficients are [line 5950]:

$$K(1,i) = E*T/\{Ro[(Ro^2 + Ri^2)/(Ro^2 - Ri^2) - \mu]\}$$
$$K(4,i) = D*C7/(Ro*C4) \qquad (2.58)$$

where [line 2040] $D = E*T^3/(12(1 - \mu^2))$ (2.59)

[line 5930] $C4 = [(1+ \mu)Ri/Ro + (1 - \mu)Ro/Ri]/2$

[line 5940] $C7 = (1 - \mu^2)*(Ro/Ri - Ri/Ro)/2$ (2.60)

(2) For a junction at the *inside* radius [line 5960]

$$K(1,i) = E*T/\{Ri[(Ro^2 + Ri^2)/(Ro^2 - Ri^2) + \mu]\}$$
$$K(4,i) = D(1 + \mu)*[1 - (Ro/Ri)^2]/\{Ri[1+ (1+ \mu)*(Ro/Ri)^2/(1 - \mu)]\} \qquad (2.61)$$

When the junction is on the plate centre line there are no freedoms for coefficients K(2,i) and K(3,i) and these default to a large stiffness value [line 5970]. Most practical structures have the connection at the plate surface rather than at the centre line. A modification to the stiffness coefficients K(1,i), K(2,i) and K(3,i) is required to cater for this situation.

With reference to FIGURE 2.13(c), an option is included in the program which allows for a $\pm$ offset distance from the plate centre line by specifying a junction position.

The junction position is defined as:

$$JP = 2*\text{offset distance}/T \qquad (2.62)$$

The offset is positive to the right of the plate centre line and negative to the left, i.e. for a junction position at the surface, the offset distance is $\pm T/2$. Therefore JP = +1 represents a junction at the right surface or -1 for a junction at the left surface. If the junction is on the plate centre line then JP=0.

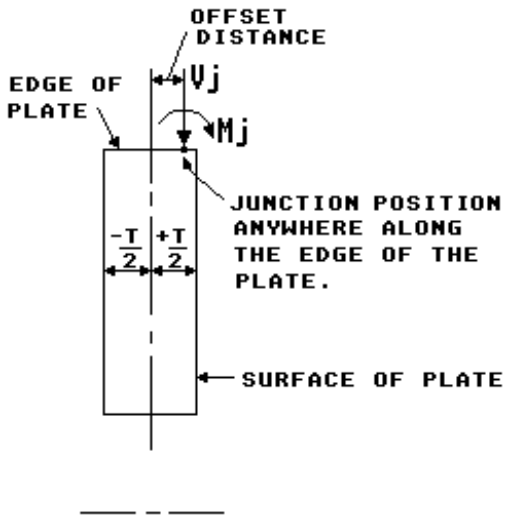

FIGURE 2.13(c) Flat plate with junction offset from the plate centre line

The displacements of the plate junction now become:

$$Y = -Vj\{1/K(1,i) + JP^2T^2/(4*K(4,i))\} - Mj*JP*T/(2*K(4,i))$$
$$\theta = -Vj*JP*T/(2*K(4,i)) - Mj/K(4,i) \qquad (2.63)$$

and the final plate coefficients now become [line 5980]:

$$K(1,i) = 1/\{1/K(1,i) + JP^2T^2/(4*K(4,i))\}$$

$$K(2,i) = -2*K(4,i)/(JP*T)$$

$$K(3,i) = -2*K(4,i)/(JP*T) \qquad (2.64)$$

$$K(4,i) \text{ is unchanged.}$$

The -ve sign for K(2,i) and K(3,i) are a result of the sign convention chosen for the displacements and the arbitrary decision to formulate the flat plates as left end components. When the junction position is to the right of the plate mid-thickness, K(2,i) and K(3,i) require a -ve sign so that the displacement sign convention of FIGURE 2.3 is maintained.

2.3.5 Compact Ring Coefficients [line 7080]

These are based on well known relationships for a ring subjected to a radial force and a moment acting at the centroid as shown in FIGURE 2.14.

$$K(1,i) = E*AR/Rc^2$$

$$K(4,i) = E*D*C/Rc^2 \qquad (2.65)$$

where Rc = centroid radius
AR = cross section area of the ring
D = section modulus $I_{NA}/|C|$
C = distance to the extreme fibre

The default properties Rc, AR, C and D are discussed in section 2.4.5. There are no freedoms for coefficients K(2,i) and K(3,i) and these default to a large stiffness value [line 7080].

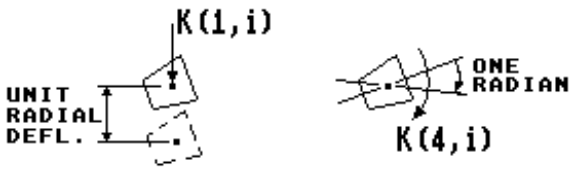

FIGURE 2.14 Stiffness coefficients for a compact ring

2.4 THE COMPONENT ANALYSIS

Once the junction analysis is complete all the loads necessary to analyse each individual component are available. The components can be analysed as separate items loaded with the junction discontinuity loads Vj and Mj plus any other applied loads, e.g. pressure, temperature, axial end load, centrifugal force etc.

The results can be obtained at the junction end or at any valid section away from the junction as shown in FIGURE 2.15. For the compact ring the stress results are listed for 9 points on the ring as discussed in section 2.4.5.

The governing equations for displacements, forces and moments and stresses are now presented for each component in terms of the section position from the junction. It is not intended to derive the equations as they are based on simple theory, well known relationships or specific references.

Program line numbers are given for cross reference in brackets [ ]. The stresses at a section are derived from the forces and moments V, N1, N2, M1 and M2 acting at that section as a result of the applied loading.

The positive directions of these forces and moments, acting on a small element at a section across the thickness of a shell, are shown in FIGURE 2.16. In some text these forces and moments are called *stress resultants*, but note that this terminology can be misleading as they do *not* have units of stress but units of force or moment per unit circumference. Stresses are calculated by applying equations (2.74) to (2.78).

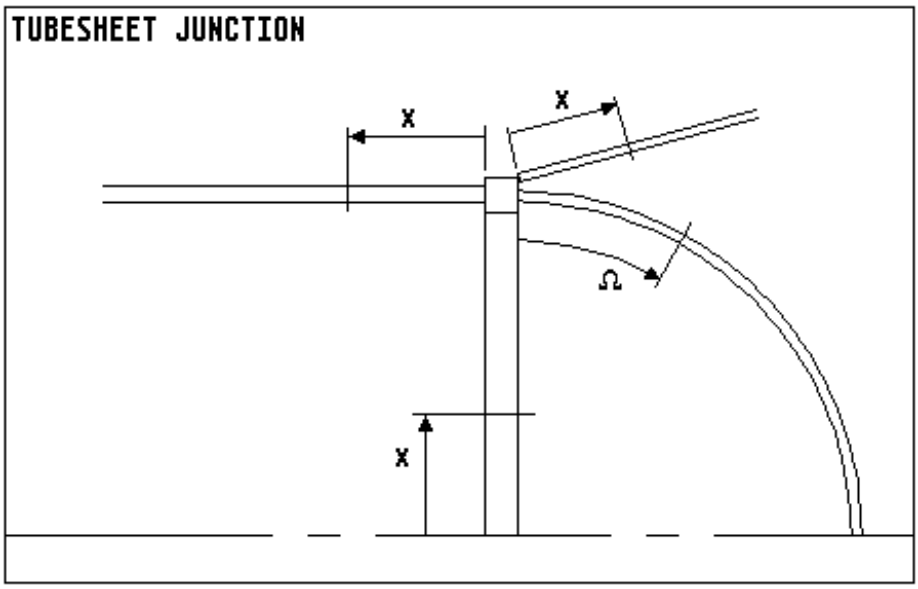

FIGURE 2.15 Component analysis, results can be obtained at the junction or any valid section away from the junction

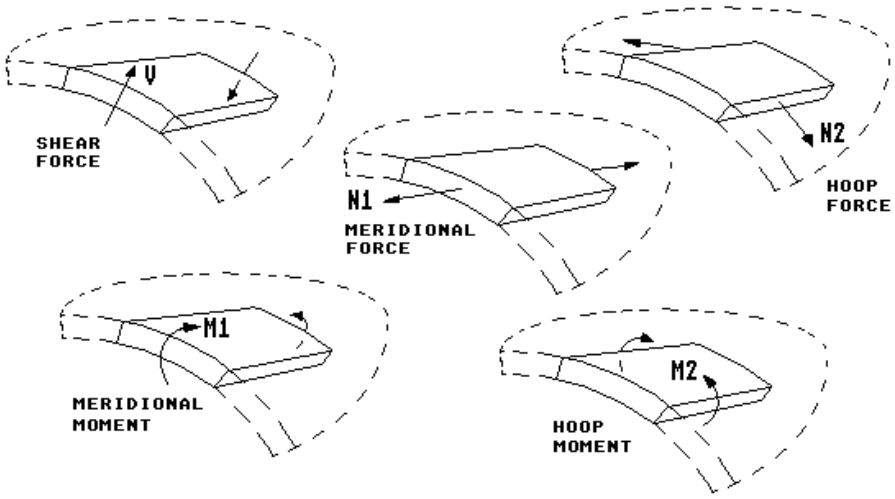

Shear force per unit circumference. +ve outward (to the right for a flat plate)

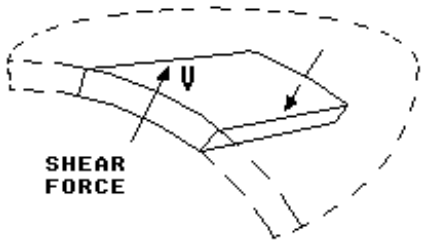

Meridional membrane force per unit circumference. +ve tensile.

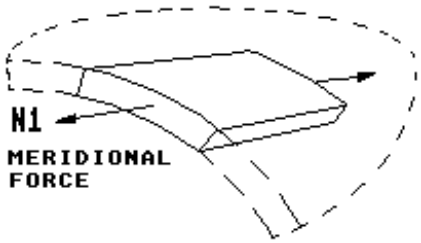

Hoop (circumferential) membrane force per unit circumference. +ve tensile.

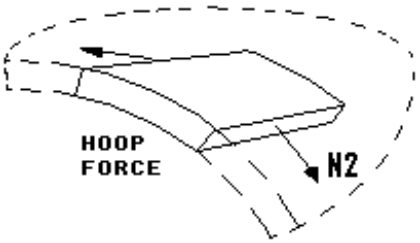

Meridional bending moment per unit circumference. +ve if it produces compression on the outside surface (the left surface if a flat plate).

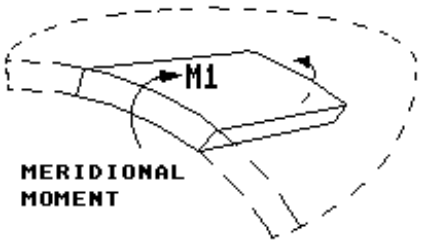

Hoop bending moment per unit circumference. +ve if it produces compression on the outside surface (the left surface if a flat plate).

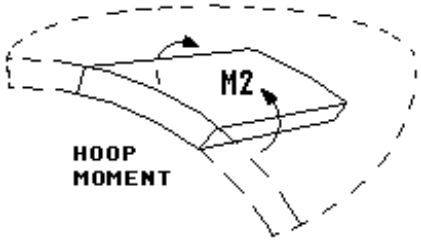

FIGURE 2.16 Positive direction of forces and moments (stress resultants) acting on a small element at a section across the component thickness

Component analysis

2.4.1 Cylindrical Shells [program lines 4870 to 4930]

The results for any distance X from the junction end can be obtained. X = 0 is at the junction end. If the cylinder is connected to a compact ring, X is from the connection point, refer to FIGURE 2.15. Note that $Z = \beta X$ is used for a cylindrical shell.

(1) Radial deflection, +ve outward.

$$\begin{aligned} Y = & -Vj*e^{-Z}COS(Z)/(2*D*\beta^3) \\ & -Mj*e^{-Z}[SIN(Z) - COS(Z)]/(2*D*\beta^2) \\ & +P*R^2(1 - \mu/2)/(E*T) \\ & -F_{AX}*\mu*R/(E*T) + R*\alpha*(Tm-Ta) \\ & +Md*(2\pi RPS)^2R^3/E \end{aligned} \qquad (2.66)$$

(2) Rotation of a tangent to the meridian, radians, +ve anti-clockwise.

$$\begin{aligned} \theta = & Vj*e^{-Z}[COS(Z) + SIN(Z)]/(2*D*\beta^2) \\ & -Mj*e^{-Z}COS(Z)/(D*\beta) \\ & -R*\alpha*Gj \end{aligned} \qquad (2.67)$$

(3) Transverse shear force, +ve outward.

$$V = -Vj*e^{-Z}[COS(Z) - SIN(Z)] - 2*Mj*\beta*e^{-Z}SIN(Z) \qquad (2.68)$$

(4) Meridional membrane force, +ve tensile.

$$N1 = F_O = P*R/2 + F_{AX} \qquad (2.69)$$

(5) Hoop (circumferential) membrane force, +ve tensile. Note that here the radial deflection, Y is due to loads Vj and Mj only.

$$N2 = P*R + Y*E*T/R + Md*(2\pi RPS)^2R^2T \qquad (2.70)$$

(6) Meridional bending moment, +ve if compression on outside.

$$M1 = -Vj*e^{-Z}SIN(Z)/\beta + Mj*e^{-Z}[COS(Z) + SIN(Z)] \qquad (2.71)$$

(7) Hoop bending moment, +ve if compression on outside.

$$M2 = \mu*M1 \qquad (2.72)$$

The thermal moment due to a temperature difference across the thickness is calculated by equation (2.73) and added to M1 and M2 [line 4780].

$$\text{Thermal moment} = -E*\alpha*dT*T^2/(12(1 - \mu)) \qquad (2.73)$$

Stresses are now calculated from the loads given by equations (2.68) to (2.73) [line 4790]. The stresses are positive tensile and negative compressive. Shear stresses are positive if the shear force is positive.

(8) Meridional membrane stress, $SL = N1/T$ (2.74)

(9) Hoop membrane stress, $SH = N2/T$ (2.75)

(10) Meridional bending stress, $SBL = -6*M1/T^2$ (2.76)

(11) Hoop bending stress, $SBH = -6*M2/T^2$ (2.77)

(12) Average Shear Stress, +ve if V is +ve. $SV = V/T$ (2.78)

The membrane plus bending stresses at the surface of the shell are calculated by summing the membrane and bending stresses [line 4790].

$$\begin{aligned} &\text{Meridional stress (outside surface),} && SLo = SL + SBL \\ &\text{Meridional stress (inside surface),} && SLi = SL - SBL \\ &\text{Hoop stress (outside surface),} && SHo = SH + SBH \\ &\text{Hoop stress (inside surface),} && SHi = SH - SBH \end{aligned} \qquad (2.79)$$

2.4.2 Spherical Shells [lines 5020 to 5220]

The analysis of spherical shells is based upon HETÉNYI's approximation II (ref. 12). Note however that a typographical error in reference (12) has been corrected (the shell characteristic was missing from the numerator for N2). TIMOSHENKO (ref. 13) quotes the correct expressions. In order to use the results of reference (12) it is necessary to derive four integration constants, i.e. two constants of integration for each of the loads Vj and Mj. The details of the derivation are given in section 2.4.2(9).

Results are for any angle OMEGA Ω degrees between limits $0 =< \Omega < \phi$. Where $\Omega = 0$ is at the junction end. The results tend to break down as Ω approaches the half arc angle ϕ. If the shell is connected to a compact ring then Ω is from the connection point, refer to FIGURE 2.15. Note that $Z = \beta\Omega$ is used for spherical shells and Rs is the mean spherical radius.

(1) Radial deflection, +ve outward.

$$\begin{aligned} Y = {} & Cv*Rs*\beta*K3*SIN(\phi - \Omega)*[COS(Z + \S) - K2*SIN(Z + \S)]/(E*T) \\ & +Cm*Rs*\beta*K3*SIN(\phi - \Omega)*[COS(Z) - K2*SIN(Z)]/(E*T) \\ & +P*Rs^2(1 - \mu)SIN(\phi - \Omega)/(2*E*T) \\ & -F_{AX}*Rs*(1 + \mu)SIN(\phi)/(E*T*SIN(\phi - \Omega)) \\ & +Rs*\alpha*(Tm - Ta)SIN(\phi - \Omega) \\ & +Md*(2\pi RPS)^2(Rs*SIN(\phi - \Omega))^3/E \end{aligned} \qquad (2.80)$$

where:
$$\begin{aligned} K1 &= 1 - (1 - 2*\mu)/(2*\beta*TAN(\phi - \Omega)) \\ K2 &= 1 - (1 + 2*\mu)/(2*\beta*TAN(\phi - \Omega)) \\ K3 &= e^{-Z}/(SIN(\phi - \Omega))^{1/2} \end{aligned} \qquad (2.81)$$

and Cv, Cm and § are constants of integration derived in section 2.4.2(9) below.

(2) Rotation of a tangent to the meridian, radians +ve anti-clockwise.

$$\begin{aligned} \theta = {} & -Cv*2*\beta^2K3*COS(Z + \S)/(E*T) \\ & -Cm*2*\beta^2K3*COS(Z)/(E*T) \\ & -Rs*\alpha*Gj \qquad \text{[Corrected was } -Rs*\alpha*Gj*SIN\ \phi\text{]} \\ & -Md*(2\pi RPS)^2Rs^2SIN(\phi - \Omega)*COS(\phi - \Omega)*(3 + \mu)/E \end{aligned} \qquad (2.82)$$

(3) Transverse shear force, +ve outward.

$$V = -Cv*K3*SIN(Z + \S) - Cm*K3*SIN(Z) \qquad (2.83)$$

(4) Meridional membrane force, +ve tensile.

$$\begin{aligned} N1 = {} & -Cv*K3*SIN(Z + \S)/TAN(\phi - \Omega) \\ & -Cm*K3*SIN(Z)/TAN(\phi - \Omega) \\ & +P*Rs/2 \\ & +F_{AX}*SIN(\phi)/SIN^2(\phi - \Omega) \end{aligned} \qquad (2.84)$$

(5) Hoop membrane force, +ve tensile

$$\begin{aligned} N2 = {} & Cv*\beta*K3[2*COS(Z + \S) - (K1 + K2)SIN(Z + \S)]/2 \\ & +Cm*\beta*K3[2*COS(Z) - (K1 + K2)SIN(Z)]/2 \\ & +P*Rs/2 \\ & -F_{AX}*SIN(\phi)/SIN^2(\phi - \Omega) \\ & +Md*(2\pi RPS)^2(Rs*SIN(\phi - \Omega))^2T \end{aligned} \qquad (2.85)$$

(6) Meridional bending moment, +ve if compression on the outside

$$\begin{aligned} M1 = {} & Cv*Rs*K3[K1*COS(Z + \S) + SIN(Z + \S)]/(2*\beta) \\ & + Cm*Rs*K3[K1*COS(Z) + SIN(Z)]/(2*\beta) \end{aligned} \qquad (2.86)$$

(7) Hoop bending moment, +ve if compression on the outside

$$\begin{aligned} M2 = {} & Cv*Rs*K3\{[(1 + \mu^2)(K1 + K2) - 2*K2]COS(Z + \S) + 2*\mu^2SIN(Z + \S)\}/(4*\mu*\beta) \\ & +Cm*Rs*K3\{[(1 + \mu^2)(K1 + K2) - 2*K2]COS(Z) + 2*\mu^2SIN(Z)\}/(4*\mu*\beta) \end{aligned} \qquad (2.87)$$

(8) As for a cylinder, the thermal moment, equation (2.73), is added to M1 and M2 [line 4780] and the stresses are calculated by equations (2.74) to (2.79).

(9) The constants of integration Cv, Cm and § are derived from the boundary conditions as follows:

If we consider a radial force Vj acting at the end of the shell, as shown in FIGURE 2.17(a). At the end $\Omega = 0$ therefore Z = 0 and $K3 = 1/(SIN\ \phi)^{1/2}$ hence the meridional membrane force N1, from equation (2.84), can be written as:

$$N1 = -Cv*SIN(\S)/((SIN\ \phi)^{1/2}TAN\ \phi) \qquad (2.88)$$

the force N1 must equal $Vj*COS\ \phi$ therefore by rearrangement the constant of integration Cv must be:

$$Cv = -Vj*(SIN\ \phi)^{3/2}/SIN\ \S \qquad (2.89)$$

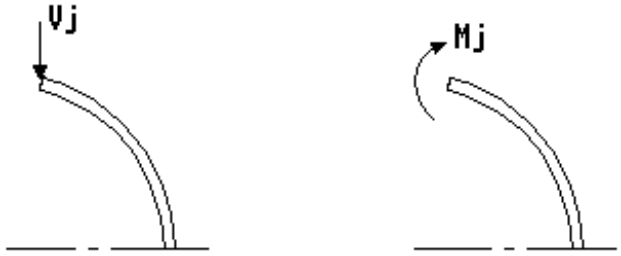

(a) (b)

FIGURE-2.17-Edge-loads-acting-on-a-spherical-shell

The constant of integration § is found by considering the meridional moment M1, which is zero at the end. From equation (2.86).

$$M1 = Cv*Rs*K3[K1*COS(Z + \S) + SIN(Z + \S)]/(2*\beta) = 0 \qquad (2.90)$$

Since $Cv*Rs*K3/(2*\beta)$ cannot be zero and since Z = 0 (as $\Omega = 0$ at the end), then [K1*COS § + SIN §] must be zero. Therefore:

$$\S = TAN^{-1}(-K1) \qquad (2.91)$$

The next two constants of integration are obtained by considering only a meridional bending moment Mj at the end of the shell, FIGURE 2.17(b). Equation (2.86) can be written:

$$M1 = Cm*Rs*K1/(2*\beta*(SIN\ \phi)^{1/2}) = Mj \qquad (2.92)$$

Therefore $Cm = Mj*2*\beta*(SIN\ \phi)^{1/2}/(Rs*K1)$ (2.93)

The constant of integration § associated with Cm is found by considering the shear force V, which is zero at the end. From equation (2.83) we write (including §):

$$V = -Cm*K3*SIN(Z + §) = 0 \quad (2.94)$$

Since Cm*K3 cannot be zero and as Z = 0 then § must be zero for all terms associated with Cm.

2.4.3 Conical Shells [lines 5470 to 5870]

The analysis of conical shells subjected to end loads Vj and Mj are based upon the work of C.E. TAYLOR (ref. 28). Appendix 5 contains a summary of the important terms used, together with a cross reference of the symbols used by TAYLOR in reference (28) compared to that used in "AJAP1".

Results can be obtained for values of distance X along the cone from the junction end. X = 0 is at the junction end. The results tend to break down as X approaches the apex. If the cone is connected to a compact ring then X is from the connection point, FIGURE 2.15.

The following terms are added to Y, θ, N1 and N2 at lines 5810 to 5870.

(1) Radial deflection, +ve outward

$$\begin{aligned} Y = &\ Y(\text{due to Vj and Mj}) \\ &+P*Rx^2(1 - \mu/2)/(E*T*COS\ \phi) \\ &-F_{AX}*\mu*Rj/(E*T*COS\ \phi) \\ &+Rx*\alpha*(Tm - Ta) \\ &+Md*(2\pi RPS)^2Rx^3/E \end{aligned} \quad (2.95)$$

(2) Rotation, radians +ve anti-clockwise. For a junction at the *large* end

$$\begin{aligned} \theta = &\ \theta\ (\text{due to Vj and Mj}) \\ &-3*P*Rx*TAN(\phi)/(2*E*T*COS\ \phi) \\ &+F_{AX}*Rj*TAN(\phi)/(E*T*Rx*COS\ \phi) \\ &-Rj*\alpha*Gj/COS\ \phi \\ &-Md*(2\pi RPS)^2Rx^2TAN(\phi)*(3 + \mu)/E \end{aligned} \quad (2.96)$$

For junction at the *small* end the terms containing P, F_{AX} and Md change sign.

(3) Meridional membrane force, +ve tensile

$$\begin{aligned} N1 = &\ N1(\text{due to Vj and Mj}) \\ &+P*Rx/(2*COS\ \phi) \\ &+F_{AX}*Rj/(Rx*COS\ \phi) \end{aligned} \quad (2.97)$$

(4) Hoop membrane force, +ve tensile

$$\begin{aligned} N2 = &\ N2(\text{due to Vj and Mj}) \\ &+P*Rx/COS(\phi) \\ &+Md*(2\pi RPS)^2Rx^2T \end{aligned} \quad (2.98)$$

(5) As for a cylinder, the thermal moment, equation (2.73), is added to M1 and M2 (due to Vj and Mj) [line 4780] and the stresses are calculated by equations (2.74) to (2.79).

2.4.4 Flat Plates

The analysis of flat plates subjected to point loads, pressure and temperature difference across the thickness are based on the well known theory of circular plates. It is not intended to detail the solution for the above loads as the theory is given in many text, e.g. references 13, 21 and 26. The equations for YL, θ, V, M1, M2 are detailed in lines 6020 to 7040. Results can be obtained for values of radius X between inside and outside radius inclusive.

Results for radial deflection and membrane forces due to internal pressure qi, external pressure qo, radial force Vj, radial temperature difference dTr and centrifugal force are also given. The results are based on the well known thick cylinder equations assuming that the plate is a disk.

(1) Radial deflection, +ve outward

For a junction at the *outside* radius and when the inside radius Ri >0 [lines 6550 and 6570 to 6590].

$$\begin{aligned} Y = {} & qi*X*Ri^2[(1 - \mu) + (1 + \mu)(Ro/X)^2]/(E(Ro^2 - Ri^2)) \\ & -(qo + Vj/T)*X*Ro^2[(1 - \mu) + (1 + \mu)(Ri/X)^2]/(E(Ro^2 - Ri^2)) \\ & +0.5*X*\alpha*dTr[f1]/Ln(Ro/Ri) \\ & +X*\alpha*(Tm - Ta) \\ & +Md*(2\pi RPS)^2X*(3 + \mu)(1 - \mu)[f4]/(8*E) \end{aligned} \qquad (2.99)$$

If the inside radius Ri = 0, then equation (2.99) reduces to [line 7000]:

$$\begin{aligned} Y = {} & -(qo + Vj/T)*X*(1 - \mu)/E \\ & +X*\alpha*(Tm - Ta) \\ & +Md*(2\pi RPS)^2(1 - \mu)*X*[(3 + \mu)Ro^2 - (1 + \mu)*X^2]/(8*E) \end{aligned} \qquad (2.100)$$

For a junction at the *inside* radius [lines 6560 to 6590].

$$\begin{aligned} Y = {} & (qi - Vj/T)*X*Ri^2[(1 - \mu) + (1 + \mu)(Ro/X)^2]/(E(Ro^2 - Ri^2)) \\ & -qo*X*Ro^2[(1 - \mu) + (1 + \mu)(Ri/X)^2]/(E(Ro^2 - Ri^2) \\ & +0.5*X*\alpha*dTr*[f1]/Ln(Ro/Ri) \\ & +X*\alpha*(Tm - Ta) \\ & +Md*(2\pi RPS)^2X*(3 + \mu)(1 - \mu)[f4]/(8*E) \end{aligned} \qquad (2.101)$$

where $[f1] = \{1 - Ln(Ro/X)(1 - \mu) - Ri^2Ln(Ro/Ri)[1 - \mu + (1 + \mu)(Ro/X)^2]/(Ro^2 - Ri^2)\}$

and $[f4] = [Ro^2 + Ri^2 + (1 + \mu)Ro^2Ri^2/((1 - \mu)*X^2) - (1 + \mu)*X^2/(3 + \mu)]$

(2) Meridional (radial) membrane force, +ve tensile

For junction at the *outside* radius and when the inside radius Ri >0 [Lines 6600, 6610 and 6650]

$$\begin{aligned} N1 = {} & -qi*T*Ri^2(Ro^2 - X^2)/(X^2(Ro^2 - Ri^2)) \\ & -(qo*T + Vj)*Ro^2(X^2 - Ri^2)/(X^2(Ro^2 - Ri^2)) \\ & +0.5*\alpha*E*T*dTr*[f2]/Ln(Ro/Ri) \\ & +Md*(2\pi RPS)^2(3 + \mu)[f5]*T/8 \end{aligned} \qquad (2.102)$$

where $[f2] = [-Ln(Ro/X) - Ri^2(1 - (Ro/X)^2)Ln(Ro/Ri)/(Ro^2 - Ri^2)]$

and $[f5] = [Ro^2 + Ri^2 - Ro^2Ri^2/X^2 - X^2]$

If the inside radius Ri = 0 then equation (2.102) reduces to equation (2.103) [Line 7010 and 7020]:

$$N1 = -(qo*T + Vj) + Md*(2\pi RPS)^2(3 + \mu)(Ro^2 - X^2)*T/8 \qquad (2.103)$$

For junction at the *inside* radius [Lines 6600,6610 and 6690]

$$N1 = (-qi*T + Vj)*Ri^2(Ro^2 - X^2)/(X^2(Ro^2 - Ri^2)) \\ -qo*T*Ro^2(X^2 - Ri^2)/(X^2(Ro^2 - Ri^2)) \\ +0.5*\alpha*E*T*dTr*[f2]/Ln(Ro/Ri) \\ +Md*(2\pi RPS)^2(3 + \mu)[f5]*T/8 \quad (2.104)$$

(3) Hoop membrane force, +ve tensile

For junction at the *outside* radius and inside radius Ri >0 [Lines 6620, 6630 and 6660]

$$N2 = qi*T*Ri^2(Ro^2 + X^2)/(X^2(Ro^2 - Ri^2)) \\ -(qo*T + Vj)*Ro^2(Ri^2 + X^2)/(X^2(Ro^2 - Ri^2)) \\ +0.5*\alpha*E*T*dTr*[f3]/Ln(Ro/Ri) \\ +Md*(2\pi RPS)^2(3 + \mu)[f6]*T/8 \quad (2.105)$$

where $[f3] = [1 - Ln(Ro/X) - Ri^2(1 + (Ro/X)^2)Ln(Ro/Ri)/(Ro^2 - Ri^2)]$
and $[f6] = [Ro^2 + Ri^2 + Ro^2Ri^2/X^2 - (1 + 3\mu)*X^2/(3 + \mu)]$

If the inside radius Ri = 0 then equation (2.105) reduces to equation (2.106) [Line 7010 and 7030]:

$$N2 = -(qo*T + Vj) + Md*(2\pi RPS)^2(3 + \mu)[Ro^2 - (1 + 3\mu)*X^2/(3 + \mu)]*T/8 \quad (2.106)$$

For junction at the *inside* radius [Lines 6620,6630 and 6700]

$$N2 = (qi*T - Vj)*Ri^2(Ro^2 + X^2)/(X^2(Ro^2 - Ri^2)) \\ -qo*T*Ro^2(Ri^2 + X^2)/(X^2(Ro^2 - Ri^2)) \\ +0.5*\alpha*E*T*dTr*[f3]/Ln(Ro/Ri) \\ +Md*(2\pi RPS)^2(3 + \mu)[f6]*T/8 \quad (2.107)$$

(4) Stresses SL, SH, SBL, SBH, and SV are calculated as before, equations (2.74) to (2.78). The membrane plus bending stresses at the plate surfaces become:

$$\text{Meridional stress (left-surface)}, \quad SLl = SL + SBL$$
$$\text{Meridional stress (right-surface)}, \quad SLr = SL - SBL$$
$$\text{Hoop-stress (left-surface)}, \quad SHl = SH + SBH$$
$$\text{Hoop-stress (right-surface)}, \quad SHr = SH - SBH \quad (2.108)$$

2.4.5 Compact Ring [lines 7110 to 7150]

The analysis is based on a ring subjected to a uniform distributed radial force and moment, mean temperature and centrifugal force.

(1) Radial deflection, +ve outward

$$Y = -(Vj + Vr)*Rc^2/(E*AR) \\ +Rc*\alpha*(Tm - Ta) \\ +Md*(2\pi RPS)^2Rc^3/E \quad (2.109)$$

(2) Rotation, radians +ve anti-clockwise

$$\theta = -(Mj + Mr)*Rc^2/(E*D*C) \quad (2.110)$$

Where D is the section modulus $I_{NA}/|C|$, refer to section 2.4.5(8) below.

Component analysis, compact ring

(3) Radial shear force at the ring centroid, +ve outward

$$V = -(Vj + Vr) \tag{2.111}$$

(4) Bending moment about the ring centroid, +ve clockwise

$$M = Mj + Mr \tag{2.112}$$

(5) Hoop membrane stress

$$SH = V*Rc/AR + Md*(2\pi RPS)^2Rc^2 \tag{2.113}$$

(6) Maximum hoop bending stress

$$SBH = -M*Rc/D \tag{2.114}$$

(7) The membrane + bending stresses are calculated at nine points on the ring, refer to section 2.4.5(8) below and FIGURE 2.18(b).

$$\text{Hoop-Stress } SH(c_P) = SH - M*Rc*Lx/I_{NA} \tag{2.115}$$

Where c_P is the connection point number on the ring and Lx is the axial offset distance from the axis N-A passing through the centroid of the ring to the point c_P.

(8) Compact Ring Properties [lines 1220 to 1370]

The properties are based on a tapered conical ring as shown in FIGURE 2.18(a)

$$\text{Cross-section Area, } AR = H(T_L + Tr)/2 \tag{2.116}$$

$$\text{Centroid Radius, } Rc = R_L \pm H_1*SIN(\delta) \tag{2.117}$$

$$\text{Attitude angle of the ring, } \delta = TAN^{-1}[(R_L - Rr)/L] \tag{2.118}$$

$$\text{Position of the centroid, } H_1 = H(2*Tr + T_L)/(3(Tr + T_L)) \tag{2.119}$$

$$\text{Section modulus about axis N-A, } D = I_{NA}/|C| \tag{2.120}$$

Terms H, L and C are distances shown on FIGURE 18(a). Distance H is the distance between points 1 and 5 along the Y-Y axis. Distance L is the axial distance (length) between points 1 and 5, i.e. the length parallel to the axisymmetric centre line. The distance H is related to L by the relationship $H = L/COS(\delta)$. Distance C is the distance to the extreme fibre from the centroid axis N-A. C is positive to right of the axis and negative to the left.

I_{NA} is the second moment of area about the centroid axis N-A

$$\begin{aligned} I_{NA} &= Iy*COS^2(\pi/2 - \delta) + Ix*SIN^2(\pi/2 - \delta) \\ Ix &= H^3(T_L^2 + 4*T_L*Tr + Tr^2)/(36(T_L + Tr)) \\ Iy &= H(T_L^3 + T_L^2Tr + Tr^2T_L + Tr^3)/48 \end{aligned} \tag{2.121}$$

The stresses in the compact ring are proportional to the axial distance from the centroid axis N-A. Stresses are calculated at 9 points on the ring as shown on FIGURE 2.18(b). Points 1, 3, 5 and 7 are on the faces of the ring and points 2, 4, 6 and 8 are at the corners. Point 9 is at the ring centroid. The points are numbered clockwise from the left side mean radius. If the ring is vertical the left radius is the inside radius. The distances Lx1 to Lx9 can be altered independent of the section properties at the input data stage. Note that when there is a membrane stress in the ring the centroid axis N-A will not be a neutral axis.

In addition to the hoop stresses just discussed the program includes an option to allow average shear stresses and meridional stresses to be calculated on the faces of the compact ring. This option is

important where the ring dimensions are smaller than the thickness of the connected components. In these cases the magnitude of the shear or meridional stresses may be higher than the ring hoop stress.

The magnitude of the shear and meridional stresses are calculated by applying the equal but opposite junction end loads from those components that are connected to any of the faces of the ring, i.e. faces 1, 3, 5 and 7 as shown in FIGURE 2.19. Loading from any components connected to the corners of the ring are not included, as it is not possible to estimate the shear and meridional stresses at a sharp corner. Stresses are calculated from equations (2.74), (2.76) and (2.78) using the face length in place of the thickness T. The necessary correction to the hoop stresses, for the Poisson's ratio effect, is made by putting N2 = μ*N1 and M2 = μ*M1 and applying equations (2.75) and (2.77).

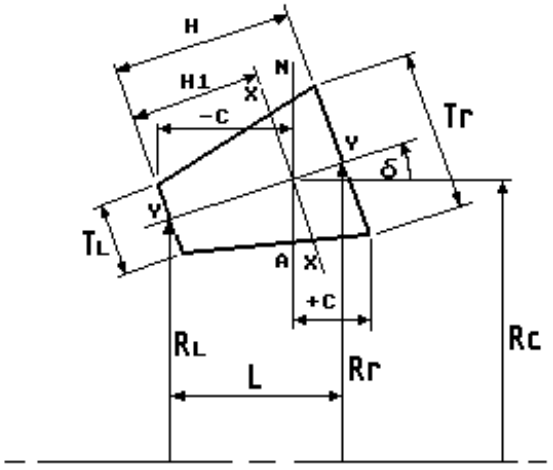

FIGURE 2.18(a) Geometry of tapered conical ring

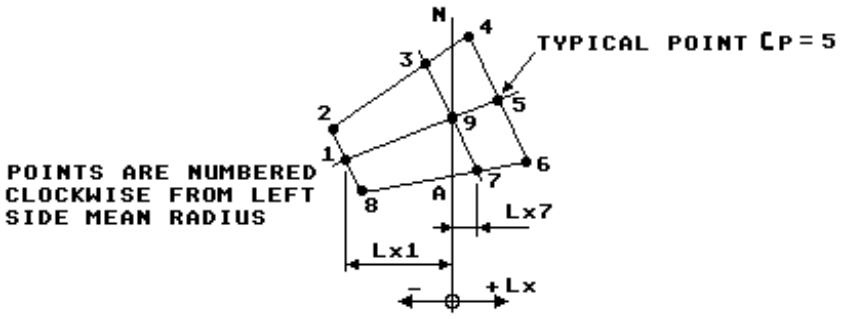

FIGURE 2.18(b) Compact ring, stresses are calculated at the nine points indicated

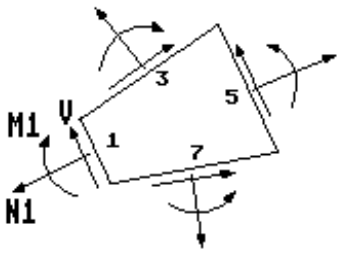

FIGURE 2.19 Positive directions of the shear force, meridional membrane force and meridional moment applied to the faces of a compact ring

3.0 THE COMPUTER PROGRAM

This book is supplied with BASIC programs on floppy disk suitable for use on an IBM PC compatible microcomputer or an Atari ST microcomputer. Make sure the original disk is write protected and make a back up copy. The PC compatible version is supplied in both 5¼" and 3½" disks. Both disks are formatted double sided double density and both text only and graphics versions of the program are supplied. The Atari ST version is formatted single sided and contains programs for all three Atari ST resolutions.

The program name is "AJAP1" which simply stands for: "Axisymmetric Junction Analysis Program version 1". The program is interactive and has been error trapped for most of the common input errors likely to occur. A list of the error traps is given in appendix 3. Output is to a VDU screen or hard copy to a printer.

The disk contains a README text file that gives the details for loading and running the program. If using an IBM PC or compatible microcomputer the README text can be read using DOS commands. A>TYPE README.TXT will list the text on the VDU screen. If the screen scrolls too fast to read use the CTRL NUM LOCK keys to pause the listing. Alternatively use the MORE command. MORE<README.TXT to pause the listing. Press any character key to continue the listing. The file can be printed either by pressing the CTRL PRTSC keys immediately before TYPE or use the command A>TYPE README.TXT>PRN. If using an Atari ST microcomputer, simply open the README.TXT file from the GEM desktop.

There are several AJAP1 programs provided on the floppy disk. The programs are nominally identical except for the details relating to the graphics display. Where applicable a RUNME program is provided to load the appropriate program to suit your VDU resolution. The RUNME program is not essential to the running of the AJAP1 programs. If using a hard disk it is not necessary to store every program, the README.TXT file gives details of the resolution of the programs currently available.

This chapter now discusses the program details required by the user. It is essential that section 3.2 Limitations, section 3.3 Defaults and section 3.4 Input Data Instructions be followed.

3.1 PROGRAM ORGANISATION

The flow diagram for the program is shown in FIGURE 3.1. The program is organised in the following sequence of steps:

(1) Input data
(2) Initialise arrays
(3) More input data
(4) Initialise defaults
(5) Revise defaults (if required)
(6) Main calculation
(7) Results output and plot
(8) Stop or return to input

The overall control of the program is by subroutines at lines 70 to 350. The details of the main calculation steps for a junction analysis have previously been discussed in section 2.2 and FIGURE 2.1. The calculation of the stiffness coefficients and component analysis for each component type are carried out within subroutines applicable to each component type, the line numbers are given in TABLE 3.1 for information.

Details of the default stiffness coefficients and component analysis are as previously discussed in sections 2.3 and 2.4. It should be possible to develop the program to include other component types outside the scope of the current text.

CYLINDERS;	Stiffness coefficients, lines 4830 - 4840
	Component analysis, lines 4870 - 4940
SPHERICAL SHELLS;	Stiffness coefficients, lines 4970 - 4990
	Component analysis, lines 5020 - 5230
CONES;	Stiffness coefficients, lines 5260 - 5440
	Component analysis, lines 5470 - 5880
FLAT PLATES;	Stiffness coefficients, lines 5910 - 5990
	Component analysis, lines 6020 - 7050
COMPACT RING;	Stiffness coefficients, lines 7080 - 7090
	Component analysis, lines 7110 - 7160
	Face stresses, lines 30000 - 30490

TABLE 3.1 Program line numbers for stiffness coefficients and component analysis subroutines

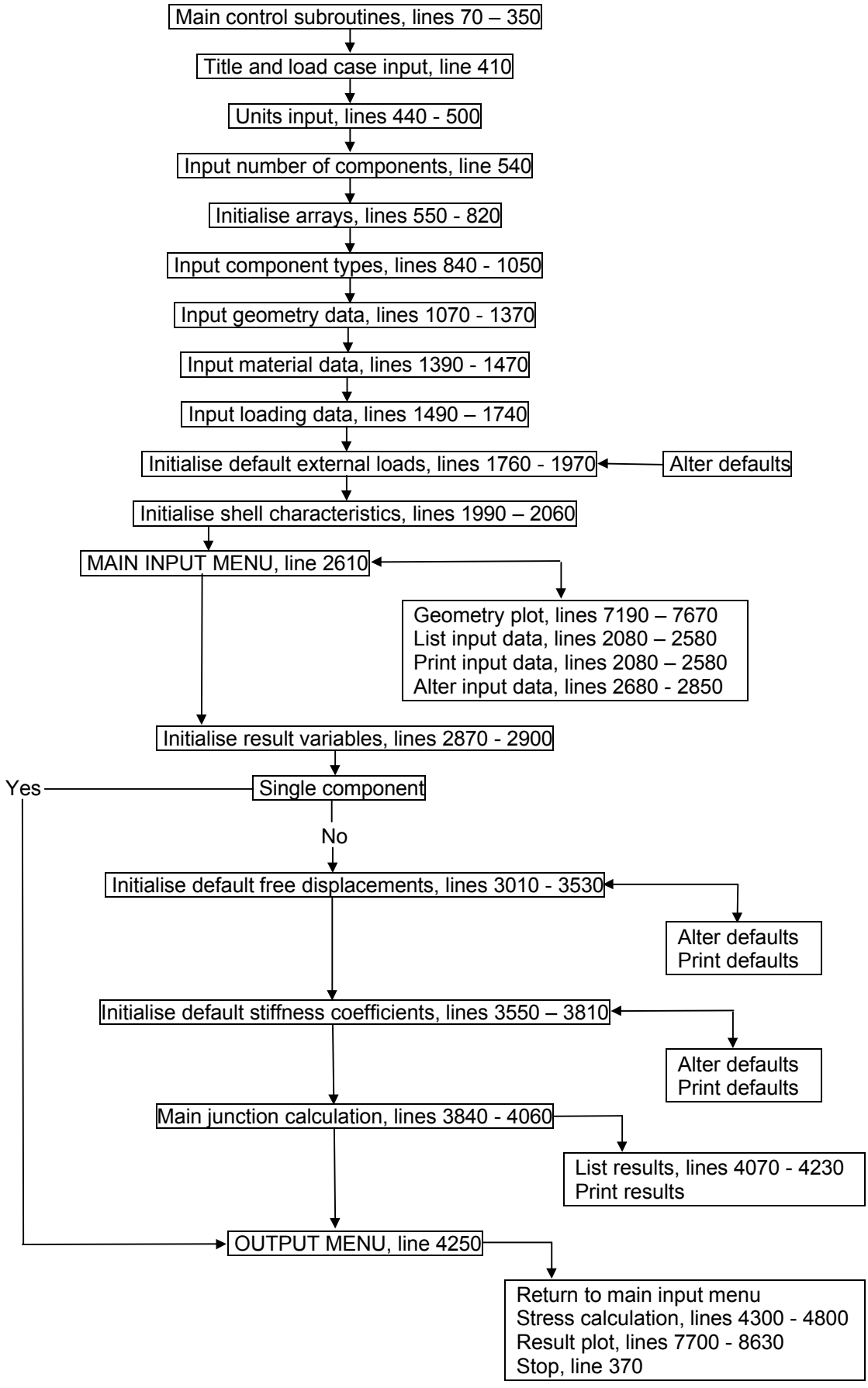

FIGURE 3.1 Flow diagram of program "AJAP1"

3.2 LIMITATIONS

There are five main limitations. These can be simply stated as follows:

(1) Only one junction can be analysed at a time.
(2) Any number of components can be connected at a junction within the memory limits of the computer except that only one compact ring is allowed.
(3) The geometry and loading are axisymmetric.
(4) The analysis is linear elastic.
(5) The material properties are isotropic.

Each component type has specific limitations. The program will give the results outside these limits so the user will have to decide on the validity of the results. As an aid to the user, the specific limits are now briefly discussed. These are not hard and fast rules but should be considered as guidance only. For example, a ratio of R/T >=10 is usually assumed for thin shells but in practice the results are often used at ratios of R/T <10.

3.2.1 Cylindrical Shell Limitations

Cylinders should be long so that the loading conditions at one end do not significantly effect the stresses and deformations at the other end. For most cases a length >=2.5$(R*T)^{1/2}$ would be considered sufficiently long. ASME SECTION VIII (ref.10) suggests that a length of cylinder is sufficiently long if the length is >=3/β.

Cylinders should be thin and radial deflections should be small compared to the wall thickness. A ratio of R/T >10 is often assumed for thin cylinders and radial deflections should be <½ the thickness. If the cylinder is very short then the equations for a compact ring become applicable. The limits for a compact ring are discussed in section 3.2.5.

3.2.2 Spherical Shell Limitations

The solution is for closed non-shallow shells. The half arc angle ϕ should be in the range ϕ_{MIN}=< ϕ <=ϕ_{MAX} as shown in FIGURE 3.2. Shells that have an edge less than ϕ_{MIN} or greater than ϕ_{MAX}, where the shell is almost vertical like a plate, require shallow shell theory. It is generally considered that shallow shell theory applies when COT $\phi \approx 1/\phi$. If a 5% error is assumed then ϕ = 21.5 degrees. Therefore we can say that the applicable angle for non-shallow shells is approximately in the range 21.5=< ϕ <=158.5 degrees.

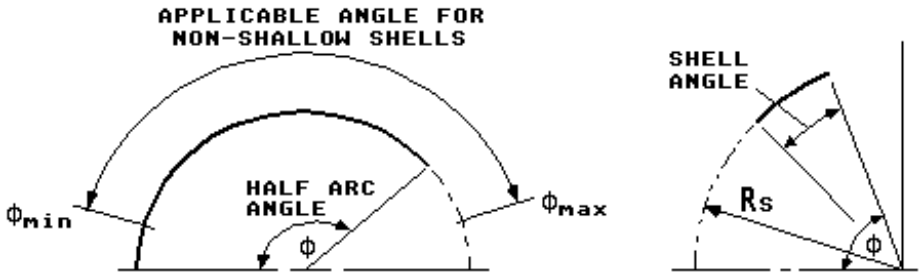

FIGURE 3.2 Applicable spherical shells

ASME SECTION VIII code (reference 10) also puts limitations on closed spherical shells where: 0.9*π/β=< ϕ <=(1-0.9/β)π radians and Rs/T >=10, i.e. the applicable angle is a function of the shell characteristic. TABLE 3.2(a) lists the applicable range of angle for several values of Rs/T and a Poisson's ratio of 0.3.

Rs/T	half arc angle, degrees
10	40=< ϕ <=140
50	18=< ϕ <=162
100	12.5=< ϕ <=167.5
500	5.5=< ϕ <=174.5
1000	4=< ϕ <=176

TABLE 3.2(a) Approximate applicable range of non-shallow shell theory

For non-shallow shells the effects of the edge discontinuity become insignificant a short distance from the edge. BAKER (ref. 8) discusses this aspect and suggests that the end effects become insignificant by about 20 degrees. This means that open spherical shells could be considered where the ends of the shell angle are greater than about 20 degrees from each other as shown in FIGURE 3.2. It is also possible to consider other shell shapes provided that the first 20 degrees can be approximated to an equivalent spherical shell. Limits for open spherical shells are also given in ASME SECTION VIII (ref. 10) where: ϕ =<(1-0.9/β)π radians and the shell angle >=π/β radians. TABLE 3.2(b) lists the applicable shell angle for several values of Rs/T and a Poisson's ratio of 0.3.

Rs/T	shell angle, degrees
10	>=44
50	>=20
100	>=14
500	>=6
1000	>=4.5

TABLE 3.2(b) Approximate required shell angle for open shells

3.2.3 Conical Shell Limitations

Cones should be thin, i.e. Rx/(T*COS ϕ) >10. The discontinuity results are based on the solution by TAYLOR (ref. 28). TAYLOR and WENK (ref. 55) found the results to be in error by about 10% for values of the cone shell parameter xi = 10. The error reduces with higher values of cone parameter. W.C. YOUNG in his discussion on cones (ref. 11) considered the results to be accurate for values of the cone parameter >5. TABLE 3.3 lists values of the cone parameter for several values of Rj/T, half apex angle ϕ and a Poisson's ratio of 0.3. It can be seen that only with thick cones or those with a large half apex angle would the results be in doubt.

The cones should be long, i.e. it is assumed that the conditions at one edge do not affect the results at the other edge. The results presented by TAYLOR in reference (28) show that the cone can be considered sufficiently long when the length parameter LP is > about 4. For values of LP > about 4 the discontinuity results have reduced to negligible values. The values of |xi| and LP are output with the results so users can make a judgement on the validity of the results.

Rj/T = 5	ϕ = 15°	xi = 30.8	Rj/T = 10	ϕ = 15°	xi = 43.6
	ϕ = 30°	xi = 15.1		ϕ = 30°	xi = 21.3
	ϕ = 60°	xi = 6.6		ϕ = 60°	xi = 9.3
	ϕ = 80°	xi = 3.4		ϕ = 80°	xi = 4.8
Rj/T = 100	ϕ = 15°	xi = 138.0	Rj/T = 1000	ϕ = 15°	xi = 436.5
	ϕ = 30°	xi = 67.6		ϕ = 30°	xi = 213.9
	ϕ = 60°	xi = 29.6		ϕ = 60°	xi = 93.8
	ϕ = 80°	xi = 15.3		ϕ = 80°	xi = 48.6

TABLE 3.3 Values of cone shell parameter xi

3.2.4 Flat plate limitations

The usual limitations are: the plate should be flat and of uniform thickness. The thickness should not be more than about ¼ of the radius. The maximum deflection should not be more than about ½ the thickness. No deflections due to shear strains are included.

3.2.5 Compact ring limitations

The main requirement is that the ring should be compact and not widely spread. The maximum width of ring should be small compared to the radius. BAKER (ref.8) suggests that if the length of a cylinder or cone is $<(R*T)^{1/2}$ then the cylinder or cone is essentially a circular ring instead of a shell. ASME SECTION VIII (ref.10) suggests that ring theory can be used when the cylinder length is <=0.5/β, i.e. for a Poisson's ratio of 0.3 the length should be approximately $<=0.4(R*T)^{1/2}$.

3.3 PROGRAM DEFAULTS

The program is written with the Pressure Vessel engineer in mind and has inbuilt defaults which are now described. These defaults may not be applicable in every case but they can be overwritten where necessary. The defaults are based on simple theory, well known relationships or specified references.

3.3.1 Pressure End Load, F_P and Meridional Load, F_O

The usual case of a closed vessel is assumed. The axial pressure end load is calculated, [lines 2950 and 2960], and added to any applied axial end load F_{AX} as shown in FIGURE 3.3. If the pressure end load is not required it can be negated by putting on an equal but opposite axial end load. The meridional load is calculated directly from F_P and F_{AX} [lines 2950 and 2960]. These loads are per unit circumference and the values of F_P and F_O calculated by the program are listed in the input data. A positive value indicates tension and a negative value indicates compression.

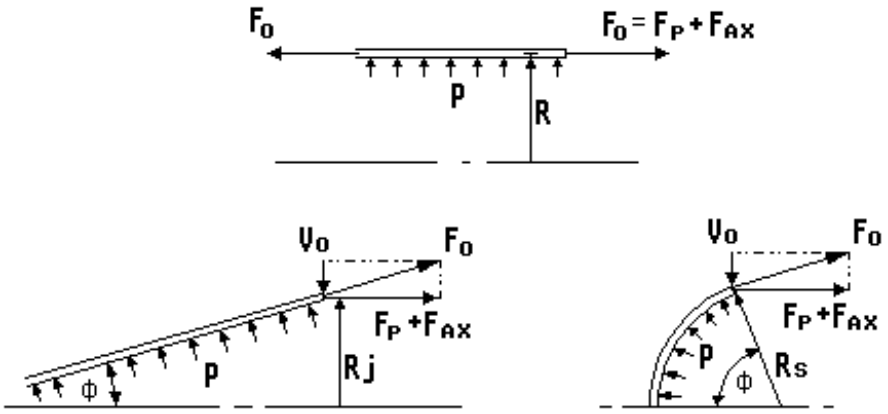

FIGURE 3.3 Axial and radial forces applied to shells

(1) for a cylinder the pressure end load, $F_P = P*R/2$ (3.1)

and the meridional load, $F_O = F_P + F_{AX}$ (3.2)

(2) for a spherical shell, $F_P = 0.5*P*Rs*SIN\ \phi$ (3.3)

$F_O = (F_P + F_{AX})/SIN\ \phi$ (3.4)

(3) for a cone, $F_P = P*Rj/2$ (3.5)

$F_O = (F_P + F_{AX})/COS\ \phi$ (3.6)

3.3.2 Applied External Radial Force, Vo

For spherical shells and cones the equations governing the membrane action of these components are based on the meridional load equations (3.4) and (3.6). It is usual to obtain the end load effects by applying a radial force Vo as shown on FIGURE 3.3.

The program calculates the radial force for each component and sums these to obtain the default applied radial force Vo acting at the junction [lines 1810, 1820, and 1840]. Vo is per unit circumference and is positive inwards.

(1) for a spherical shell, $Vo = F_O*COS\ \phi$ (3.7)

(2) for a conical shell, $Vo = F_O*SIN\ \phi$ (3.8)

3.3.3 Applied External Moment, Mo

In cases where the junction radii are different, there will be a moment applied at the junction due to the difference in radii times any end loads. The end loads can be produced by pressure or other axial loads such as F_{AX} applied to shells or point loads W applied to flat plates. The program calculates the moment due to the end load and applies this as a default external moment Mo about the last component [lines 1800 to 1830]. Mo is per unit circumference and is positive clockwise.

For example, a common case is for two connected cylinders to have different radii as shown in FIGURE 3.4(a). When subjected to pressure or axial end load there is a moment at the junction given by equation (3.9).

$$Mo = -(F_{P1} + F_{AX1})*(R_1 - R_2) \qquad (3.9)$$

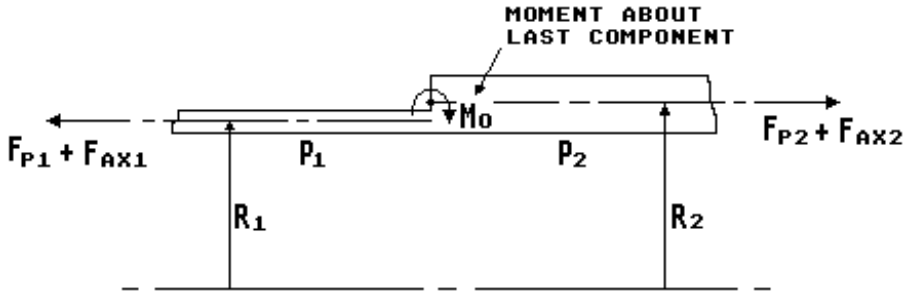

FIGURE 3.4(a) Components connected with different radii

If a compact ring is at the junction the moment will be about the centroid of the ring. If any spherical shell or cone is connected to the ring, for example as shown in FIGURE 3.4(b), then the radial force Vo (as discussed in section 3.3.2) acting offset from the centroid axis N-A, is included as an external moment [line 1830]. Detailed properties of the ring are as discussed in section 2.4.5(8).

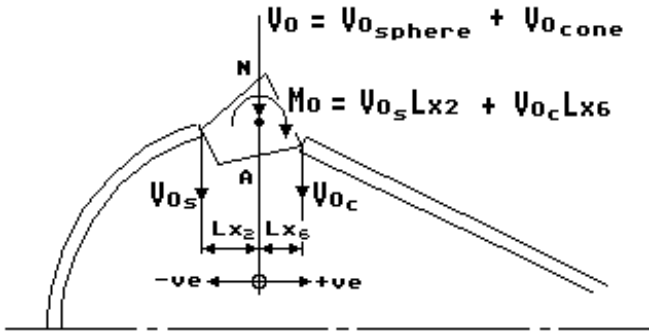

FIGURE 3.4(b) Default external loads applied to the centroid of a compact ring

3.3.4 Thermal End Moment

For shells a temperature difference dT across the thickness is allowed and surface stresses for a restrained plate are assumed, equation (3.10).

$$SBL = SBH = \pm 0.5*E*\alpha*dT/(1 - \mu) \qquad (3.10)$$

Stresses are tensile on outside when dT is positive, i.e. when the temperature of the inside surface is at a higher temperature than the outside surface. The stresses are obtained by applying restraining moments M1 and M2 given by equation (3.11) [line 4790].

$$M1 = M2 = -E*\alpha*dT*T^2/(12(1 - \mu)) \qquad (3.11)$$

In order to obtain a free edge an equal but opposite meridional moment to M1 is applied as an external moment Mo as shown in FIGURE 3.5 [line 1790].

For flat plates the free rotation due to dT is calculated directly and is discussed in section 3.3.5(4).

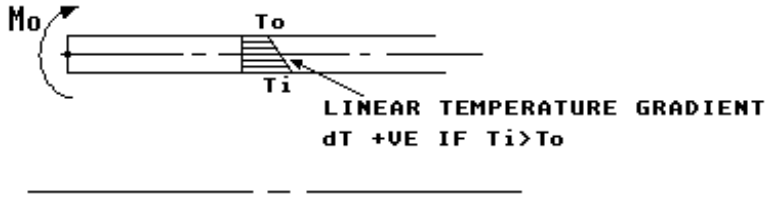

$$Mo = E^*\alpha^*dT^*T^2/(12(1 - \mu))$$

FIGURE 3.5 Default external moment applied to the end of a shell subjected to a temperature difference across its thickness

3.3.5 Free Displacements at the Junction

For a junction analysis the default free displacements of each component at the junction are calculated [lines 3010 to 3530]. It is the relative difference in these displacements (together with any applied external loads) which cause the junction discontinuity. Yf is the radial deflection positive outward. θf is the rotation of the tangent to a meridian in radians positive anti-clockwise.

The displacements are stored in array Z( ) [line 3340]. Where: Z(2*i) = Yf and Z(2*i -1) = θf and i is the component number under consideration.

(1) for cylindrical shells

The free deflections due to pressure differential, axial end load, mean temperature and centrifugal force are given by [line 3040]:

$$\begin{aligned} Yf = {} & P^*R^2(1 - \mu/2)/(E^*T) \\ & -F_{AX}^*\mu^*R/(E^*T) \\ & +R^*\alpha^*(Tm - Ta) \\ & +Md^*(2\pi RPS)^2R^3/E \end{aligned} \qquad (3.12)$$

The free rotation due to an axial thermal gradient is given by [lines 3030 - 3040]:

$$\theta f = Fc^*R^*\alpha^*Gj \qquad (3.13)$$

(2) for spherical shells

The free deflections due to pressure differential, axial end load, mean temperature and centrifugal force are given by [line 3050]:

$$\begin{aligned} Yf = {} & P^*Rs^2(1 - \mu)SIN(\phi)/(2^*E^*T) \\ & -F_{AX}^*Rs^*(1 + \mu)/(E^*T) \\ & +Rs^*\alpha^*(Tm - Ta)SIN(\phi) \\ & +Md^*(2\pi RPS)^2(Rs^*SIN\ \phi)^3/E \end{aligned} \qquad (3.14)$$

The free rotation due to a thermal gradient and centrifugal force is given by [lines 3030 and 3050]:

$$\theta f = Fc^*Rs^*\alpha^*Gj + Fc^*Md^*(2\pi RPS)^2(3 + \mu)^*Rs^2SIN(\phi)^*COS(\phi)/E \qquad (3.15)$$

(3) for conical shells

The free deflections due to pressure, axial end load, mean temperature and centrifugal force are given by [line 3060]:

$$\begin{aligned} Yf = {} & P^*Rj^2(1 - \mu/2)/(E^*T^*COS\ \phi) \\ & -F_{AX}^*\mu^*Rj/(E^*T^*COS\ \phi) \\ & +Rj^*\alpha^*(Tm - Ta) \\ & +Md^*(2\pi RPS)^2Rj^3/E \end{aligned} \qquad (3.16)$$

The free rotation due to pressure, axial end load, thermal gradient and centrifugal force is given by:

For cones sloping up to the *right* [line 3070]

$$\begin{aligned}\theta f = {} & 3*P*Rj*TAN(\phi)/(2*E*T*COS\ \phi) \\ & -F_{AX}*TAN(\phi)/(E*T*COS\ \phi) \\ & +Fc*Rj*\alpha*Gj/COS(\phi) \\ & +Md*(2\pi RPS)^2(3 + \mu)*Rj^2TAN(\phi)/E\end{aligned} \qquad (3.17)$$

For cones sloping up to the *left* [line 3080]

$$\begin{aligned}\theta f = {} & -3*P*Rj*TAN(\phi)/(2*E*T*COS\ \phi) \\ & +F_{AX}*TAN(\phi)/(E*T*COS\ \phi) \\ & +Fc*Rj*\alpha*Gj/COS(\phi) \\ & -Md*(2\pi RPS)^2(3 + \mu)*Rj^2TAN(\phi)/E\end{aligned} \qquad (3.18)$$

(4) for flat plates with the junction at the *outside* radius

The free deflection due to radial internal and external pressure, mean thermal expansion, radial temperature difference and centrifugal force are [lines 3310 and 3330]:

$$\begin{aligned}Yf = {} & qi*2*Ro*Ri^2/[E*(Ro^2 - Ri^2)] \\ & -qo*Ro[(Ro^2 + Ri^2)/(Ro^2 - Ri^2) - \mu]/E \\ & +Ro*\alpha*(Tm - Ta) \\ & +0.5*\alpha*dTr*Ro*[1 - 2*Ri^2Ln(Ro/Ri)/(Ro^2 - Ri^2)]/Ln(Ro/Ri) \\ & +Md*(2\pi RPS)^2Ro*(3 + \mu)(1 - \mu)[f7]/(8*E)\end{aligned} \qquad (3.19)$$

where: $[f7] = Ro^2 + Ri^2 + (1 + \mu)*Ri^2/(1 - \mu) - (1 + \mu)*Ro^2/(3 + \mu)$

Equation (3.19) is based on the well known thick cylinder theory. The term containing the radial logarithmic temperature difference dTr is based on the theory of a thin disk. The longitudinal stress is assumed to be zero and the $(1 - \mu)$ term is not included in the denominator. There are no free rotations due to the above loading.

The free rotations due to pressure difference, applied point loads and temperature difference across the thickness are based on the theory of simply supported circular flat plates. The theory is given in many textbooks.

When the inside radius, Ri >0 [lines 3200 and 3270]

$$\begin{aligned}\theta f = {} & P*Ro^3(C4*L17/C7 - L14)/D \\ & +W*Ro^2(C4*L9/C7 - L6)/D \\ & +\alpha(1 + \mu)*dT*Ro[L5 + C4(1 - L8)/C7]/T\end{aligned} \qquad (3.20)$$

where: $D = E*T^3/(12(1 - \mu^2))$

$C4 = [(1 + \mu)*Ri/Ro + (1 - \mu)*Ro/Ri]/2$

$C7 = (1 - \mu^2)(Ro/Ri - Ri/Ro)/2$

$C9 = Ri/Ro\ *\{(1 + \mu)*Ln(Ro/Ri)/2 + (1 - \mu)*[1 – (Ri/Ro)^2]/4\}$ [Added]

$L5 = [1 - (Ri/Ro)^2]/2$

$L6 = Rw[(Rw/Ro)^2 - 1 + 2*Ln(Ro/Rw)]/(4*Ro)$

$L8 = [1 + \mu + (1 - \mu)(Ri/Ro)^2]/2$

$L9 = Rw\{0.5(1 + \mu)*Ln(Ro/Rw) + 0.25(1 - \mu)[1 - (Rw/Ro)^2]\}/Ro$

$L14 = [1 - (Ri/Ro)^4 - 4(Ri/Ro)^2Ln(Ro/Ri)]/16$

$L17 = \{1 - (1 - \mu)[1 - (Ri/Ro)^4]/4 - (Ri/Ro)^2[1 + (1 + \mu)*Ln(Ro/Ri)]\}/4$

When the inside radius Ri = 0 the rotation reduces to the following [line 3120]:

$$\theta f = P*Ro^3/(8*D(1 + \mu)) + W*Rw(Ro^2 – Rw^2)/(2*D(1 + \mu)Ro) + \alpha*dT*Ro/T \qquad (3.21)$$

Computer program, defaults

The free deflection due to the rotation is calculated by equation (3.22) [line 3300] and added to equation (3.19).

$$Yf = JP*\theta f*T/2 \qquad (3.22)$$

Where JP is the junction position = -1 at the left surface
0 at the plate centre line
1 at the right surface

(5) for flat plates with the junction at the *inside* radius

The free deflection due to radial internal and external pressure, mean thermal expansion and radial temperature difference are given by [line 3320 and 3335]:

$$\begin{aligned} Yf = & -qo*2*Ro^2Ri/[E*(Ro^2 - Ri^2)] \\ & +qi*Ri[(Ro^2 + Ri^2)/(Ro^2 - Ri^2) + \mu]/E \\ & +Ri*\alpha*(Tm - Ta) \\ & +0.5*\alpha*dTr*Ri[1 - 2*Ro^2Ln(Ro/Ri)/(Ro^2 - Ri^2)]/Ln(Ro/Ri) \\ & +Md*(2\pi RPS)^2Ri(3 + \mu)(1 - \mu)[f8]/(8*E) \end{aligned} \qquad (3.23)$$

Where: $[f8] = Ro^2 + Ri^2 + (1 + \mu)*Ro^2/(1 - \mu) - (1 + \mu)*Ri^2/(3 + \mu)$

The free rotation due to pressure difference, applied point loads and temperature difference across the plate thickness are based on the well known theory of simply supported flat plates [lines 3210 and 3280].

$$\begin{aligned} \theta f = & -P*Ro^3[C9(Ro^2 - Ri^2)/(2*Ro*Ri) - L17]/(D*C7) \\ & -W*Ro^2(Rw*C9/Ri - L9)/(D*C7) \\ & +\alpha*(1 + \mu)*dT*Ro(1 - L8)/(T*C7) \end{aligned} \qquad (3.24)$$

Where: terms C7, C9, D, L8, L9 and L17 are as defined above.

The free deflection due to the rotation is calculated as before equation (3.22) and added to equation (3.23).

(7) compact ring

The free deflection at the ring centroid due to an applied radial force, mean temperature and centrifugal force is given by [line 3090]:

$$\begin{aligned} Yf = & -Vr*Rc^2/(E*AR) \\ & +Rc*\alpha*(Tm - Ta) \\ & +Md*(2\pi RPS)^2Rc^3/E \end{aligned} \qquad (3.25)$$

The free rotation due to an applied moment is given by:

$$\theta f = -Mr*Rc^2/(E*D*C) \qquad (3.26)$$

Where the terms Rc, AR, D and C are as previously defined in section 2.4.5.

For the compact ring the displacements above refer to the centroid of the ring. In order to allow for the usual case of components connected to the edge of the ring, the offset distance Lx (as discussed in section 2.2.4) is allowed for by calculating the deflection at the ring edge due to rotation of the ring, equation (3.27).

$$Yf = Yf(\text{at centroid}) - \theta f*Lx \qquad (3.27)$$

Since the offset Lx is component dependent, the calculation of equation (3.27) is carried out in the main junction analysis [line 3880].

3.3.6 Compact Ring Properties

The default properties are based on a tapered conical ring. Section 2.4.5(8) discusses the full details. The properties can be overwritten at the input data stage so it is possible to simulate other shapes of ring.

3.3.7 Stiffness Coefficients

The default coefficients are discussed in detail in section 2.3. The coefficients are listed prior to solving the junction analysis. Each coefficient can be individually overwritten so that it is possible to carry out a junction analysis for components not specifically covered by the defaults.

3.4 INPUT DATA INSTRUCTIONS

The detailed input data instructions are now presented. The format used is that of an instruction manual. This has been done to minimise the risk of users inputting the wrong data. The input has been error trapped for the common errors likely to occur. A list of the error traps is given in appendix 3.

The input data is arranged into eight sub-sections as follows:

(1) Title data
(2) Units data
(3) Geometry data
(4) Material data
(5) Loading data
(6) Applied external loads
(7) Free displacements
(8) Stiffness coefficients

Sub-sections (1) to (5) will require input data but sub-sections (6), (7) and (8) initially give default values which can be overwritten later if required. The sub-sections will now be discussed in detail. It is essential that the sign directions are followed and the previous sections on limitations and defaults should be read and understood.

A README.TXT file is included on the floppy disk. This file gives the details of loading and running the program. The program is interactive and will initially ask for some information about your printer hardware. This simply sets the left margin for some well known printer types. The following data will then be asked for.

3.4.1 Title Data

"TITLE"	enter any title information.
"LOAD CASE"	enter any load case information.

3.4.2 Units Data

Any consistent set of units may be used. The following are suggested. S.I. use: mm, N, Kg, degC.
Imperial use: in, Lbf, Lb, degF.

"LENGTH UNITS"	enter units
"FORCE UNITS" `	enter units
"MASS UNITS"	enter units
"TEMPERATURE UNITS"	enter units

the screen is cleared

3.4.3 Geometry Data

Enter the NUMBER OF COMPONENTS. A single component or a multi component junction is allowed. Only one compact ring is allowed at a junction.

the screen is cleared

A menu of component types is listed, refer to TABLE 2.1.

Enter the COMPONENT TYPE. Enter the type number from the menu. The order of entering the components is not important except that if a compact ring is specified it should be the *last* component.

the screen is cleared

You are now asked for the geometry data required for each component in turn. Refer to FIGURES 3.6 to 3.10. If a single component is specified the end of the component (if a shell) is assumed to be on the *left* end.

(1) for a cylinder enter: MEAN RADIUS, R
THICKNESS. T

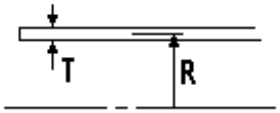

FIGURE 3.6 Cylindrical shell geometry

(2) for a spherical shell enter: MEAN SPHERICAL RADIUS, Rs
THICKNESS, T
ANGLE PHI(degrees), ϕ

where $0< \phi <180°$ but refer to the limitations discussed in section 3.2.2. $\phi = 90°$ is a hemisphere.

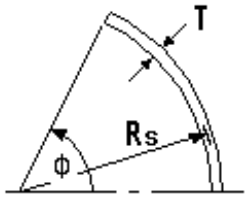

FIGURE 3.7 Spherical shell geometry

(3) for a cone enter: MEAN JUNCTION RADIUS, Rj
THICKNESS, T
ANGLE PHI(degrees), ϕ

where $0< \phi <90°$ but refer also to the limitations discussed in section 3.2.3.

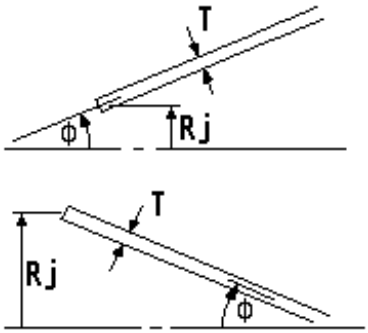

FIGURE 3.8 Conical shell geometry

(4) for a flat plate enter: OUTSIDE RADIUS, Ro
INSIDE RADIUS, Ri
THICKNESS, T
JUNCTION POSITION, JP

where -1=< JP <=1 (refer to section 2.3.4 for additional information) likely practical values are:

-1 for a junction at the left surface (offset = -T/2)
0 for a junction at the centre line of the plate
1 for a junction at the right surface (offset = T/2)

If a flat plate with junction at the outside is specified, you can have a flat head closure by putting the inside radius = 0. If you want to apply a radial temperature difference on the flat head you will have to specify a small inside radius. Only one junction position is allowed per flat plate. If more than one position is required you will have to use the compact ring at the junction.

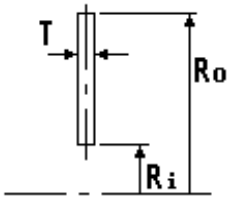

FIGURE 3.9 Flat plate geometry

(5) for a compact ring enter: LEFT MEAN RADIUS, R_L
LEFT THICKNESS, T_L
RIGHT MEAN RADIUS, Rr
RIGHT THICKNESS, Tr
AXIAL LENGTH, L

If the axial length L = 0, i.e. the ring is vertical the *left* radius is taken to be the *inside* radius.

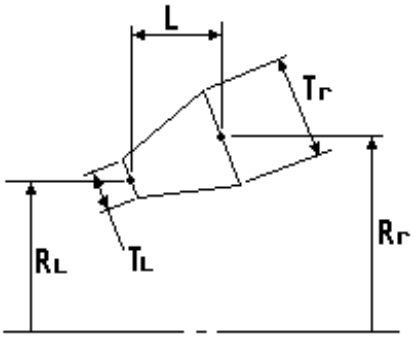

FIGURE 3.10 Compact ring geometry

The properties of the ring are calculated and listed. Details of the properties are discussed in section 2.4.5(8). You can alter these properties as required. The stress results will be calculated at the 9 points on the ring as shown in FIGURE 2.18(b). The offset distances Lx from the centroid axis to the 9 points are listed. The distances can be altered without affecting the previous ring parameters. Distances are +ve to the right of the centroid axis and -ve to the left. Point 9 is on the centroid. It may be useful in some cases to alter the distances to give a better connection with the other components or to simulate a different shape.

You are now asked to enter the connection point numbers for each component connecting to the compact ring. Enter the number, 1 to 9, which is nearest the component offset.

the screen is cleared

3.4.4 Material Data

You are now asked for material properties for each component in turn.

YOUNG'S MODULUS, E enter a value >0
POISSON'S RATIO, PR enter 0=< PR <0.5 (for PR = 0 the program defaults to a small value 1E-6)
COEFFICIENT OF EXPANSION, ALPHA (enter a non-zero value if there are thermal loads)
MASS DENSITY, Md (enter a value >0 if there is centrifugal loading)

the screen is cleared

3.4.5 Loading Data

You are now asked for the loading data for each component in turn, refer to FIGURES 3.11 to 3.14.

(1) For shells enter:

PRESSURE DIFFERENCE ACROSS THE THICKNESS, P +ve outward (internal).
AXIAL END LOAD, F_{AX} per unit circumference of the junction. +ve if it tends to produce tension in the component. The pressure end load is included as a default, refer to the discussion in section 3.3.1

You are now asked for any thermal loads, enter the following:

AMBIENT TEMPERATURE of the surrounds, Ta
MEAN TEMPERATURE of the shell, Tm

Shells continued.

TEMPERATURE DIFFERENCE ACROSS THE THICKNESS of the shell, dT. The assumed temperature distribution is linear. dT is +ve if the inside surface is at a higher temperature than the outside surface.
THERMAL GRADIENT AT THE JUNCTION along the shell, Gj. +ve if the heat flows away from the junction. Units of Gj are temperature/length along the shell.

FIGURE 3.11(a) Pressure and axial end load acting on a cylinder

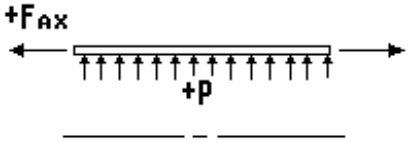

FIGURE 3.11(b) Pressure and axial end load acting on a spherical shell

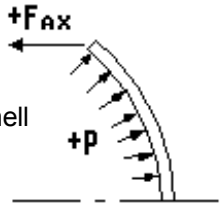

FIGURE 3.11(c) Pressure and axial end load acting on a cone

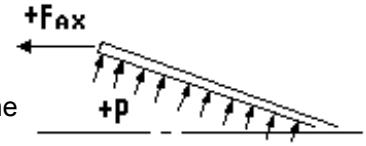

(2) For flat plates enter:

PRESSURE DIFFERENCE across the thickness of the entire plate, P,
+ve to the right.
RADIAL PRESSURE AT THE OUTSIDE DIAMETER, qo.
+ve if the pressure is external.
RADIAL PRESSURE AT THE INSIDE DIAMETER, qi. +ve if the pressure is internal.
If the inside diameter is zero then qi is not asked for.

HOW MANY POINT LOADS, MAX = 12 (enter 0 for no loads)
POINT LOAD, W. +ve to the right.
RADIUS OF LOAD W, Rw

W is per unit circumference at radius Rw. The maximum number of point loads can be increased by altering the value of MPL at line 520. If a moment is required this can be simulated by a couple, i.e. apply equal but opposite loads at slightly different radii.

FIGURE 3.12 Pressure and point loads acting on a flat plate

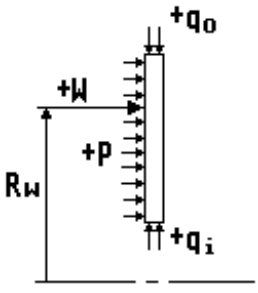

You are now asked for any thermal loads, enter the following:

AMBIENT TEMPERATURE of the surrounds, Ta
MEAN TEMPERATURE of the plate, Tm

Flat Plates, continued.

TEMPERATURE DIFFERENCE, dT, across the thickness of the entire plate. dT is +ve if right surface is at a higher temperature than the left surface. A linear temperature distribution is assumed.
RADIAL TEMPERATURE DIFFERENCE, dTr, across the radius of the plate. If the inside diameter is zero then dTr will not be asked for. dTr is +ve if the inside diameter is at a higher temperature than the outside diameter. A logarithmic temperature distribution is assumed.

(3) For a compact ring enter the following:

MOMENT, Mr +ve clockwise
RADIAL FORCE, Vr +ve inward
Mr and Vr are per unit circumference at the centroid radius. Alternatively these loads can be applied as external loads Mo and Vo as discussed below.

FIGURE 3.13 Moment and radial force acting at the centroid of the compact ring

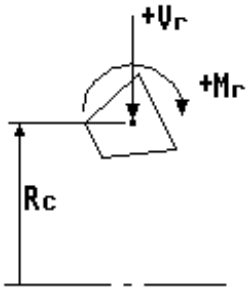

You are now asked for any thermal loads, enter the following:

AMBIENT TEMPERATURE of surrounds, Ta
MEAN TEMPERATURE of the compact ring, Tm

This completes the input data for individual components. You are now asked if there is any Centrifugal Loading. If so then enter the rotation about the axisymmetric centre line in REVOLUTIONS PER SECOND as shown in FIGURE 3.14.

FIGURE 3.14 Centrifugal loading, rotation in revolutions per second

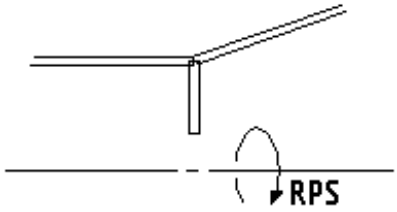

the screen is cleared

3.4.6 Applied External Loads

The default external loads as discussed in sections 3.3.2 to 3.3.4 are calculated and listed. The defaults can be accepted or overwritten.

MOMENT, Mo +ve clockwise
RADIAL FORCE, Vo +ve inward
Loads Mo and Vo are per unit circumference at the junction. Positive directions are shown in FIGURE 3.15.

FIGURE 3.15 Applied external loads

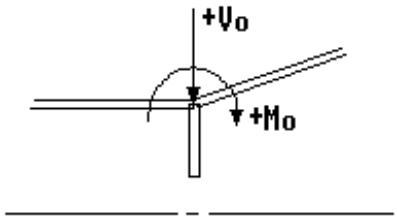

Applied External Loads, continued.

If a compact ring is modelled the loads are applied at the centroid of the ring, alternatively the loads can be applied as Mr and Vr at component loading stage discussed above.

For single components Mo and Vo are applied to the *left* end of the component at the mean radius or the centroid if the component is a compact ring.

the screen is cleared

A main input menu is presented. You can now get a geometry plot, a list of the input data, a copy of the input data or you can alter the data.

the screen is cleared

3.4.7 Free Displacements

If a junction analysis is being carried out the program calculates and lists the default free displacements for each component as discussed in section 3.3.5. The default displacements can be accepted or overwritten.

A copy of the displacements can be obtained. The radial deflection Yf is positive outward and the rotation THf is positive anti-clockwise.

the screen is cleared

3.4.8 Stiffness Coefficients

Prior to solving the junction analysis the default stiffness coefficients are listed for each component as discussed in section 2.3. The coefficients can be accepted or overwritten. A copy of the coefficients can be obtained.

The Junction Analysis proceeds. After a few seconds the junction results are listed. The positive directions are shown in FIGURE 2.2. A copy of the junction results can be obtained.

the screen is cleared

An output menu is presented. You can obtain a component stress calculation and output the results to a printer. A result plot can be obtained for all but the compact ring results. You can return to the main input menu or drop into BASIC command level by using the STOP option.

3.5 OUTPUT RESULTS

Output is to a VDU screen or to a printer. The following information can be obtained:

(1) Input data listing
(2) Geometry plot
(3) Calculated results
(4) Results plot

Typical output listings are given with the examples in section 3.6. Some additional notes and position of the component sections have been added to the geometry plots for information. The notation and input data should be carefully checked including the sign directions. Positive directions of junction forces and moments are shown in FIGURE 2.2 and a summary of the component output is listed in TABLE 3.4.

3.5.1 Graphical Options

The floppy disk contains versions of the program for use with several different graphic displays. The README.TXT on the floppy disk gives the details of the current versions available. The README.TXT gives some guidance on how to modify the program graphics to suit other displays not yet included on the disk.

Two graphical subroutines are included with the program, a geometry plot and a result plot. These routines are not essential for the analysis but it is recommended that they be used.

Typical geometry plots [lines 7190 - 7670] are shown with the examples in section 3.6. The plot should highlight any gross errors in the input geometry data. Cylinders and cones with the junction at the small end are assumed to be $5(R*T)^{1/2}$ in length for plotting purposes.

A typical result plot [lines 7700 - 8630] is shown in FIGURE 3.16. NP is the number of points plotted. DX is the distance between points on the X-axis. The result (meridional moment M1 in this example) is plotted on the Y-axis. The maximum value calculated is printed out together with its position on the X-axis. The result plot should automatically give a reasonable scale to the Y-axis in most cases. There may be some instances where a change to the input units gives an improved plot.

A list of the results that can be plotted is given in TABLE 3.4. The results are plotted at specific points along the component from the origin at the junction or in the case of a single component the left end. For flat plates the origin is indicated by the inside or outside radius. The number of points and distance (or angle for spherical shells) between points is specified by the user.

In many cases the maximum result value occurs at the junction, but this is not true in every case so it is important not to choose too large a step between points. As a first trial try 17 points with distance between points $<=0.3(R*T)^{1/2}$ or for spherical shells the angle between points $<=17.5/(Rs/T)^{1/2}$ degrees.

There is no plot of results for the compact ring.

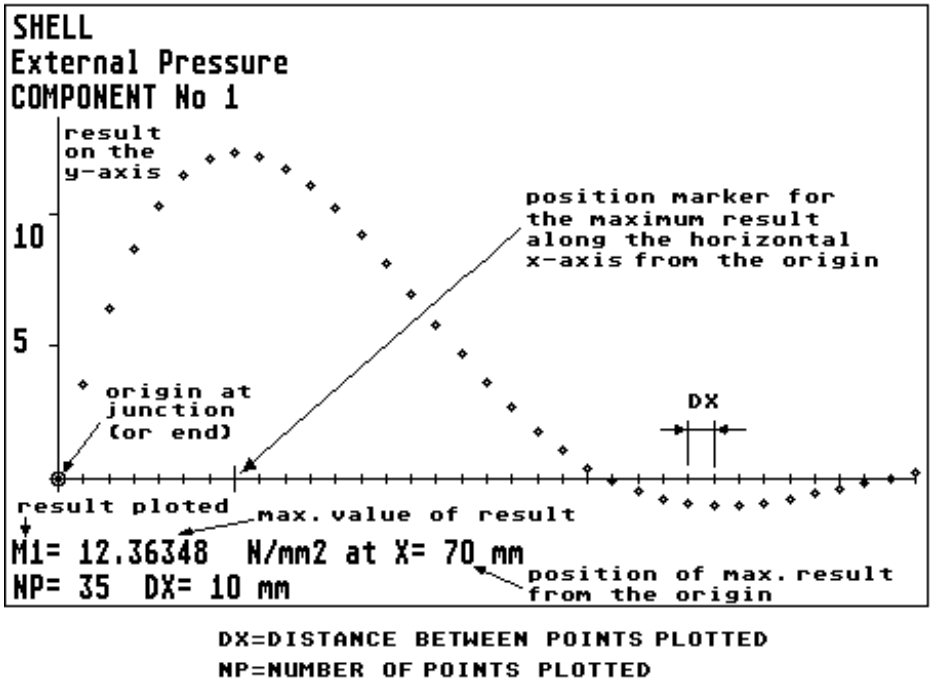

FIGURE 3.16 A typical result plot

Y Radial deflection, +ve outward

YL Transverse deflection for a flat plate +ve to the right

THETA Rotation, radians. +ve anti-clockwise

V Shear force/unit circumference. +ve outward (to right for a plate)

M1 Meridional bending moment/unit circumference. +ve if compression on the outside surface (left surface for a flat plate)

M2 Hoop bending moment/unit circumference. +ve as for M1

N1 Meridional membrane force/unit circumf. +ve tensile

N2 Hoop membrane force/unit circumference. +ve tensile

STRESSES +ve tensile, -ve compression.

SL Meridional membrane stress

SH Hoop membrane stress

SBL Meridional bending stress, ± at surface. Note the plot of SBL gives results for the outside surface (left surface if a flat plate)

SBH Hoop bending stress, ± at the surface. Note the plot of SBH gives results for the outside surface(left surface if a flat plate).

SLi Meridional stress on the shell inside surface

SLo Meridional stress on the shell outside surface

SHi Hoop stress on the shell inside surface

SHo Hoop stress on the shell outside surface

SLl Meridional stress on flat plate, left surface

SLr Meridional stress on flat plate, right surface

SHl Hoop stress on flat plate, left surface

SHr Hoop stress on flat plate, right surface

SV Average transverse shear stress, +ve if V is +ve.

TABLE 3.4 Summary of output results

3.6 PROGRAM EXAMPLES

In this section worked examples are presented in detail. The examples have been specially prepared for the following reasons.

(1) To show typical Input Data Sets for the "AJAP1" program.
(2) To show the working and features of the program.
(3) To show how the program can be used to analyse practical problems.
(4) To provide results that can be used as benchmarks for programmers.

Example 3.1 RING SUPPORTED THIN DOME

The thin reinforced concrete dome shown in FIGURE 3.17(a) is subjected to a uniform external pressure. The ends of the dome are embedded in a concrete ring. The ring is required to resist the radial force component Vo of the meridional load Fo as discussed in section 3.3.2. The ring is supported in the way of its centroid.

The input data set and the program defaults are given in FIGURE 3.17(c). A geometry plot is shown in FIGURE 3.17(b). The default applied junction moment and force are the applied external radial force and moment discussed in sections 3.3.2 and 3.3.3. The default free displacement is calculated as discussed in section 3.3.5. The default stiffness coefficients are as discussed in sections 2.3.2 and 2.3.5.

The junction results are given in FIGURE 3.17(d). The stress results for the meridional bending stress SBL and the hoop membrane stress SH along the dome from the junction with the concrete ring are listed in TABLE 3.5 case 1. Plots of SBL and SH are shown in FIGURES 3.17(e) and (f). Note that the results for spherical shells tend to break down as you approach the vertex, hence no solution is obtained at the vertex. On a plot, the break down in results tend to show up as an unexpected "tail", like that shown in FIGURE 3.17(f) at 39 degrees.

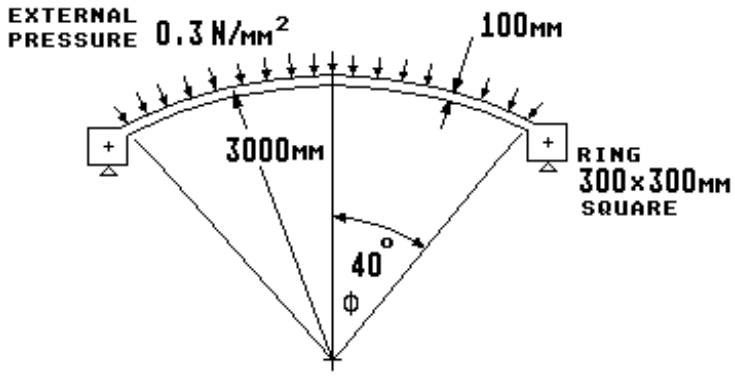

FIGURE 3.17(a) Thin dome subjected to external pressure

The effects of different end conditions can be investigated by altering the stiffness of the compact ring. This can be done by modifying the Young's modulus or by overwriting the default stiffness coefficients with specified values. For example if the Young's modulus of the ring is given a large value (say 1E15) the effects of a rigid ring can be obtained. The results are given in TABLE 3.5 case 2 and plots are shown in FIGURE 3.17(g) and (h). A comparison of these results show that the stiffness of the ring has a significant effect on the magnitude of the stresses and on the shape of the stress distribution local to the junction. For example, when the ring is concrete, the maximum bending stress is 8 degrees from the junction and the hoop stress is tensile at the junction. If the ring is rigid the maximum bending stress occurs at the junction but the hoop stress is compression throughout the dome. This sensitivity to the stiffness is very typical of a junction discontinuity analysis. Example 3.3 later will show how to analyse the dome when the edge has no ring support.

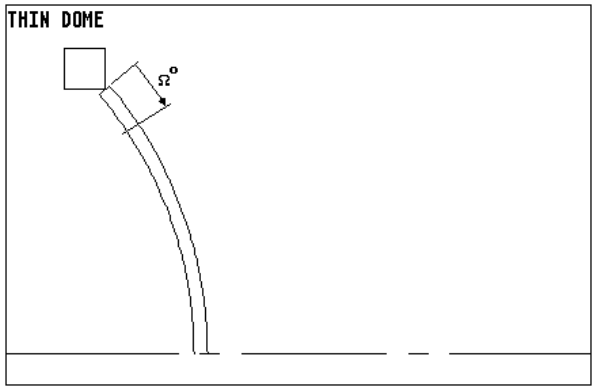

FIGURE 3.17(b) Geometry plot for example 3.1

	Meridional Bending Stress SBL (on outside surface) N/mm^2		Hoop Membrane Stress SH N/mm^2	
Ω°	Case 1 (concrete ring)	Case 2 (rigid ring)	Case 1 (concrete ring)	Case 2 (rigid ring)
0	1.58	7.21	2.21	-0.76
5	-3.23	1.08	-1.09	-1.46
10	-3.51	-1.31	-3.47	-2.86
15	-2.25	-1.59	-4.64	-3.95
20	-0.98	-1.09	-4.97	-4.52
25	-0.17	-0.52	-4.92	-4.70
30	0.18	-0.13	-4.76	-4.70
35	0.25	0.03	-4.65	-4.64

TABLE 3.5 Comparison of stresses in the thin dome, example 3.1

INPUT DATA, PROGRAM AJAP1

THIN DOME
External Pressure

COMPONENT No. 1
SPHERICAL SHELL, JUNCTION AT LEFT END
Rs= 3000 mm
T= 100 mm
PHI= 40 degrees
E= 24000 N/mm2
PR= .2
BETA= 7.135242
P= -.3 N/mm2
Fp= -289.2545 N/mm
Fo= -450 N/mm

COMPONENT No. 2
COMPACT RING AT JUNCTION
Rl= 2078.363 mm
Tl= 300 mm
Rr= 2078.363 mm
Tr= 300 mm
L= 300 mm
Rc= 2078.363 mm
AREA= 90000.01 mm2
Ina/C= 4500001 mm3
C= -150 mm
Lx 1 = -150 mm
Lx 2 = -150 mm
Lx 3 = 0 mm
Lx 4 = 150 mm
Lx 5 = 150 mm
Lx 6 = 150 mm
Lx 7 = 0 mm
Lx 8 = -150 mm
Lx 9 = 0 mm
CONNECTION 6 ,
E= 24000 N/mm2
PR= .2

APPLIED JUNCTION MOMENT & FORCE
Mo= -8319.816 Nmm/mm anti-clockwise
Vo= -344.72 N/mm outward

FREE DISPLACEMENTS AT JUNCTION
COMPONENT No. 1
Yf= -.2892545 mm inward
THf= 0 radians

COMPONENT No. 2
Yf= 0 mm
THf= 0 radians

STIFFNESS COEFFICIENTS
per mm circumference

COMPONENT No. 1
K(1 , 1)= 140.1774 N/mm
K(2 , 1)= 34831.4 Nmm/mm
K(3 , 1)= 34831.4 N/radian
K(4 , 1)= 4706749 Nmm/radian

COMPONENT No. 2
K(1 , 2)= 500.0472 N/mm
K(2 , 2)= 1E+15 Nmm/mm
K(3 , 2)= 1E+15 N/radian
K(4 , 2)= 3750355 Nmm/radian

FIGURE 3.17(c) Input data set and defaults for example 3.1 case 1

JUNCTION RESULTS	RESULTS COMPONENT No. 1
DISCONTINUITY FORCES & MOMENTS	THIN DOME
THIN DOME	External Pressure
External Pressure	OMEGA= 0 degrees
	Y= .2392662 mm
Mj 1 = -2635.202 Nmm/mm anti-clockwise	THETA= -1.871605E-03 radians
Vj 1 = -84.69193 N/mm outward	V= 54.43893 N/mm
	N1= -385.1222 N/mm
at centroid	N2= 220.7612 N/mm
Mj 2 = 7019.182 Nmm/mm clockwise	M1= -2635.204 Nmm/mm
Vj 2 = -260.0281 N/mm outward	M2= 959.9512 Nmm/mm
	STRESSES N/mm2
	SV= .5443893
	SL= -3.851222
	SH= 2.207612
Results for case 1	SBL=+or- 1.581122
with a concrete ring	SBH=+or- .5759708
(component 2, E=24000 N/mm^2)	SLo= -2.2701
	SLi= -5.432345
	SHo= 1.631641
	SHi= 2.783583

JUNCTION RESULTS	RESULTS COMPONENT No. 1
DISCONTINUITY FORCES & MOMENTS	THIN DOME
THIN DOME	External Pressure
External Pressure	OMEGA= 0 degrees
	Y= -1.788139E-07 mm
Mj 1 = -12010.87 Nmm/mm anti-clockwise	THETA= 2.328307E-10 radians
Vj 1 = -88.88416 N/mm outward	V= 57.13364 N/mm
	N1= -381.9108 N/mm
at centroid	N2= -76.38236 N/mm
Mj 2 = 17023.68 Nmm/mm clockwise	M1= -12010.87 Nmm/mm
Vj 2 = -255.8358 N/mm outward	M2= -2402.175 Nmm/mm [Corrected was M1]
	STRESSES N/mm2
	SV= .5713364
	SL= -3.819108
	SH= -.7638236
Results for case 2	SBL=+or- 7.206524
with a rigid ring	SBH=+or- 1.441305
(component 2, E=1E15 N/mm^2)	SLo= 3.387416
	SLi= -11.02563
	SHo= .6774814
	SHi= -2.205129

FIGURE 3.17(d) Junction results for the thin dome

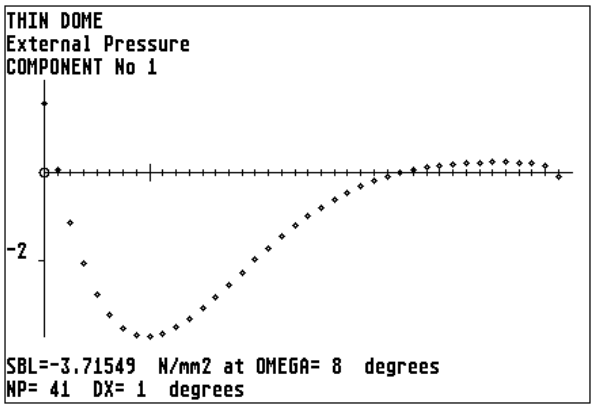

FIGURE 3.17(e) Meridional bending stress along the outside surface of the dome, case 1 with a concrete ring.

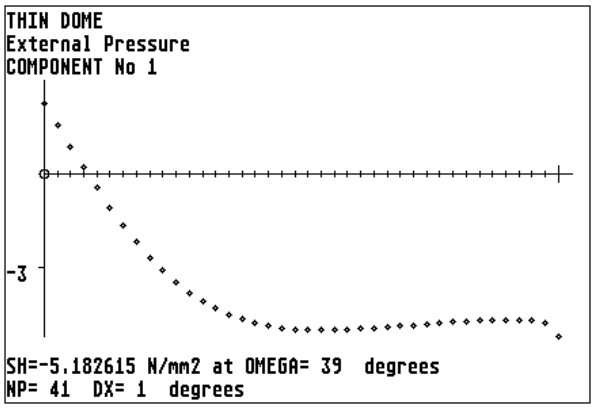

FIGURE 3.17(f) Hoop membrane stress in dome, case 1 with concrete ring.

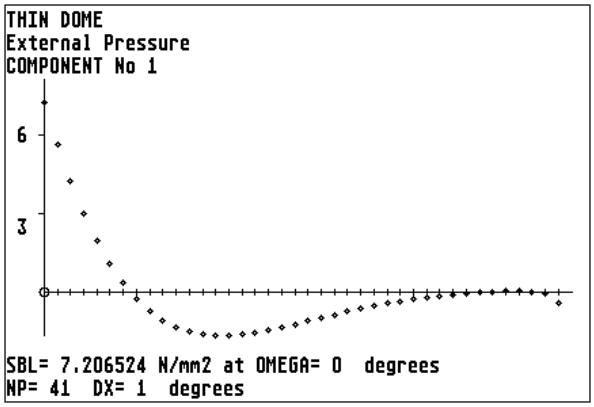

FIGURE 3.17(g) Meridional bending stress along the outside surface of the dome, case 2 with a rigid ring.

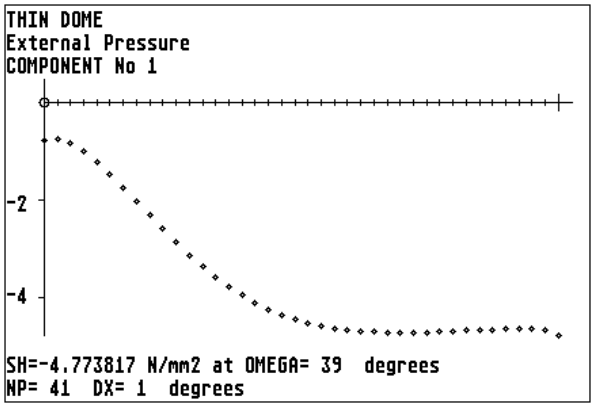

FIGURE 3.17(h) Hoop membrane stress in dome, case 2 with a rigid ring.

Example 3.2 STIFFENED CYLINDER

Many shell structures have circular rings or plates attached to the inside or outside surfaces. There can be several reasons for these attachments, for example:

(1) Thin shells that are subjected to external pressure often have stiffeners to maintain circularity and prevent buckling of the shell (but care must be taken that the stiffener itself does not sideways buckle).
(2) Fins are often attached to the shell to increase the gas side heat transfer coefficient.
(3) Ring attachments are often used for supporting the shell or there can be internals to be supported within the shell.
(4) Some mechanical items such as flanges have a stiffening effect on the shell.

The following cases show how "AJAP1" can be used to analyse a cylinder with an internal stiffener as shown in FIGURE 3.18(a). Three load cases will be considered as shown in FIGURE 3.18(b): internal pressure, a temperature differential and an internal support load.

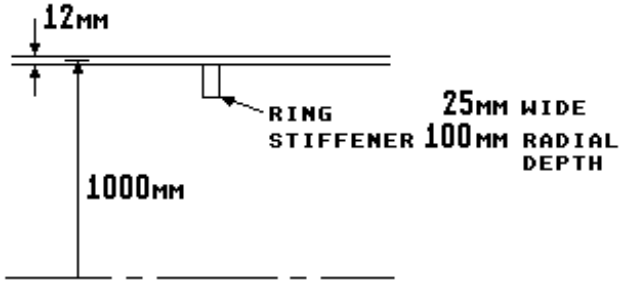

FIGURE 3.18(a) Cylinder with a ring stiffener, example 3.2

This example is analysed as a three component junction, i.e. two cylinders (components 1 and 2) and a flat plate (component 3) as the ring stiffener. FIGURE 3.18(c) shows the geometry plot for all three cases.

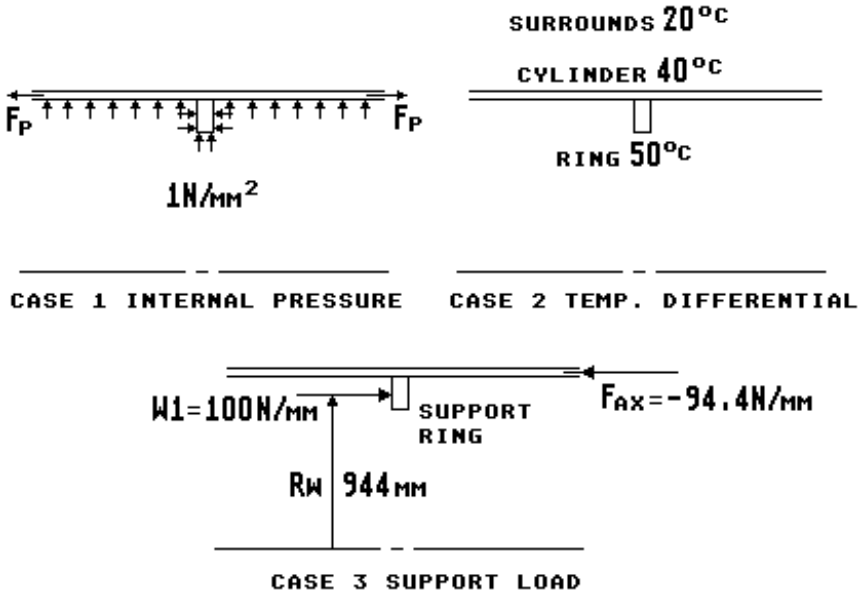

FIGURE 3.18(b) Loadings applied to the stiffened cylinder, example 3.2

Case 1 internal pressure. The loading is shown in FIGURE 3.18(b) and the input data set is given in FIGURE 3.18(d).

An internal pressure of P = 1 N/mm^2 is applied to the cylinders and also to the inside edge of the ring, qi = 1 N/mm^2. The default pressure end load Fp is applied to the cylinders, i.e. it is assumed that there are end caps closing the cylinder remote from the stiffening ring. There is an equal pressure on both sides of the ring so there is no net transverse pressure across the ring in the axial direction.

The junction results for both cylinders and the stiffener are shown in FIGURE 3.18(e). Due to symmetry of the geometry, materials and loading the stresses in the cylinders are identical.

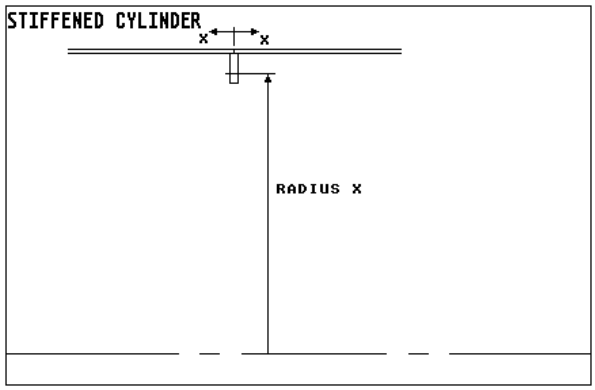

FIGURE 3.18(c) Geometry plot for a stiffened cylinder, example 3.2

INPUT DATA, PROGRAM AJAP1

STIFFENED CYLINDER
Internal pressure

COMPONENT No. 1
CYLINDER, JUNCTION AT RIGHT END
R= 1000 mm
T= 12 mm
E= 200000 N/mm2
PR= .3
BETA= 1.173411E-02 /mm
D= 3.164835E+07 Nmm
P= 1 N/mm2
Fp= 500 N/mm
Fo= 500 N/mm

COMPONENT No. 2
CYLINDER, JUNCTION AT LEFT END
R= 1000 mm
T= 12 mm
E= 200000 N/mm2
PR= .3
BETA= 1.173411E-02 /mm
D= 3.164835E+07 Nmm
P= 1 N/mm2
Fp= 500 N/mm
Fo= 500 N/mm

COMPONENT No. 3
FLAT PLATE, JUNCTION AT O.D.
JUNCTION POSITION, CENTRE
JP= 0
OFFSET= 0 mm
Ro= 994 mm
Ri= 894 mm
T= 25 mm
E= 200000 N/mm2
PR= .3
D= 2.861722E+08 Nmm
qo= 0 N/mm2
qi= 1 N/mm2

FREE DISPLACEMENTS AT JUNCTION
COMPONENT No. 1
Yf= .3541667 mm outward
THf= 0 radians

COMPONENT No. 2
Yf= .3541667 mm outward
THf= 0 radians

COMPONENT No. 3
Yf= 4.207842E-02 mm outward
THf= 0 radians

STIFFNESS COEFFICIENTS
per mm circumference

COMPONENT No. 1
K(1 , 1)= 102.2659 N/mm
K(2 , 1)= 8715.274 Nmm/mm
K(3 , 1)= 8715.274 N/radian
K(4 , 1)= 371365.1 Nmm/radian

COMPONENT No. 2
K(1 , 2)= 102.2659 N/mm
K(2 , 2)= 8715.274 Nmm/mm
K(3 , 2)= 8715.274 N/radian
K(4 , 2)= 371365.1 Nmm/radian

COMPONENT No. 3
K(1 , 3)= 548.758 N/mm
K(2 , 3)= 1E+15 Nmm/mm
K(3 , 3)= 1E+15 N/radian
K(4 , 3)= 28581.15 Nmm/radian

FIGURE 3.18(d) Input data set and defaults for example 3.2 case 1

The hoop membrane stress remote from the junction with the ring is SH = 83.33 N/mm^2. FIGURE 3.18(f) shows a plot of the hoop membrane stress along the cylinder from the junction. It is seen that there

is a significant reduction in the hoop membrane stress close to the junction with the ring, but that only a short distance from the ring the hoop stress has returned to its remote value. Many closely spaced stiffening rings are required to sufficiently stiffen a cylinder so that the general level of the hoop stress is reduced. The highest stress in the cylinder is the meridional membrane plus bending stress on the inside surface, SLi. FIGURE 3.18(g) shows a plot of this stress. The highest stress is 106.59 N/mm^2 at the junction with the ring. This value is 28% higher than the hoop membrane stress remote from the junction. Had the stiffening ring been considered as rigid (by putting Young's modulus to a large value, E=1E15 N/mm^2 and Poisson's ratio to a small value, PR=1E-6) then the meridional stress would have increased to 170.28 N/mm^2 and approaches the value predicted by equation (1.6).

The highest stress in the ring stiffener is the hoop membrane stress. A plot of this stress is shown in FIGURE 3.18(h). The stress is almost uniform across the plate. This indicates that a compact ring could also have been used to solve this case.

JUNCTION RESULTS
DISCONTINUITY FORCES & MOMENTS
STIFFENED CYLINDER
Internal Pressure

Mj 1 = 1558.313 Nmm/mm anti-clockwise
Vj 1 = 36.57081 N/mm inward

Mj 2 = 1558.313 Nmm/mm clockwise
Vj 2 = 36.57081 N/mm inward

Mj 3 = -2.051008E-09 Nmm/mm anti-clockwise
Vj 3 = -73.14161 N/mm outward

RESULTS COMPONENT No. 1
STIFFENED CYLINDER
Internal Pressure
X= 0 in
Y= .1753641 mm
THETA= 4.656613E-10 radians
V= -36.57081 N/mm
N1= 500 N/mm
N2= 570.8739 N/mm
M1= 1558.313 Nmm/mm
M2= 467.4939 Nmm/mm
STRESSES N/mm2
SV= -3.047568
SL= 41.66667
SH= 47.57283
SBL=+or- 64.9297
SBH=+or- 19.47891
SLo= -23.26304
SLi= 106.5964
SHo= 28.09392
SHi= 67.05174

RESULTS COMPONENT No. 2
STIFFENED CYLINDER
Internal Pressure
X= 0 mm
Y= .1753641 mm
THETA= -4.656613E-10 radians
V= -36.57081 N/mm
N1= 500 N/mm
N2= 570.8739 N/mm
M1= 1558.313 Nmm/mm
M2= 467.4939 Nmm/mm
STRESSES N/mm2
SV= -3.047568
SL= 41.66667
SH= 47.57283
SBL=+or- 64.9297
SBH=+or- 19.47891
SLo= -23.26304
SLi= 106.5964
SHo= 28.09392
SHi= 67.05174

RESULTS COMPONENT No. 3
STIFFENED CYLINDER
Internal Pressure
radius X= 994 mm
YL= -8.673618E-19 mm
Y= .1753641 mm
THETA= 7.176088E-14 radians
V= 0 N/mm
N1= 73.14161 N/mm
N2= 904.0559 N/mm
M1= 2.051008E-09 Nmm/mm
M2= 1.941583E-08 Nmm/mm
STRESSES N/mm2
SV= 0
SL= 2.925665
SH= 36.16224
SBL=+or- 1.968968E-11
SBH=+or- 1.86392E-10
SLl= 2.925665
SLr= 2.925665
SHl= 36.16224
SHr= 36.16224

FIGURE 3.18(e) Junction results for example 3.2 case 1

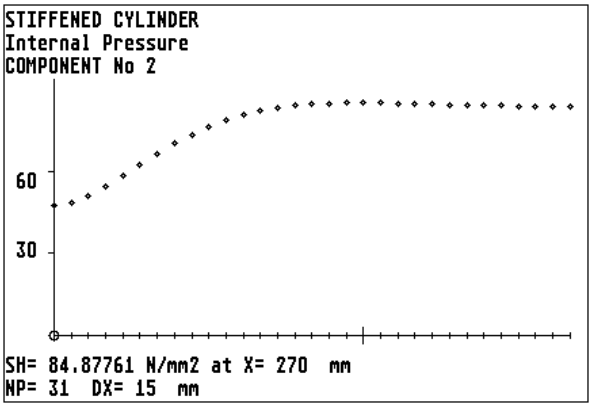

FIGURE 3.18(f) Hoop membrane stress along the cylinder from the junction

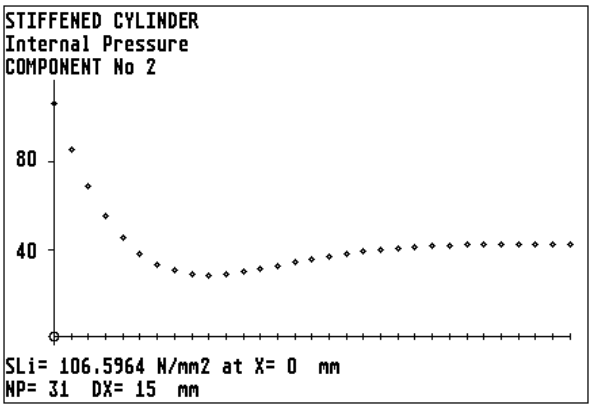

FIGURE 3.18(g) Meridional stress along the inside surface of the cylinder from the junction

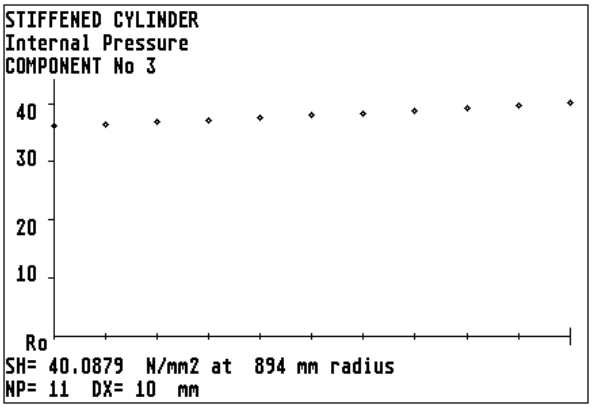

FIGURE 3.18(h) Hoop membrane stress along the ring stiffener from the outside radius (the junction) to the inside radius

Case 2 temperature differential. The loading is shown in FIGURE 3.18(b) and the input data set is given in FIGURE 3.18(i).

The cylinder is at a uniform temperature of 40°C and the surrounding ambient temperature is 20°C. Due to the process fluid within the cylinder the internal ring is at a temperature 10°C higher than the mean temperature of the cylinder. The material of the cylinder and ring is a carbon steel with a coefficient of thermal expansion of 0.000012 mm/mm°C. The cylinder will therefore be pushed outward by the radial expansion of the stiffener ring.

The junction results for both cylinders and the internal ring are shown in FIGURE 3.18(j). Due to symmetry of the geometry, materials and loading the stresses in the cylinders are identical. The highest stress is the meridional bending stress of 24.51 N/mm^2 at the junction. The hoop membrane plus bending stress on the outside surface is not quite as high at 20.85 N/mm^2. This stress is mainly due to the hoop membrane stress of 13.5 N/mm^2 as a result of the ring expansion pushing the cylinder outward. If the ring had been considered as rigid the maximum bending stress would have been 42.79 N/mm^2, i.e. approaching the value predicted by equation (1.7).

The expansion of the ring produces both bending and membrane stresses in the cylinder at the junction. FIGURES 3.18(k) and (L) show the plots of the meridional bending stress SBL and the hoop membrane stress SH along the cylinder from the junction. The stresses reduce rapidly away from the junction. At points remote from the junction the cylinder stresses are zero.

Example 3.2, temperature differential

INPUT DATA, PROGRAM AJAP1

STIFFENED CYLINDER
Temperature Differential

COMPONENT No. 1
CYLINDER, JUNCTION AT RIGHT END
R= 1000 mm
T= 12 mm
E= 200000 N/mm2
PR= .3
ALPHA= .000012 /degC
BETA= 1.173411E-02 /mm
D= 3.164835E+07 Nmm
Ta= 20 degC
Tm= 40 degC

COMPONENT No. 2
CYLINDER, JUNCTION AT LEFT END
R= 1000 mm
T= 12 mm
E= 200000 N/mm2
PR= .3
ALPHA= .000012 /degC
BETA= 1.173411E-02 /mm
D= 3.164835E+07 Nmm
Ta= 20 degC
Tm= 40 degC

COMPONENT No. 3
FLAT PLATE, JUNCTION AT O.D.
JUNCTION POSITION, CENTRE
JP= 0
OFFSET= 0 mm
Ro= 994 mm
Ri= 894 mm
T= 25 mm
E= 200000 N/mm2
PR= .3
ALPHA= .000012 /degC
D= 2.861722E+08 Nmm
Ta= 20 degC
Tm= 50 degC

FREE DISPLACEMENTS AT JUNCTION
COMPONENT No. 1
Yf= .24 mm outward
THf= 0 radians

COMPONENT No. 2
Yf= .24 mm outward
THf= 0 radians

COMPONENT No. 3
Yf= .35784 mm outward
THf= 0 radians

STIFFNESS COEFFICIENTS
per mm circumference

COMPONENT No. 1
K(1 , 1)= 102.2659 N/mm
K(2 , 1)= 8715.274 Nmm/mm
K(3 , 1)= 8715.274 N/radian
K(4 , 1)= 371365.1 Nmm/radian

COMPONENT No. 2
K(1 , 2)= 102.2659 N/mm
K(2 , 2)= 8715.274 Nmm/mm
K(3 , 2)= 8715.274 N/radian
K(4 , 2)= 371365.1 Nmm/radian

COMPONENT No. 3
K(1 , 3)= 548.758 N/mm
K(2 , 3)= 1E+15 Nmm/mm
K(3 , 3)= 1E+15 N/radian
K(4 , 3)= 28581.15 Nmm/radian

FIGURE 3.18(i) Input data set and defaults for example 3.2 case 2

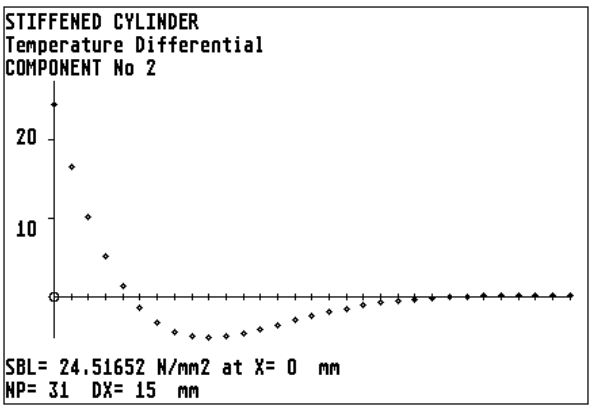

FIGURE 3.18(k) Meridional bending stress along outside surface of the cylinder from the junction

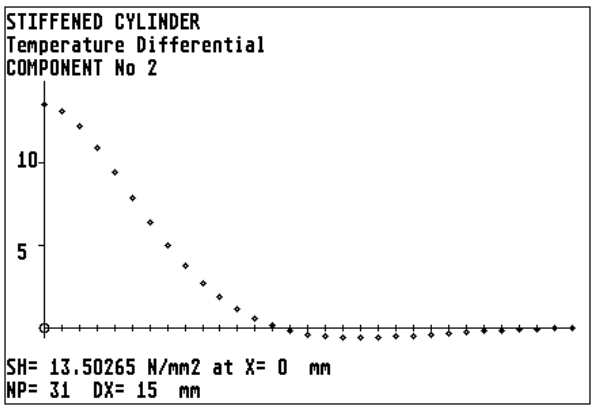

FIGURE 3.18(L) Hoop membrane stress along the the cylinder from the junction

JUNCTION RESULTS
DISCONTINUITY FORCES & MOMENTS
STIFFENED CYLINDER
Temperature Differential

Mj 1 = -588.3963 Nmm/mm clockwise
Vj 1 = -13.80861 N/mm outward

Mj 2 = -588.3963 Nmm/mm anti-clockwise
Vj 2 = -13.80861 N/mm outward

Mj 3 = 7.74431E-10 Nmm/mm clockwise
Vj 3 = 27.61721 N/mm inward

RESULTS COMPONENT No. 1
STIFFENED CYLINDER
Temperature Differential
X= 0 in
Y= .3075132 mm
THETA= -1.164153E-10 radians
V= 13.80861 N/mm
N1= 0 N/mm
N2= 162.0318 N/mm
M1= -588.3963 Nmm/mm
M2= -176.5189 Nmm/mm
STRESSES N/mm2
SV= 1.150717
SL= 0
SH= 13.50265
SBL=+or- 24.51652
SBH=+or- 7.354954
SLo= 24.51652
SLi= -24.51652
SHo= 20.8576
SHi= 6.147693

RESULTS COMPONENT No. 2
STIFFENED CYLINDER
Temperature Differential
X= 0 mm
Y= .3075132 mm
THETA= 1.164153E-10 radians
V= 13.80861 N/mm
N1= 0 N/mm
N2= 162.0318 N/mm
M1= -588.3963 Nmm/mm
M2= -176.5189 Nmm/mm
STRESSES N/mm2
SV= 1.150717
SL= 0
SH= 13.50265
SBL=+or- 24.51652
SBH=+or- 7.354954
SLo= 24.51652
SLi= -24.51652
SHo= 20.8576
SHi= 6.147693

RESULTS COMPONENT No. 3
STIFFENED CYLINDER
Temperature Differential
radius X= 994 mm
YL= 0 mm
Y= .3075132 mm
THETA= -2.709587E-14 radians
V= 0 N/mm
N1= -27.61721 N/mm
N2= -261.4379 N/mm
M1= -7.744309E-10 Nmm/mm
M2= -7.331137E-09 Nmm/mm
STRESSES N/mm2
SV= 0
SL= -1.104688
SH= -10.45752
SBL=+or- 7.434536E-12
SBH=+or- 7.037892E-11
SLl= -1.104688
SLr= -1.104688
SHl= -10.45752
SHr= -10.45752

FIGURE 3.18(j) Junction results for example 3.2 case 2

Case 3 support load. The loading is shown in FIGURE 3.18(b) and the input data set is given in FIGURE 3.18(m).

The internal support ring is subjected to a uniform load W1 of 100 N/mm circumference at a radius Rw of 944 mm. This load is transmitted to the ground via the cylinder, component 2. The axial load F_{AX} in the cylinder is calculated from the applied load W1 as follows:

Load at radius R = Applied load at radius Rw times radius Rw/radius R
therefore F_{AX} = W1*Rw/R = 100*944/1000 = -94.4 N/mm
A negative sign is applied to the input since F_{AX} is in compression.

The default applied junction moment Mo = -566.4 Nmm/mm is due to the axial load times the radial distance to the junction, in this case half the cylinder thickness.

therefore Mo = F_{AX}*T/2 = 94.4*12/2 = -566.4 Nmm/mm
The negative sign is due to the moment acting anti-clockwise.

Example 3.2, support load

The junction results for both cylinders and the support ring are shown in FIGURE 3.18(n). Due to the axial loading on the cylinder, component 2, the stresses in the cylinders will *not* be identical (had there been no axial load, the stresses would have been equal but opposite sign).

The highest stress in the cylinder is the meridional membrane plus bending stress SLi= -115.77 N/mm^2 on the inside surface of component No.2 at the junction. A plot of this stress is shown in FIGURE 3.18(o). At distances remote from the junction this stress reduces to the membrane value of SL= -7.86 N/mm^2.

The highest stress in the support is the meridional bending stress SBL= 44.85 N/mm^2. A plot of this stress and a plot of the average shear stress, between the junction radius and inside radius, is shown in FIGURES 3.18(p) and 3.18(q). These plots show a typical cantilever stress distribution between the support load radius and the junction radius. A plot of the hoop bending stress in the support is shown in FIGURE 3.18(r). This stress is a result of the support tending to rotate as a ring.

Although in this case the highest stress occurred in the cylinder, in general, it is possible for high stresses to be generated in the support ring. This usually occurs when the ring is thinner than the cylinder. In cases where the ring is narrow in the radial direction and subjected to heavy loads the shear stress in the ring may be significant.

INPUT DATA, PROGRAM AJAP1

STIFFENED CYLINDER
Support Load

COMPONENT No. 1
CYLINDER, JUNCTION AT RIGHT END
R= 1000 mm
T= 12 mm
E= 200000 N/mm2
PR= .3
BETA= 1.173411E-02 /mm
D= 3.164835E+07 Nmm

COMPONENT No. 2
CYLINDER, JUNCTION AT LEFT END
R= 1000 mm
T= 12 mm
E= 200000 N/mm2
PR= .3
BETA= 1.173411E-02 /mm
D= 3.164835E+07 Nmm
Fax= -94.4 N/mm
Fo= -94.4 N/mm

COMPONENT No. 3
FLAT PLATE, JUNCTION AT O.D.
JUNCTION POSITION, CENTRE
JP= 0
OFFSET= 0 mm
Ro= 994 mm
Ri= 894 mm
T= 25 mm
E= 200000 N/mm2
PR= .3
D= 2.861722E+08 Nmm
W 1 = 100 N/mm
Rw= 944 mm

APPLIED JUNCTION MOMENT & FORCE
Mo= -566.4 Nmm/mm anti-clockwise
Vo= 0 N/mm

FREE DISPLACEMENTS AT JUNCTION
COMPONENT No. 1
Yf= 0 mm
THf= 0 radians

COMPONENT No. 2
Yf= .0118 mm outward
THf= 0 radians

COMPONENT No. 3
Yf= 0 mm
THf= .1670666 radians anti-clockwise

STIFFNESS COEFFICIENTS
per mm circumference

COMPONENT No. 1
K(1 , 1)= 102.2659 N/mm
K(2 , 1)= 8715.274 Nmm/mm
K(3 , 1)= 8715.274 N/radian
K(4 , 1)= 371365.1 Nmm/radian

COMPONENT No. 2
K(1 , 2)= 102.2659 N/mm
K(2 , 2)= 8715.274 Nmm/mm
K(3 , 2)= 8715.274 N/radian
K(4 , 2)= 371365.1 Nmm/radian

COMPONENT No. 3
K(1 , 3)= 548.758 N/mm
K(2 , 3)= 1E+15 Nmm/mm
K(3 , 3)= 1E+15 N/radian
K(4 , 3)= 28581.15 Nmm/radian

FIGURE 3.18(m) Input data set and defaults for example 3.2 case 3

JUNCTION RESULTS
DISCONTINUITY FORCES & MOMENTS
STIFFENED CYLINDER
Support Load

Mj 1 = 2648.737 Nmm/mm anti-clockwise
Vj 1 = 30.82288 N/mm inward

Mj 2 = -2589.818 Nmm/mm anti-clockwise
Vj 2 = -29.44013 N/mm outward

Mj 3 = 4672.183 Nmm/mm clockwise
Vj 3 = -1.382722 N/mm outward

RESULTS COMPONENT No. 1
STIFFENED CYLINDER
Support Load
X= 0 in
Y= 2.519727E-03 mm
THETA= 3.595785E-03 radians
V= -30.82288 N/mm
N1= 0 N/mm
N2= 6.047344 N/mm
M1= 2648.737 Nmm/mm
M2= 794.6212 Nmm/mm
STRESSES N/mm2
SV= -2.568573
SL= 0
SH= .5039454
SBL=+or- 110.3641
SBH=+or- 33.10922
SLo= -110.3641
SLi= 110.3641
SHo= -32.60528
SHi= 33.61316

RESULTS COMPONENT No. 2
STIFFENED CYLINDER
Support Load
X= 0 mm
Y= 2.519736E-03 mm
THETA= 3.595785E-03 radians
V= 29.44013 N/mm
N1= -94.4 N/mm
N2= -22.27264 N/mm
M1= -2589.818 Nmm/mm
M2= -776.9453 Nmm/mm
STRESSES N/mm2
SV= 2.453344
SL= -7.866667
SH= -1.856053
SBL=+or- 107.9091
SBH=+or- 32.37272
SLo= 100.0424
SLi= -115.7757
SHo= 30.51667
SHi= -34.22877

RESULTS COMPONENT No. 3
STIFFENED CYLINDER
Support load
radius X= 994 mm
YL= -2.886634E-06 mm
Y= 2.519729E-03 mm
THETA= 3.595817E-03 radians
V= -94.96982 N/mm
N1= 1.382722 N/mm
N2= 13.08951 N/mm
M1= -4672.183 Nmm/mm
M2= -459.5921 Nmm/mm
STRESSES N/mm2
SV= -3.798793
SL= 5.530888E-02
SH= .5235806
SBL=+or- 44.85296
SBH=+or- 4.412085
SLl= 44.90827
SLr= -44.79765
SHl= 4.935665
SHr= -3.888504

FIGURE 3.18(n) Junction results for example 3.2 case 3

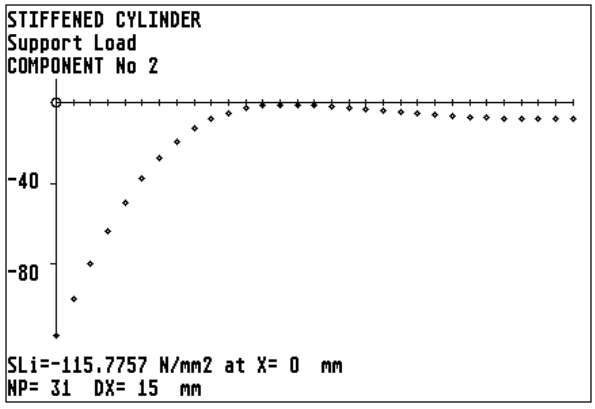

FIGURE 3.18(o) Meridional stress along the inside surface of the cylinder from the junction

FIGURE 3.18(p) Meridional bending stress along the left surface of the support ring

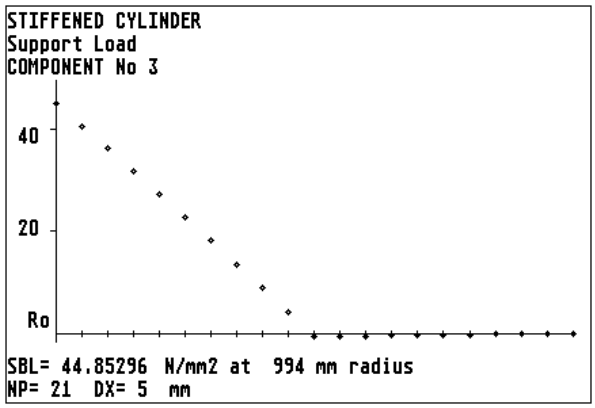

FIGURE 3.18(q) Average shear stress in the support ring

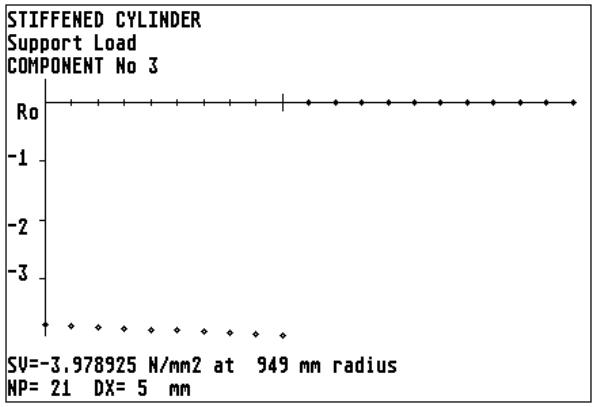

FIGURE 3.18(r) Hoop bending stress along the left surface of the support ring

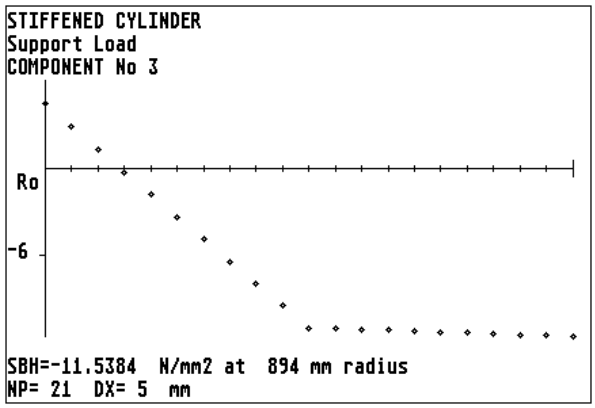

Example 3.3 SIMPLY SUPPORTED THIN DOME

This example illustrates how to analyse components that are simply supported. The thin reinforced concrete dome of Example 3.1 will be used in this example but without the ring support. The geometry and loading are shown in FIGURE 3.19(a).

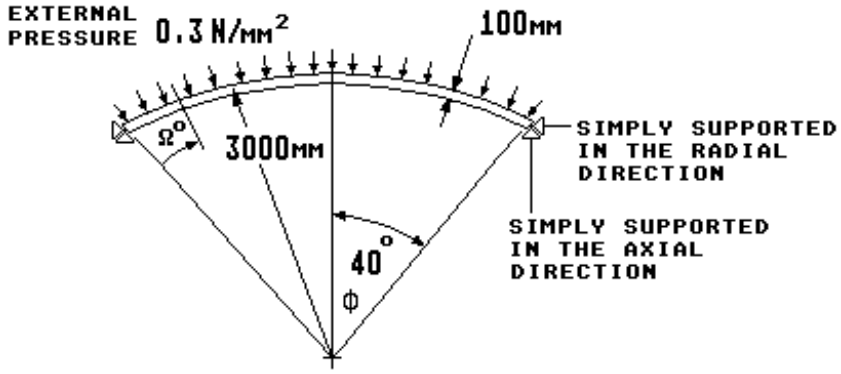

FIGURE 3.19(a) Simply supported thin dome subjected to external pressure

Two load cases will be considered:

(1) supported in the axial direction only
(2) supported in both axial and radial direction

Case 1 supported in the axial direction only. The input data set and result at Ω = 0 (at the support) are shown in FIGURE 3.19(b).

The results for this case are obtained directly due to the program defaults discussed in section 3.3.1 and 3.3.2, i.e. the pressure end load Fp is obtained by the application of the meridional load Fo and the applied radial force Vo. TABLE 3.6 case 1 lists the meridional bending stress SBL and the hoop membrane stress SH at several points from the supported edge. Plots of these stresses are shown in FIGURES 3.19(c) and (d). By comparison these stresses are significantly higher than those in Example 3.1 where a ring support is provided.

INPUT DATA, PROGRAM AJAP1	RESULTS COMPONENT No. 1
	SIMPLY SUPPORTED THIN DOME
SIMPLY SUPPORTED THIN DOME	External Pressure
External Pressure	OMEGA= 0 degrees
SPHERICAL SHELL	Y= 2.169913 mm
Rs= 3000 mm	THETA= -9.896815E-03 radians
T= 100 mm	V= 221.5817 N/mm
PHI= 40 degrees	N1= -185.9293 N/mm
E= 24000 N/mm2	N2= 2663.443 N/mm
PR= .2	M1= -4.031447E-03 Nmm/mm
BETA= 7.135242	M2= 7863.03 Nmm/mm
P= -.3 N/mm2	STRESSES N/mm2
Fp= -289.2545 N/mm	SV= 2.215817
Fo= -450 N/mm	SL= -1.859293
	SH= 26.63443
APPLIED END MOMENT & FORCE	SBL=+or- 2.418868E-06
Mo= 0 Nmm/mm	SBH=+or- 4.717818
Vo= -344.72 N/mm outward	SLo= -1.85929
	SLi= -1.859295
	SHo= 21.91661
	SHi= 31.35224

FIGURE 3.19(b) Input data set and result at Ω = 0 for case 1 external pressure and axial support only

	Meridional Bending Stress SBL (on outside surface) N/mm^2		Hoop Membrane Stress SH N/mm^2	
Ω°	Case 1 (axial support)	Case 2 (axial & radial support)	Case 1 (axial support)	Case 2 (axial & radial support)
0	0.0	0.0	26.63	-0.84
5	-18.31	-2.15	10.02	-2.80
10	-17.04	-2.00	-0.95	-4.08
15	-10.05	-1.18	-5.87	-4.66
20	-3.90	-0.46	-7.00	-4.80
25	-0.32	-0.04	-6.48	-4.73
30	1.09	0.13	-5.64	-4.63
35	1.28	0.15	-5.14	-4.57

TABLE 3.6 Comparison of stresses in the thin dome, example 3.3 [Corrected was example 3.1]

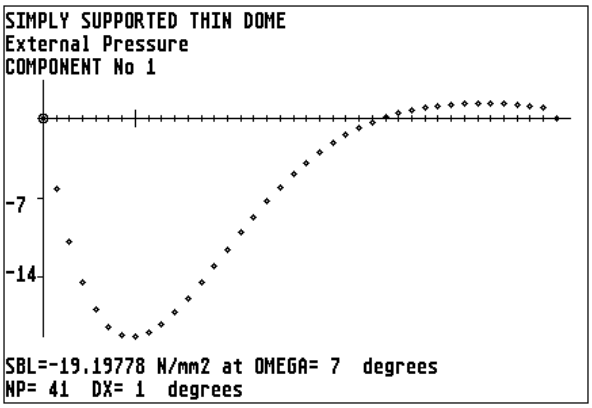

FIGURE 3.19(c) Meridional bending stress along the outside of the dome from the support, case 1 with axial support only.

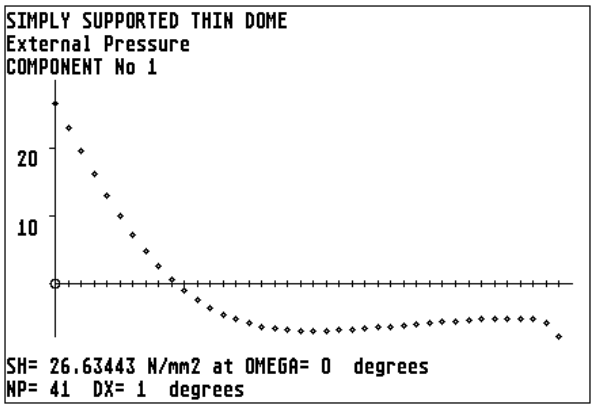

FIGURE 3.19(d) Hoop membrane stress, case 1 with axial support.

Case 2 supported in both the axial and radial direction. In this case a solution cannot be obtained directly, we must proceed in the following manner:

(1) A unit radial force case is run to obtain the radial deflection at the support. FIGURE 3.19(e) shows the input data set and results at Ω = 0. The radial deflection Y = 0.0071338 mm for a radial force Vo = 1 N/mm.

(2) The external pressure case 1 above is run with the axial support only. FIGURE 3.19(b) shows that the radial deflection at the end (Ω = 0) with no radial support is Y = 2.1699 mm and the default radial force Vo = -344.72 N/mm outward.

(3) The force necessary to bring the end support radial deflection in (2) back to zero is calculated, by hand, knowing the radial deflection in (1) for a unit radial force. i.e. Vo = 2.1699/0.0071338 = 304.173 N/mm inward.

(4) The net radial force at the support is calculated, by hand, knowing the default value in (2) and the value in (3) required to bring the support radial deflection to zero. i.e. Vo = -344.72 + 304.173 = -40.547 N/mm outward.

(5) Finally the solution is obtained by running "AJAP1" for external pressure and overwriting the default Vo with the value calculated in (4).

The input data set and result at Ω = 0 (at the support) are shown in FIGURE 3.19(f). TABLE 3.6 case 2 lists the meridional bending stress SBL and the hoop membrane stress SH at several points from the supported edge.

Plots of these stresses are shown in FIGURES 3.19(g) and (h). These stresses are significantly different from case 1 stresses. By comparison these case 2 stresses are of a similar order of magnitude to the results of Example 3.1 where a ring support is provided. This confirms the necessity of providing adequate support at the edges of shell structures.

Example 3.3

INPUT DATA, PROGRAM AJAP1	RESULTS COMPONENT No. 1
	SIMPLY SUPPORTED THIN DOME
SIMPLY SUPPORTED THIN DOME	Unit Radial Force
Unit Radial Force	OMEGA= 0 degrees
SPHERICAL SHELL	Y= -7.133815E-03 mm
Rs= 3000 mm	THETA= 2.870972E-05 radians
T= 100 mm	V= -.6427876 N/mm
PHI= 40 degrees	N1= -.7660443 N/mm
E= 24000 N/mm2	N2= -9.031804 N/mm
PR= .2	M1= 1.169485E-05 Nmm/mm
BETA= 7.135242	M2= -22.80991 Nmm/mm
	STRESSES N/mm2
APPLIED END MOMENT & FORCE	SV= -6.427876E-03
Mo= 0 Nmm/mm	SL= -7.660443E-03
Vo= 1 N/mm inward	SH= -9.031804E-02
	SBL=+or- 7.016908E-09
	SBH=+or- 1.368594E-02
FIGURE 3.19(e) Input data set	SLo= -7.66045E-03
and result at Ω = 0 for a unit	SLi= -7.660436E-03
radial force Vo	SHo= -.0766321
	SHi= -.104004

INPUT DATA, PROGRAM AJAP1	RESULTS COMPONENT No. 1
SIMPLY SUPPORTED THIN DOME	SIMPLY SUPPORTED THIN DOME
External Pressure	External Pressure
SPHERICAL SHELL	OMEGA= 0 degrees
Rs= 3000 mm	Y= 2.980232E-07 mm
T= 100 mm	THETA= -1.164093E-03 radians
PHI= 40 degrees	V= 26.06311 N/mm
E= 24000 N/mm2	N1= -418.9392 N/mm
PR= .2	N2= -83.78745 N/mm
BETA= 7.135242	M1= -4.74191E-04 Nmm/mm
P= -.3 N/mm2	M2= 924.8733 Nmm/mm
Fp= -289.2545 N/mm	STRESSES N/mm2
Fo= -450 N/mm	SV= .2606311
	SL= -4.189392
APPLIED END MOMENT & FORCE	SH= -.8378745
Mo= 0 Nmm/mm	SBL=+or- 2.845146E-07
Vo= -40.547 N/mm outward	SBH=+or- .554924
	SLo= -4.189392
FIGURE 3.19(f) Input data set and result	SLi= -4.189393
at Ω = 0 for case 2 external pressure with	SHo= -1.392798
axial and radial support	SHi= -.2829505

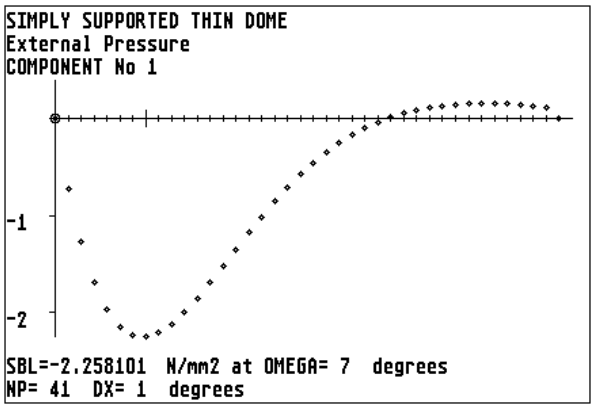

FIGURE 3.19(g) Meridional bending stress along the outside of the dome from the support, case 2 with axial and radial support.

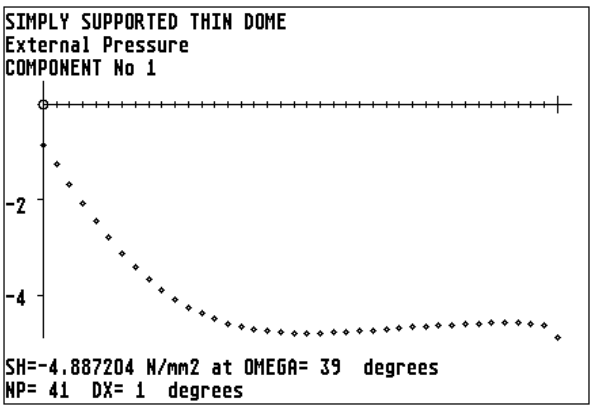

FIGURE 3.19(h) Hoop membrane stress, case 2 with axial and radial support.

Example 3.4 CONE-SPHERE JUNCTION

This example is chosen to test the validity of the conical shell solution. The test makes use of the suggestion, by HETÉNYI in reference (12), that the equations for spherical shells can be used for approximate calculations for conical shells. In order to test this a 45 degree cone is connected to a spherical shell as shown in FIGURE 3.20(a). The junction of the cone and sphere is loaded by an applied radial force of 50 N/mm circumference.

The input data set is shown in FIGURE 3.20(b) and the results for the junction are given in FIGURE 3.20(c). TABLE 3.7 shows the comparison of results at equivalent positions on the two components, i.e. at X= Ω*Rs*π/180 on the cone. By inspection it is seen that the results are in agreement close to the junction. This also tends to confirm BAKER's (ref. 8) suggestion that the shape of the shell beyond 20 degrees does not seriously affect the solution at the loaded end.

The above test can be repeated for an applied moment in place of the radial force. The same conclusions can be obtained.

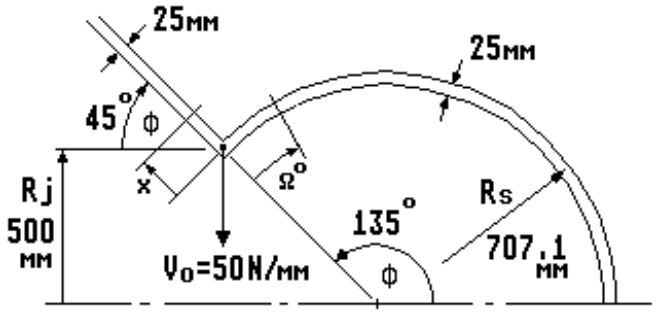

FIGURE 3.20(a) Cone and sphere junction subjected to a radial force Vo

		Meridional Moment M1		Hoop Bending Moment M2	
X mm	Ω°	CONE Nmm/mm	SPHERE Nmm/mm	CONE Nmm/mm	SPHERE Nmm/mm
0	0	912.19	912.19	274.41	272.89
30.85	2.5	435.79	436.11	156.29	153.96
61.71	5	132.69	124.93	73.89	67.29
123.41	10	-129.06	-145.97	-9.76	-21.72
185.11	15	-157.34	-164.81	-30.42	-39.16
246.82	20	-111.82	-104.79	-26.14	-28.28
308.53	25	-60.95	-45.89	-16.14	-13.45
370.23	30	-25.31	-10.52	-7.75	-3.48
431.94	35	-5.67	4.06	-2.55	0.98
493.65	40	2.82	6.81	1.97	1.96
		Meridional Force N1		Hoop Membrane Force N2	
X mm	Ω°	CONE N/mm	SPHERE N/mm	CONE N/mm	SPHERE N/mm
0	0	17.83	17.52	-127.71	-127.80
30.85	2.5	12.03	11.17	-113.06	-114.03
61.71	5	7.47	6.46	-90.22	-91.17
123.41	10	1.91	1.29	-45.65	-44.59
185.11	15	-0.28	-0.32	-16.41	-13.69
246.82	20	-0.80	-0.48	-2.00	0.56
308.53	25	-0.68	-0.27	3.17	4.46
370.23	30	-0.43	-0.10	3.87	3.84
431.94	35	-0.21	-0.02	2.95	2.15
493.65	40	-0.08	0.0006	1.78	0.80

TABLE 3.7 Results comparison for cone and sphere, example 3.4

```
INPUT DATA, PROGRAM AJAP1

CONE-SPHERE JUNCTION
Applied Radial Force

COMPONENT No. 1
CONE, JUNCTION AT SMALL RIGHT END
Rj= 500 mm
T= 25 mm
PHI= 45 degrees
E= 200000 N/mm2
PR= .3

COMPONENT No. 2
SPHERICAL SHELL, JUNCTION AT LEFT END
Rs= 707.1 mm
T= 25 mm
PHI= 135 degrees
E= 200000 N/mm2
PR= .3
BETA= 6.836142

APPLIED JUNCTION MOMENT & FORCE
Mo= 0 Nmm/mm
Vo= 50 N/mm inward
```

FIGURE 3.20(b) Input data set for example 3.4

```
JUNCTION RESULTS
DISCONTINUITY FORCES & MOMENTS
CONE-SPHERE JUNCTION
Applied Radial Force

Mj 1 = 912.195 Nmm/mm anti-clockwise
Vj 1 = 25.21672 N/mm inward

Mj 2 = 912.1951 Nmm/mm clockwise
Vj 2 = 24.78328 N/mm inward

RESULTS COMPONENT No. 1
CONE-SPHERE JUNCTION
Applied Radial Force
X= 0 mm
XI= 19.33562    LP= 0
Y= -1.330636E-02 mm
THETA= -2.061658E-06 radians
V= -17.83091 N/mm
N1= 17.83092 N/mm
N2= -127.7143 N/mm
M1= 912.195 Nmm/mm
M2= 274.4178 Nmm/mm
STRESSES N/mm2
SV= -.7132366
SL= .7132366
SH= -5.108573
SBL=+or-  8.757071
SBH=+or-  2.634411
SLo= -8.043835
SLi= 9.470308
SHo= -7.742984
SHi= -2.474162

RESULTS COMPONENT No. 2
CONE-SPHERE JUNCTION
Applied Radial Force
OMEGA= 0 degrees
Y= -1.330636E-02 mm
THETA= -2.061832E-06 radians
V= -17.52442 N/mm
N1= 17.52443 N/mm
N2= -127.8076 N/mm
M1= 912.1952 Nmm/mm
M2= 272.8992 Nmm/mm
STRESSES N/mm2
SV= -.7009768
SL= .7009771
SH= -5.112304
SBL=+or-  8.757073
SBH=+or-  2.619833
SLo= -8.056096
SLi= 9.458051
SHo= -7.732137
SHi= -2.492472
```

FIGURE 3.20(c) Junction results for example 3.4

Example 3.5 CYLINDER WITH AN END CLOSURE

Cylindrical pressure vessels are the most common type of vessel produced. The ends of the cylinder have to be closed by a welded on shell or plate known as a "head" or "end". FIGURE 3.21(a) shows some ends that can be analysed by "AJAP1". These include hemispherical, spherical, conical and flat ends.

The hemispherical end represents a junction with a relatively smooth transition to the cylinder and hence the discontinuity effects are small, although the end and transition generally require more forming at manufacture. The flat end is relatively simple to manufacture but has a much more severe discontinuity. The discontinuity effects of other ends generally lie between these two extremes.

As an example of the relative discontinuity effects TABLE 3.8 summarises the results for a cylindrical vessel of 500 mm mean radius, 15 mm thick shell and subjected to an internal pressure of 0.5 N/mm^2. A typical input data set for a domed end is given in FIGURE 3.21(b).

The maximum stresses are given for both the cylinder and the end for various shapes of the end. The ends are all 15 mm thick. The hoop membrane stress in the cylinder remote from the junction is SH=16.66 N/mm^2. The stress ratio is calculated from: maximum stress/hoop membrane stress in the cylinder remote from the junction. It can be seen that the hemisphere has the lowest stress and the flat end by far the highest stress. The stresses in this flat end are so high that they would be considered unacceptable to the pressure vessel codes. A doubling of the flat end thickness to 30 mm would be required to keep the stresses within code limits. Section 4.6 discusses the assessment of this end closure later. The increase in stress as the ratio of R/h_E increases is the main reason for the pressure vessel codes requiring a knuckle radius, to form a torispherical end, to be provided to minimise the stresses local to the junction with the cylinder.

The right column in TABLE 3.8 gives the maximum compressive hoop membrane stress in the end. This stress increases with larger ratios of R/h_E. With some very thin ends this stress is high enough to cause buckling and is one reason why ends with high ratios (>2) of R/h_E are not generally used in practice. GALLETLY discusses this aspect in detail in reference (17).

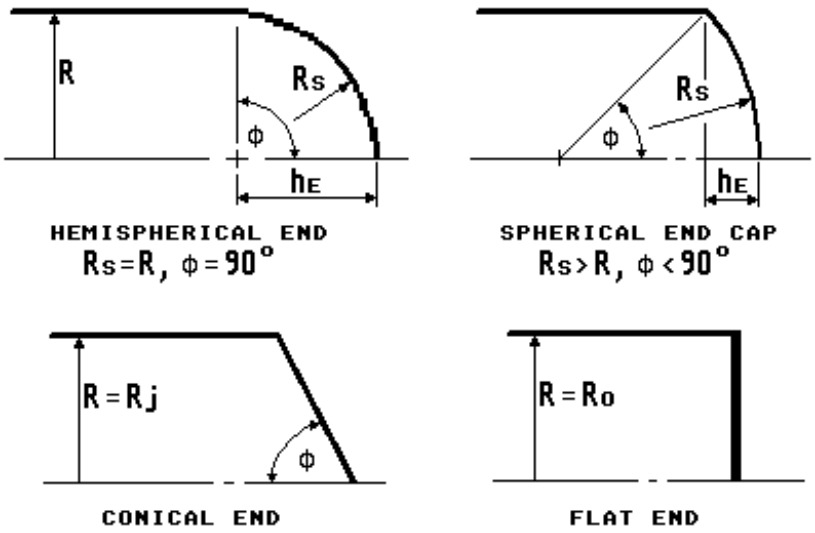

FIGURE 3.21(a) Some vessel ends that can be analysed by "AJAP1"

INPUT DATA, PROGRAM AJAP1

HEMISPHERICAL END
Internal Pressure

COMPONENT No. 1
CYLINDER, JUNCTION AT RIGHT END
R= 500 mm
T= 15 mm
E= 200000 N/mm2
PR= .3
BETA= .0148426 /mm
D= 6.181319E+07 Nmm
P= .5 N/mm2
Fp= 125 N/mm
Fo= 125 N/mm

COMPONENT No. 2
SPHERICAL SHELL, JUNCTION AT LEFT END
Rs= 500 mm
T= 15 mm
PHI= 90 degrees
E= 200000 N/mm2
PR= .3
BETA= 7.421301
P= .5 N/mm2
Fp= 125 N/mm
Fo= 125 N/mm

APPLIED JUNCTION MOMENT & FORCE
Mo= 0 Nmm/mm
Vo= -2.036509E-05 N/mm outward

FIGURE 3.21(b) Input data set and defaults for a cylindrical vessel with a hemispherical end subjected to internal pressure

---

End type	Maximum stress N/mm^2 cyl.	end	Stress ratio Max.stress/16.66 cyl.	end	Compression hoop stress SH N/mm^2 in end
hemisphere, R/h_E = 1 Rs= 500mm, ϕ= 90°	17.18 (X=130mm)	12.5 (Ω=0°)	1.03	0.75	all tensile
spherical, R/h_E = 1.5 Rs= 541.667mm, ϕ= 67.38°	31.24 (X=0mm)	31.35 (Ω=0°)	1.87	1.88	-0.02 (Ω=1°)
spherical, R/h_E = 2 Rs= 625.0mm, ϕ= 53.13°	48.07 (X=0mm)	48.29 (Ω=0°)	2.88	2.89	-8.18 (Ω=1°)
spherical, R/h_E = 3 Rs= 833.33mm, ϕ= 36.87°	73.6 (X=0mm)	74.24 (Ω=0°)	4.42	4.46	-19.41(Ω=0°)
spherical, R/h_E = 4 Rs= 1062.59mm, ϕ= 28.07°	94.03 (X=0mm)	95.07 (Ω=0°)	5.64	5.71	-27.29 (Ω=0°)
spherical, R/h_E = 5 Rs= 1300.0mm, ϕ= 22.62°	111.57 (X=0mm)	113.12 (Ω=0°)	6.69	6.79	-33.24 (Ω=0°)
flat end Ro=500mm,15mm thick	355.05 (X=0mm)	404.32 (X=500mmR)	21.3	24.27	-------

TABLE 3.8 Comparison of results for various end types subjected to internal pressure

In view of the severe discontinuity produced by a cylindrical vessel with a flat end closure, a detailed analysis will be carried out on the geometry and loading shown in FIGURE 3.21(c).

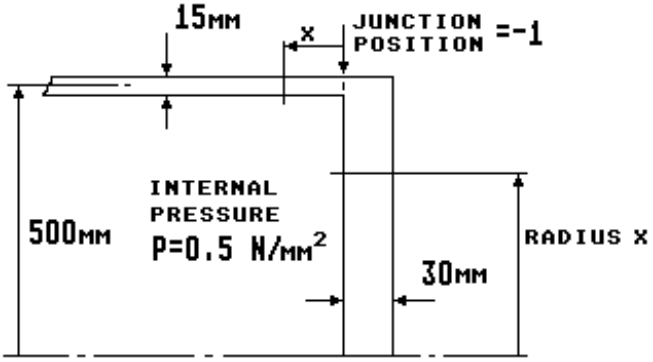

FIGURE 3.21(c) Cylindrical vessel with a flat end closure subjected to internal pressure

The reason for the severe discontinuity can be seen from the free body diagram shown in FIGURE 3.21(d). When subjected to internal pressure the cylinder has a radial deflection outward but no rotation at the end. The flat end if simply supported would rotate anti-clockwise and the plate corner at the junction with the cylinder moves radially inward. It can be seen that the difference in free radial deflection is large and if a radial inward force is applied to close the gap, the cylinder end will rotate clockwise, FIGURE 3.21(e), i.e. opposite to the free rotation of the flat end. The result is that the connected junction has a relatively severe discontinuity and is a good case for an assessment example. The detailed assessment, to a pressure vessel code, is given later in section 4.6.

The input data set and defaults are given in FIGURE 3.21(f). Results at the junction and other selected points are given in FIGURE 3.21(g).

Plots of maximum stress for both cylinder and the flat end are shown on FIGURES 3.21(h) to (k). The overall maximum stress is the longitudinal membrane plus bending stress at the inside surface of the cylinder, at the junction, SLi = 239.27 N/mm^2. The maximum stress in the flat end is the hoop and longitudinal membrane plus bending stresses, at the centre, on the outside(right) surface, SHr = SLr = 103.43 N/mm^2. Note that, in general, the maximum stress in the end does *not* always occur at the centre. It

can occur at the junction, as was the case when the end thickness was 15 mm, refer to the TABLE 3.8 results.

Although the maximum stress occurred in the cylinder, at the junction, the maximum hoop membrane stress occurs away from the junction. This is clearly seen in the plot shown in FIGURE 3.21(i) and can have important implications in a code assessment which requires the local membrane stress to be limited. This is discussed further in section 4.6.

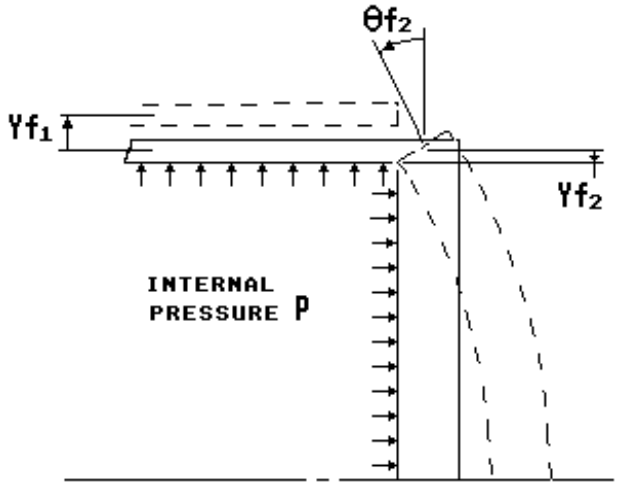

FIGURE 3.21(d) Free body diagram for a cylinder with a flat end closure subjected to internal pressure

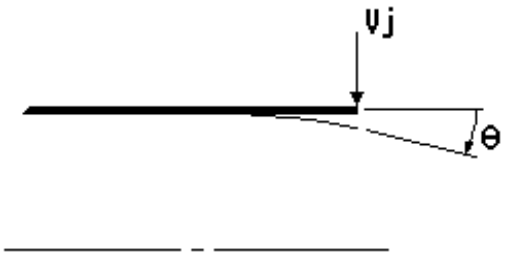

FIGURE 3.21(e) Rotation of a cylinder subjected to a radial force

INPUT DATA, PROGRAM AJAP1

CYLINDER WITH FLAT END CLOSURE
Internal Pressure

COMPONENT No. 1
CYLINDER, JUNCTION AT RIGHT END
R= 500 mm
T= 15 mm
E= 200000 N/mm2
PR= .3
BETA= .0148426 /mm
D= 6.181319E+07 Nmm
P= .5 N/mm2
Fp= 125 N/mm
Fo= 125 N/mm

COMPONENT No. 2
FLAT PLATE, JUNCTION AT O.D.
JUNCTION POSITION, LEFT SURFACE
JP= -1
OFFSET= -15 mm
Ro= 500 mm
Ri= 0 mm
T= 30 mm
E= 200000 N/mm2
PR= .3
D= 4.945055E+08 Nmm
P= .5 N/mm2

FREE DISPLACEMENTS AT JUNCTION
COMPONENT No. 1
Yf= 3.541667E-02 mm outward
THf= 0 radians

COMPONENT No. 2
Yf= -.1822917 mm inward
THf= 1.215278E-02 radians anti-clockwise

FIGURE 3.21(f) Input data set and defaults for example 3.5

JUNCTION RESULTS
DISCONTINUITY FORCES & MOMENTS
CYLINDER WITH FLAT END CLOSURE
Internal Pressure

Mj 1 = 8660.149 Nmm/mm anti-clockwise
Vj 1 = 160.559 N/mm inward

Mj 2 = 8660.152 Nmm/mm clockwise
Vj 2 = -160.5591 N/mm outward

RESULTS COMPONENT No. 1
CYLINDER WITH FLAT END CLOSURE
Internal Pressure
X= 0 mm
Y= -4.379281E-02 mm
THETA= 3.543913E-03 radians
V= -160.559 N/mm
N1= 125 N/mm
N2= -225.2569 N/mm
M1= 8660.149 Nmm/mm
M2= 2598.045 Nmm/mm
STRESSES N/mm2
SV= -10.70393
SL= 8.333333
SH= -15.01712
SBL=+or- 230.9373
SBH=+or- 69.28119
SLo= -222.604
SLi= 239.2706
SHo= -84.29831
SHi= 54.26407

RESULTS COMPONENT No. 1
CYLINDER WITH FLAT END CLOSURE
Internal Pressure
X= 40 mm
Y= -9.908588E-02 mm
THETA= -1.991284E-04 radians
V= -103.3198 N/mm
N1= 125 N/mm
N2= -557.0153 N/mm
M1= 3297.821 Nmm/mm
M2= 989.3464 Nmm/mm
STRESSES N/mm2
SV= -6.88799
SL= 8.333333
SH= -37.13435
SBL=+or- 87.9419
SBH=+or- 26.38257
SLo= -79.60857
SLi= 96.27524
SHo= -63.51692
SHi= -10.75178

RESULTS COMPONENT No. 2
CYLINDER WITH FLAT END CLOSURE
Internal Pressure
radius X= 500 mm
YL= 0 mm
Y= 9.365946E-03 mm
THETA= 3.543913E-03 radians
V= -125 N/mm
N1= 160.5591 N/mm
N2= 160.5591 N/mm
M1= -11068.54 Nmm/mm
M2= -131.0398 Nmm/mm
STRESSES N/mm2
SV= -4.166667
SL= 5.351969
SH= 5.351969
SBL=+or- 73.79026
SBH=+or- .8735986
SLi= 79.14223
SLr= -68.4383
SHl= 6.225568
SHr= 4.478371

RESULTS COMPONENT No. 2
CYLINDER WITH FLAT END CLOSURE
Internal Pressure
radius X= 0 mm
YL= 1.873392 mm
Y= 0 mm
THETA= 0 radians
V= 0 N/mm
N1= 160.5591 N/mm
N2= 160.5591 N/mm
M1= 14712.71 Nmm/mm
M2= 14712.71 Nmm/mm
STRESSES N/mm2
SV= 0
SL= 5.351969
SH= 5.351969
SBL=+or- 98.08474
SBH=+or- 98.08474
SLi= -92.73278
SLr= 103.4367
SHl= -92.73278
SHr= 103.4367

FIGURE 3.21(g) Results for example 3.5

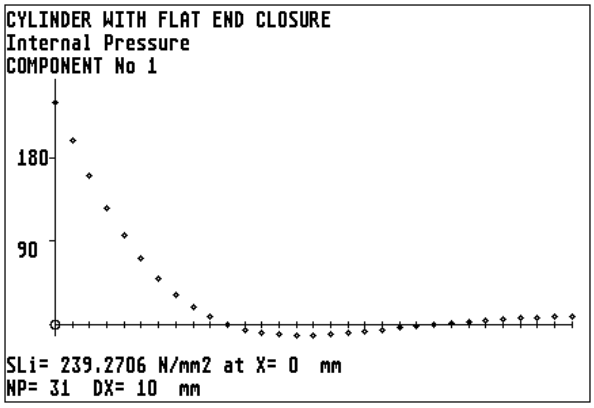

FIGURE 3.21(h) Meridional stress along the inside of the cylinder from the junction.

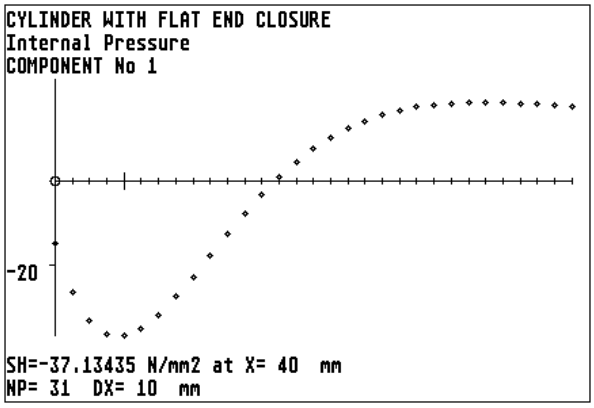

FIGURE 3.21(i) Hoop membrane stress along the cylinder from the junction.

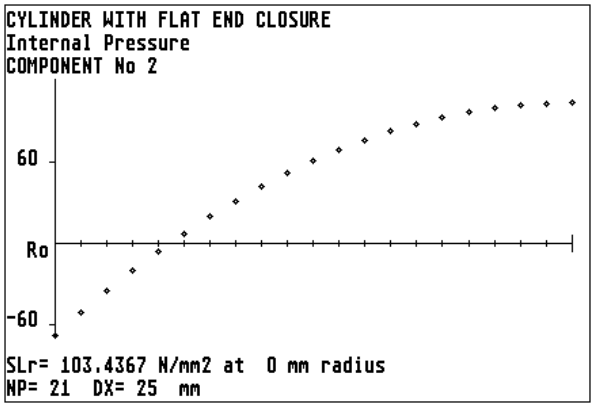

FIGURE 3.21(j) Meridional stress along the right surface of the flat end.

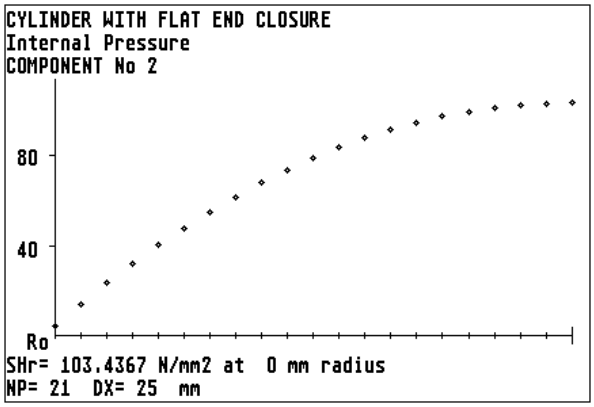

FIGURE 3.21(k) Hoop stress along the right surface of the flat end.

Example 3.6 CYLINDRICAL WATER TANK

A cylindrical tank filled with a liquid is a well known test example. This particular example is chosen to illustrate how to analyse a vessel subjected to a hydrostatic pressure of water.

The geometry and loading are shown in FIGURE 3.22(a). In this example the tank is made from reinforced concrete and has a rigid base. However, in "AJAP1" any thickness or stiffness of base could be investigated. The rigid base is simulated by a thick flat end with a high Young's modulus (1E15) and low Poisson's ratio (1E-6).

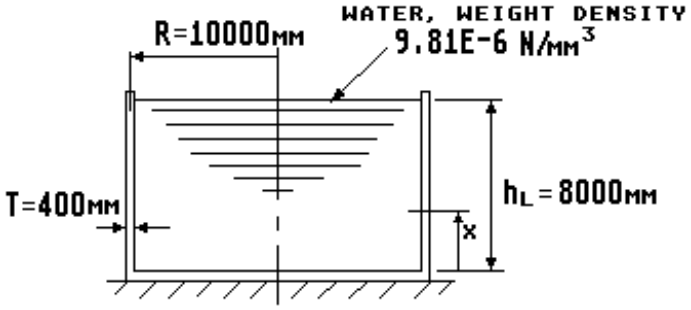

FIGURE 3.22(a) Cylindrical water tank

The loading on the tank is due to the hydrostatic pressure of the water. The program does not cater for this type of loading directly, but the discontinuity loads and stresses can still be obtained by applying the free displacements due to the hydrostatic pressure at the bottom of the tank. The procedure is as follows.

With reference to FIGURE 3.22(b). The displacements at the bottom of the tank, from simple theory, are given by equation (3.28).

$$\text{Free deflection, } Yf = Wd*R^2h_L/(E*T)$$
$$\text{Free rotation, } \theta f = Wd*R^2/(E*T) \qquad (3.28)$$

where: Wd is the weight density of the liquid = mass density times the acceleration due to gravity = Md*g.
g = 9.81 m/s^2 and for water Md = 1000 Kg/m^3. Therefore Wd = 9810 N/m^3 $\equiv$ 9.81E-6 N/mm^3.
h_L is the height of the liquid from the base.

For the dimensions and loading given in FIGURE 3.22(a) the free displacements for a reinforced concrete tank with Young's modulus E = 24000 N/mm^2 are: Yf = 0.8175 mm outward and θf = 0.0001021 radians anti-clockwise. These free displacements are applied as input at the junction. The input data set is shown in FIGURE 3.22(c) and the junction results are given in FIGURE 3.22(d).

Plots of the shear stress, meridional bending stress and the hoop membrane stress are shown in FIGURES 3.22(e) to (g). These results are as expected. Note that the discontinuity effects, at the tank bottom, diffuse away well before the top of the tank. The results for the hoop membrane stress do *not* include the stress due the hydrostatic pressure loading. This can be calculated, by hand, from equation (3.29) and added to the discontinuity results from "AJAP1".

$$\text{Hoop stress due to pressure, } SH = Wd*h_L*R*(1 - X/h_L)/T \qquad (3.29)$$

[Corrected h_L was h_E]

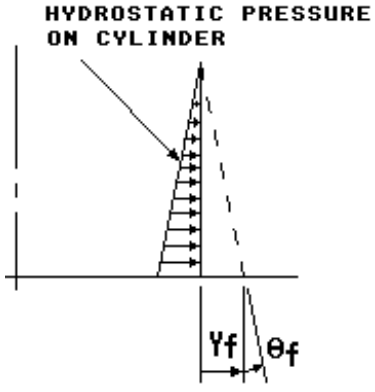

FIGURE 3.22(b) Free body diagram for the cylindrical water tank

INPUT DATA, PROGRAM AJAP1

CYLINDRICAL WATER TANK
Displacements, Hydrostatic Pressure

COMPONENT No. 1
CYLINDER, JUNCTION AT RIGHT END
R= 10000 mm
T= 400 mm
E= 24000 N/mm2
PR= .2
BETA= 6.513558E-04 /mm
D= 1.333333E+11 Nmm

COMPONENT No. 2
FLAT PLATE, JUNCTION AT O.D.
JUNCTION POSITION, LEFT SURFACE
JP= -1
OFFSET= -200 mm
Ro= 10000 mm
Ri= 0 mm
T= 400 mm
E= 1E+15 N/mm2
PR= .000001
D= 5.333334E+21 Nmm

FREE DISPLACEMENTS AT JUNCTION
COMPONENT No. 1
Yf= .8175 mm outward
THf= .0001021 radians anti-clockwise

COMPONENT No. 2
Yf= 0 in
THf= 0 radians

FIGURE 3.22(c) Input data set and applied displacements

JUNCTION RESULTS
DISCONTINUITY FORCES & MOMENTS
CYLINDRICAL WATER TANK
Displacements, Hydrostatic Pressure

Mj 1 = 74755.4 Nmm/mm anti-clockwise
Vj 1 = 108.936 N/mm inward

Mj 2 = 74755.38 Nmm/mm clockwise
Vj 2 = -108.9362 N/mm outward

RESULTS COMPONENT No. 1
CYLINDRICAL WATER TANK
Displacements, Hydrostatic Pressure
X= 0 mm
Y= -.8175 mm
THETA= -1.020998E-04 radians
V= -108.936 N/mm
N1= 0 N/mm
N2= -784.8 N/mm
M1= 74755.4 Nmm/mm
M2= 14951.08 Nmm/mm
STRESSES N/mm2
SV= -.27234
SL= 0
SH= -1.962
SBL=+or- 2.803327
SBH=+or- .5606655
SLo= -2.803327
SLi= 2.803327
SHo= -2.522665
SHi= -1.401334

FIGURE 3.22(d) Junction results for example 3.6

TABLE 3.9 summarises the total of the pressure and discontinuity stresses at several points along the cylinder, where X is from the bottom of the tank. The highest hoop membrane stress is tensile and occurs approximately 3000 mm from the tank bottom.

Example 3.6

X	SH due to pressure equation 3.29	SH from "AJAP1"	Total SH
mm	N/mm^2	N/mm^2	N/mm^2
0	1.962	-1.962	0
1000	1.717	-1.315	0.402
2000	1.471	-0.557	0.914
3000	1.226	-0.104	1.122
4000	0.981	0.065	1.046
5000	0.736	0.082	0.818
6000	0.49	0.05	0.54
7000	0.245	0.019	0.264
8000	0	0.002	0.002

TABLE 3.9 Total hoop membrane stress along the cylindrical tank from the bottom of the tank

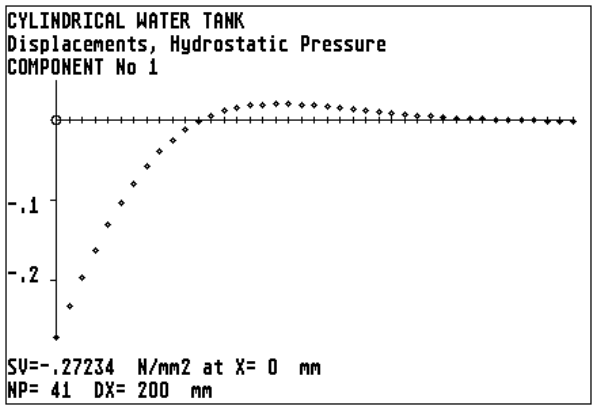

FIGURE 3.22(e) Average shear stress along the cylindrical tank from the bottom of the tank

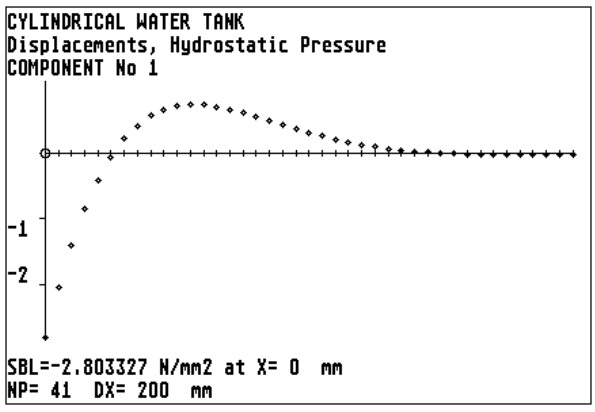

FIGURE 3.22(f) Meridional bending stress along the cylindrical tank from the bottom of the tank

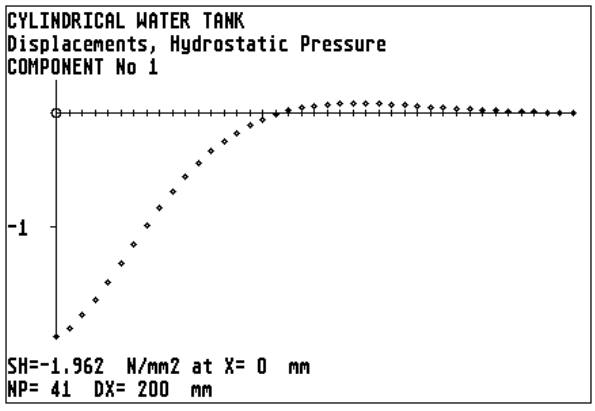

FIGURE 3.22(g) Hoop membrane stress along the cylindrical tank from the bottom of the tank

Example 3.7 TRANSVERSE LOADED FLAT PLATE

Flat plates are often subjected to transverse loading. The following example shows how to analyse this type of plate. FIGURE 3.23(a) shows a plate simply supported at both edges and subjected to a linear distributed pressure. Any distributed loading can be simulated in "AJAP1" by several point loads at specified radii. By default a total of 12 loads can be applied, but this number can be increased or decreased by altering the value of MPL at line 520. For the present example the distributed pressure is simulated by three loads as follows:

W1 = 36.66 N/mm at a radius of 250 mm
W2 = 30.00 N/mm at a radius of 230 mm
W3 = 23.34 N/mm at a radius of 210 mm

The plate is simply supported at both the inside and outside edge. Since "AJAP1" is formulated for plates supported only at the inside or the outside but not both, a solution must be run in steps like Example 3.3. A single flat plate with a support at the outside is chosen (the solution can also be obtained using the plate with a support at the inside). The solution proceeds by following the steps (1) to (3) below.

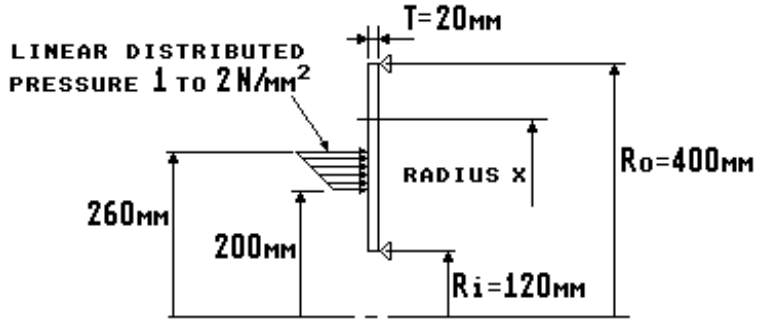

FIGURE 3.23(a) Flat plate subjected to a distributed loading

(1) A first run is made with the plate simply supported at the outside edge and subjected to the three loads discussed above. The input data set and result at the inside edge (radius X= 120mm) is shown in FIGURE 3.23(b). The transverse deflection YL is 5.533702 mm at the inside edge.

(2) The plate is loaded with a unit point load of -1 N/mm at the inside edge only. The input data set is shown in FIGURE 3.23(c). The results at the inside edge gives YL= -0.0552821 mm, hence the required point load at the inside edge to bring the transverse deflection in (1) to zero is 5.533702/(-0.0552821) = -100.1 N/mm.

(3) The final load case is run with the three point loads discussed above and the -100.1 N/mm load (W4) at the inside radius (Rw= 120mm). The input data set is shown in FIGURE 3.23(d).

A plot of the transverse deflection is shown in FIGURE 3.23(e). This shows that the deflection is zero at the inside and outside edges as expected for a plate simply supported at both edges. The maximum transverse deflection is 0.227 mm at 246 mm radius.

The maximum stresses in the plate are the meridional and hoop bending stresses. Plots of these stresses are shown in FIGURES 3.23(f) and (g). There are no membrane stresses in the plate all the loading is resisted by bending of the plate.

A result plot for the shear stress in the plate is shown in FIGURE 3.23(h). This plot shows clearly the sudden changes in shear forces to be expected when point loads are applied to a flat plate. At the position of a point load there is a singularity, i.e. the magnitude of the function is indeterminate. It is necessary to consider points just to the side of the load in order to get a better plot of the function, hence the need to put the distance between points DX = 13.9999 rather than 14 mm order to get close to the true value of the applied shear force at the inside edge.

INPUT DATA, PROGRAM AJAP1	RESULTS COMPONENT No. 1
	SIMPLY SUPPORTED FLAT PLATE
SIMPLY SUPPORTED FLAT PLATE	Linear Distributed Pressure
Linear Distributed Pressure	radius X= 120 mm
FLAT PLATE, support at O.D.	YL= 5.533702 mm
Ro=400mm	Y= 0 mm
Ri=120 mm	THETA= 1.926927E-02 radians
T= 20 mm	V= 0 N/mm
E= 200000 N/mm2	N1= 0 N/mm
PR= .3	N2= 0 N/mm
D= 1.465202E+08 Nmm	M1= 0 N/mm
W 1 = 36.66 N/mm	M2= 21410.3 Nmm/mm
Rw= 250 mm	STRESSES N/mm2
W 2 = 30 N/mm	SV= 0
Rw= 230 mm	SL= 0
W 3 = 23.34 N/mm	SH= 0
Rw= 210 mm	SBL=+or- 0
	SBH=+or- 321.1545
	SLl= 0
	SLr= 0
	SHl= -321.1545
	SHr= 321.1545

FIGURE 3.23(b) Input data set and result at X = 120mm radius for a support at the outside edge only

INPUT DATA, PROGRAM AJAP1	RESULTS COMPONENT No. 1
	SIMPLY SUPPORTED FLAT PLATE
SIMPLY SUPPORTED FLAT PLATE	Unit Point Load at inside radius
Unit Point Load at inside radius	radius X= 120 mm
FLAT PLATE, support at O.D.	YL= -.0552821 mm
Ro=400mm	Y= 0 mm
Ri=120 mm	THETA= -2.235558E-04 radians
T= 20 mm	V= 0 N/mm
E= 200000 N/mm2	N1= 0 N/mm
PR= .3	N2= 0 N/mm
D= 1.465202E+08 Nmm	M1= 0 N/mm
W 1 = -1 N/mm	M2= -248.3953 Nmm/mm
Rw= 120 mm	STRESSES N/mm2
	SV= 0
	SL= 0
	SH= 0
	SBL=+or- 0
	SBH=+or- 3.72593
	SLl= 0
	SLr= 0
	SHl= 3.72593
	SHr= -3.72593

FIGURE 3.23(c) Input data set and result for a unit point load at the inside edge

Example 3.7

INPUT DATA, PROGRAM AJAP1	RESULTS COMPONENT No. 1
	SIMPLY SUPPORTED FLAT PLATE
SIMPLY SUPPORTED FLAT PLATE	Linear Distributed Pressure
Linear Distributed Pressure	radius X= 120 mm
FLAT PLATE, support at O.D.	YL= -3.671646E-05 mm
Ro=400mm	Y= 0 mm
Ri=120 mm	THETA= -3.108664E-03 radians
T= 20 mm	V= 0 N/mm
E= 200000 N/mm2	N1= 0 N/mm
PR= .3	N2= 0 N/mm
D= 1.465202E+08 Nmm	M1= 0 N/mm
W 1 = 36.66 N/mm	M2= -3454.07 Nmm/mm
Rw= 250 mm	STRESSES N/mm2
W 2 = 30 N/mm	SV= 0
Rw= 230 mm	SL= 0
W 3 = 23.34 N/mm	SH= 0
Rw= 210 mm	SBL=+or- 0
W 4 = -100.1 N/mm	SBH=+or- 51.81106
Rw= 120 mm	SLI= 0
	SLr= 0
	SHI= 51.81106
	SHr= -51.81106

FIGURE 3.23(d) The final input data set and result at X = 120mm radius

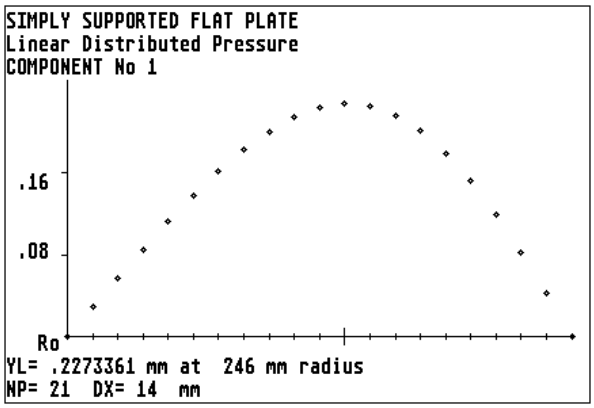

FIGURE 3.23(e) Transverse deflection of the flat plate from the outside to the inside radius.

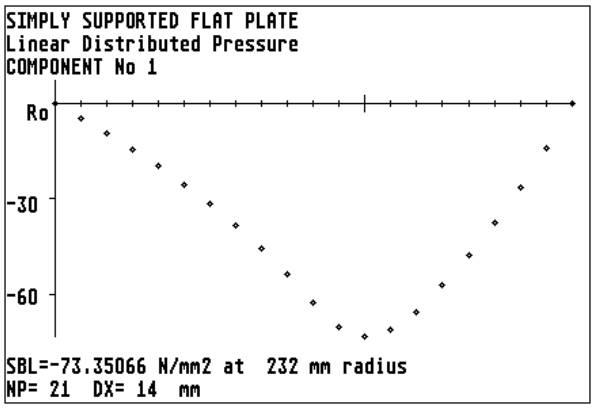

FIGURE 3.23(f) Meridional bending stress on the left surface of the plate from the outside to the inside radius.

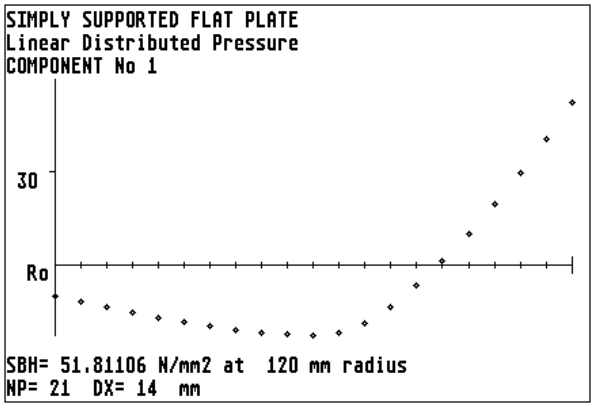

FIGURE 3.23(g) Hoop bending stress on the left surface of the plate from the outside to the inside radius.

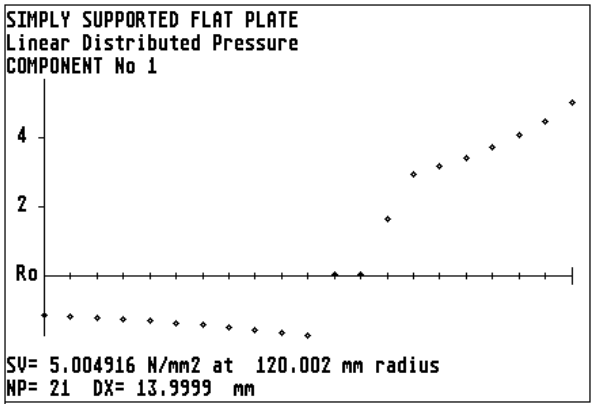

FIGURE 3.23(h) Average shear stress across the plate thickness from the outside to the inside radius.

Example 3.8 THICK CYLINDERS

The flat plates have been formulated to suit LAMÉ thick cylinder equations without end caps. This example illustrates the use of "AJAP1" to solve the case of two cylinders subjected to an internal pressure and an interference fit between the cylinders. There are many examples of this form of construction particularly where there is a need to avoid stress concentrating features such as keyways. This particular example is a case of "autofrettage" where two cylinders are shrunk together to form a pressure tube and jacket. The geometry and loading are shown in FIGURE 3.24(a).

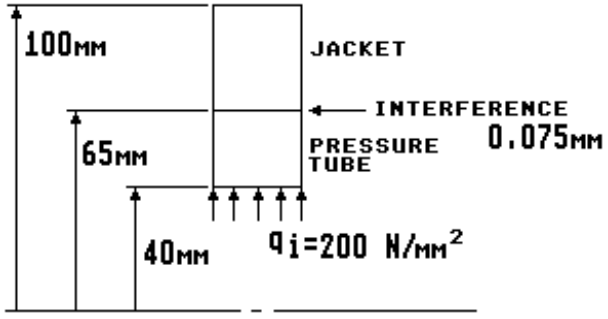

FIGURE 3.24(a) Thick cylinders subjected to internal pressure and a interference fit

In "AJAP1" a solution can be obtained by connecting the two cylinders at a common junction. The input data set for internal pressure of 200 N/mm^2 only is shown in FIGURE 3.24(b) and the results are summarised in TABLE 3.10 case 1.

For a combined pressure and interference it is only necessary to apply a negative interference to the free displacements of the outer cylinder. The input data set for this case is shown in FIGURE 3.24(c) and the results are summarised in TABLE 3.10 case 2.

A comparison of the results given in TABLE 3.10 show that the interference significantly reduces the stresses in the pressure tube while increasing the stresses in the jacket. It is known that for thick cylinders the stresses vary significantly with radius. This effect is clearly seen in the stress plots of FIGURES 3.24(d) to (g).

INPUT DATA, PROGRAM AJAP1	COMPONENT No. 2
	FLAT PLATE, JUNCTION AT I.D.
THICK CYLINDERS	JUNCTION POSITION, CENTRE
Internal Pressure	JP= 0
	OFFSET= 0 mm
COMPONENT No. 1	Ro= 100 mm
FLAT PLATE, JUNCTION AT O.D.	Ri= 65 mm
JUNCTION POSITION, CENTRE	T= 1 mm
JP= 0	E= 200000 N/mm2
OFFSET= 0 mm	PR= .3
Ro= 65 mm	D= 18315.02 Nmm
Ri= 40 mm	
T= 1 mm	FREE DISPLACEMENTS AT JUNCTION
E= 200000 N/mm2	COMPONENT No. 1
PR= .3	Yf= .0792381 mm outward
D= 18315.02 Nmm	THf= 0 radians
qo= 0 N/mm2	
qi= 200 N/mm2	COMPONENT No.2
	Yf= 0 mm
	THf= 0 radians

FIGURE 3.24(b) Input data set for example 3.8 case 1 internal pressure only

INPUT DATA, PROGRAM AJAP1

THICK CYLINDERS
Internal Pressure + Interference

COMPONENT No. 1
FLAT PLATE, JUNCTION AT O.D.
JUNCTION POSITION, CENTRE
JP= 0
OFFSET= 0 mm
Ro= 65 mm
Ri= 40 mm
T= 1 mm
E= 200000 N/mm2
PR= .3
D= 18315.02 Nmm
qo= 0 N/mm2
qi= 200 N/mm2

COMPONENT No. 2
FLAT PLATE, JUNCTION AT I.D.
JUNCTION POSITION, CENTRE
JP= 0
OFFSET= 0 mm
Ro= 100 mm
Ri= 65 mm
T= 1 mm
E= 200000 N/mm2
PR= .3
D= 18315.02 Nmm

FREE DISPLACEMENTS AT JUNCTION
COMPONENT No. 1
Yf= .0792381 mm outward
THf= 0 radians

COMPONENT No.2
Yf= -.075 mm inward
THf= 0 radians

FIGURE 3.24(c) Input data set for example 3.8 case 2 internal pressure plus interference

Stresses N/mm^2		Case 1 Pressure	Case 2 Pressure + interference
Tube at inner surface	Radial Stress SL	-200.00	-200.00
(X=40 mm radius)	Hoop Stress SH	276.19	117.54
Tube at interface	Radial Stress SL	-52.07	-101.36
(X=65 mm radius)	Hoop Stress SH	128.26	18.89
Jacket at interface	Radial Stress SL	-52.07	-101.36
(X=65 mm radius)	Hoop Stress SH	128.26	249.66
Jacket outer surface	Radial Stress SL	0	0
(X=100 mm radius)	Hoop Stress SH	76.19	148.30

TABLE 10 Comparison of results for example 3.8

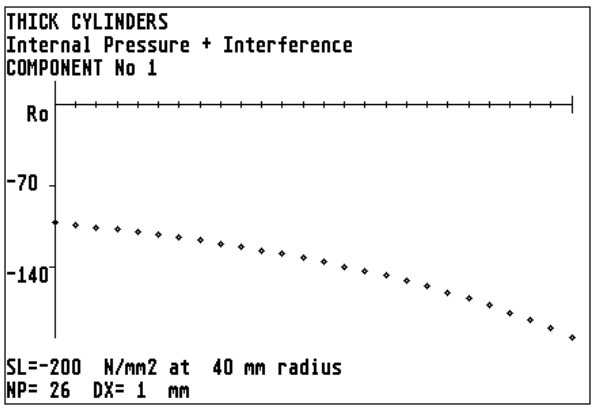

FIGURE 3.24(d) Meridional (radial) stress from the outside radius to the inside radius of the pressure tube.

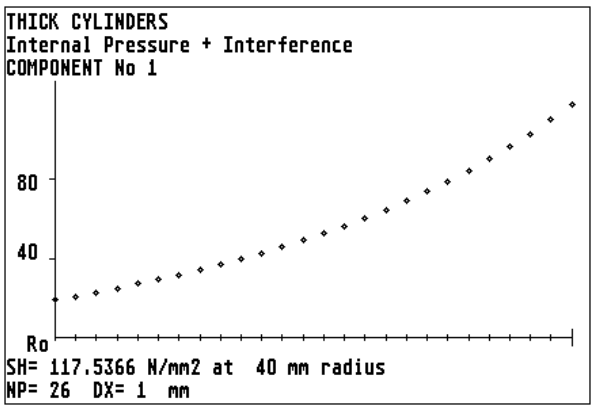

FIGURE 3.24(e) Hoop stress from the outside radius to the inside radius of the pressure tube.

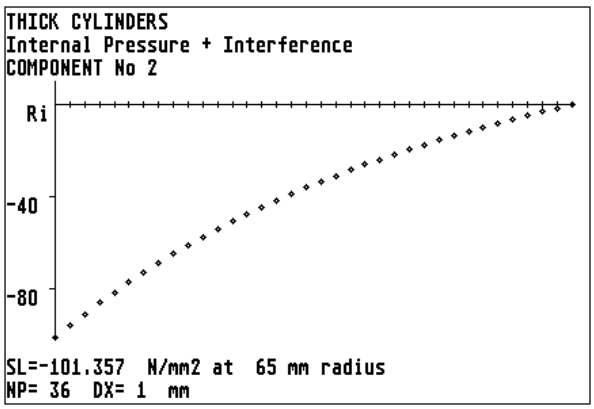

FIGURE 3.24(f) Meridional (radial) stress from the inside radius to the outside radius of the jacket.

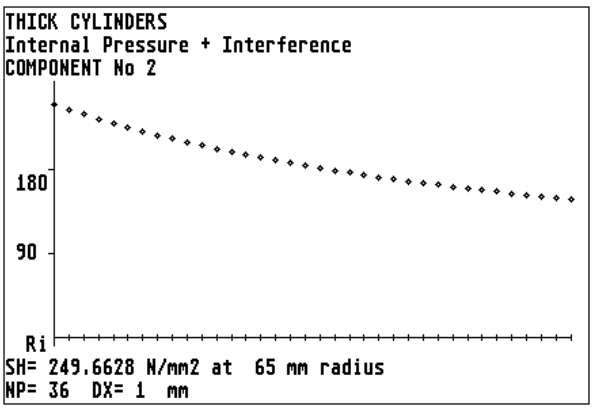

FIGURE 3.24(g) Hoop stress from the inside radius to the outside radius of the jacket.

Example 3.9 SPHERE TO NOZZLE JUNCTION

Nozzles are one of the most common attachments welded to pressure vessels. They provide openings for services, manways, safety devices, etc. The presence of the opening locally weakens the shell. It is usual to reinforce the opening, so that the stress levels local to the opening are kept within acceptable limits. All the major pressure vessel codes provide rules for the amount of reinforcement to be provided, although each set of code rules differ in method and in detail.

The "AJAP1" program can analyse the nozzle as a cylinder to sphere junction. FIGURE 3.25(a) shows some nozzles that can be analysed. The loading has to be axisymmetric so only pressure and thrust loading can be considered. The limits imposed by the spherical shell approximation used (HETÉNYI approximation II) means that the results are strictly valid only in the non-shallow shell region, as discussed in section 3.2.2, realistic results *cannot* be expected for the full range of nozzle sizes.

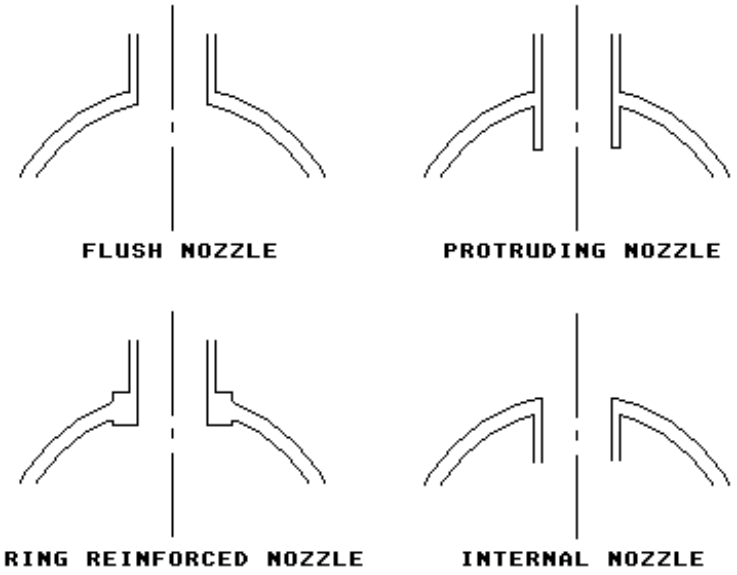

FIGURE 3.25(a) Some typical nozzles that can be analysed

As an example of what can be analysed, the sphere with a protruding nozzle junction, as shown in FIGURE 3.25(b), has been chosen with an opening angle of about 20 degrees. In "AJAP1" the protruding nozzle is simulated by two cylinders connected at a common junction to the sphere. A geometry plot is shown in FIGURE 3.25(c). The sphere is component 1, the nozzle is component 2 and the internal protrusion is component 3. The input data sets with junction results, for internal pressure and thrust loading, are shown in FIGURES 3.25(d) to (g).

A method of calculating the stresses in a sphere, local to a junction, is given in Appendix G of BS5500 (ref. 14). The background to these rules is discussed in Part 2 of British Standards published document PD6550 (ref. 25). The method is based on the work by LECKIE and PENNY (ref. 29) and is not restricted to the shallow shell region.

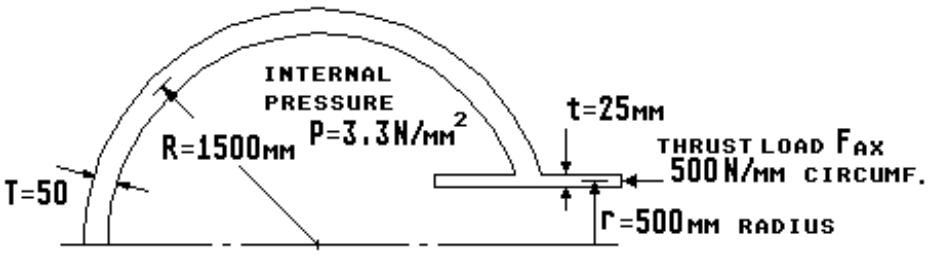

FIGURE 3.25(b) Sphere with a protruding nozzle subjected to internal pressure and a thrust load

A comparison of results for the example shown in FIGURE 3.25(b) is given in TABLE 3.11. These results are for the maximum stress in the spherical shell at the junction, but note that the "AJAP1" results given in FIGURES 3.25(e) and (g) both show that stresses are higher in the nozzle(component 2) than in the sphere.

FIGURE 3.25(c) Geometry plot for example 3.9

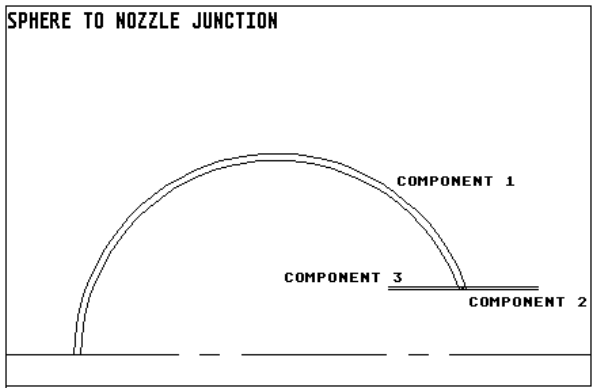

In order that a better idea of the scope of validity of the "AJAP1" results, a comparison of stress concentration factors (SCF) for flush and protruding nozzles subject to pressure and thrust loading has been carried out. The results are summarised in TABLES 3.12 and 3.13.

Inspection of these results show that for pressure loading the results are reasonable throughout the range considered. For the thrust loading the "AJAP1" results deviate significantly from the BS5500 results at the smaller values of shell parameter. The "AJAP1" results should *not* be used for thrust loading at these small parameters.

Stresses N/mm^2 in sphere at junction with nozzle	"AJAP1"	BS5500
Internal Pressure 3.3 N/mm^2	190.5	207.9
Thrust Load 500 N/mm	74.1	84.9

TABLE 3.11 Results comparison for sphere to nozzle junction

```
INPUT DATA, PROGRAM AJAP1

SPHERE TO NOZZLE JUNCTION
Internal Pressure

COMPONENT No. 1
SPHERICAL SHELL, JUNCTION AT RIGHT END
Rs= 1500 mm
T= 50 mm
PHI= 160.529 degrees
E= 200000 N/mm2
PR= .3
BETA= 7.040464
P= 3.3 N/mm2
Fp= 824.9901 N/mm
Fo= 2475 N/mm

COMPONENT No. 2
CYLINDER, JUNCTION AT LEFT END
R= 500 mm
T= 25 mm
E= 200000 N/mm2
PR= .3
BETA= 1.149703E-02 /mm
D= 2.861722E+08 Nmm
P= 3.3 N/mm2
Fp= 825 N/mm
Fo= 825 N/mm

COMPONENT No. 3
CYLINDER, JUNCTION AT RIGHT END
R= 500 mm
T= 25 mm
E= 200000 N/mm2
PR= .3
BETA= 1.149703E-02 /mm
D= 2.861722E+08 Nmm

APPLIED JUNCTION MOMENT & FORCE
Mo= 0 Nmm/mm
Vo= -2333.456 N/mm outward

FREE DISPLACEMENTS AT JUNCTION
COMPONENT No. 1
Yf= 8.662396E-02 mm outward
THf= 0 radians

COMPONENT No. 2
Yf= .14025 mm outward
THf= 0 radians

COMPONENT No. 3
Yf= 0 mm
THf= 0 radians
```

FIGURE 3.25(d) Input data set for example 3.9, internal pressure case

JUNCTION RESULTS
DISCONTINUITY FORCES & MOMENTS
SPHERE TO NOZZLE JUNCTION
Internal Pressure

Mj 1 = -19461.46 Nmm/mm clockwise
Vj 1 = -1295.119 N/mm outward

Mj 2 = -32309.1 Nmm/mm anti-clockwise
Vj 2 = -570.0489 N/mm outward

Mj 3 = -12847.65 Nmm/mm clockwise
Vj 3 = -468.288 N/mm outward

RESULTS COMPONENT No. 1
SPHERE TO NOZZLE JUNCTION
Internal Pressure
OMEGA= 0 degrees
Y= .3685698 mm
THETA= 2.285004E-03 radians
V= 431.7013 N/mm
N1= 1253.948 N/mm
N2= 7747.669 N/mm
M1= -19461.47 Nmm/mm
M2= -14814.9 Nmm/mm
STRESSES N/mm2
SV= 8.634024
SL= 25.07896
SH= 154.9534
SBL=+or- 46.70752
SBH=+or- 35.55577
SLo= 71.78648
SLi= -21.62855
SHo= 190.5091
SHi= 119.3976

RESULTS COMPONENT No. 2
SPHERE TO NOZZLE JUNCTION
Internal Pressure
X= 0 mm
Y= .3685697 mm
THETA= 2.285006E-03 radians
V= 570.0489 N/mm
N1= 825 N/mm
N2= 3933.197 N/mm
M1= -32309.1 Nmm/mm
M2= -9692.731 Nmm/mm
STRESSES N/mm2
SV= 22.80196
SL= 33
SH= 157.3279
SBL=+or- 310.1674
SBH=+or- 93.05021
SLo= 343.1674
SLi= -277.1674
SHo= 250.3781
SHi= 64.27767

RESULTS COMPONENT No. 3
SPHERE TO NOZZLE JUNCTION
Internal Pressure
X= 0 mm
Y= .3685697 mm
THETA= 2.285004E-03 radians
V= 468.288 N/mm
N1= 0 N/mm
N2= 3685.697 N/mm
M1= -12847.65 Nmm/mm
M2= -3854.295 Nmm/mm
STRESSES N/mm2
SV= 18.73152
SL= 0
SH= 147.4279
SBL=+or- 123.3374
SBH=+or- 37.00123
SLo= 123.3374
SLi= -123.3374
SHo= 184.4391
SHi= 110.4267

FIGURE 3.25(e) Results for example 3.9, internal pressure case

INPUT DATA, PROGRAM AJAP1

SPHERE TO NOZZLE JUNCTION
Thrust Loading

COMPONENT No. 1
SPHERICAL SHELL, JUNCTION AT RIGHT END
Rs= 1500 mm
T= 50 mm
PHI= 160.529 degrees
E= 200000 N/mm2
PR= .3
BETA= 7.040464
Fax= -500 N/mm
Fo= -1500.018 N/mm

COMPONENT No. 2
CYLINDER, JUNCTION AT LEFT END
R= 500 mm
T= 25 mm
E= 200000 N/mm2
PR= .3
BETA= 1.149703E-02 /mm
D= 2.861722E+08 Nmm
Fax= -500 N/mm
Fo= -500 N/mm

COMPONENT No. 3
CYLINDER, JUNCTION AT RIGHT END
R= 500 mm
T= 25 mm
E= 200000 N/mm2
PR= .3
BETA= 1.149703E-02 /mm
D= 2.861722E+08 Nmm

APPLIED JUNCTION MOMENT & FORCE
Mo= 0 Nmm/mm
Vo= 1414.233 N/mm inward

FREE DISPLACEMENTS AT JUNCTION
COMPONENT No. 1
Yf= 9.749999E-02 mm outward
THf= 0 radians

COMPONENT No. 2
Yf= .015 mm outward
THf= 0 radians

COMPONENT No. 3
Yf= 0 mm
THf= 0 radians

FIGURE 3.25(f) Input data set for example 3.9, thrust loading case

JUNCTION RESULTS
DISCONTINUITY FORCES & MOMENTS
SPHERE TO NOZZLE JUNCTION
Thrust Loading

Mj 1 = 19579.35 Nmm/mm anti-clockwise
Vj 1 = 1009.595 N/mm inward

Mj 2 = 18588.43 Nmm/mm clockwise
Vj 2 = 321.3947 N/mm inward

Mj 3 = -990.9189 Nmm/mm clockwise
Vj 3 = 83.24348 N/mm inward

RESULTS COMPONENT No. 1
SPHERE TO NOZZLE JUNCTION
Thrust Loading
OMEGA= 0 degrees
Y= -.1088034 mm
THETA= -1.401506E-03 radians
V= -336.5277 N/mm
N1= -548.1613 N/mm
N2= -2340.543 N/mm
M1= 19579.35 Nmm/mm
M2= 11379.51 Nmm/mm
STRESSES N/mm2
SV= -6.730553
SL= -10.96323
SH= -46.81086
SBL=+or- 46.99045
SBH=+or- 27.31083
SLo= -57.95367
SLi= 36.02722
SHo= -74.12169
SHi= -19.50003

RESULTS COMPONENT No. 2
SPHERE TO NOZZLE JUNCTION
Thrust Loading
X= 0 mm
Y= -.1088034 mm
THETA= -1.401506E-03 radians
V= -321.3947 N/mm
N1= -500 N/mm
N2= -1238.034 N/mm
M1= 18588.43 Nmm/mm
M2= 5576.529 Nmm/mm
STRESSES N/mm2
SV= -12.85579
SL= -20
SH= -49.52135
SBL=+or- 178.4489
SBH=+or- 53.53468
SLo= -198.4489
SLi= 158.4489
SHo= -103.056
SHi= 4.013329

RESULTS COMPONENT No. 3
SPHERE TO NOZZLE JUNCTION
Thrust Loading
X= 0 mm
Y= -.1088034 mm
THETA= -1.401506E-03 radians
V= -83.24348 N/mm
N1= 0 N/mm
N2= -1088.034 N/mm
M1= -990.9189 Nmm/mm
M2= -297.2757 Nmm/mm
STRESSES N/mm2
SV= -3.329739
SL= 0
SH= -43.52137
SBL=+or- 9.512822
SBH=+or- 2.853847
SLo= 9.512822
SLi= -9.512822
SHo= -40.66752
SHi= -46.37522

FIGURE 3.25(g) Results for example 3.9, thrust loading case

			FLUSH NOZZLE		PROTRUDING NOZZLE	
RHO	r/R	t/T	SCF (BS5500)	SCF (AJAP1)	SCF (BS5500)	SCF (AJAP1)
0.07	0.013	0	2.2	2.15	2.2	2.15
0.07	0.013	0.25	1.8	1.48 +	1.6	1.66 +
0.07	0.013	0.5	1.8	1.88		
0.07	0.013	1.0	1.8	1.83		
0.16	0.029	0	2.6	2.64	2.6	2.64
0.16	0.029	0.25	2.0	1.98 +	2.0	2.05 +
0.16	0.029	0.5	1.8	1.66 +	1.5	1.44 +
0.16	0.029	1.0	1.7	1.7		
0.36	0.067	0	3.2	3.45	3.2	3.45
0.36	0.067	0.25	2.7	2.76 +	2.5	2.70 +
0.36	0.067	0.5	2.1	1.88 +	1.9	1.87 +
0.36	0.067	1.0	1.8	1.57	1.3	1.18 +
0.64	0.116	0	4.0	4.3	4.0	4.3
0.64	0.116	0.25	3.5	3.52 +	3.3	3.39 +
0.64	0.116	0.5	2.6	2.50 +	2.4	2.33 +
0.64	0.116	1.0	2.0	1.75 +	1.6	1.42 +
1.09	0.2	0	5.2	5.46	5.2	5.46
1.09	0.2	0.25	4.6	4.58 +	4.3	4.34 +
1.09	0.2	0.5	3.5	3.35 +	3.1	2.99 +
1.09	0.2	1.0	2.5	2.37 +	1.9	1.77 +
1.82	0.333	0	7.3	7.06	7.3	7.06
1.82	0.333	0.25	6.3	5.99 +	5.9	5.58 +
1.82	0.333	0.5	4.8	4.44 +	4.2	3.85 #
1.82	0.333	1.0	3.6	3.16 +	2.5	2.24 +
2.7	0.5	0	9.6	8.5	9.6	8.5
2.7	0.5	0.25	8.0	7.29 +	7.9	6.67 +
2.7	0.5	0.5	6.0	5.40 +	5.5	4.57 +
2.7	0.5	1.0	4.7	3.87	3.2	2.64 +
3.65	0.666	0	11.0	9.05	11.0	9.5
3.65	0.666	0.25	9.7	7.90 +	9.3	7.12 +
3.65	0.666	0.5	7.3	5.90 +	6.4	4.85 +
3.65	0.666	1.0	5.7	4.22	3.8	2.79 +

+ "AJAP1" predicts a higher stress in the nozzle
# Result corresponding to example 3.9

RHO = Shell parameter = $(r/R)(R/T)^{1/2}$

SCF = Maximum stress in sphere at junction/(0.5*P*R/T)

R = 1500mm T = 50mm E = 200000 N/mm^2 μ = 0.3

TABLE 3.12 Comparison of results for internal pressure

			FLUSH NOZZLE		PROTRUDING NOZZLE	
RHO	r/R	t/T	SCF (BS5500)	SCF (AJAP1)	SCF (BS5500)	SCF (AJAP1)
0.07	0.013	0	1.4	12.4	1.4	12.4
0.07	0.013	0.25	1.2	12.6	1.2	10.5 +
0.07	0.013	0.5	0.9	11.7	0.98	7.30 +
0.07	0.013	1.0	0.9	8.9	0.7	7.03
0.16	0.029	0	2.15	6.43	2.15	6.43
0.16	0.029	0.25	1.8	6.00	1.8	5.32 +
0.16	0.029	0.5	1.3	5.00	1.2	3.55 +
0.16	0.029	1.0	1.4	3.60	1.4	3.63
0.36	0.067	0	2.8	3.97	2.8	3.97
0.36	0.067	0.25	2.35	3.07 +	2.25	2.92 +
0.36	0.067	0.5	1.6	1.84 +	1.45	1.62 +
0.36	0.067	1.0	1.75	2.00	1.75	2.15
0.64	0.116	0	3.1	3.57	3.1	3.57
0.64	0.116	0.25	2.45	2.74 +	2.45	2.65 +
0.64	0.116	0.5	1.7	1.75 +	1.6	1.65 +
0.64	0.116	1.0	1.8	1.96	1.8	2.05
1.09	0.2	0	2.9	3.16	2.9	3.16
1.09	0.2	0.25	2.3	2.43 +	2.25	2.35 +
1.09	0.2	0.5	1.75	1.63 +	1.6	1.54 +
1.09	0.2	1.0	1.8	1.8	1.75	1.77
1.82	0.333	0	2.7	2.77	2.7	2.77
1.82	0.333	0.25	2.1	2.12 +	2.0	2.01 +
1.82	0.333	0.5	1.7	1.46 +	1.55	1.35 #
1.82	0.333	1.0	1.75	1.60	1.6	1.44 +
2.7	0.5	0.5	1.65	1.25 +	1.4	1.12 +
2.7	0.5	1.0	1.65	1.37	1.4	1.16 +
3.65	0.666	0.5	1.5	1.00 +	1.25	0.88 +
3.65	0.666	1.0	1.5	1.14	1.25	0.94 +

+ "AJAP1" predicts a higher stress in the nozzle
# Result corresponding to example 3.9

RHO = Shell parameter = $(r/R)(R/T)^{1/2}$

SCF = Maximum stress in sphere at junction/$[(F_{AX}/T)(R/T)^{1/2}]$

R = 1500mm T = 50mm E = 200000 N/mm^2 μ = 0.3

TABLE 3.13 Comparison of results for thrust loading

Example 3.10 CYLINDER WITH A RADIAL THERMAL GRADIENT

Vessels that contain fluids often have the contents at a different temperature from the ambient surrounds. The resulting temperature difference across the vessel thickness induces bending stresses in the vessel wall. For a thin walled vessel the temperature distribution is essentially linear and the bending stresses remote from the ends can be calculated by equation (1.9).

For a component with a free end it is known that the hoop membrane plus bending stress at the end is approximately 25% higher than bending stresses remote from the end. If we consider the cylinder shown in FIGURE 3.26(a), the bending stresses remote from the end are given by equation (1.9):

$$SBL = SBH = \pm 0.5*E*\alpha*dT/(1 - \mu)$$

$$= \pm 0.5*200000*0.000013*250/(1 - 0.3)$$

$$= \pm 464.28 \text{ N/mm}^2 \text{ +ve tensile on outside surface}$$

The stress at the free end is given by equation (1.12).

$$\text{i.e. Maximum stress} = 0.893*E*\alpha*dT = 580.45 \text{ N/mm}^2$$

The input data set is given in FIGURE 3.26(b). The default applied moment, Mo = 48363.1 Nmm/mm, is the thermal end moment as discussed previously in section 3.3.4.

The results for the free end (X=0) and remote from the end (X=1000 mm) are given in FIGURE 3.26(c). The results are satisfactory.

The maximum stress is the hoop stress on the outside of the cylinder. A plot of this stress along the cylinder is shown in FIGURE 3.26(d). This stress plot shows a highly damped stress field typical of that produced by a discontinuity and confirms that the stress is higher at the free end.

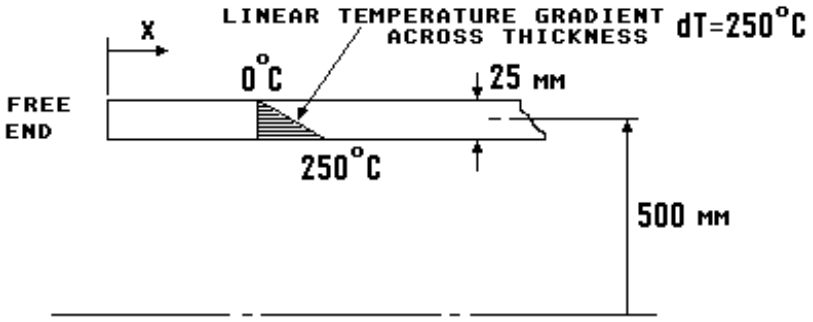

Material properties: Young's modulus, E = 200000 N/mm^2
Poisson's ratio, μ = 0.3
Coefficient of expansion, α = 13.0E-6/°C

FIGURE 3.26(a) Geometry and loading for example 3.10

INPUT DATA, PROGRAM AJAP1

CYLINDER WITH FREE END
Radial Thermal Gradient
CYLINDER
R= 500 mm
T= 25 mm
E= 200000 N/mm2
PR= .3
ALPHA= .000013 /degC
BETA= 1.149703E-02 /mm
D= 2.861722E+08 Nmm
dT= 250 degC

APPLIED END MOMENT & FORCE
Mo= 48363.1 Nmm/mm clockwise
Vo= 0 N/mm

FIGURE 3.26(b) Input data set for example 3.10

RESULTS COMPONENT No. 1	RESULTS COMPONENT No. 1
CYLINDER WITH FREE END	CYLINDER WITH FREE END
Radial Thermal Gradient	Radial Thermal Gradient
X= 0 mm	X= 1000 mm
Y= .6392716 mm	Y= 8.817719E-06 mm
THETA= -1.469945E-02 radians	THETA= -7.179283E-08 radians
V= 0 N/mm	V= 9.907751E-03 N/mm
N1= 0 N/mm	N1= 0 N/mm
N2= 6392.716 N/mm	N2= 8.817718E-02 N/mm
M1= 0 N/mm	M1= -48363.3 Nmm/mm
M2= -33854.17 Nmm/mm	M2= -48363.16 Nmm/mm
STRESSES N/mm2	STRESSES N/mm2
SV= 0	SV= 3.9631E-04
SL= 0	SL= 0
SH= 255.7086	SH= 3.527087E-03
SBL=+or- 0	SBL=+or- 464.2876
SBH=+or- 325	SBH=+or- 464.2863
SLo= 0	SLo= 464.2876
SLi= 0	SLi= -464.2876
SHo= 580.7086	SHo= 464.2899
SHi= -69.29138	SHi= -464.2828

FIGURE 3.26(c) Results for example 3.10

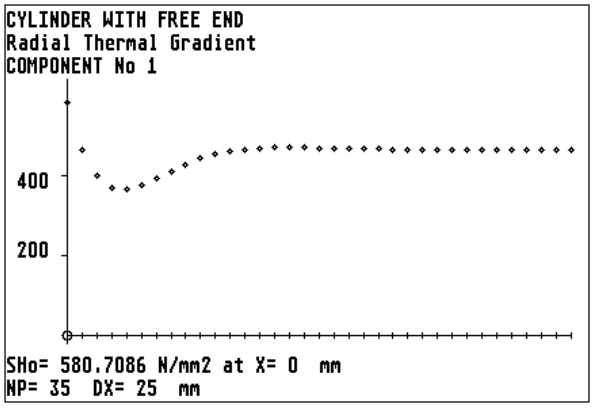

FIGURE 3.26(d) Hoop stress along the outside of the cylinder from the free end.

Example 3.11 CYLINDER WITH AN AXIAL THERMAL GRADIENT

Local heating or cooling of shells due to heat treatment or process requirements often lead to thermal gradients being set up along the length of the shell. The resulting angle of discontinuity produces thermal stresses at the point where the thermal gradient changes slope.

The following example of an axial thermal gradient occurs when it is impracticable, due to the length of a vessel, to post weld heat treat the complete vessel in a furnace. FIGURE 3.27(a) shows a carbon steel vessel that is being heat treated in a furnace. Part of the vessel is inside the furnace and is at a temperature of 600°C. The other part of the vessel is outside the furnace and is shielded such that the temperature falls linearly from 600 to 300°C over a length of 700 mm. With reference to Example 1.4 and FIGURE 1.8 the axial thermal gradient Gj is given by equation (3.30).

$$Gj = (Tm - Ta)/Le \qquad (3.30)$$

where: Tm is the temperature of the cylinder in the furnace = 600°C
Ta is the temperature of the cylinder at the specified length Le outside the furnace = 300°C
Le is the specified length = 700 mm

therefore Gj = (600 - 300)/700 = 0.428°C/mm

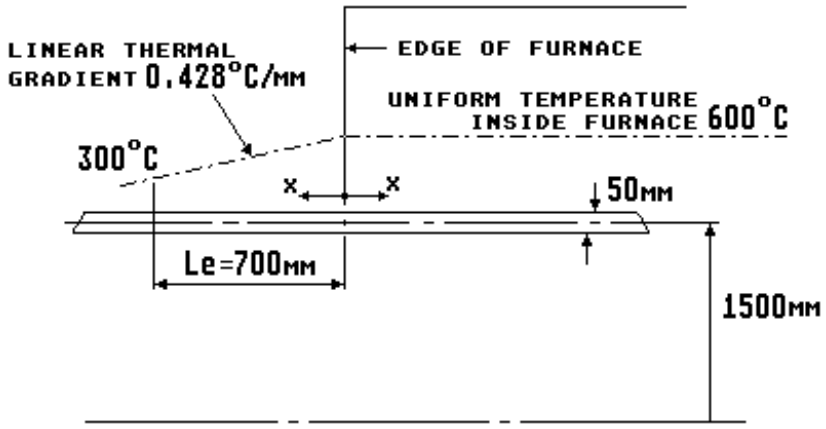

Material properties: Young's modulus, E=165000 N/mm^2
Poisson's ratio, μ = 0.3
Coefficient of expansion, α = 14.5E-6/°C

FIGURE 3.27(a) Cylindrical vessel subjected to an axial linear thermal gradient

The "AJAP1" solution is obtained by a two cylinder junction. The input data set is shown in FIGURE 3.27(b). The junction (at the edge of the furnace) is loaded with the thermal gradient applied to one of the cylinders (component No. 1). The gradient is positive as the heat flows away from the junction and results in a default free rotation of 0.009309 radians anti-clockwise at the junction.

INPUT DATA, PROGRAM AJAP1

VESSEL P.W.H.T.
Axial Thermal Gradient

COMPONENT No. 1
CYLINDER, JUNCTION AT RIGHT END
R= 1500 mm
T= 50 mm
E= 165000 N/mm2
PR= .3
ALPHA= .0000145 /degC
BETA= 4.693643E-03 /mm
D= 1.888736E+09 Nmm
Gj= .428 degC/mm

COMPONENT No. 2
CYLINDER, JUNCTION AT LEFT END
R= 1500 mm
T= 50 mm
E= 165000 N/mm2
PR= .3
ALPHA= .0000145 /degC
BETA= 4.693643E-03 /mm
D= 1.888736E+09 Nmm

FREE DISPLACEMENTS AT JUNCTION
COMPONENT No. 1
Yf= 0 in
THf= 9.309001E-03 radians anti-clockwise

COMPONENT No. 2
Yf= 0 in
THf= 0 radians

FIGURE 3.27(b) Input data set for example 3.11

The junction results and plot of the maximum stress along component No.2 (the part of the cylinder within the furnace) are shown in FIGURES 3.27(c) and (d).

The maximum stress is the meridional bending stress at the junction, SBL= ±99.02 N/mm^2. This is a high stress for carbon steel at 600°C and illustrates the importance of avoiding severe thermal gradients during heat treatment. A hoop membrane stress is also present and FIGURE 3.27(e) shows that this stress is compressive at the junction. All stresses are negligible by about 500 mm from the edge of the furnace. Note that the stress results along component No.1 are a mirror image of the component 2 results.

It is sometimes necessary to carry out a *local* post weld heat treatment by means of a circumferential heating band. This results in both sides of the weld being subjected to a thermal gradient. A solution to this case is obtained by applying the gradient to *both* components. The result will be a doubling of the stresses.

JUNCTION RESULTS
DISCONTINUITY FORCES & MOMENTS
VESSEL P.W.H.T.
Axial Thermal Gradient

Mj 1 = -41262.4 Nmm/mm clockwise
Vj 1 = -6.103516E-05 N/mm outward

Mj 2 = -41262.38 Nmm/mm anti-clockwise
Vj 2 = 3.051758E-05 N/mm inward

RESULTS COMPONENT No. 1
VESSEL P.W.H.T.
Axial Thermal Gradient
X= 0 mm
Y= -.4958303 mm
THETA= .0046545 radians
V= 6.103516E-05 N/mm
N1= 0 N/mm
N2= -2727.067 N/mm
M1= -41262.4 Nmm/mm
M2= -12378.72 Nmm/mm
STRESSES N/mm2
SV= 1.220703E-06
SL= 0
SH= -54.54133
SBL=+or- 99.02975
SBH=+or- 29.70893
SLo= 99.02975
SLi= -99.02975
SHo= -24.8324
SHi= -84.25025

RESULTS COMPONENT No. 2
VESSEL P.W.H.T.
Axial Thermal Gradient
X= 0 mm
Y= -.4958303 mm
THETA= .0046545 radians
V= -3.051758E-05 N/mm
N1= 0 N/mm
N2= -2727.067 N/mm
M1= -41262.38 Nmm/mm
M2= -12378.71 Nmm/mm
STRESSES N/mm2
SV= -6.103516E-07
SL= 0
SH= -54.54133
SBL=+or- 99.02971
SBH=+or- 29.70891
SLo= 99.02971
SLi= -99.02971
SHo= -24.83242
SHi= -84.25024

FIGURE 3.27(c) Junction results for example 3.11

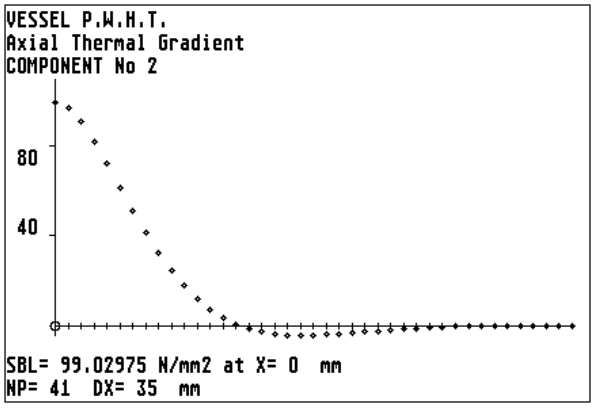

FIGURE 3.27(d) Meridional bending stress along the outside surface of the cylinder from the edge of the furnace.

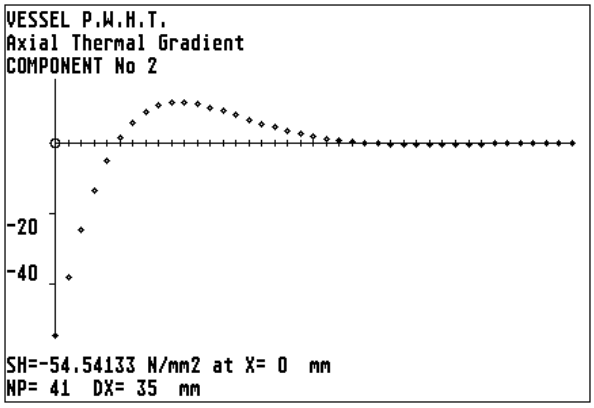

FIGURE 3.27(e) Hoop membrane stress along the cylinder from the edge of the furnace.

Example 3.12 CYLINDER WITH A MATERIAL DISCONTINUITY

Environmental and operating conditions often demand that components be manufactured from different materials joined together by welding.

A common example is the case of two cylinders welded together, where one cylinder is ferritic steel and the other is an austenitic stainless steel. The austenitic stainless steel has a higher coefficient of thermal expansion than the ferritic steel. Under changing thermal conditions the resulting discontinuity stresses at the weld junction can be a potential problem, as there are many features of welded construction that can influence the service performance, such as: local weld geometry, metallurgical variation in properties, residual stresses and manufacturing defects. GRAY and SPENCE discuss these aspects in some detail in reference 20. Other references (40), (41) and (51) provide additional background reading.

The example shown in FIGURE 3.28(a) is a weld junction in a pipeline subjected to an internal pressure of 6 N/mm^2 and a uniform temperature of 280°C. The material properties are listed in TABLE 3.14. The pressure will induce membrane stresses in the pipe wall, but the difference in thermal expansion will produce discontinuity stresses, local to the junction, as the temperature changes from ambient at 20°C to the steady state operating temperature of 280°C.

In "AJAP1" this problem is solved as a two cylinder junction. The input data set and junction results are shown in FIGURES 3.28(b) and (c).

The highest stress is the hoop membrane plus bending stress on the inside surface of the ferritic steel cylinder. A plot of this stress and the meridional stress is shown in FIGURES 3.28(d) and (e). Corresponding stresses in the stainless steel cylinder are shown in FIGURES 3.28(f) and (g). The reason for the stresses being higher in the ferritic steel cylinder is due to the combined effect of the internal pressure and discontinuity force acting together.

The highest stress in the stainless steel cylinder is the meridional membrane plus bending stress on the outside surface. A plot of this stress and the hoop stress is shown in FIGURE 3.28(h) and (i). These stresses reach a maximum a short distance away from the junction. The stresses are much less than the stresses in the ferritic steel cylinder due to the stainless steel cylinder being pulled inward by the discontinuity force against the internal pressure. The affects of the material discontinuity diffuse away by about 100 mm on each side of the weld junction.

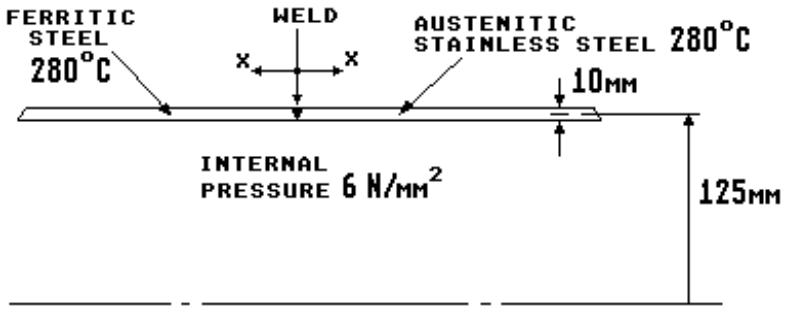

FIGURE 3.28(a) Cylinder with a material discontinuity

Note that if there had been no internal pressure the stresses in this particular example would have been reduced from a maximum of 166.8 to 90.4 N/mm^2.

In general, when different combinations of mechanical and thermal loading occur, it is necessary to analyse each loading combination to establish the worst condition.

Ferritic steel	Stainless steel
E= 184000 N/mm^2	E= 176000 N/mm^2
μ= 0.3	μ= 0.3
α= 13.2E-6/°C	α= 17.0E-6/°C

TABLE 3.14 Material properties used in example 3.12

INPUT DATA, PROGRAM AJAP1

CYLINDER WITH MATERIAL DISCONTINUITY
Pressure plus Uniform Temperature

COMPONENT No. 1
CYLINDER, JUNCTION AT RIGHT END
R= 125 mm
T= 10 mm
E= 184000 N/mm2
PR= .3
ALPHA= .0000132 /degC
BETA= .0363568 /mm
D= 1.684982E+07 Nmm
P= 6 N/mm2
Fp= 375 N/mm
Fo= 375 N/mm
Ta= 20 degC
Tm= 280 degC

COMPONENT No. 2
CYLINDER, JUNCTION AT LEFT END
R= 125 mm
T= 10 mm
E= 176000 N/mm2
PR= .3
ALPHA= .000017 /degC
BETA= .0363568 /mm
D= 1.611722E+07 Nmm
P= 6 N/mm2
Fp= 375 N/mm
Fo= 375 N/mm
Ta= 20 degC
Tm= 280 degC

FREE DISPLACEMENTS AT JUNCTION
COMPONENT No. 1
Yf= .4723085 mm outward
THf= 0 radians

COMPONENT No. 2
Yf= .597777 mm outward
THf= 0 radians

FIGURE 3.28(b) Input data set for example 3.12

JUNCTION RESULTS
DISCONTINUITY FORCES & MOMENTS
CYLINDER WITH MATERIAL DISCONTINUITY
Pressure plus Uniform Temperature

Mj 1 = 30.36743 Nmm/mm anti-clockwise
Vj 1 = -99.36521 N/mm outward

Mj 2 = 30.36768 Nmm/mm clockwise
Vj 2 = 99.36525 N/mm inward

RESULTS COMPONENT No. 1
CYLINDER WITH MATERIAL DISCONTINUITY
Pressure plus Uniform Temperature
X= 0 mm
Y= .5343455 mm
THETA= 2.280255E-03 radians
V= 99.36521 N/mm
N1= 375 N/mm
N2= 1663.186 N/mm
M1= 30.36743 Nmm/mm
M2= 9.110229 Nmm/mm
STRESSES N/mm2
SV= 9.936521
SL= 37.5
SH= 166.3186
SBL=+or- 1.822046
SBH=+or- .5466138
SLo= 35.67796
SLi= 39.32205
SHo= 165.7719
SHi= 166.8652

RESULTS COMPONENT No. 2
CYLINDER WITH MATERIAL DISCONTINUITY
Pressure plus Uniform Temperature
X= 0 mm
Y= .5343455 mm
THETA= 2.280254E-03 radians
V= -99.36525 N/mm [Sign corrected]
N1= 375 N/mm
N2= -143.1155 N/mm
M1= 30.36768 Nmm/mm
M2= 9.110303 Nmm/mm
STRESSES N/mm2
SV= -9.936526
SL= 37.5
SH= -14.31155
SBL=+or- 1.822061
SBH=+or- .5466183
SLo= 35.67794
SLi= 39.32206
SHo= -14.85817
SHi= -13.76494

FIGURE 3.28(c) Junction results for example 3.12

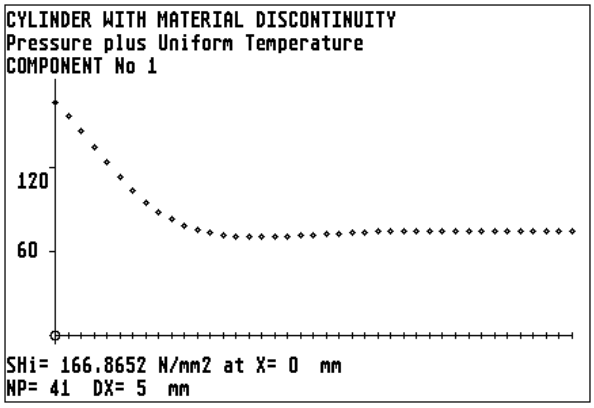

FIGURE 3.28(d) Hoop stress along the inside of the ferritic steel cylinder from the weld junction.

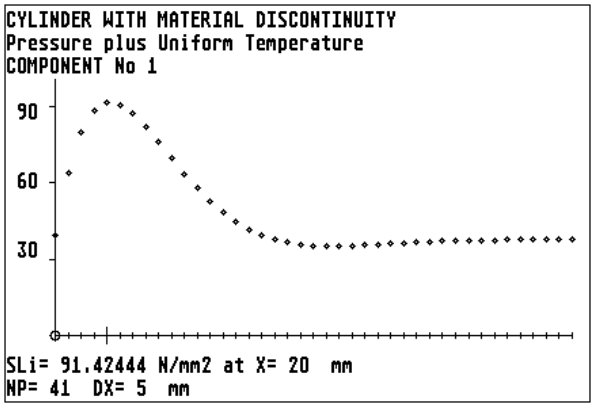

FIGURE 3.28(e) Meridional stress along the inside of the ferritic steel cylinder from the weld junction.

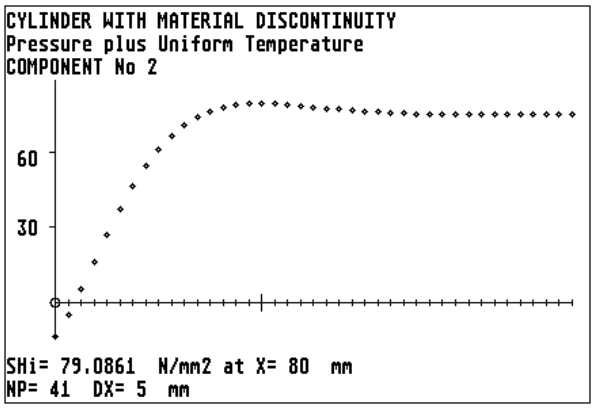

FIGURE 3.28(f) Hoop stress along the inside of the stainless steel cylinder from the weld junction.

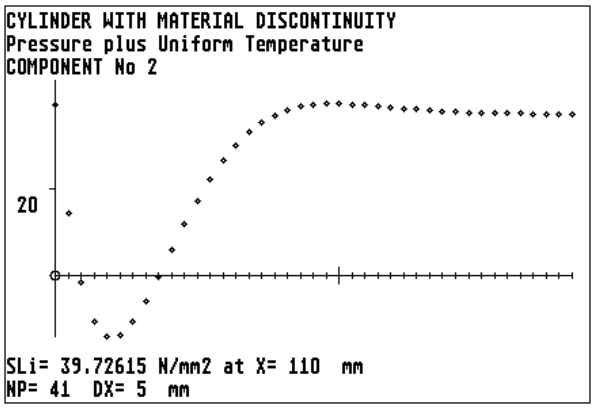

FIGURE 3.28(g) Meridional stress along the inside of the stainless steel cylinder from the weld junction.

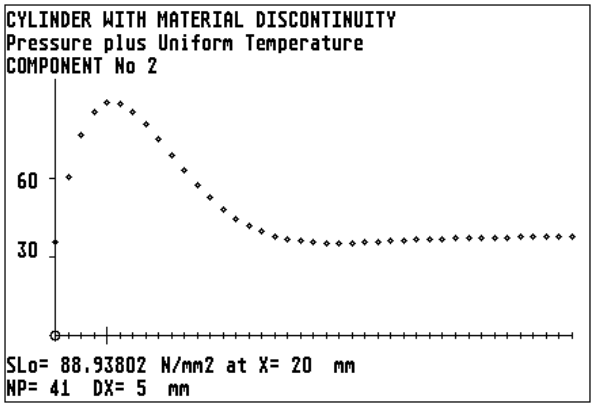

FIGURE 3.28(h) Meridional stress along the outside of the stainless steel cylinder from the weld junction.

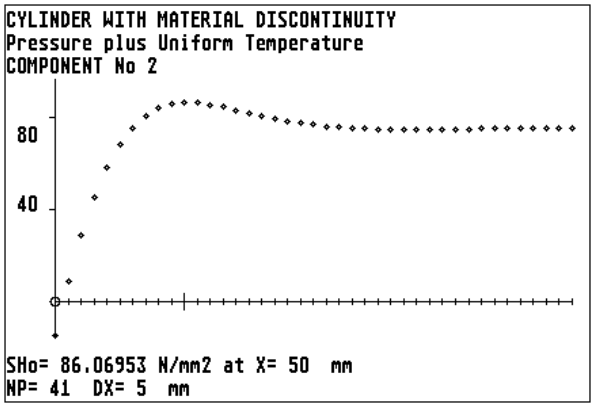

FIGURE 3.28(i) Hoop stress along the outside of the stainless steel cylinder from the weld junction.

Example 3.13 SPHERICAL HOT WATER TANK

Vessels that are part filled with hot liquids can have a discontinuity due to the thermal differential expansion between the hot and cold parts of the vessel. FLÜGGE draws attention to this type of discontinuity in reference (4).

The following example consists of a spherical steel tank that is part filled with a hot liquid as shown in FIGURE 3.29(a). In "AJAP1" the tank is simulated as a two component junction, by two spherical shells. The bottom shell is at the liquid temperature of 80°C the top shell is at a mean metal temperature of 35°C. The ambient temperature is 20°C.

A typical input data set is shown in FIGURE 3.29(b) and the junction results are given in FIGURE 3.29(c). Plots of meridional bending stress SBL and hoop membrane stress SH close to the junction, for component No.1, are shown in FIGURES 3.29(d) and (e). The stress results for component No. 2 are almost equal and opposite sign to those of component No.1. Inspection of the results show that the maximum hoop stress occurs at the junction but the maximum bending stress occurs about 1.5 degrees away from the junction. The results show that it is possible to generate significant thermal stresses due to modest temperature differentials, and is the reason why sudden changes in temperature should be avoided whenever possible.

Although the results presented are for one particular liquid level, a solution can easily be obtained for other levels by specifying the appropriate half arc angles for each component.

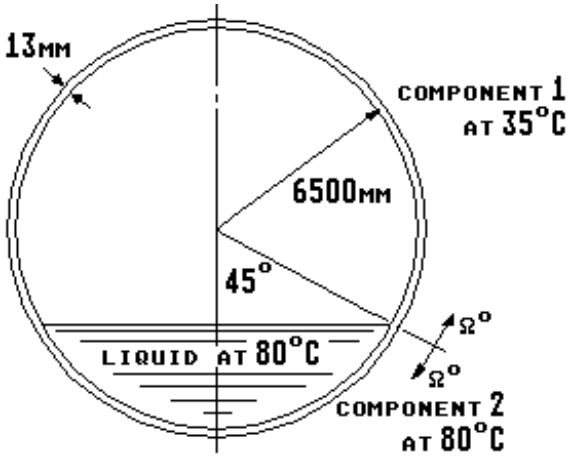

Component No. 1	Component No. 2
E= 200000 N/mm^2	E= 194000 N/mm^2
μ= 0.3	μ= 0.3
α= 15.3E-6/°C	α= 15.8E-6/°C

FIGURE 3.29(a) Spherical tank part filled with a hot liquid

INPUT DATA, PROGRAM AJAP1

SPHERICAL HOT WATER TANK
Part Filled

COMPONENT No. 1
SPHERICAL SHELL, JUNCTION AT RIGHT END
Rs= 6500 mm
T= 13 mm
PHI= 135 degrees
E= 200000 N/mm2
PR= .3
ALPHA= .0000153 /degC
BETA= 28.74258
Ta= 20 degC
Tm= 35 degC

FIGURE 3.29(b) Input data set for example 3.13

COMPONENT No. 2
SPHERICAL SHELL, JUNCTION
Rs= 6500 mm AT LEFT END
T= 13 mm
PHI= 45 degrees
E= 194000 N/mm2
PR= .3
ALPHA= .0000158 /degC
BETA= 28.74258
Ta= 20 degC
Tm= 80 degC

FREE DISPLACEMENTS AT JUNCTION
COMPONENT No. 1
Yf= 1.054826 mm outward
THf= 0 radians

COMPONENT No. 2
Yf= 4.357193 mm outward
THf= 0 radians

JUNCTION RESULTS
DISCONTINUITY FORCES & MOMENTS
SPHERICAL HOT WATER TANK
Part Filled

Mj 1 = 40.15283 Nmm/mm anti-clockwise
Vj 1 = -22.63761 N/mm outward

Mj 2 = 40.15405 Nmm/mm clockwise
Vj 2 = 22.63761 N/mm inward

RESULTS COMPONENT No. 1
SPHERICAL HOT WATER TANK
Part Filled
OMEGA= 0 degrees
Y= 2.71642 mm
THETA= 1.032621E-02 radians
V= 16.00721 N/mm
N1= -16.00722 N/mm
N2= 935.1369 N/mm
M1= 40.15252 Nmm/mm
M2= -46.12541 Nmm/mm
STRESSES N/mm2
SV= 1.231324
SL= -1.231324
SH= 71.93361
SBL=+or- 1.425533
SBH=+or- 1.637589
SLo= -2.656858
SLi= .194209
SHo= 73.5712
SHi= 70.29602

RESULTS COMPONENT No. 2
SPHERICAL HOT WATER TANK
Part Filled
OMEGA= 0 degrees
Y= 2.716419 mm
THETA= 1.032622E-02 radians
V= -16.00721 N/mm
N1= -16.00721 N/mm
N2= -905.1187 N/mm
M1= 40.15405 Nmm/mm
M2= -44.37915 Nmm/mm
STRESSES N/mm2
SV= -1.231324 [Sign corrected]
SL= -1.231324
SH= -69.62452
SBL=+or- 1.425588
SBH=+or- 1.575591
SLo= -2.656911
SLi= .1942637
SHo= -68.04893
SHi= -71.20011

FIGURE 3.29(c) Junction results for example 3.13

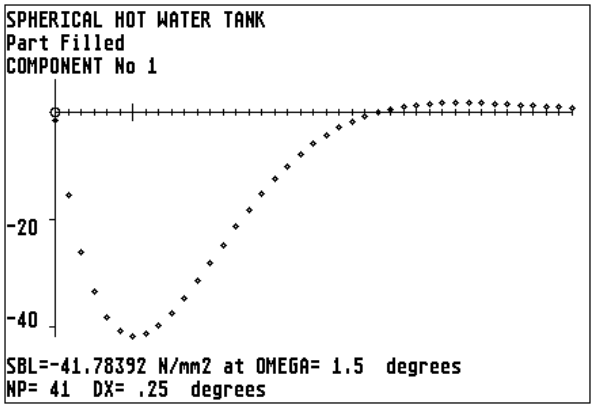

FIGURE 3.29(d) Meridional bending stress around the outside of the spherical shell from the junction at the liquid surface

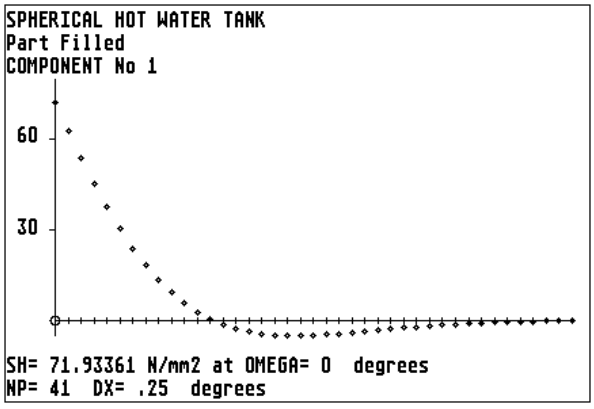

FIGURE 3.29(e) Hoop membrane stress around the spherical shell from the junction at the liquid surface

Example 3.14 FLAT DISK WITH A RADIAL TEMPERATURE GRADIENT

Heated components that are thick walled are more likely to have a higher radial temperature difference than thin wall components. The temperature distribution across a thick walled component is logarithmic and the resulting stress distribution is non-linear.

The following is an example of a thick flat disk with a ratio of outside radius to inside radius of 3, as shown in FIGURE 3.30(a). The inside surface temperature is 100°C higher than the outside surface temperature, i.e. there is a radial temperature difference dTr of +100°C. A positive sign indicates that the inside temperature is higher than the outside surface temperature.

This problem can be solved using a single flat plate. The input data set is shown in FIGURE 3.30(b). The support can be at the inside or the outside. Results at the inside and outside radii are given in FIGURE 3.30(c).

Plots of the hoop and meridional(radial) stress distribution across the disk are shown in FIGURES 3.30(d) and (e). The results are as expected. The maximum stress is the hoop membrane stress at the inside radius. The meridional stress is zero at the inside and outside radii and reaches a maximum at a radius of 40 mm.

FIGURE 3.30(f) shows a plot of the radial deflection. Note that the deflection is inward at the inside radius, this happens because a mean temperature was not specified. This inward deflection can have important consequences in cases where a close fit is required such as a disk shrunk onto a hub. In these cases it is necessary to carefully analyse each operating condition to ensure that gross yielding does not occur, or on the other hand, that the shrink fit is not lost.

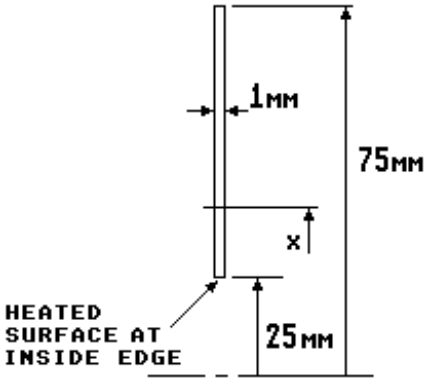

Material properties
E=200000 N/mm^2
μ= 0.3
α= 13E-6 /°C

FIGURE 3.30(a) Flat disk subjected to a radial temperature gradient

INPUT DATA, PROGRAM AJAP1

FLAT DISK
Radial Temperature Gradient
FLAT PLATE, support at I.D.
Ro= 75 mm
Ri= 25 mm
T= 1 mm
E= 200000 N/mm2
PR= .3
ALPHA= .000013 /degC
D= 18315.02 Nmm
dTr= 100 degC

FIGURE 3.30(b) Input data set for example 3.14

RESULTS COMPONENT No. 1	RESULTS COMPONENT No. 1
FLAT DISK	FLAT DISK
Radial Temperature Gradient	Radial Temperature Gradient
radius X= 25 mm	radius X= 75 mm
YL= 0 mm	YL= 0 mm
Y= -2.177111E-02 mm	Y= 3.218666E-02 mm
THETA= 0 radians	THETA= 0 radians
V= 0 N/mm	V= 0 N/mm
N1= 0 N/mm	N1= 0 N/mm
N2= -174.1689 N/mm	N2= 85.83109 N/mm
M1= 0 Nmm/mm	M1= 0 Nmm/mm
M2= 0 Nmm/mm	M2= 0 Nmm/mm
STRESSES N/mm2	STRESSES N/mm2
SV= 0	SV= 0
SL= 0	SL= 0
SH= -174.1689	SH= 85.83109
SBL=+or- 0	SBL=+or- 0
SBH=+or- 0	SBH=+or- 0
SLl= 0	SLl= 0
SLr= 0	SLr= 0
SHl= -174.1689	SHl= 85.83109
SHr= -174.1689	SHr= 85.83109

FIGURE 3.30(c) Results at the inside and outside radii for example 3.14

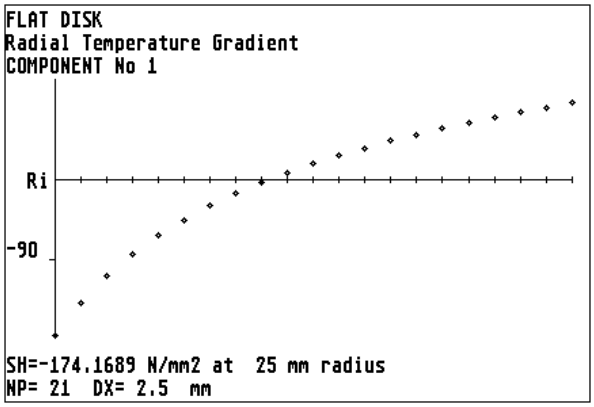

FIGURE 3.30(d) Hoop membrane stress from the inside to the outside radius of the disk.

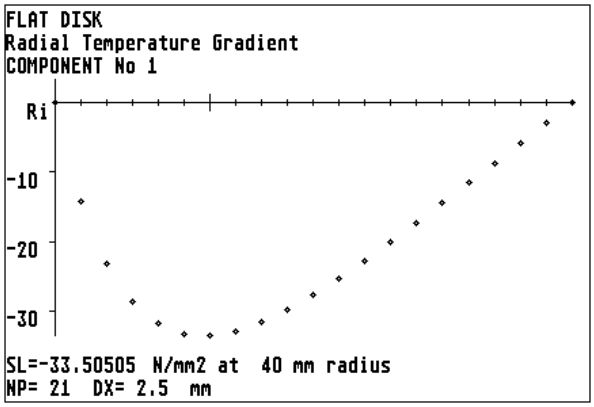

FIGURE 3.30(e) Meridional membrane stress from the inside to the outside radius of the disk.

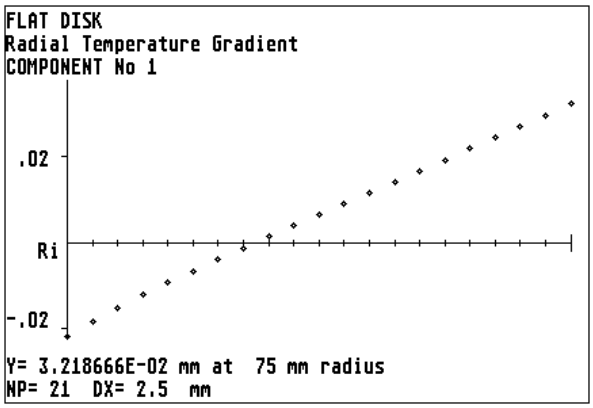

FIGURE 3.30(f) Radial deflection from the inside to the outside radius of the disk.

Example 3.15 SUPPORT SKIRTS AND THERMAL SLEEVES

Vessel support skirts and nozzle thermal sleeves, like the examples shown in FIGURES 3.31(a), (b) and (c), are structures that can be analysed as a three or four component junction. These junctions are often subjected to a combination of loadings, including: pressure, weight, pipe thrust, and thermal loads due to operating conditions. The following are two cases chosen to show how these junctions can be analysed using "AJAP1".

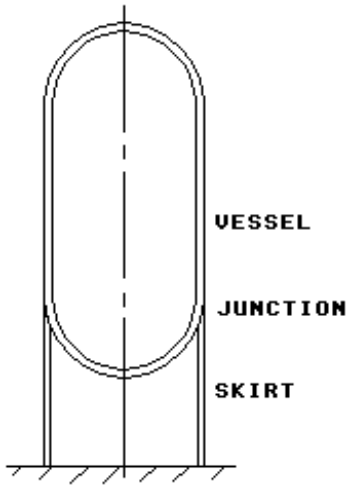

FIGURE 3.31(a) Vertical vessel with a skirt support

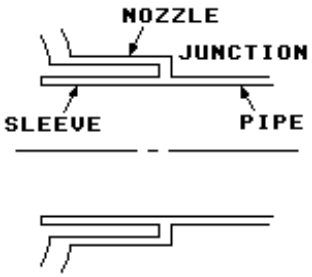

FIGURE 3.31(b) External nozzle with a thermal sleeve

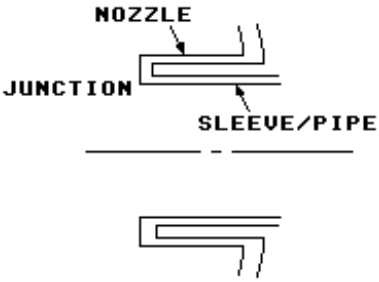

FIGURE 3.31(c) Internal nozzle with a thermal sleeve

Case 1 Vessel Support Skirt. The following is an example of a support skirt junction for a vertical vessel. The geometry and loading are detailed in FIGURE 3.32(a). In this case the skirt is a cone and is welded to the outside of the cylindrical part of the vessel near to the junction with the hemispherical end.

The vessel is subjected to an internal pressure of 3 N/mm^2 and a mean temperature of 200°C. There is a total axial end load on the vessel cylinder of 235620 N due to deadweight and contents.

$$\text{i.e. } F_{AX} = 235620/(2*\pi*1250) = -30 \text{ N/mm circumference.}$$

The negative sign indicates compression of the cylinder at the junction. The total axial end load on the hemispherical end, again due to deadweight and contents, is 62832 N.

$$\text{i.e. } F_{AX} = 62832/(2*\pi*1250) = +8 \text{ N/mm circumference at the junction.}$$

The sign is positive as the end will be in tension due to the axial end load.

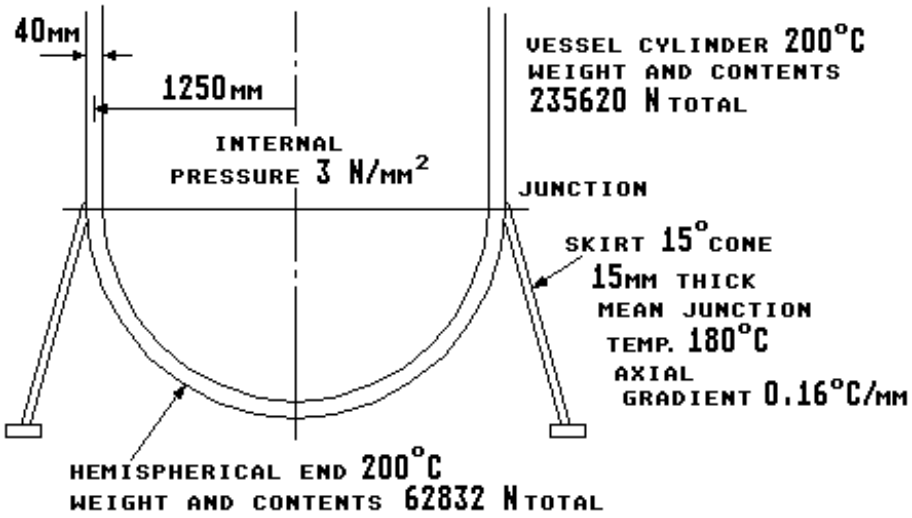

FIGURE 3.32(a) Geometry and loading on a vessel support skirt

The conical skirt is of sufficient length such that the ground support does not affect the junction at the vessel. The skirt junction is subjected to a mean temperature of 180°C and an axial thermal gradient of 0.16°C/mm. An axial end load is applied due to the deadweight and contents of the vessel adjusted for the difference in mean radius.

i.e. F_{AX} for skirt = (30 + 8)*1250/1270 = -37.4 N/mm

The negative sign is required as the skirt will be in compression.

A geometry plot of the junction is shown in FIGURE 3.32(b) and the input data set is shown in FIGURE 3.32(c). The program defaults calculate the pressure end load on the vessel, as discussed in section 3.3.1. The defaults also calculate the applied junction moment and radial force due to the axial end load on the skirt, as discussed in sections 3.3.2 and 3.3.3.

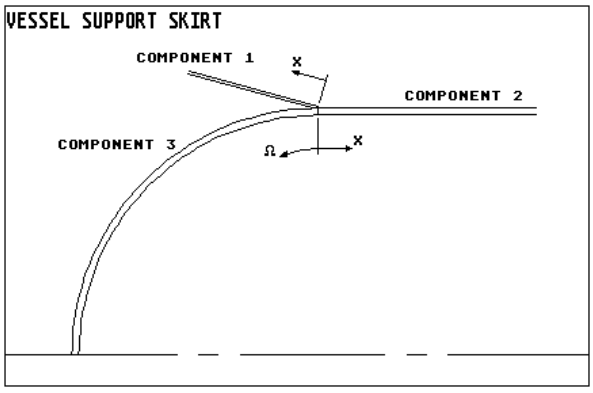

FIGURE 3.32(b) Geometry plot for example 3.15 case 1

The junction results are given in FIGURE 3.32(d). The highest stress is the meridional membrane plus bending stress in the skirt at the junction, SLi = -202.46 N/mm^2. A plot of this stress is shown in FIGURE 3.32(e). The skirt stresses are high due to the severe bending moments occurring at the junction.

The stresses in the vessel are much lower. Plots of the highest stresses in the vessel are shown in FIGURES 3.32(f) and (g). In general, the highest stress can sometimes occur in the vessel. In practice it is necessary to investigate each component and each operating condition to establish the worst case.

INPUT DATA, PROGRAM AJAP1

VESSEL SUPPORT SKIRT
Total Loads

COMPONENT No. 1
CONE, JUNCTION AT SMALL RIGHT END
Rj= 1270 mm
T= 15 mm
PHI= 15 degrees
E= 198000 N/mm2
PR= .3
ALPHA= .0000125 /degC
Fax= -37.4 N/mm
Fo= -38.71933 N/mm
Ta= 20 degC
Tm= 180 degC
Gj= .16 degC/mm

COMPONENT No. 2
CYLINDER, JUNCTION AT LEFT END
R= 1250 mm
T= 40 mm
E= 198000 N/mm2
PR= .3
ALPHA= .0000125 /degC
BETA= 5.748517E-03 /mm
D= 1.16044E+09 Nmm
P= 3 N/mm2
Fp= 1875 N/mm
Fax= -30 N/mm
Fo= 1845 N/mm
Ta= 20 degC
Tm= 200 degC

COMPONENT No. 3
SPHERICAL SHELL, JUNCTION AT RIGHT END
Rs= 1250 mm
T= 40 mm
PHI= 90 degrees
E= 198000 N/mm2
PR= .3
ALPHA= .0000125 /degC
BETA= 7.185642
P= 3 N/mm2
Fp= 1875 N/mm
Fax= 8 N/mm
Fo= 1883 N/mm
Ta= 20 degC
Tm= 200 degC

APPLIED JUNCTION MOMENT & FORCE
Mo= 748 Nmm/mm clockwise
Vo= 10.02099 N/mm inward

FREE DISPLACEMENTS AT JUNCTION
COMPONENT No. 1
Yf= 2.544967 mm outward
THf= 2.626109E-03 radians anti-clockwise

COMPONENT No. 2
Yf= 3.316998 mm outward
THf= 0 radians

COMPONENT No. 3
Yf= 3.018008 mm outward
THf= 0 radians

FIGURE 3.32(c) Input data set for example 3.15 case 1

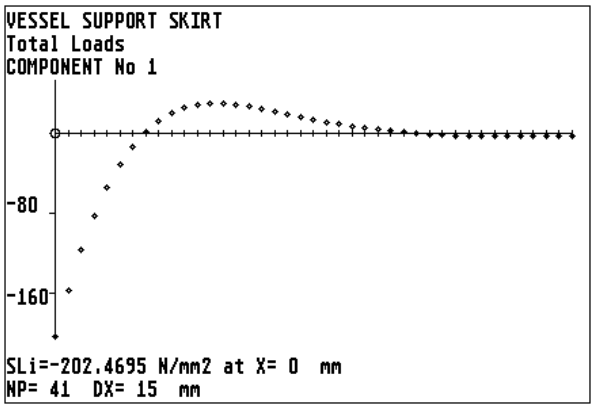

FIGURE 3.32(e) Meridional stress along the inside surface of the skirt from the junction.

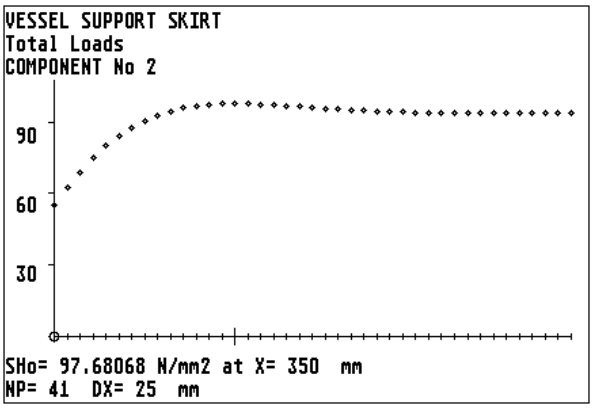

FIGURE 3.32(f) Hoop stress along the outside of the vessel cylinder from the junction.

FIGURE 3.32(g) Meridional stress along the inside surface of the hemispherical end from the junction

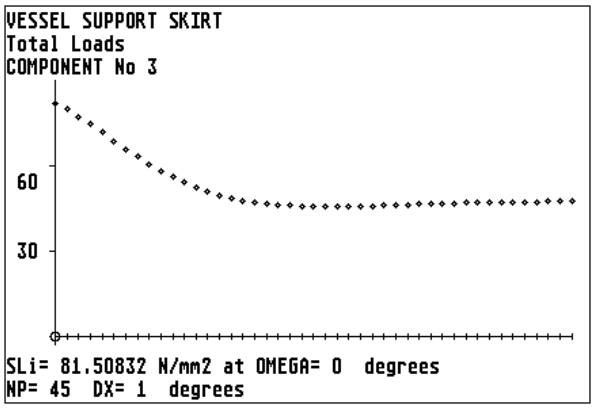

JUNCTION RESULTS
DISCONTINUITY FORCES & MOMENTS
VESSEL SUPPORT SKIRT
Total Loads

Mj 1 = -7415.278 Nmm/mm clockwise
Vj 1 = -124.4615 N/mm outward

Mj 2 = 2514.934 Nmm/mm clockwise
Vj 2 = 113.987 N/mm inward

Mj 3 = 9182.217 Nmm/mm anti-clockwise
Vj 3 = 20.49551 N/mm inward

RESULTS COMPONENT No. 1
VESSEL SUPPORT SKIRT
Total Loads
X= 0 mm
XI= 127.0333 LP= 0
Y= 3.091245 mm
THETA= 1.109223E-03 radians
V= 120.2206 N/mm
N1= -70.93234 N/mm
N2= 1267.853 N/mm
M1= -7415.278 Nmm/mm
M2= -2207.369 Nmm/mm
STRESSES N/mm2
SV= 8.014704
SL= -4.728822
SH= 84.52352
SBL=+or- 197.7407
SBH=+or- 58.86316
SLo= 193.0119
SLi= -202.4695
SHo= 143.3867
SHi= 25.66036

RESULTS COMPONENT No. 2
VESSEL SUPPORT SKIRT
Total Loads
X= 0 mm
Y= 3.091245 mm
THETA= 1.109242E-03 radians
V= -113.987 N/mm
N1= 1845 N/mm
N2= 2319.629 N/mm
M1= 2514.934 Nmm/mm
M2= 754.4801 Nmm/mm
STRESSES N/mm2
SV= -2.849675
SL= 46.125
SH= 57.99073
SBL=+or- 9.431001
SBH=+or- 2.829301
SLo= 36.694
SLi= 55.556
SHo= 55.16143
SHi= 60.82003

RESULTS COMPONENT No. 3
VESSEL SUPPORT SKIRT
Total Loads
OMEGA= 0 degrees
Y= 3.091245 mm
THETA= 1.109242E-03 radians
V= -20.49551 N/mm
N1= 1883 N/mm
N2= 2331.029 N/mm
M1= 9182.217 Nmm/mm
M2= 2754.666 Nmm/mm
STRESSES N/mm2
SV= -.5123877
SL= 47.075
SH= 58.27572
SBL=+or- 34.43331
SBH=+or- 10.33
SLo= 12.64169
SLi= 81.50832
SHo= 47.94572
SHi= 68.60571

FIGURE 3.32(d) Junction results for example 3.15 case 1

Example 3.15

Case 2 Nozzle Thermal Sleeve. The following is an example of a pressure vessel nozzle that requires a thermal sleeve due a severe thermal downshock as a result of a thermal transient. The geometry and loading are detailed in FIGURE 3.33(a). The nozzle is sufficiently long, i.e. $>2.5(R*T)^{1/2}$, so that the junction with the vessel does not interact with the junction with the pipe and sleeve. This is a necessary requirement. If the nozzle is made too short and stiff the pipe and/or the sleeve will be overstressed. The junction is modelled by four components, i.e. three cylinders and a compact ring. A geometry plot is shown in FIGURE 3.33(b) and the input data set is given in FIGURE 3.33(d). The cylinders are of length $5(R*T)^{1/2}$ for plotting purposes.

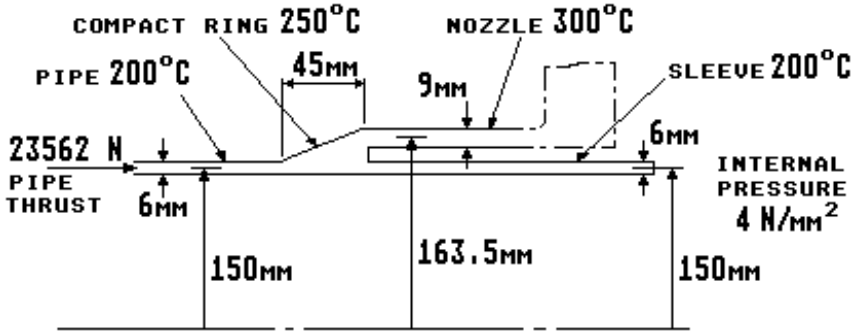

FIGURE 3.33(a) Geometry and loading on a nozzle with a thermal sleeve

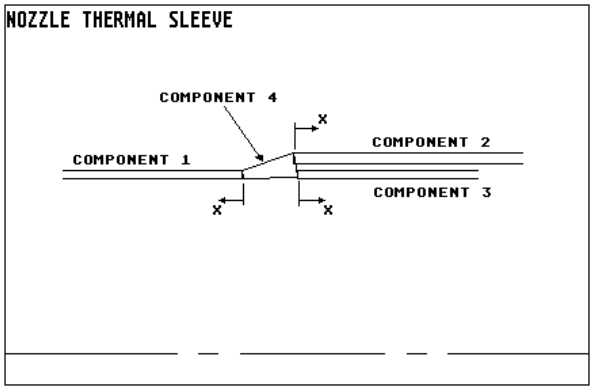

FIGURE 3.33(b) Geometry plot for example 3.15 case 2

The nozzle, pipe and ring are subjected to an internal pressure of 4 N/mm^2. There is no pressure difference across the sleeve. During steady state conditions all components are at 300°C but due to the thermal downshock the temperature of the pipe and sleeve are reduced to 200°C. There is a total axial end load of 23562 N due to pipe thrust.

$$\text{i.e. } F_{AX} = 23562/(2*\pi*150) = -25 \text{ N/mm circumference.}$$

The negative sign indicates compression of the pipe at the junction. This thrust is taken out by the nozzle to the vessel and then to ground. The axial end load on the nozzle becomes:

$$F_{AX} = 23562/(2*\pi*163.5) = -22.936 \text{ N/mm circumference.}$$

The effects of the axial end loads and pressure end loads produce a default moment Mo = 3975.691 Nmm/mm circumference at the centroid of the compact ring. In addition to this moment, the ring is subjected to a pressure loading at its inside radius and there is an axial thrust due to the pressure acting in the gap between the sleeve and the nozzle. In this case the gap is small and the thrust acts almost through the centroid. The moment produced by this thrust will be small and can be ignored in this case. The pressure loading at the inside radius must be considered and is applied to the ring as follows. With reference to FIGURE 3.33(c) the radial force at the centroid of the ring due to the pressure acting on the inside of the ring is calculated from equation (3.31).

$$Vr = P*L*Ri/Rc \qquad (3.31)$$

where: P is the pressure acting at the inside radius = 4 N/mm^2
L is the axial length of the ring subjected to pressure = 45 mm
Ri is the inside radius of the ring = 147 mm
Rc is the centroid radius = 154.4444 mm as calculated by equation (2.117)

Therefore Vr = -171.324 N/mm circumference. The negative sign represents an outward force. As the force at the inside radius acts half way along the length of the ring and the force Vr is applied at the centroid, there will be a moment on the ring due to the offset distance Lo shown on FIGURE 3.33(c). This moment is calculated by equation (3.32) and applied to the centroid of the ring.

$$Mr = Vr*Lo \qquad (3.32)$$

where: $Lo = H_1*COS(\delta) - L/2$
δ is given by equation (2.118) = 0.165149 radians
H_1 is given by equation (2.119) = 27.0345 mm

Therefore Lo = 4.1667 mm and Mr = 713.856 Nmm/mm circumference, +ve clockwise.

The junction results are given in FIGURE 3.33(e). The highest stress is the meridional bending stress in the sleeve at the junction, SBL= 410.4 N/mm^2. A plot of this stress is shown in FIGURE 3.33(f). The stresses in the pipe and nozzle are much lower. Plots of the highest stresses in these components are shown in FIGURES 3.33(g) and (h). In general, the highest stress can occur in the pipe, nozzle or the sleeve. In practice it is necessary to investigate each component and each operating condition to establish the worst case.

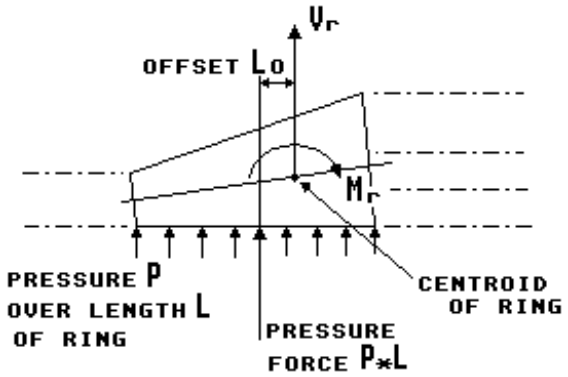

FIGURE 3.33(c) Pressure loading on the inside of the compact ring

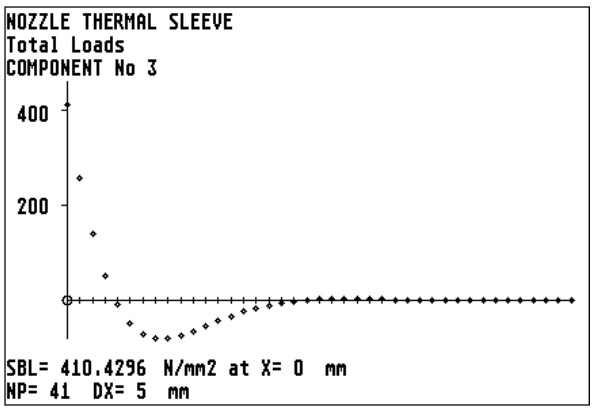

FIGURE 3.33(f) Meridional bending stress along the outside of the sleeve from the junction with the compact ring

INPUT DATA, PROGRAM AJAP1

NOZZLE THERMAL SLEEVE
Total Loads

COMPONENT No. 1
CYLINDER, JUNCTION AT RIGHT END
R= 150 mm
T= 6 mm
E= 198000 N/mm2
PR= .3
ALPHA= .0000125 /degC
BETA= .0428469 /mm
D= 3916484 Nmm
P= 4 N/mm2
Fp= 300 N/mm
Fax= -25 N/mm
Fo= 275 N/mm
Ta= 20 degC
Tm= 200 degC

COMPONENT No. 2
CYLINDER, JUNCTION AT LEFT END
R= 163.5 mm
T= 9 mm
E= 190000 N/mm2
PR= .3
ALPHA= .000013 /degC
BETA= 3.350893E-02 /mm
D= 1.268407E+07 Nmm
P= 4 N/mm2
Fp= 327 N/mm
Fax= -22.936 N/mm
Fo= 304.064 N/mm
Ta= 20 degC
Tm= 300 degC

COMPONENT No. 3
CYLINDER, JUNCTION AT LEFT END
R= 150 mm
T= 6 mm
E= 198000 N/mm2
PR= .3
ALPHA= .0000125 /degC
BETA= .0428469 /mm
D= 3916484 Nmm
Ta= 20 degC
Tm= 200 degC

COMPONENT No. 4
COMPACT RING AT JUNCTION
Rl= 150 mm
Tl= 6 mm
Rr= 157.5 mm
Tr= 21 mm
L= 45 mm
Rc= 154.4444 mm
AREA= 615.8796 mm2
Ina/C= 3445.09 mm3
C= -27.15986 mm
Lx 1 = -26.66667 mm
Lx 2 = -27.15986 mm
Lx 3 = -1.223859 mm
Lx 4 = 16.60715 mm
Lx 5 = 18.33333 mm
Lx 6 = 20.05952 mm
Lx 7 = 1.223859 mm
Lx 8 = -26.17347 mm
Lx 9 = 0 mm
CONNECTION 1 , 4 , 6 ,
E= 194000 N/mm2
PR= .3
ALPHA= .0000128 /degC
Mr= 713.856 Nmm/mm
Vr= -171.324 N/mm
Ta= 20 degC
Tm= 250 degC

APPLIED JUNCTION MOMENT & FORCE
Mo= 3975.691 Nmm/mm clockwise
Vo= 0 N/mm

FREE DISPLACEMENTS AT JUNCTION
COMPONENT No. 1
Yf= .4028409 mm outward
THf= 0 radians

COMPONENT No. 2
Yf= .6489498 mm outward
THf= 0 radians

COMPONENT No. 3
Yf= .3375 mm outward
THf= 0 radians

COMPONENT No. 4
Yf= .4888875 mm outward
THf= -9.380486E-04 radians

FIGURE 3.33(d) Input data set for example 3.15 case 2

JUNCTION RESULTS
DISCONTINUITY FORCES & MOMENTS
NOZZLE THERMAL SLEEVE
Total Loads

Mj 1 = -867.2551 Nmm/mm clockwise
Vj 1 = -81.33851 N/mm outward

Mj 2 = 3951.162 Nmm/mm clockwise
Vj 2 = 278.704 N/mm inward

Mj 3 = -2462.578 Nmm/mm anti-clockwise
Vj 3 = -204.0075 N/mm outward

at centroid
Mj 4 = -1085.361 Nmm/mm anti-clockwise
Vj 4 = 6.642046 N/mm inward

RESULTS COMPONENT No. 1
NOZZLE THERMAL SLEEVE
Total Loads
X= 0 mm
Y= .4745434 mm
THETA= 4.881802E-04 radians
V= 81.33851 N/mm
N1= 275 N/mm
N2= 1167.884 N/mm
M1= -867.2551 Nmm/mm
M2= -260.1765 Nmm/mm
STRESSES N/mm2
SV= 13.55642
SL= 45.83333
SH= 194.6473
SBL=+or- 144.5425
SBH=+or- 43.36275
SLo= 190.3758
SLi= -98.70918
SHo= 238.0101
SHi= 151.2846

RESULTS COMPONENT No. 2
NOZZLE THERMAL SLEEVE
Total Loads
X= 0 mm
Y= .4956687 mm
THETA= 4.881798E-04 radians
V= -278.704 N/mm
N1= 304.064 N/mm
N2= -949.1226 N/mm
M1= 3951.162 Nmm/mm
M2= 1185.348 Nmm/mm
STRESSES N/mm2
SV= -30.96711
SL= 33.78489
SH= -105.4581
SBL=+or- 292.6786
SBH=+or- 87.80358
SLo= -258.8938
SLi= 326.4635
SHo= -193.2616
SHi= -17.65448

RESULTS COMPONENT No. 3
NOZZLE THERMAL SLEEVE
Total Loads
X= 0 mm
Y= .4973542 mm
THETA= 4.88177E-04 radians
V= 204.0075 N/mm
N1= 0 N/mm
N2= 1266.045 N/mm
M1= -2462.578 Nmm/mm
M2= -738.7733 Nmm/mm
STRESSES N/mm2
SV= 34.00126
SL= 0
SH= 211.0076
SBL=+or- 410.4296
SBH=+or- 123.1289
SLo= 410.4296
SLi= -410.4296
SHo= 334.1364
SHi= 87.87868

RESULTS COMPONENT No. 4
NOZZLE THERMAL SLEEVE
Total Loads
Y= .4875615 mm
THETA= 4.881787E-04 radians
V= 164.682 N/mm
M= -371.5045 Nmm/mm
STRESSES N/mm2
SH= 41.29738
SBH= -16.65466
SH 1 = 24.94515
SH 2 = 24.64272
SH 3 = 40.5469
SH 4 = 51.48102
SH 5 = 52.53953
SH 6 = 53.59805
SH 7 = 42.04786
SH 8 = 25.24758
SH 9 = 41.29738

FIGURE 3.33(e) Junction results for example 3.15 case 2

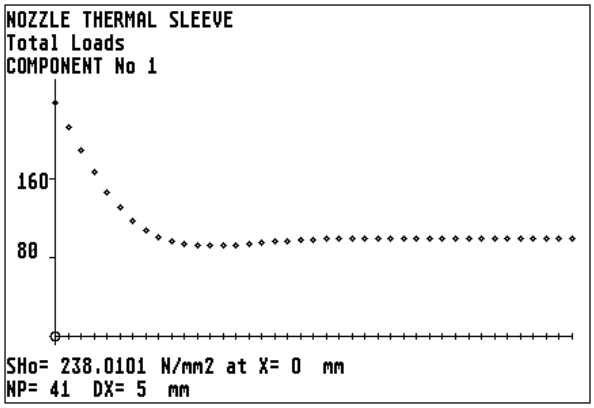

FIGURE 3.33(g) Hoop stress along the outside of the pipe from the junction with the compact ring.

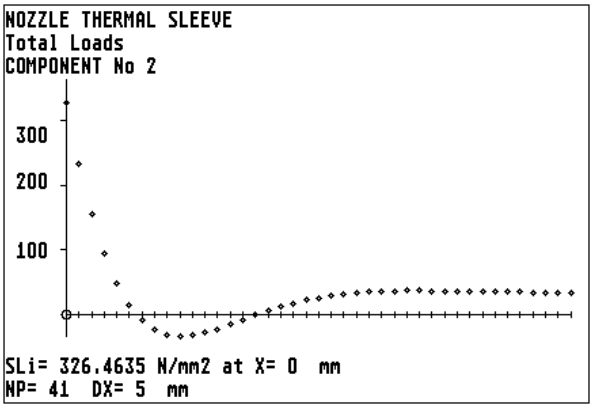

FIGURE 3.33(h) Meridional stress along the inside of the nozzle from the junction with the compact ring.

Example 3.16 SPINNING FLAT DISK

Spinning disks are a common feature of rotating equipment and are often shrunk onto a shaft to maintain concentricity and provide means to transmit torsional loading. In the following example a disk and hub is shrunk onto a solid shaft with a radial interference fit of 0.05 mm as shown in FIGURE 3.34(a). It is required to find the speed of rotation at which the shrink fit between the shaft and hub is just lost and to obtain the stresses at this speed.

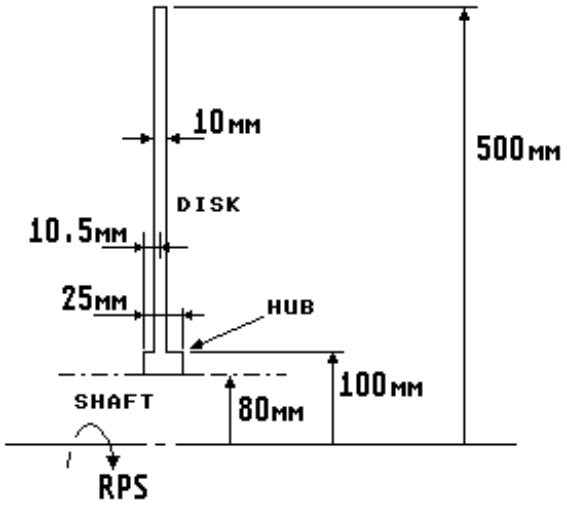

material properties
Young's modulus, E= 200000 N/mm^2
Poisson's ratio, PR= 0.3
Mass density, Md= 7.85E-6 Kg/mm^3

FIGURE 3.34(a) Geometry of spinning shaft, hub and disk

Using "AJAP1" the speed of rotation is found as follows.

(1) The shaft is modelled as a flat plate with zero inside radius. The centrifugal load is applied as a unit speed of rotation of 1 revolution per second. The input data set and the result at the outside radius is shown in FIGURE 3.34(b).

(2) The disk and hub are modelled as flat plates. Again the centrifugal load is applied as a unit speed of rotation of 1 revolution per second. The input data set and the result at the inside radius of the hub (component 2) is shown in FIGURE 3.34(c). The disk and hub have their centre lines offset by 2 mm. This is simulated by adjusting the offset option for the hub by setting the junction position, given by equation (2.62), as follows:

Junction position, JP = 2*offset/thickness of the hub = 2*2/25 = -0.16

The negative sign is required as the disk is offset to the left of the hub centre line.

(3) From the two sets of results obtained in (1) and (2) above. The difference in the radial deflection between the hub and the shaft for a unit speed can be obtained as follows:

From FIGURE 3.33(b) at the shaft outside radius (80mm) the radial deflection of the shaft is Y = 0.0001388377 mm outward.

From FIGURE 3.33(c) at the hub inside radius (80mm) the radial deflection of the hub centre line is Y = 0.01849027 mm outward and rotation (of a meridian) THETA = -0.0005559637 radians clockwise. Because of the hub rotation the right corner of the hub will move inward by:

Y = THETA*hub thickness/2 = -0.0005559637*25/2 = -0.0069487 mm inward

The hub radial deflection becomes = 0.01849027 - 0.0069487 = 0.0115414 mm outward

The difference in radial deflection between hub and shaft is:

Y_{DIFF} = 0.0115414 - 0.0001388377 = 0.0114026 mm outward

(4) The centrifugal loading (and hence the deflection) is proportional to speed squared. Therefore the speed of rotation that will just allow the hub and shaft to separate is obtained from equation (3.33).

$$\text{Speed of rotation} = \text{unit speed}*(\text{interference}/Y_{DIFF})^{1/2} = 1*(0.05/0.0114026)^{1/2} \qquad (3.33)$$

RPS = 2.094 revolutions per second

Result plots for the meridional and hoop membrane stresses in each component when spinning at 2.094 revolutions per second are shown in FIGURES 3.34(d) to (i). Due to the centre lines of the disk and hub not being in line there are bending stresses induced in these components. This results in higher stresses on the surface. Plots of the highest stresses are shown in FIGURES 3.34(j) and (k). The highest overall stress is the hoop membrane plus bending stress of 278.87 N/mm^2 at the left inside radius of the hub.

INPUT DATA, PROGRAM AJAP1	COMPONENT No. 1
	SPINNING SHAFT
SPINNING SHAFT	Unit Speed
Unit Speed	radius X= 80 mm
FLAT PLATE, support at O.D.	YL= 0 mm
Ro= 80 mm	Y= 1.388377E-04 mm
Ri= 0 mm	THETA= 0 radians
T= 25 mm	V= 0 N/mm
E= 200000 N/mm2	N1= 0 N/mm
PR= .3	N2= 8.677358 N/mm
MD= 7.85E-06 Kg/mm3	M1= 0 Nmm/mm
D= 2.861722E+08 Nmm	M2= 0 Nmm/mm
	STRESSES N/mm2
CENTRIFUGAL LOADING	SV= 0
RPS= 1 rev/s	SL= 0
	SH= .3470943
	SBL=+or- 0
	SBH=+or- 0
	SLI= 0
	SLr= 0
	SHI= .3470943
	SHr= .3470943

FIGURE 3.34(b) Input data set and result for spinning shaft

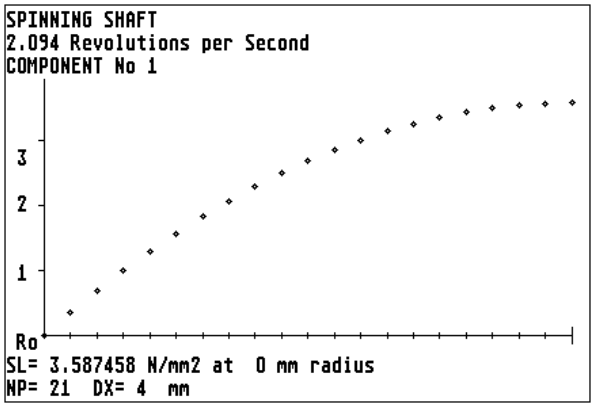

FIGURE 3.34(d) Meridional (radial) membrane stress in the shaft.

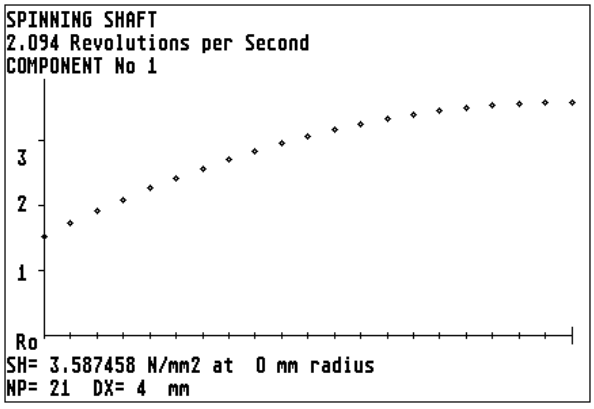

FIGURE 3.34(e) Hoop membrane stress in the shaft.

```
INPUT DATA, PROGRAM AJAP1

SPINNING DISK AND HUB
Unit Speed

COMPONENT No. 1
FLAT PLATE, JUNCTION AT I.D.
JUNCTION POSITION, CENTRE
JP= 0
OFFSET= 0
Ro= 500 mm
Ri= 100 mm
T= 10 mm
E= 200000 N/mm2
PR= .3
MD= 7.85E-06 Kg/mm3
D= 1.831502E+07 Nmm

COMPONENT No. 2
FLAT PLATE, JUNCTION AT O.D.
JUNCTION POSITION, JP= -.16
OFFSET= -2 mm
Ro= 100 mm
Ri= 80 mm
T= 25 mm
E= 200000 N/mm2
PR= .3
MD= 7.85E-06 Kg/mm3
D= 2.861722E+08 Nmm
CENTRIFUGAL LOADING
RPS= 1 rev/s

COMPONENT No. 2
SPINNING DISK AND HUB
Unit Speed
radius X= 80 mm
YL= -1.082932E-02 mm
Y= 1.849027E-02 mm
THETA= -5.559637E-04 radians
V= 0 N/mm
N1= 0 N/mm
N2= 1155.642 N/mm
M1= 0 Nmm/mm
M2= -1809.778 Nmm/mm
STRESSES N/mm2
SV= 0
SL= 0
SH= 46.22566
SBL=+or-  0
SBH=+or-  17.37387
SLl= 0
SLr= 0
SHl= 63.59953
SHr= 28.8518
```

FIGURE 3.34(c) Input data set and result for the disk and hub

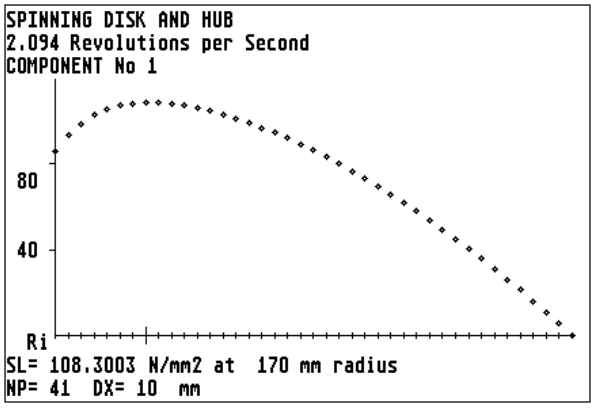

FIGURE 3.34(f) Meridional (radial) membrane stress in the disk.

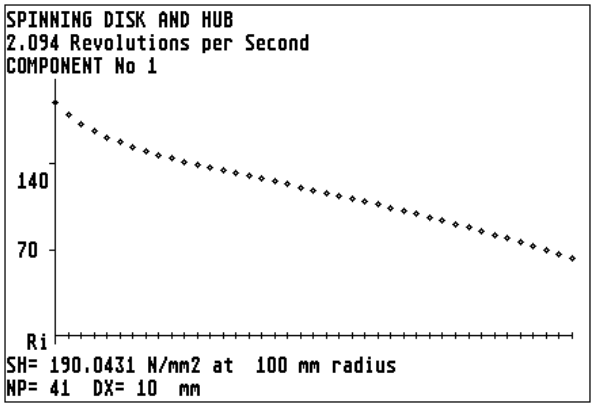

FIGURE 3.34(g) Hoop membrane stress in the disk.

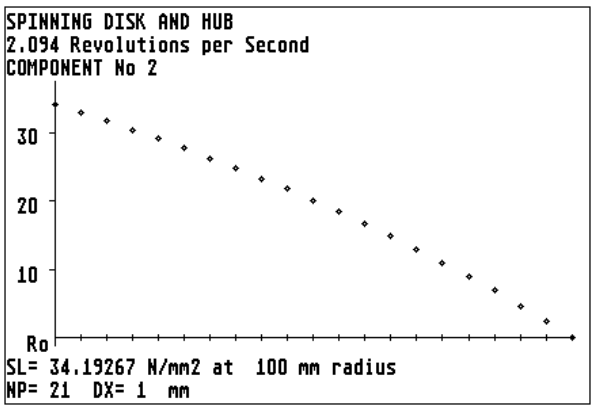

FIGURE 3.34(h) Meridional (radial) membrane stress in the hub.

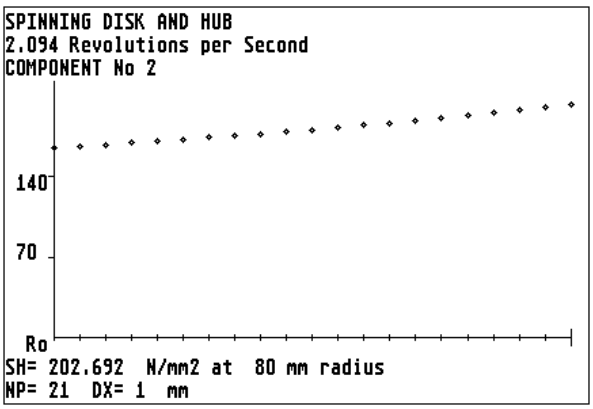

FIGURE 3.34(i) Hoop membrane stress in the hub.

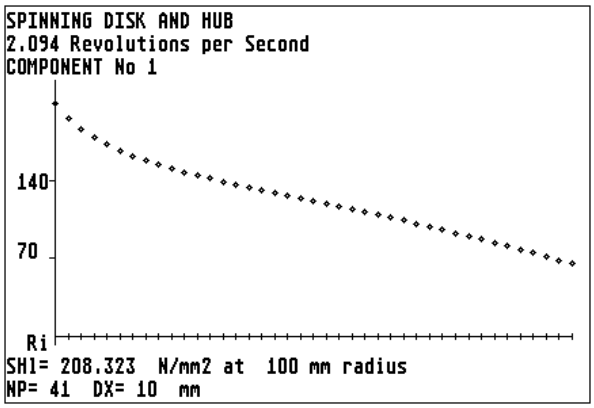

FIGURE 3.34(j) Maximum Hoop stress in the disk.

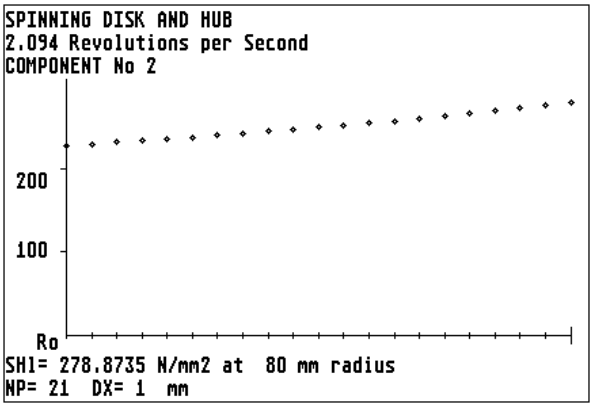

FIGURE 3.34(k) Maximum hoop stress in the hub.

Example 3.17 HEAT EXCHANGER TUBESHEET

This example shows how "AJAP1" can be used to confirm the design of a U-tube heat exchanger tubesheet. The tubesheet is a critical component as it provides a barrier between the shell side and tube side fluids and must have sufficient mechanical strength to withstand the pressure differences between the two fluids.

The thickness of the tubesheet can be calculated by rules provided in a pressure vessel code such as BS5500 (ref. 14). These rules have been developed over many years and are described in detail in the BSI published document PD6550: Part 4 (ref. 25) and in reference (53).

The thickness of the tubesheet depends on both the perforated region and on the support provided by the outer unperforated rim. It is proposed to investigate a U-tube heat exchanger for two common types of tubesheet edge support, i.e. simply supported and clamped. The stress controlling the tubesheet thickness is usually the maximum meridional (radial) bending stress, which in BS5500 terminology is limited to $\Omega\mu f$. Where Ω is a stress factor = 2.0 and μ is the ligament efficiency = ligament/tube pitch. f is the material allowable design strength value.

Hence for a tubesheet with a ligament efficiency of say 0.265 and an allowable design strength = 167 N/mm^2. The maximum radial bending stress would be limited to 88.51 N/mm^2 if the tubesheet thickness was based on BS5500 rules.

Case 1, Simply Supported Tubesheet.

The tubesheet of a typical U-tube heat exchanger is shown in FIGURE 3.35(a). In this type of exchanger the tube bundle has no axial stiffness and is free to expand in the axial direction without restraint from the pressure shell of the exchanger. The outside edge of the tubesheet is often supported by means of narrow gasket bolted flanges and the arrangement is generally considered to be simply supported. For a shell side pressure of 0.345 N/mm^2 the tubesheet thickness calculated by BS5500 rules is 31.5 mm in order to limit the radial bending stress as discussed above.

In "AJAP1" the perforated region of the tubesheet is simulated by a flat plate with equivalent modified material properties; Poison's ratio μ' = 0.04 and Young's modulus E' = 72411 N/mm^2. These properties are based on the characteristics for thin plates (thickness < 2*tube pitch) discussed in reference (25).

The unperforated outer rim is simulated as a compact ring with unmodified material properties. The shell side pressure is applied to the flat plate as a uniform pressure. The loading applied to the ring is shown in FIGURE 3.35(b). There is a shear load P*Ro/2 from the pressure acting over the flat plate as well as the pressure acting directly on the side of the ring. The effect of these loads on the ring is to put an applied twisting moment on the ring. For the support at the outer edge of the ring the applied moment about the ring centroid is given by equation (3.34).

$$\text{Moment} = -[P*R_L(Rr - R_L) + P(Rr^2 - R_L^2)*(Rr - R_L)/(Rr + R_L)]/2 \qquad (3.34)$$

$$= -3702.7 \text{ Nmm/mm circumference, negative anti-clockwise}$$

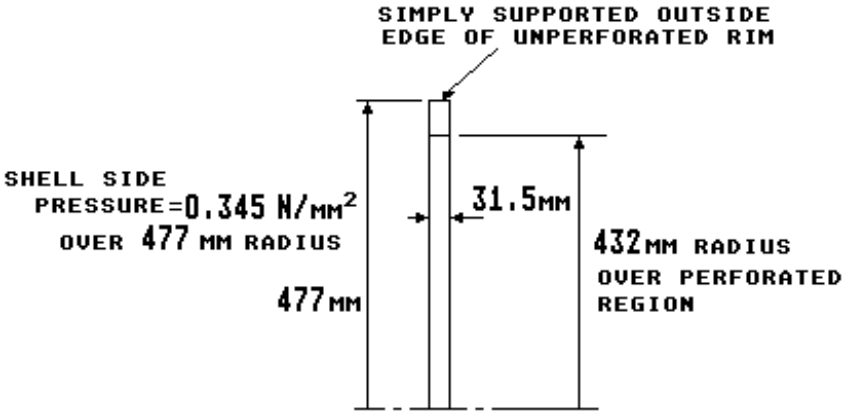

Tube details	Tubesheet details	
630 U-tubes fully expanded	1260 holes, 19.15 mm diameter	
19.05 mm outside diameter	ligament efficiency = 0.265	
1.651 mm wall thickness	E = 200000 N/mm^2	E' = 72411 N/mm^2
23.8 mm pitch	μ = 0.3	μ' = 0.04

FIGURE 3.35(a) Details of a U-Tube tubesheet

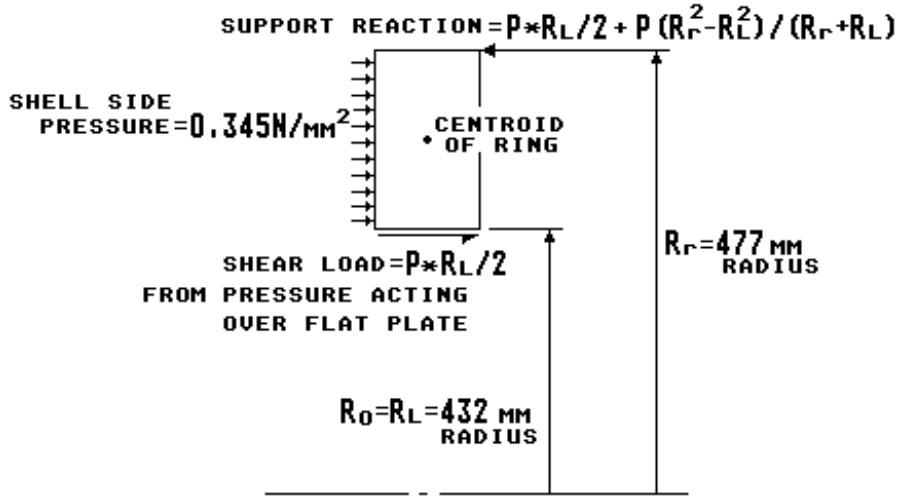

FIGURE 3.35(b) Loads acting on the outer rim of the tubesheet

This moment can be applied either as a component loading Mr or as an external load Mo. The input data set, free displacements and stiffness coefficients are shown in FIGURE 3.35(c). Inspection of the stiffness terms show that the compact ring (component 2) is only about a quarter of the stiffness of the equivalent flat plate.

Results are given in FIGURE 3.35(d) and plots of the bending stress in the equivalent flat plate are shown in FIGURES 3.35(e) and (f). These results show that the maximum stress is 82.17 N/mm^2 at the centre of the plate and is in close agreement with the limiting value of 88.51 N/mm^2. The results for the compact ring (component 2) show that the ring is stressed to 143.3 N/mm^2. This is acceptable for a material with an allowable design strength of 167 N/mm^2. Plots of the transverse deflection and rotation of the equivalent plate are shown in FIGURES 3.35(g) and (h) these can be compared with the results for the clamped case FIGURES 3.36(j) and (k).

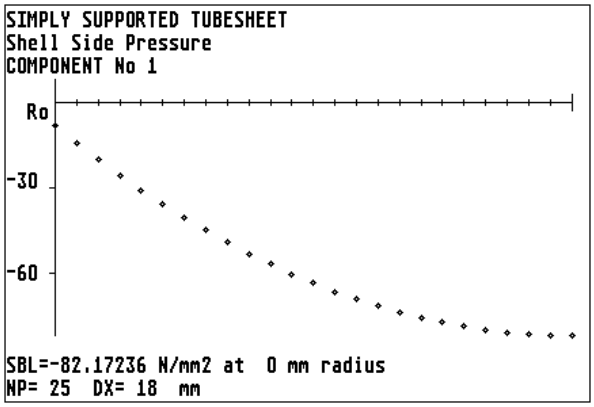

FIGURE 3.35(e) Meridional bending stress on the left surface of the equivalent flat plate from the outside edge (Ro=432mm) to the centre

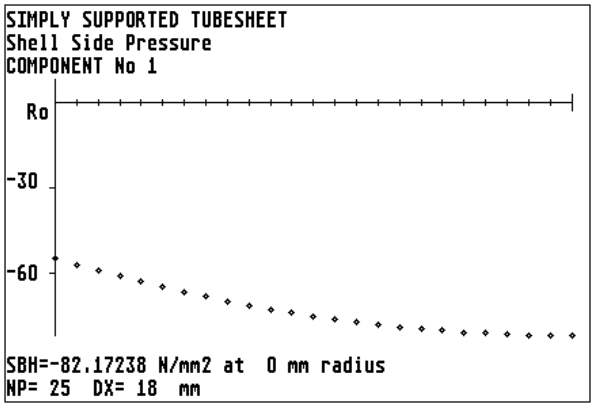

FIGURE 3.35(f) Hoop bending stress on the left surface of the equivalent flat plate from the outside edge (Ro=432mm) to the centre

Example 3.17, case 1 simply supported tubesheet

INPUT DATA, PROGRAM AJAP1

SIMPLY SUPPORTED TUBESHEET
Shell Side Pressure

COMPONENT No. 1
FLAT PLATE, JUNCTION AT O.D.
JUNCTION POSITION, CENTRE
JP= 0
OFFSET= 0 mm
Ro= 432 mm
Ri= 0 mm
T= 31.5 mm
E= 72411 N/mm2
PR= .04
D= 1.88908E+08 Nmm
P= .345 N/mm2

COMPONENT No. 2
COMPACT RING AT JUNCTION
Rl= 432 mm
Tl= 31.5 mm
Rr= 477 mm
Tr= 31.5 mm
L= 0 mm
Rc= 454.5 mm
AREA= 1417.5 mm2
Ina/C= 7441.871 mm3
C= 15.75 mm
Lx 1 = 3.665715E-06 mm
Lx 2 = -15.75 mm
Lx 3 = -15.75 mm
Lx 4 = -15.75 mm
Lx 5 = 3.665715E-06 mm
Lx 6 = 15.75 mm
Lx 7 = 15.75 mm
Lx 8 = 15.75 mm
Lx 9 = 0 mm
CONNECTION 1 ,
E= 200000 N/mm2
PR= .3

APPLIED JUNCTION MOMENT & FORCE
Mo= -3702.7 Nmm/mm anti-clockwise
Vo= 0 N/mm

FREE DISPLACEMENTS AT JUNCTION
COMPONENT No. 1
Yf= 0 mm
THf= 1.769688E-02 radians anti-clockwise

COMPONENT No. 2
at centroid
Yf= 0 mm
THf= 0 radians

STIFFNESS COEFFICIENTS
per mm circumference

COMPONENT No. 1
K(1 , 1)= 5499.968 N/mm
K(2 , 1)= 1E+15 Nmm/mm
K(3 , 1)= 1E+15 N/radian
K(4 , 1)= 454778.6 Nmm/radian

COMPONENT No. 2
K(1 , 2)= 1372.414 N/mm
K(2 , 2)= 1E+15 Nmm/mm
K(3 , 2)= 1E+15 N/radian
K(4 , 2)= 113481.5 Nmm/radian

FIGURE 3.35(c) Input data set for example 3.17 case 1

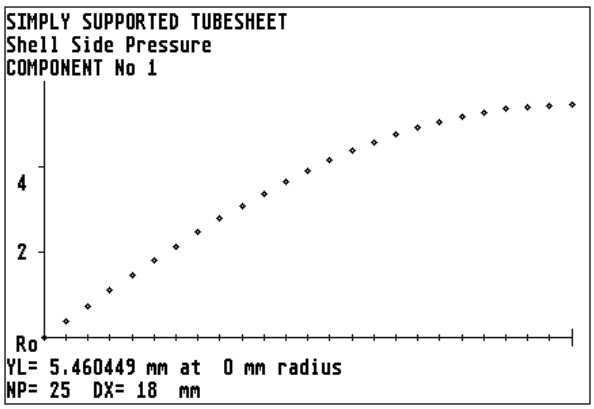

FIGURE 3.35(g) Transverse deflection of the equivalent flat plate from the outside edge (Ro=432mm) to the centre.

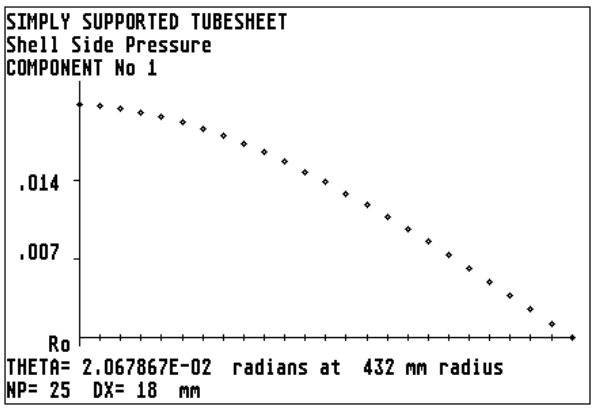

FIGURE 3.35(h) Rotation of the equivalent flat plate from the outside edge (Ro=432mm) to the centre.

JUNCTION RESULTS
DISCONTINUITY FORCES & MOMENTS
SIMPLY SUPPORTED TUBESHEET
Shell Side Pressure

Mj 1 = -1356.053 Nmm/mm anti-clockwise
Vj 1 = -8.325558E-05 N/mm outward

at centroid
Mj 2 = -2346.646 Nmm/mm anti-clockwise
Vj 2 = 8.325561E-05 N/mm inward

RESULTS COMPONENT No. 1
SIMPLY SUPPORTED TUBESHEET
Shell Side Pressure
radius X= 0 mm
YL= 5.460449 mm
Y= 0 mm
THETA= 0 radians
V= 0 N/mm
N1= 8.325558E-05 N/mm
N2= 8.325558E-05 N/mm
M1= 13589.26 Nmm/mm
M2= 13589.26 Nmm/mm
STRESSES N/mm2
SV= 0
SL= 2.643034E-06
SH= 2.643034E-06
SBL=+or- 82.17236
SBH=+or- 82.17236
SLl= -82.17236
SLr= 82.17236
SHl= -82.17236
SHr= 82.17236

RESULTS COMPONENT No. 1
SIMPLY SUPPORTED TUBESHEET
Shell Side Pressure
radius X= 432 mm
YL= 1.192093E-07 mm
Y= 1.513747E-08 mm
THETA= 2.067867E-02 radians
V= -74.52 N/mm
N1= 8.325558E-05 N/mm
N2= 8.325558E-05 N/mm
M1= 1356.053 Nmm/mm
M2= 9082.287 Nmm/mm
STRESSES N/mm2
SV= -2.365714
SL= 2.643034E-06
SH= 2.643034E-06
SBL=+or- 8.199866
SBH=+or- 54.91935
SLl= -8.199863
SLr= 8.199868
SHl= -54.91934
SHr= 54.91935

RESULTS COMPONENT No. 2
SIMPLY SUPPORTED TUBESHEET
Shell Side Pressure
Y= -6.066362E-08 mm
THETA= 2.067867E-02 radians
V= -8.325561E-05 N/mm
M= -2346.646 Nmm/mm
STRESSES N/mm2
SH= -2.669466E-05
SBH= 143.3175
SH 1 = 6.661591E-06
SH 2 = -143.3175
SH 3 = -143.3175
SH 4 = -143.3175
SH 5 = 6.661591E-06
SH 6 = 143.3175
SH 7 = 143.3175
SH 8 = 143.3175
SH 9 = -2.669466E-05

FIGURE 3.35(d) Results for example 3.17 case 1

Case 2, Clamped Tubesheet.

If the tubesheet is welded direct to the shell of the exchanger, FIGURE 3.36(a), and the bending stiffness of the shell is high relative to the tubesheet then the edge of the tubesheet can be considered clamped. FIGURE 3.36(a) shows a tubesheet attached to a cylindrical shell. The shell side pressure is 0.345 N/mm^2 as before. The thickness of the tubesheet calculated by BS5500 rules is 23.5mm in order to limit the radial bending stress to 88.51 N/mm^2 as discussed previously.

In "AJAP1" the arrangement can be simulated as a four component junction, i.e. two cylinders, a flat plate and a compact ring. A geometry plot is shown in FIGURE 3.36(b). The input data set and free displacements are shown in FIGURE 3.36(c). The default external moment Mo is due to the shear load P*Ro/2 (from the pressure acting over the flat plate) acting about the ring centroid. The stiffness coefficients are listed in FIGURE 3.36(d). Inspection of the coefficients show that the bending stiffness of the shell (the K(4,2) and K(4,3) terms) are much larger than the bending stiffness of the equivalent flat plate (the K(4,1) term) so it is reasonable to expect this arrangement to be effectively clamped.

Example 3.17, case 2 clamped tubesheet

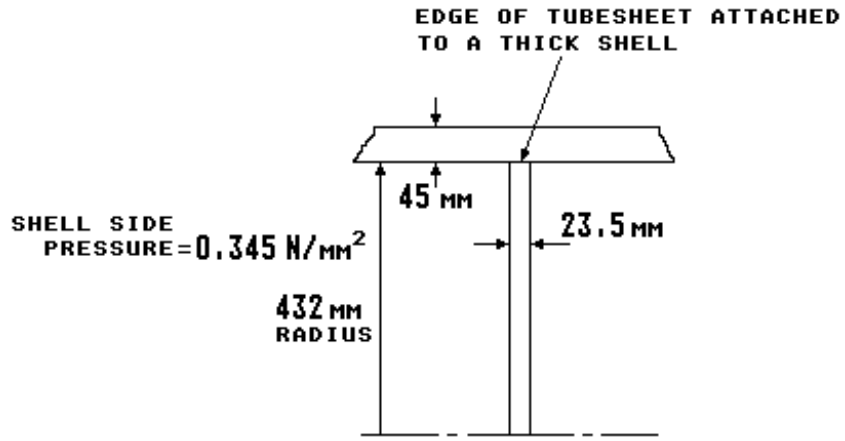

Tube details	Tubesheet details	
630 U-tubes fully expanded	1260 holes, 19.15 mm diameter	
19.05 mm outside diameter	ligament efficiency = 0.265	
1.651 mm wall thickness	E = 200000 N/mm^2	E' = 72411 N/mm^2
23.8 mm pitch	μ = 0.3	μ' = 0.04

FIGURE 3.36(a) Details of a U-Tube tubesheet attached to a shell

Junction results are listed in FIGURE 3.36(e) and stresses in the compact ring are given in FIGURE 3.36(f). In this case the ring stresses are very low as the ring is not able to twist due to the clamping of the shell. Selected results for the plate and cylindrical shells are given in FIGURE 3.36(g). Plots of the bending stress in the equivalent flat plate are shown in FIGURES 3.36(h) and (i). The maximum stress in the plate is 87.23 N/mm^2 and occurs at the outer edge of the plate (as opposed to the centre of the plate for the simply supported case). The result is in agreement with the limiting value of 88.51 N/mm^2.

Plots of the transverse deflection and rotation of the equivalent plate are shown in FIGURES 3.36(j) and (k). These plots clearly show the clamping effect of the shell. The shape of the plots are different from the simply supported case shown in FIGURES 3.35(g) and (h).

Although the above cases are for extreme edge conditions, "AJAP1" could be used to investigate a complete range of conditions and geometries.

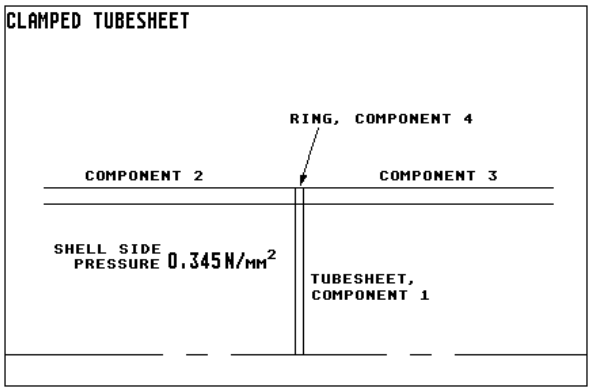

FIGURE 3.36(b) Geometry plot for example 3.17 case 2

STIFFNESS COEFFICIENTS
per mm circumference

COMPONENT No. 1
K(1 , 1)= 4103.151 N/mm
K(2 , 1)= 1E+15 Nmm/mm
K(3 , 1)= 1E+15 N/radian
K(4 , 1)= 188830.4 Nmm/radian

COMPONENT No. 2
K(1 , 2)= 2423.691 N/mm
K(2 , 2)= 269655.8 Nmm/mm
K(3 , 2)= 269655.8 N/radian
K(4 , 2)= 1.500073E+07 Nmm/radian

COMPONENT No. 3
K(1 , 3)= 2423.691 N/mm
K(2 , 3)= 269655.8 Nmm/mm
K(3 , 3)= 269655.8 N/radian
K(4 , 3)= 1.500073E+07 Nmm/radian

COMPONENT No. 4
K(1 , 4)= 1023.865 N/mm
K(2 , 4)= 1E+15 Nmm/mm
K(3 , 4)= 1E+15 N/radian
K(4 , 4)= 47119.1 Nmm/radian

FIGURE 3.36(d) Stiffness coefficients for example 3.17 case 2

```
INPUT DATA, PROGRAM AJAP1

CLAMPED TUBESHEET
Shell Side Pressure

COMPONENT No. 1
FLAT PLATE, JUNCTION AT O.D.
JUNCTION POSITION, CENTRE
JP= 0
OFFSET= 0 mm
Ro= 432 mm
Ri= 0 mm
T= 23.5 mm
E= 72411 N/mm2
PR= .04
D= 7.843725E+07 Nmm
P= .345 N/mm2

COMPONENT No. 2
CYLINDER, JUNCTION AT RIGHT END
R= 454.5 mm
T= 45 mm
E= 200000 N/mm2
PR= .3
BETA= 8.988091E-03 /mm
D= 1.668956E+09 Nmm
P= .345 N/mm2
Fp= 78.40125 N/mm
Fo= 78.40125 N/mm

COMPONENT No. 3
CYLINDER, JUNCTION AT LEFT END
R= 454.5 mm
T= 45 mm
E= 200000 N/mm2
PR= .3
BETA= 8.988091E-03 /mm
D= 1.668956E+09 Nmm

COMPONENT No. 4
COMPACT RING AT JUNCTION
RI= 432 mm
TI= 23.5 mm
Rr= 477 mm
Tr= 23.5 mm
L= 0 mm
Rc= 454.5 mm
AREA= 1057.5 mm2
Ina/C= 4141.873 mm3
C= 11.75 mm
Lx 1 = 3.665715E-06 mm
Lx 2 = -11.75 mm
Lx 3 = -11.75 mm
Lx 4 = -11.75 mm
Lx 5 = 3.665715E-06 mm
Lx 6 = 11.75 mm
Lx 7 = 11.75 mm
Lx 8 = 11.75 mm
Lx 9 = 0 mm
CONNECTION 1 , 3 , 7 ,
E= 200000 N/mm2
PR= .3

APPLIED JUNCTION MOMENT & FORCE
Mo= -1676.7 Nmm/mm anti-clockwise
Vo= 0 N/mm

FREE DISPLACEMENTS AT JUNCTION
COMPONENT No. 1
Yf= 0 mm
Thf= .0426211 radians anti-clockwise

COMPONENT No. 2
Yf= 6.730748E-03 mm outward
Thf= 0 radians

COMPONENT No. 3
Yf= 0 mm
Thf= 0 radians

COMPONENT No. 4
at centroid
Yf= 0 mm
THf= 0 radians
```

FIGURE 3.36(c) Input data set for example 3.17 case 2

JUNCTION RESULTS
DISCONTINUITY FORCES & MOMENTS
CLAMPED TUBESHEET
Shell Side Pressure

Mj 1 = 8029.018 Nmm/mm clockwise
Vj 1 = -9.03208 N/mm outward

Mj 2 = 4583.692 Nmm/mm anti-clockwise
Vj 2 = 55.06346 N/mm inward

Mj 3 = -3955.869 Nmm/mm anti-clockwise
Vj 3 = -43.77759 N/mm outward

at centroid
Mj 4 = -4.776254 Nmm/mm anti-clockwise
Vj 4 = -2.253786 N/mm outward

FIGURE 3.36(e) Junction results for example 3.17 case 2

RESULTS COMPONENT No. 4
CLAMPED TUBESHEET
Shell Side Pressure
Y= 2.201254E-03 mm
THETA= 1.013656E-04 radians
V= 2.253786 N/mm
M= -4.776254 Nmm/mm
STRESSES N/mm2
SH= .9686487
SBH= .5241126
SH 1 = .9686489
SH 2 = .4445365
SH 3 = .4445362
SH 4 = .4445365
SH 5 = .9686489
SH 6 = 1.492761
SH 7 = 1.492761
SH 8 = 1.492761
SH 9 = .9686487

FIGURE 3.36(f) Results for the compact ring example 3.17 case 2

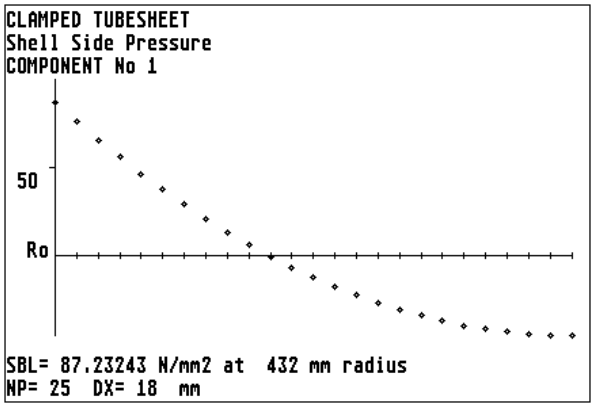

FIGURE 3.36(h) Meridional bending stress on the left surface of the equivalent flat plate from the outside edge (Ro=432mm) to the centre.

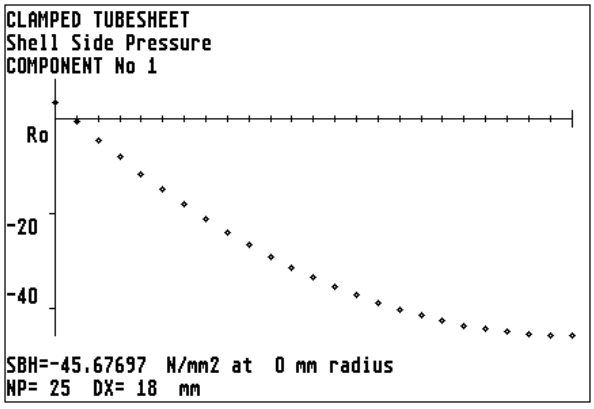

FIGURE 3.36(i) Hoop bending stress on the left surface of the equivalent flat plate from the outside edge (Ro=432mm) to the centre.

RESULTS COMPONENT No. 1
CLAMPED TUBESHEET
Shell Side Pressure
radius X= 0 mm
YL= 2.415497 mm
Y= 0 mm
THETA= 0 radians
V= 0 N/mm
N1= 9.03208 N/mm
N2= 9.03208 N/mm
M1= 4204.184 Nmm/mm
M2= 4204.184 Nmm/mm
STRESSES N/mm2
SV= 0
SL= .3843438
SH= .3843438
SBL=+or- 45.67697
SBH=+or- 45.67697
SLl= -45.29263
SLr= 46.06131
SHl= -45.29263
SHr= 46.06131

RESULTS COMPONENT No. 2
CLAMPED TUBESHEET
Shell Side Pressure
X=0 mm
Y= 1.010208E-03 mm
THETA= 1.013656E-04 radians
V= -55.06346 N/mm
N1= 78.40125 N/mm
N2= 43.52449 N/mm
M1= 4583.692 Nmm/mm
M2= 1375.107 Nmm/mm
STRESSES N/mm2
SV= -1.223632
SL= 1.74225
SH= .9672109
SBL=+or- 13.58131
SBH=+or- 4.074392
SLo= -11.83906
SLi= 15.32356
SHo= -3.107182
SHi= 5.041603

RESULTS COMPONENT No. 1
CLAMPED TUBESHEET
Shell Side Pressure
radius X= 432 mm
YL= 4.768372E-07 mm
Y= 2.201255E-03 mm
THETA= 1.013652E-04 radians
V= -74.52 N/mm
N1= 9.03208 N/mm
N2= 9.03208 N/mm
M1= -8029.018 Nmm/mm
M2= -302.7855 Nmm/mm
STRESSES N/mm2
SV= -3.171064
SL= .3843438
SH= .3843438
SBL=+or- 87.23243
SBH=+or- 3.289657
SLl= 87.61678
SLr= -86.84808
SHl= 3.674001
SHr= -2.905313

RESULTS COMPONENT No. 3
CLAMPED TUBESHEET [Corrected was simply supported]
Shell Side Pressure
X= 0 mm
Y= 3.392301E-03 mm
THETA= 1.013656E-04 radians
V= 43.77759 N/mm
N1= 0 N/mm
N2= 67.17426 N/mm
M1= -3955.869 Nmm/mm
M2= -1186.761 Nmm/mm
STRESSES N/mm2
SV= .9728354
SL= 0
SH= 1.492761
SBL=+or- 11.72109
SBH=+or- 3.516328
SLo= 11.72109
SLi= -11.72109
SHo= 5.009089
SHi= -2.023566

FIGURE 3.36(g) Example 3.17 case 2, results for the equivalent flat plate (component 1) and the cylindrical shells (component No. 2 and 3)

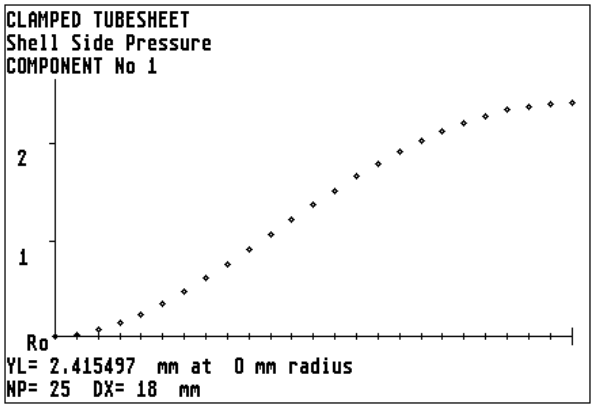

FIGURE 3.36(j) Transverse deflection of the equivalent flat plate from the outside edge (Ro=432mm) to the centre.

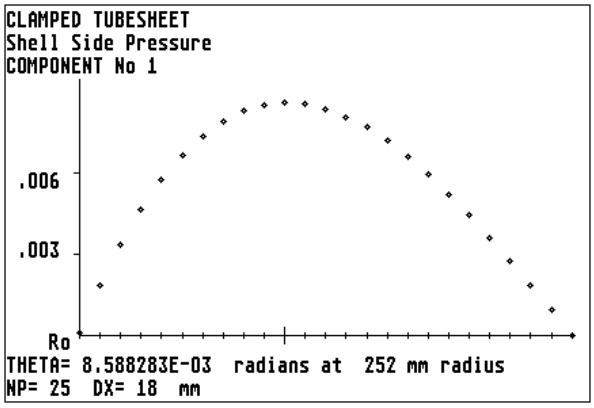

FIGURE 3.36(k) Rotation of the equivalent flat plate from the outside edge (Ro=432mm) to the centre.

Example 3.18 BOLTED FLANGES

Bolted flanges are often used in pressure vessel manways and associated pressure pipe lines. Flanges are generally identified as one of two possible types depending on the form of the gasket seating face: (1) the *raised* face (narrow face) type or (2) the *full* face type. FIGURE 3.37(a) to (d) shows some of the types of raised face flange that can be analysed by "AJAP1". The full face type can also be analysed provided the pressure distribution between the flange faces can be estimated.

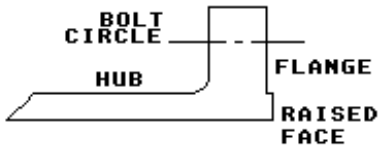

FIGURE 3.37(a) Conventional integral hub flange.

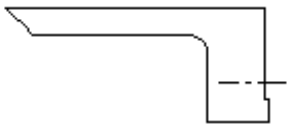

FIGURE 3.37(b) Reversed integral hub flange.

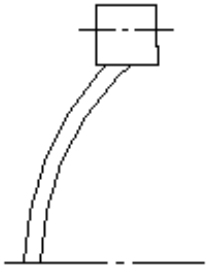

FIGURE 3.37(c) Spherical domed flange.

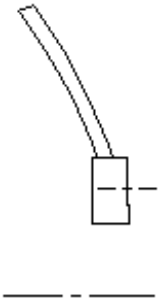

FIGURE 3.37(d) Studded connection.

In "AJAP1" the flange and its connecting shell are simulated by using the component types permitted, e.g. flat plate(s) or compact ring for the flange and cylinder, cone, spherical cap for the shell as appropriate. The loading on the flange and shell can be internal or external pressure plus any other mechanical and temperature loading permitted for the component. The following cases show examples of the main types of flange shown in FIGURE 3.37(a) to (d), when subjected to operating and bolting up conditions. It should be appreciated that the stress analysis and functioning of bolted flanges is a complex subject. The flange can also leak if it is not stiff enough or the bolting is not preloaded correctly or the gasket is fitted incorrectly or damaged.

For a better understanding of the subject it is necessary to consider the following references: ROSE in chapter 6 of GILL (ref. 7), POLAK (ref. 15), WATERS et al (ref. 31), Modern Flange Design (ref. 32), MURRAY and STUART (ref. 33).

Case 1 Conventional Hub Flange. FIGURE 3.38(a) shows a 24" Class 900 Long Weld Neck (LWN) flange. These particular flanges feature a flange and bolting corresponding to the dimensions given in BS1560 (ref. 30) and a relatively thick straight hub that is welded to the vessel shell. There is often sufficient thickness in the hub to reinforce the opening in the vessel without the need for additional reinforcement.

A geometry plot is shown in FIGURES 3.38(b). The cylindrical shell is component No.1 and the flange is simulated by two flat plates, components 2 and 3, connected at the mean junction radius with the shell. The cylindrical shell and the inside edge of the flange (component 3) are subjected to the internal pressure of 6.02 N/mm^2. The flange is subjected to transverse loads from the bolting, the gasket and the internal pressure. In most cases the actual service bolt loads on a flange are unknown. For the purpose of this example the four transverse loads required by the pressure vessel codes, BS5500 and ASME SECTION VIII, to *size* the flange will be used to load the flange. The basis for the use of these loads is discussed in reference (31) and (32).

(1) A bolt load W_{M1}= 2836888 N total. This load is applied as a point load W1= 1001.45 N/mm at a radius of 450.85 mm to component No.2. Positive acting to the right.

(2) A Hydrostatic end force from the shell H_D= 1756128N total, due to the pressure acting over the inside diameter of the shell. This load is applied as a point load W2= -822.726 N/mm at the junction radius of 339.72 mm to component No.2. Negative acting to the left. Note that the difference in the value of this load and F_P for the shell is simply due to "AJAP1" calculating the end load based on mean radius. For most cases the difference is not significant.

(3) A gasket reaction load H_G= 739318.7 N total. This load is applied as a point load W1= -353.229 N/mm at a radius of 333.116 mm to component No.3. Negative acting to the left. H_G is calculated on the basis of a spiral wound gasket with a gasket factor = 3 and minimum seating stress = 69 N/mm^2. Note in some cases this load may act at a larger radius than the junction radius. In these cases the load would be applied as a point load W3 to component No.2.

(4) A Hydrostatic end force H_T= 341441.8 N total due to the pressure acting on the flange face between the inside diameter and the gasket reaction diameter. This load is applied as a point load W2= -170.374 N/mm at a radius of 318.958 mm to component No. 3 [Corrected was No. 2]. Negative acting to the left.

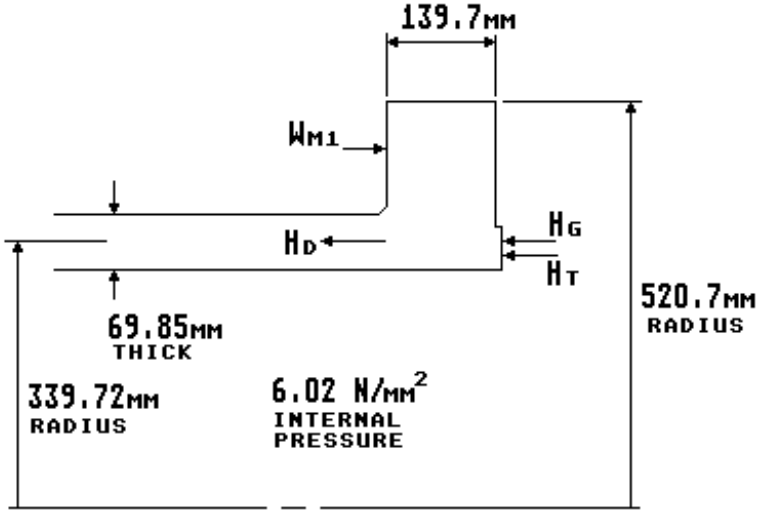

FIGURE 3.38(a) 24 inch class 900 long weld neck flange

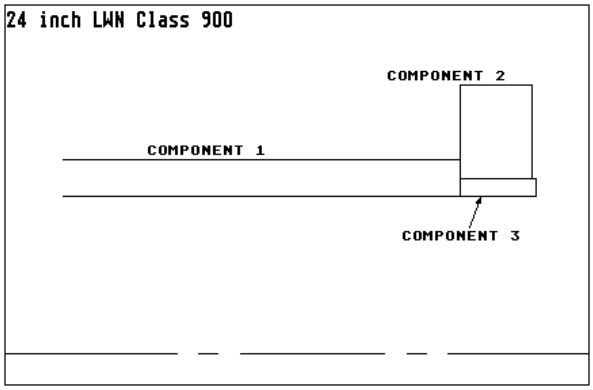

FIGURE 3.38(b) Geometry plot for example 3.18 case 1

The input data set and default free displacements are given in FIGURE 3.38(c) for the operating condition, i.e. internal pressure plus the flange loads as discussed above. No assumptions are made as regard to points of zero radial deflection and no allowance is made for the effect of the bolt holes in reducing the stiffness of the flange.

The junction results are presented in FIGURE 3.38(d). The highest stress is the longitudinal membrane plus bending stress SLo = 92.2 N/mm^2 on the outside of the hub at the junction with the flange. A plot of this stress is shown in FIGURE 3.38(e). The highest hoop stress in the hub is SHo = 56.7 N/mm^2 on the outside surface 30 mm from the junction with the flange. A plot of this stress is shown in FIGURE 3.38(f). The highest stresses in the flange are the hoop membrane plus bending stress SHI = 37.04 N/mm^2 and the meridional membrane plus bending stress SLr = -34.8 N/mm^2. Both stresses occur at the junction radius. Plots of these stresses are shown in FIGURES 3.38(g) and (h).

```
INPUT DATA, PROGRAM AJAP1

24 inch LWN Class 900
Operating Condition

COMPONENT No. 1
CYLINDER, JUNCTION AT RIGHT END
R= 339.72 mm
T= 69.85 mm
E= 178000 N/mm2
PR= .3
BETA= 8.344436E-03 /mm
D= 5.55516E+09 Nmm
P= 6.02 N/mm2
Fp= 1022.557 N/mm
Fo= 1022.557 N/mm

COMPONENT No. 2
FLAT PLATE, JUNCTION AT I.D.
JUNCTION POSITION, LEFT SURFACE
JP= -1
OFFSET= -69.85 mm
Ro= 520.7 mm
Ri= 339.72 mm
T= 139.7 mm
E= 178000 N/mm2
PR= .3
D= 4.444128E+10 Nmm
W 1 = 1001.45 N/mm
Rw= 450.85 mm
W 2 = -822.726 N/mm
Rw= 339.72 mm

COMPONENT No. 3
FLAT PLATE, JUNCTION AT O.D.
JUNCTION POSITION, LEFT SURFACE
JP= -1
OFFSET= -73.05 mm
Ro= 339.72 mm
Ri= 304.8 mm
T= 146.1 mm
E= 178000 N/mm2
PR= .3
D= 5.083327E+10 Nmm
qo= 0 N/mm2
qi= 6.02 N/mm2
W 1 = -353.229 N/mm
Rw= 333.116 mm
W 2 = -170.374 N/mm
Rw= 318.958 mm

FREE DISPLACEMENTS AT JUNCTION
COMPONENT No. 1
Yf= 4.749755E-02 mm outward
THf= 0 radians

COMPONENT No. 2
Yf= .2220231 mm outward
THf= -3.178569E-03 radians clockwise

COMPONENT No. 3
Yf= .1219292 mm outward
THf= -3.706663E-04 radians clockwise
```

FIGURE 3.38(c) Input data set for example 3.18 case 1 operating condition

The displacement of the flange can be important in some cases. FIGURES 3.38(i) and (j) show the rotation and transverse deflection of the flange relative to the junction radius. Excessive rotation would indicate that the flange is not stiff enough and gasket leakage may be increased. ASME SECTION VIII division 1, appendix S (and division 2 appendix M) have rules for estimating the flange rigidity in order to give some control of the leakage. It is also sometimes necessary to calculate the axial and rotational stiffness of the flange in order that the actual service bolt loads can be established.

It is usual in flange design to check the bolting-up condition at atmospheric temperature. In some cases the stresses can be more critical than the operating condition at design temperature. FIGURES 3.38 (k) and (l) show the input data set and junction results for the bolting-up condition. There is no pressure on the flange or hub. The only loads are the flange design bolt load W = 7613922 N total [Correction reference to W_{M1} removed] and its reaction at the gasket. These loads are applied as a point load W1= 2687.797 N/mm at a radius of 450.85 mm to component No. 2 and as a point load W1= -3637.752 N/mm at a radius of 333.116 mm to component No. 3.

The results show that the highest stress is the meridional bending stress SBL = 216.5 N/mm^2 in the hub at the junction with the flange. The highest stresses in the flange are SHr = -105.2 and SLI = 102.4 N/mm^2. A plot of these stresses are shown in FIGURES 3.38(m) to (p). Plots of the displacements are shown in FIGURES 3.38(q) and (r).

TABLE 3.15 summarises the results for several Class 900 long weld neck flanges compared with BS5500 rules. These results are based on an operating condition of 6.02 N/mm^2 at 450°C and a bolting-up condition at ambient temperature. Assumed materials were A105 carbon steel for the flange and BS4882 grade B7A bolts [Corrected was B7]. TABLE 3.16 lists the results for extreme gasket factor and seating stress. These results show that stresses and displacements increase with increased gasket factor and seating stress. The sign of the stresses and displacements are the same between the operating and bolting-up conditions.

The above results are for flanges with hubs of uniform thickness. Many flanges are manufactured with tapered hubs. In "AJAP1" it is possible to model the taper hub by the compact ring. *Case 5* shows that the compact ring tends to overestimate the stresses at the taper hub compared to a BS5500 analysis.

JUNCTION RESULTS
DISCONTINUITY FORCES & MOMENTS
24 inch LWN Class 900
Operating Condition

Mj 1 = -63104.87 Nmm/mm clockwise
Vj 1 = -558.3499 N/mm outward

Mj 2 = -122863.7 Nmm/mm anti-clockwise
Vj 2 = -203.7285 N/mm outward

Mj 3 = 59758.82 Nmm/mm clockwise
Vj 3 = 762.0781 N/mm inward

RESULTS COMPONENT No. 1
24 inch LWN Class 900
Operating Condition
X= 0 mm
Y= .0524199 mm
THETA= -.0006396 radians
V= 558.3499 N/mm
N1= 1022.557 N/mm
N2= 2225.266 N/mm
M1= -63104.87 Nmm/mm
M2= -18931.46 Nmm/mm
STRESSES N/mm2
SV= 7.993556
SL= 14.63933
SH= 31.85778
SBL=+or- 77.6035
SBH=+or- 23.28105
SLo= 92.24282
SLi= -62.96417
SHo= 55.13883
SHi= 8.576727

RESULTS COMPONENT No. 2
24 inch LWN Class 900
Operating Condition
radius X= 339.72 mm
YL= 0 mm
Y= 7.743866E-03 mm
THETA= -6.396007E-04 radians
V= 506.3208 N/mm
N1= -203.7285 N/mm
N2= 505.7119 N/mm
M1= -108633.3 Nmm/mm
M2= -108730.5 Nmm/mm
STRESSES N/mm2
SV= 3.624344
SL= -1.458329
SH= 3.619985
SBL=+or- 33.39806
SBH=+or- 33.42795
SLI= 31.93973
SLr= -34.85639
SHI= 37.04794
SHr= -29.80797

RESULTS COMPONENT No. 3
24 inch LWN Class 900
Operating Condition
radius X= 339.72 mm
YL= 2.125489E-09 mm
Y= 5.697109E-03 mm
THETA= -6.395997E-04 radians
V= 506.324 N/mm
N1= -762.0781 N/mm
N2= 207.4937 N/mm
M1= -4089.008 Nmm/mm
M2= -88318.35 Nmm/mm
STRESSES N/mm2
SV= 3.465599
SL= -5.21614
SH= 1.420217
SBL=+or- 1.149394
SBH=+or- 24.82572
SLI= -4.066746
SLr= -6.365534
SHI= 26.24593
SHr= -23.4055

FIGURE 3.38(d) Junction results for example 3.18 case 1 operating condition

Example 3.18, case 1 conventional hub flange

Loading	4" BS5500	4" AJAP1	8" BS5500	8" AJAP1
Operating condition	Sh = 62.1 Sr = 51.4 St = 30.9	SLo = 61.9 SLr = -48.3 SHl = 31.3	Sh = 60.1 Sr = 60.2 St = 25.8	SLo = 63.0 SLr = -51.8 SHl = 30.7
Bolt-up condition	Sh = 178.9 Sr = 148.0 St = 89.1	SBL = 161.7 SLl = 154.3 SHr = -102.7	Sh = 157.8 Sr = 158.2 St = 67.9	SBL = 145.8 SLl = 151.6 SHr = -96.7
Loading	16" BS5500	16" AJAP1	24" BS5500	24" AJAP1
Operating condition	Sh = 89.1 Sr = 50.9 St = 30.3	SLo = 97.2 SLr = -45.4 SHl = 38.5	Sh = 81.3 Sr = 37.0 St = 28.9	SLo = 92.2 SLr = -34.8 SHl = 37.0
Bolt-up condition	Sh = 221.5 Sr = 126.5 St = 75.5	SBL = 210.9 SLl = 121.1 SHr = -108.5	Sh = 222.7 Sr = 101.3 St = 79.2	SBL = 216.5 SLl = 102.4 SHr = -105.2

TABLE 3.15 Comparison of highest stresses (N/mm^2) for Long Weld Neck flanges

	Operating condition	Bolting-up condition
Gasket factor	0	0
Seating stress, N/mm^2	0	0
Hub stress, N/mm^2	SLo = 71.2	SLo = 199.3
Flange radial stress	SLr = -26.7	SLl = 94.3
Flange hoop stress	SHl = 31.4	SHr = -96.8
Flange rotation, radians	θ = -0.00054	θ = -0.00137
Flange deflection, mm	YL = 0.095	YL = 0.239
Gasket factor	6.5	6.5
Seating stress, N/mm^2	179	179
Hub stress, N/mm^2	SLo = 116.7	SLo = 236.5
Flange radial stress	SLr = -44.3	SLl = 111.9
Flange hoop stress	SHl = 43.6	SHr = -114.9
Flange rotation, radians	θ = -0.00089	θ = -0.00162
Flange deflection, mm	YL = 0.157	YL = 0.284

TABLE 3.16 "AJAP1" results for the highest stresses and displacements for extreme gasket parameters, example 3.18 case 1, 24" class 900 LWN flange

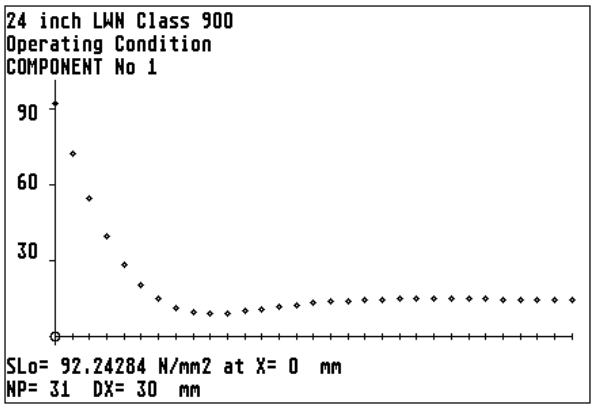

FIGURE 3.38(e) Meridional stress along the outside surface of the cylinder (hub) from the junction with the flange.

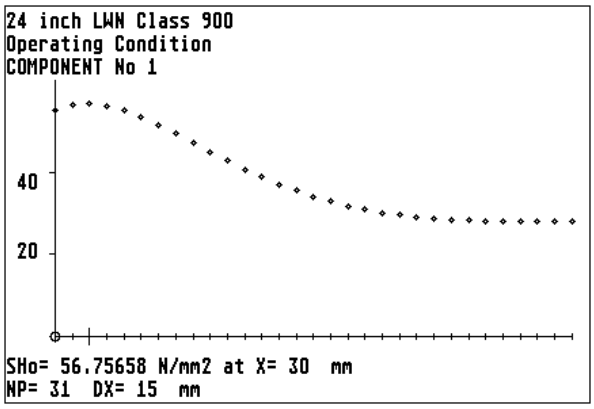

FIGURE 3.38(f) Hoop stress along the outside surface of the cylinder (hub) from the junction with the flange.

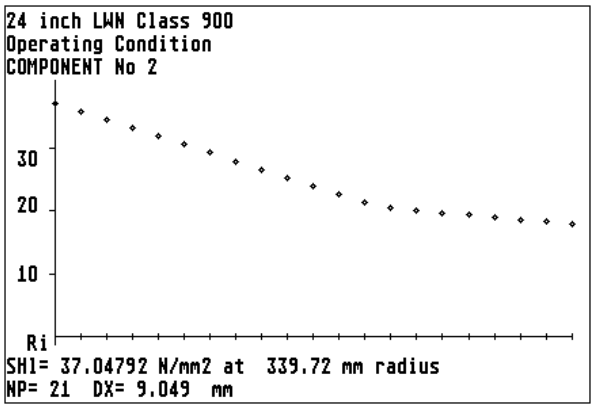

FIGURE 3.38(g) Hoop stress along the left surface of the flange from the junction radius.

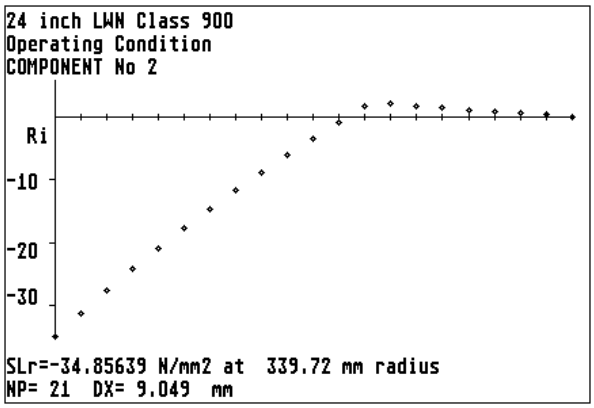

FIGURE 3.38(h) Meridional (radial) stress along the right surface of the flange from the junction radius.

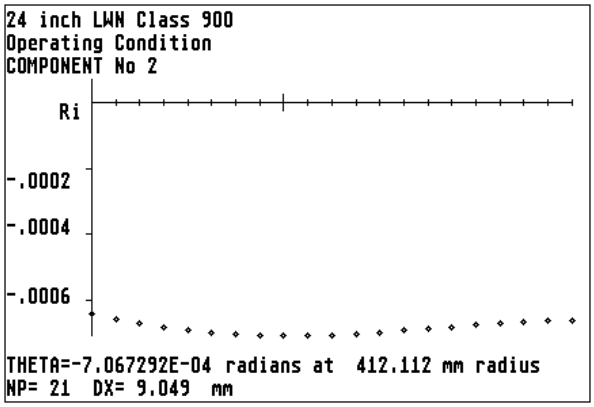

FIGURE 3.38(i) Rotation of the flange from the junction radius.

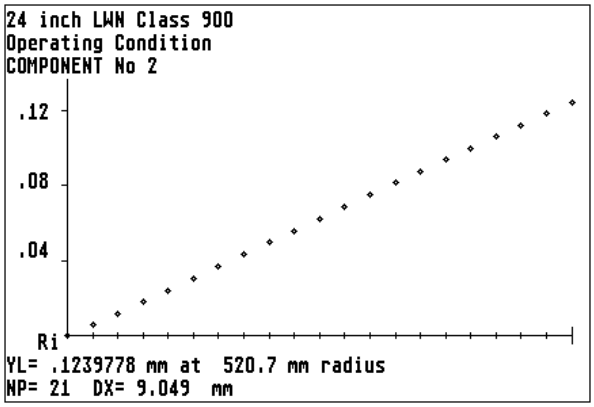

FIGURE 3.38(j) Transverse deflection of the flange from the junction radius.

INPUT DATA, PROGRAM AJAP1

24 inch LWN Class 900
Bolting-up Condition

COMPONENT No. 1
CYLINDER, JUNCTION AT RIGHT END
R= 339.72 mm
T= 69.85 mm
E= 200000 N/mm2
PR= .3
BETA= 8.344436E-03 /mm
D= 6.241753E+09 Nmm

COMPONENT No. 2
FLAT PLATE, JUNCTION AT I.D.
JUNCTION POSITION, LEFT SURFACE
JP= -1
OFFSET= -69.85 mm
Ro= 520.7 mm
Ri= 339.72 mm
T= 139.7 mm
E= 200000 N/mm2
PR= .3
D= 4.993403E+10 Nmm
W 1 = 2687.797 N/mm
Rw= 450.85 mm

COMPONENT No. 3
FLAT PLATE, JUNCTION AT O.D.
JUNCTION POSITION, LEFT SURFACE
JP= -1
OFFSET= -73.05 mm
Ro= 339.72 mm
Ri= 304.8 mm
T= 146.1 mm
E= 200000 N/mm2
PR= .3
D= 5.711604E+10 Nmm
W 1 = -3637.752 N/mm
Rw= 333.116 mm

FREE DISPLACEMENTS AT JUNCTION
COMPONENT No. 1
Yf= 0 mm
THf= 0 radians

COMPONENT No. 2
Yf= .5303411 mm outward
THf= -7.592571E-03 radians clockwise

COMPONENT No. 3
Yf= .1009304 mm outward
THf= -1.381662E-04 radians clockwise

FIGURE 3.38(k) Input data set for example 3.18 case 1 bolting-up condition

JUNCTION RESULTS
DISCONTINUITY FORCES & MOMENTS
24 inch LWN Class 900
Bolting-up Condition

Mj 1 = -176062.6 Nmm/mm clockwise
Vj 1 = -1803.775 N/mm outward

Mj 2 = -209281.3 Nmm/mm anti-clockwise
Vj 2 = 1331.157 N/mm inward

Mj 3 = 33218.51 Nmm/mm clockwise
Vj 3 = 472.6174 N/mm inward

RESULTS COMPONENT No. 1
24 inch LWN Class 900
Bolting-up Condition
X= 0 mm
Y= 4.613599E-02 mm
THETA= -1.305204E-03 radians
V= 1803.775 N/mm
N1= 0 N/mm
N2= 1897.209 N/mm
M1= -176062.6 Nmm/mm
M2= -52818.8 Nmm/mm
STRESSES N/mm2
SV= 25.82356
SL= 0
SH= 27.16119
SBL=+or- 216.5139
SBH=+or- 64.95415
SLo= 216.5139
SLi= -216.5139
SHo= 92.11533
SHi= -37.79296

RESULTS COMPONENT No. 2
24 inch LWN Class 900
Bolting-up Condition
radius X= 339.72 mm
YL= 0 mm
Y= -4.503243E-02 mm
THETA= -1.305203E-03 radians
V= 3567.036 N/mm
N1= 1331.157 N/mm
N2= -3304.309 N/mm
M1= -302262.6 Nmm/mm
M2= -265259 Nmm/mm
STRESSES N/mm2
SV= 25.53354
SL= 9.528686
SH= -23.65289
SBL=+or- 92.92719
SBH=+or- 81.55085
SLi= 102.4559
SLr= -83.39851
SHi= 57.89795
SHr= -105.2037

RESULTS COMPONENT No. 3
24 inch LWN Class 900
Bolting-up Condition
radius X= 339.72 mm
YL= 6.960818E-09 mm
Y= -4.920912E-02 mm
THETA= -1.305204E-03 radians
V= 3567.036 N/mm
N1= -472.6174 N/mm
N2= -4374.362 N/mm
M1= 1306.193 Nmm/mm
M2= -199298.3 Nmm/mm
STRESSES N/mm2
SV= 24.41503
SL= -3.23489
SH= -29.94087
SBL=+or- .3671625
SBH=+or- 56.02147
SLi= -3.602052
SLr= -2.867727
SHi= 26.0806
SHr= -85.96233

FIGURE 3.38(l) Junction results for example 3.18 case 1 bolting-up condition

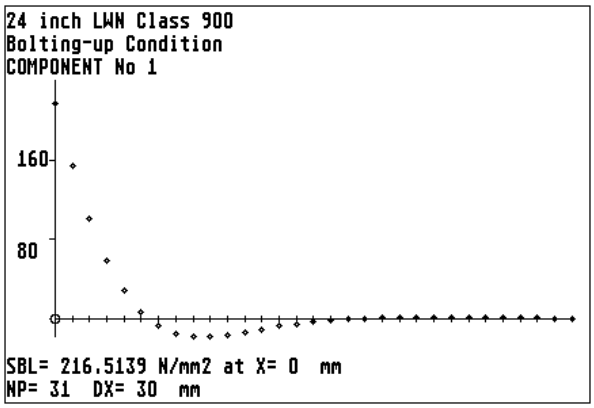

FIGURE 3.38(m) Meridional bending stress along the outside surface of the cylinder (hub) from the junction with the flange.

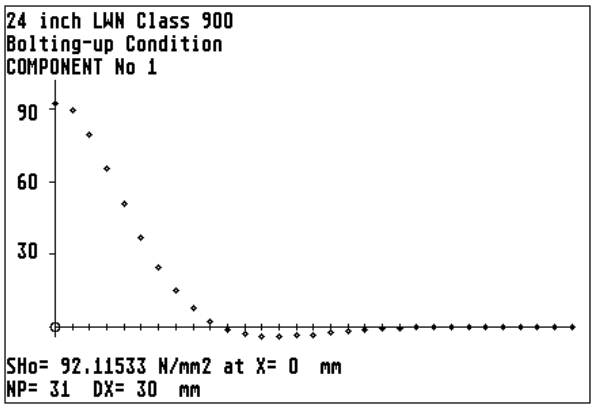

FIGURE 3.38(n) Hoop stress along the outside surface of the cylinder (hub) from the junction with the flange.

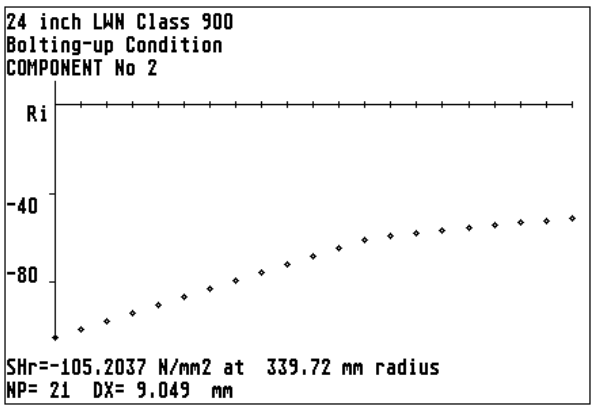

FIGURE 3.38(o) Hoop stress along the right surface of the flange from the junction radius.

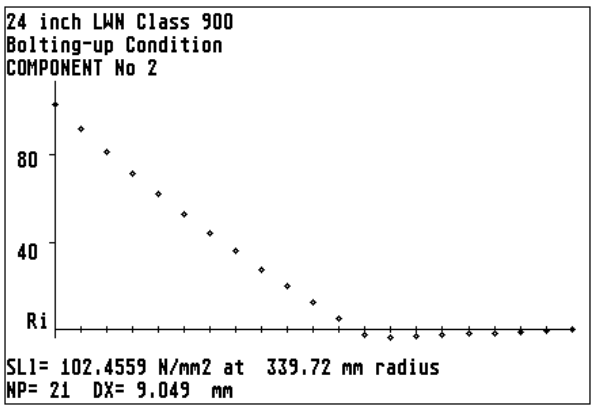

FIGURE 3.38(p) Meridional (radial) stress along the left surface of the flange from the junction radius.

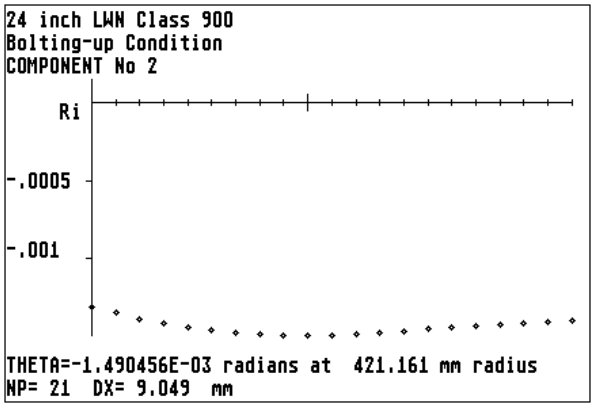

FIGURE 3.38(q) Rotation of the flange from the junction radius.

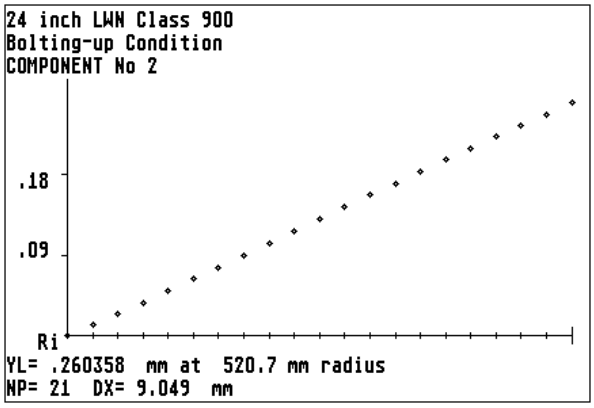

FIGURE 3.38(r) Transverse deflection of the flange from the junction radius.

Case 2 Reversed Hub Flange. The basic form of a reversed integral hub flange consists of a shell connected to a flat head (the flange) with a central opening. FIGURE 3.39(a) shows a part of a low alloy steel pump casing consisting of a cylindrical shell connected to the outside of a flat head with a central opening. The opening, raised face, gasket and bolting, mate with a conventional 24" class 900 flange.

A geometry plot is shown in FIGURES 3.39(b). The cylindrical shell is component No.1 and the flange is simulated by two flat plates (components 2 and 3) connected at the mean junction radius with the shell.

The cylindrical shell and inside edge of the plate (component 3) are subjected to the internal pressure of 6.02 N/mm^2. The effect of the internal pressure on the flange left face is simulated by a load H_T described below. The flange [Corrected was flange face] is subjected to four transverse loads as follows.

(1) A bolt load W_{M1} = 2836888 N total. This load is applied as a point load W1 = 1001.45 N/mm at a radius of 450.85 mm to component No.3. Positive acting to the right.

(2) A hydrostatic end force from the shell H_D = 6817717N total, due to the pressure acting over the inside diameter of the shell. This load is applied as a point load W2 = -1707.27 N/mm at the junction radius of 635.56 mm to component No.3. Negative acting to the left. Note that the difference in the value of this load and F_P for the shell is simply due to "AJAP1" calculating the end load based on mean radius. For most cases the difference is not significant.

(3) A gasket reaction load H_G = 739318.7 N total. This load is applied as a point load W3 = -353.229 N/mm at a radius of 333.116 mm to component No.3. Negative acting to the left. H_G is calculated on the basis of a spiral wound gasket with a gasket factor = 3 and minimum seating stress = 69 N/mm^2.

(4) A Hydrostatic end force H_T = 4722537.9 N total due to the pressure acting on the flange face between the inside diameter of the shell and the gasket reaction diameter. This load is applied as a point load W4 = 1610.013 N/mm at a radius of 466.838 mm to component No.3. Positive acting to the right. In this case this radius is greater than the bolt circle. In other cases the radius may be smaller than the bolt circle.

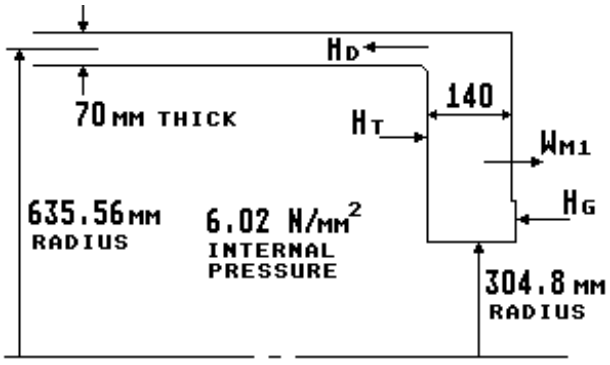

FIGURE 3.39(a) Reversed integral hub flange

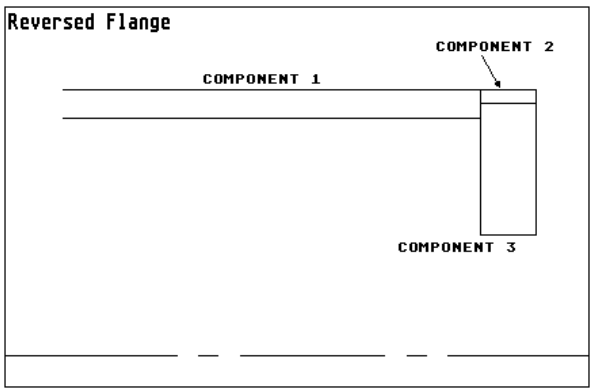

FIGURE 3.39(b) Geometry plot for example 3.18 case 2

Example 3.18, case 2 reversed hub flange

The input data set and default free displacements are given in FIGURE 3.39(c) for the operating condition, i.e. internal pressure plus the flange loads as discussed above. No assumptions are made as regard to points of zero radial deflection and no allowance is made for the effect of the bolt holes in reducing the stiffness of the flange. The junction results are presented in FIGURE 3.39(d). The highest stress is the longitudinal membrane plus bending stress SLi = 187.7 N/mm^2 on the inside of the hub at the junction with the flange. The highest stress in the flange is the hoop membrane plus bending stress SHr = 83.3 N/mm^2 at the inside edge. Plots of these stresses and the displacement of the flange are shown in FIGURES 3.39(e) to (h).

INPUT DATA, PROGRAM AJAP1

Reversed Flange
Operating Condition

COMPONENT No. 1
CYLINDER, JUNCTION AT RIGHT END
R= 635.56 mm
T= 70 mm
E= 178000 N/mm2
PR= .3
BETA= 6.094156E-03 /mm
D= 5.591026E+09 Nmm
P= 6.02 N/mm2
Fp= 1913.036 N/mm
Fo= 1913.036 N/mm

COMPONENT No. 2
FLAT PLATE, JUNCTION AT I.D.
JUNCTION POSITION, LEFT SURFACE
JP= -1
OFFSET= -70 mm
Ro= 670.56 mm
Ri= 635.56 mm
T= 140 mm
E= 178000 N/mm2
PR= .3
D= 4.472821E+10 Nmm

COMPONENT No. 3
FLAT PLATE, JUNCTION AT O.D.
JUNCTION POSITION, LEFT SURFACE
JP= -1
OFFSET= -70 mm
Ro= 635.56 mm
Ri= 304.8 mm
T= 140 mm
E= 178000 N/mm2
PR= .3
D= 4.472821E+10 Nmm
qo= 0 N/mm2
qi= 6.02 N/mm2
W 1 = 1001.45 N/mm
Rw= 450.85 mm
W 2 = -1707.27 N/mm
Rw= 635.56 mm
W 3 = -353.229 N/mm
Rw= 333.116 mm
W 4 = 1610.013 N/mm
Rw= 466.838 mm

FREE DISPLACEMENTS AT JUNCTION
COMPONENT No. 1
Yf= .1658863 mm outward
THf= 0 radians

COMPONENT No. 2
Yf= 0 mm
THf= 0 radians

COMPONENT No. 3
Yf= -.3601042 mm inward
THf= 5.327784E-03 radians anti-clockwise

FIGURE 3.39(c) Input data set for example 3.18 case 2 operating condition

For the bolting-up condition the input data set and default free displacements are shown in FIGURE 3.39(i). There is no pressure on the flange or hub. The only loads are the flange design bolt load W = 7613922 N total [Correction reference to W_{M1} removed] and its reaction at the gasket. These loads are applied as a point load W1 = 2687.797 N/mm at a radius of 450.85 mm and as a point load W2 = -3637.752 N/mm [Corrected was W1] at a radius of 333.116 mm to component No. 3.

The junction results are presented in FIGURE 3.39(j). The highest stress is the meridional bending stress SBL = 119.4 N/mm^2 in the hub at the junction with the flange. This stress is compressive on the inside surface of the hub. The highest stress in the flange is the hoop membrane plus bending stress SHr = -119.54 N/mm^2 at the inside edge. Plots of these stresses and the displacement of the flange are shown in FIGURES 3.39(k) to (n).

Inspection of these results show several interesting features of reversed flanges. The highest stresses are at the *inside* of the hub as opposed to the *outside* for a conventional hub flange. There is a change of sign in the stress between the operating condition and bolting-up condition, i.e. there is a stress range of 187.7 - (-119.4) = 307.1 N/mm^2 at the inside of the hub at the junction with the flange. Stress ranges of this magnitude, occurring at re-entrant corners, are potential sources of fatigue failure. The reason for this change of sign is due to the behaviour of the flange when subjected to the transverse loads.

Comparison of the displacements, FIGURES 3.39(g),(h),(m) and (n) show that the sign of the flange rotation and deflection are different between the operating and bolting-up conditions. This indicates that the net moment on the flange is in the opposite direction for these two conditions.

JUNCTION RESULTS
DISCONTINUITY FORCES & MOMENTS
Reversed Flange
Operating Condition

Mj 1 = 131000.8 Nmm/mm anti-clockwise
Vj 1 = 1241.804 N/mm inward

Mj 2 = -10187.07 Nmm/mm anti-clockwise
Vj 2 = -104.3221 N/mm outward

Mj 3 = 141187.9 Nmm/mm clockwise
Vj 3 = -1137.48 N/mm outward

RESULTS COMPONENT No. 1
Reversed Flange
Operating Condition
X= 0 mm
Y= -9.339005E-03 mm
THETA= 8.54529E-04 radians
V= -1241.804 N/mm
N1= 1913.036 N/mm
N2= 390.822 N/mm
M1= 131000.8 Nmm/mm
M2= 39300.25 Nmm/mm
STRESSES N/mm2
SV= -17.74006
SL= 27.32908
SH= 5.583172
SBL=+or- 160.4092
SBH=+or- 48.12276
SLo= -133.0801
SLi= 187.7383
SHo= -42.53959
SHi= 53.70593

RESULTS COMPONENT No. 3
Reversed Flange
Operating Condition
radius X= 635.56 mm
YL= 1.862645E-07 mm
Y= 5.047807E-02 mm
THETA= 8.545314E-04 radians
V= -1707.868 N/mm
N1= 1137.48 N/mm
N2= 2320.464 N/mm
M1= -220811.4 Nmm/mm
M2= -11517.36 Nmm/mm
STRESSES N/mm2
SV= -12.19906
SL= 8.124853
SH= 16.57475
SBL=+or- 67.59533
SBH=+or- 3.525721
SLl= 75.72018
SLr= -59.47048
SHl= 20.10047
SHr= 13.04903

RESULTS COMPONENT No. 3
Reversed Flange
Operating Condition
radius X= 304.8 mm
YL= .3988832 mm
Y= 5.569552E-02 mm
THETA= 1.28693E-03 radians
V= 0 N/mm
N1= -842.7999 N/mm
N2= 4300.744 N/mm
M1= 0 Nmm/mm
M2= 171855.3 Nmm/mm
STRESSES N/mm2
SV= 0
SL= -6.02
SH= 30.7196
SBL=+or- 0
SBH=+or- 52.60875
SLl= -6.02
SLr= -6.02
SHl= -21.88915
SHr= 83.32835

FIGURE 3.39(d) Junction and flange results for example 3.18 case 2 operating condition

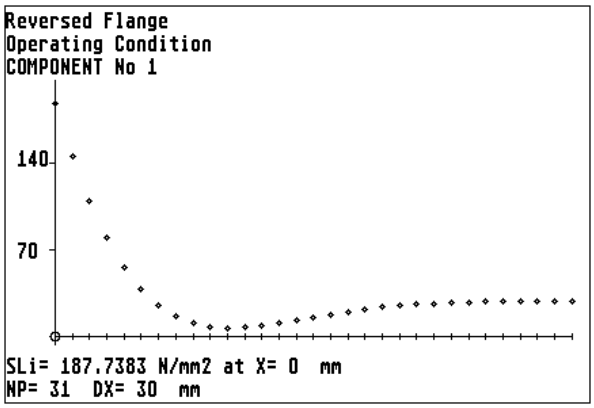

FIGURE 3.39(e) Meridional stress along the inside surface of the cylinder (hub) from the junction with the flange.

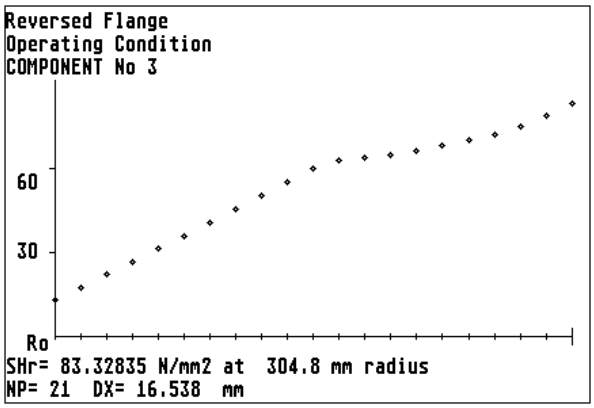

FIGURE 3.39(f) Hoop stress along the right surface of the flange from the junction radius.

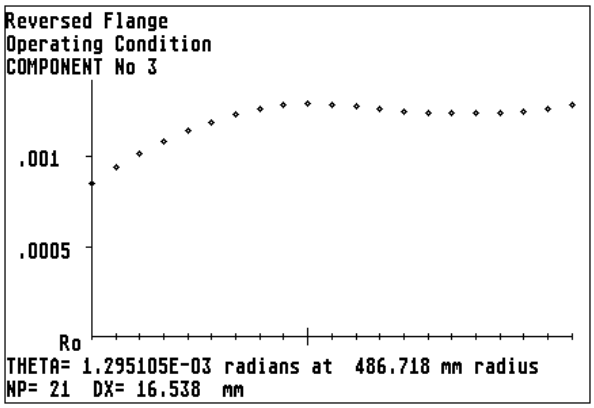

FIGURE 3.39(g) Rotation of the flange from the junction radius.

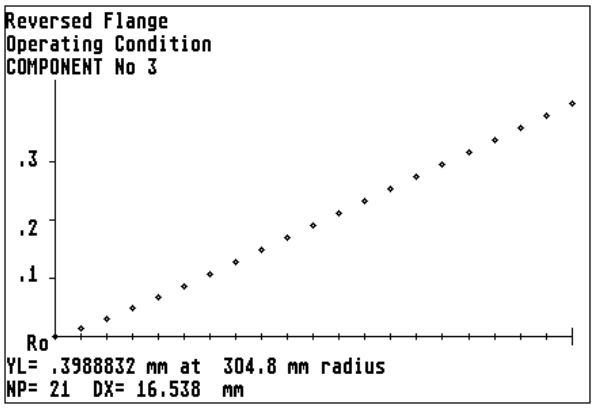

FIGURE 3.39(h) Transverse deflection of the flange from the junction radius.

INPUT DATA, PROGRAM AJAP1

Reversed Flange
Bolting-up Condition

COMPONENT No. 1
CYLINDER, JUNCTION AT RIGHT END
R= 635.56 mm
T= 70 mm
E= 200000 N/mm2
PR= .3
BETA= 6.094156E-03 /mm
D= 6.282051E+09 Nmm

COMPONENT No. 2
FLAT PLATE, JUNCTION AT I.D.
JUNCTION POSITION, LEFT SURFACE
JP= -1
OFFSET= -70 mm
Ro= 670.56 mm
Ri= 635.56 mm
T= 140 mm
E= 200000 N/mm2
PR= .3
D= 5.025641E+10 Nmm

COMPONENT No. 3
FLAT PLATE, JUNCTION AT O.D.
JUNCTION POSITION, LEFT SURFACE
JP= -1
OFFSET= -70 mm
Ro= 635.56 mm
Ri= 304.8 mm
T= 140 mm
E= 200000 N/mm2
PR= .3
D= 5.025641E+10 Nmm
W 1 = 2687.797 N/mm
Rw= 450.85 mm
W 2 = -3637.752 N/mm
Rw= 333.116 mm

FREE DISPLACEMENTS AT JUNCTION
COMPONENT No. 1
Yf= 0 mm
THf= 0 radians

COMPONENT No. 2
Yf= 0 mm
THf= 0 radians
COMPONENT No. 3
Yf= .2609678 mm outward
THf= -3.728111E-03 radians clockwise

FIGURE 3.39(i) Input data set for example 3.18 case 2 bolting-up condition

JUNCTION RESULTS
DISCONTINUITY FORCES & MOMENTS
Reversed Flange
Bolting-up Condition

Mj 1 = -97528.66 Nmm/mm clockwise
Vj 1 = -731.8723 N/mm outward

Mj 2 = 6992.413 Nmm/mm clockwise
Vj 2 = 46.84442 N/mm inward

Mj 3 = -104521.1 Nmm/mm anti-clockwise
Vj 3 = 685.0278 N/mm inward

RESULTS COMPONENT No. 1
Reversed Flange
Bolting-up Condition
X= 0 mm
Y= 4.835995E-02 mm
THETA= -9.790458E-04 radians
V= 731.8723 N/mm
N1= 0 N/mm
N2= 1065.264 N/mm
M1= -97528.66 Nmm/mm
M2= -29258.6 Nmm/mm
STRESSES N/mm2
SV= 10.45532
SL= 0
SH= 15.21806
SBL=+or- 119.4229
SBH=+or- 35.82686
SLo= 119.4229
SLi= -119.4229
SHo= 51.04492
SHi= -20.6088

RESULTS COMPONENT No. 3
Reversed Flange
Bolting-up Condition
radius X= 635.56 mm
YL= 0 mm
Y= -.0201732 mm
THETA= -9.790461E-04 radians
V= 0 N/mm
N1= -685.0278 N/mm
N2= -1094.252 N/mm
M1= 152473 Nmm/mm
M2= -24707.83 Nmm/mm
STRESSES N/mm2
SV= 0
SL= -4.893056
SH= -7.816084
SBL=+or- 46.67542
SBH=+or- 7.563623
SLi= -51.56848
SLr= 41.78237
SHi= -.252461
SHr= -15.37971

RESULTS COMPONENT No. 3
Reversed Flange
Bolting-up Condition
radius X= 304.8 mm
YL= -.5620771 mm
Y= -1.936873E-02 mm
THETA= -2.325984E-03 radians
V= 0 N/mm
N1= 0 N/mm
N2= -1779.279 N/mm
M1= 0 Nmm/mm
M2= -348999.3 Nmm/mm
STRESSES N/mm2
SV= 0
SL= 0
SH= -12.70914
SBL=+or- 0
SBH=+or- 106.8365
SLi= 0
SLr= 0
SHi= 94.12738
SHr= -119.5457

FIGURE 3.39(j) Junction and flange results for example 3.18 case 2 bolting-up condition

Example 3.18, case 2 reversed hub flange

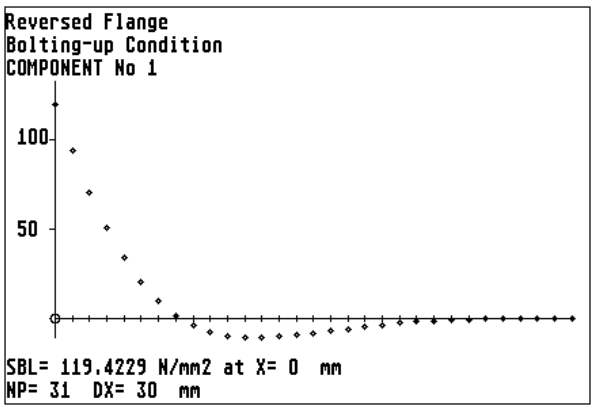

FIGURE 3.39(k) Meridional bending stress along the outside surface of the cylinder (hub) from the junction with the flange.

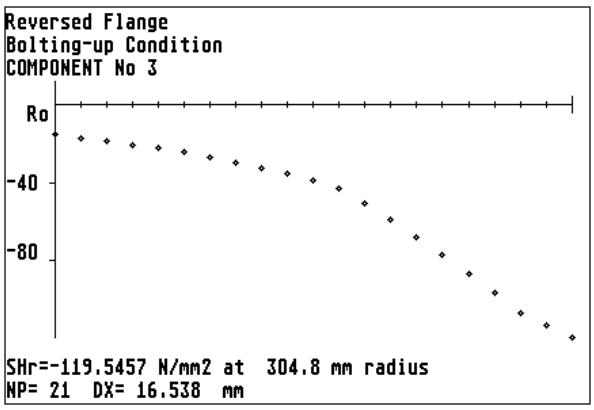

FIGURE 3.39(l) Hoop stress along the right surface of the flange from the junction radius.

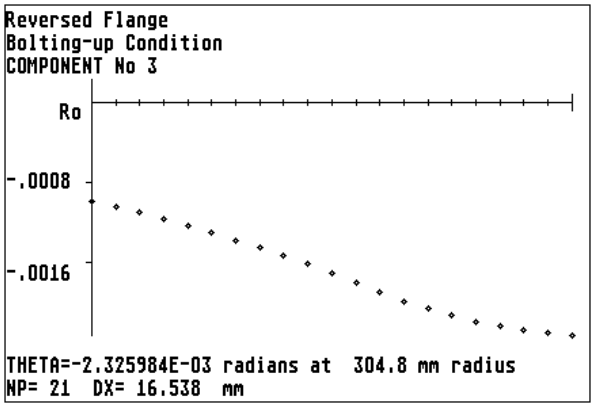

FIGURE 3.39(m) Rotation of the flange from the junction radius.

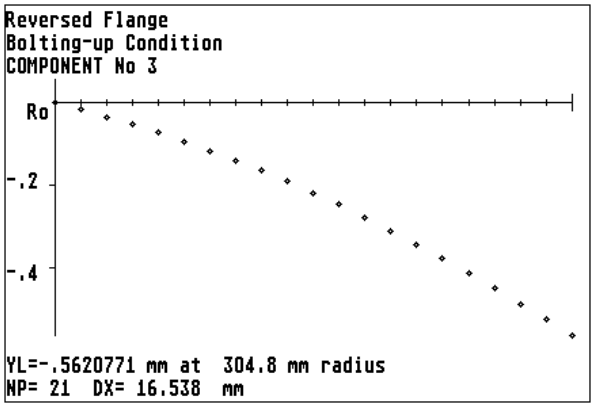

FIGURE 3.39(n) Transverse deflection of the flange from the junction radius.

TABLE 3.17 summarises the results for extreme gasket factor and seating stress. These results are based on an operating condition of 6.02 N/mm^2 at 450°C and a bolting-up condition at ambient temperature. The sign of the stresses and displacements are different between the operating and bolting-up conditions. Note also that for the operating condition the results with zero gasket factor are higher than the results with an increased gasket factor. The reason for this is that the gasket reaction load H_G is zero when the gasket factor is zero. Hence, by inspection of the load directions shown in FIGURE 3.39(a), the net moment on the flange is *increased* when H_G is zero (or of a low magnitude).

	Operating condition	Bolting-up condition
Gasket factor	0	0
Seating stress, N/mm^2	0	0
Hub stress N/mm^2	SLi = 199.3	SLi = -109.9
Flange radial stress	SLI = 80.7	SLI = -70.21
Flange hoop stress	SHr = 94.9	SHr = -110.0
Flange rotation, radians	θ = 0.00154	θ = -0.00214
Flange deflection, mm	YL = 0.46	YL = -0.517
Gasket factor	6.5	6.5
Seating stress, N/mm^2	179	179
Hub stress, N/mm^2	SLi = 174.2	SLi = -130.4
Flange radial stress	SLI = 69.8	SLI = -83.3
Flange hoop stress	SHr = 69.7	SHr = -130.6
Flange rotation, radians	θ = 0.00109	θ = -0.00254
Flange deflection, mm	YL = 0.327	YL = -0.614

TABLE 3.17 "AJAP1" results for the highest stresses and displacements for extreme gasket parameters, example 3.18 case 2, reversed flange

Case 3 Spherical Domed Flange. The basic form of a spherical domed and bolted flange consists of a spherical shell connected to the inside edge of a flat head (the flange). FIGURE 3.40(a) shows a typical domed flange suitable for connecting to a 24" class 900 flange.

A geometry plot is shown in FIGURES 3.40(b). The spherical shell is component No.1 and the flange (component No. 2) is simulated by a flat plate. In cases where the flange is compact, the compact ring could be used to simulate the flange in place of the plate.

The spherical shell and part of the inside edge of the flange are subjected to an internal pressure of 6.02 N/mm^2. The flange [Corrected was flange face] is subjected to four transverse loads as follows.

(1) A bolt load W_{M1} = 2836888 N total. This load is applied as a point load W1 = 1001.45 N/mm at a radius of 450.85 mm. Positive acting to the right.

(2) A Hydrostatic end force from the shell H_D = 1757018N total, due to the pressure acting over the inside diameter of the flange. This load is applied as a point load W2 = -917.448 N/mm at a radius of 304.8 mm. Negative acting to the left.

(3) A gasket reaction load H_G = 739318.7 N total. This load is applied as a point load W3 = -353.229 N/mm at a radius of 333.116 mm. Negative acting to the left. H_G is calculated on the basis of a spiral wound gasket with a gasket factor = 3 and minimum seating stress = 69 N/mm^2.

(4) A Hydrostatic end force H_T = 341441.8 N total, due to the pressure acting on the flange face between the inside of the flange and the gasket reaction diameter. This load is applied as a point load W4 = -170.374 N/mm [Corrected was W2] at a radius of 318.958 mm. Negative acting to the left.

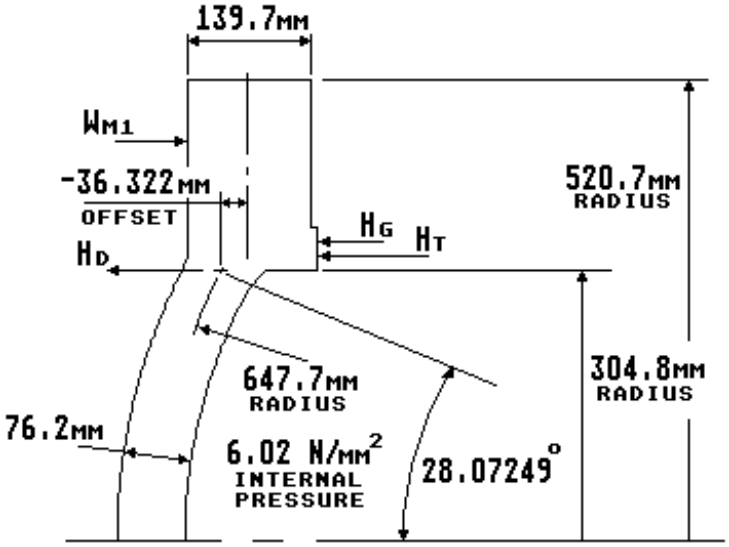

FIGURE 3.40(a) Spherical domed flange

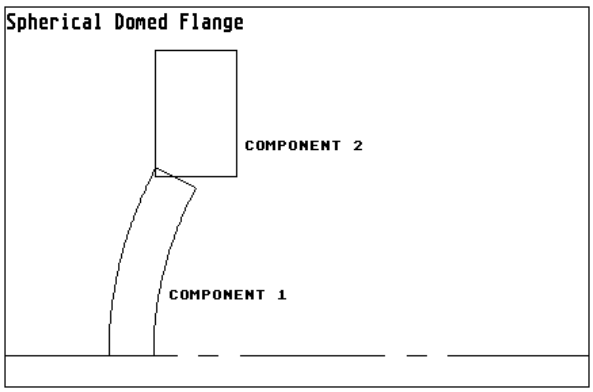

FIGURE 3.40(b) Geometry plot for example 3.18 case 3

Example 3.18, case 3 spherical domed flange

The input data set and default free displacements are given in FIGURE 3.40(c) for the operating condition, i.e. internal pressure plus the flange loads as discussed above. As before, no assumptions are made as regard to points of zero radial deflection and no allowance is made for the effect of the bolt holes in reducing the stiffness of the flange.

INPUT DATA, PROGRAM AJAP1

Spherical Domed Flange

Operating Condition

COMPONENT No. 1
SPHERICAL SHELL, JUNCTION AT RIGHT END
Rs= 647.7 mm
T= 76.2 mm
PHI= 28.07249 degrees
E= 178000 N/mm2
PR= .3
BETA= 3.747574
P= 6.02 N/mm2
Fp= 917.4482 N/mm
Fo= 1949.577 N/mm

COMPONENT No. 2
FLAT PLATE, JUNCTION AT I.D.
JUNCTION POSITION,
JP= -.52
OFFSET= -36.322 mm
Ro= 520.7 mm
Ri= 304.8 mm
T= 139.7 mm
E= 178000 N/mm2
PR= .3
D= 4.444128E+10 Nmm
W 1 = 1001.45 N/mm
Rw= 450.85 mm
W 2 = -917.448 N/mm
Rw= 304.8 mm
W 3 = -353.229 N/mm
Rw= 333.116 mm
W 4 = -170.374 N/mm
Rw= 318.958 mm

APPLIED JUNCTION MOMENT & FORCE
Mo= -28323.14 Nmm/mm anti-clockwise
Vo= 1340.955 N/mm inward

FREE DISPLACEMENTS AT JUNCTION
COMPONENT No. 1
Yf= 3.066751E-02 mm outward
THf= 0 radians

COMPONENT No. 2
Yf= .1140844 mm outward
THf= -3.140917E-03 radians clockwise

FIGURE 3.40(c) Input data set for example 3.18 case 3 operating condition

Inspection of the input data set shows that an applied junction moment and force have been applied. The magnitude and point of application of these loads are critically dependent on the exact position of the junction of the shell and flange. In this case the junction offset is 36.322 mm to the left (negative) of the plate centre line. The loads have been evaluated as follows. With reference to FIGURE 3.40(d) the program will calculate, by default, a radial force of 1720.215 N/mm acting inward due to the pressure acting on the spherical shell as discussed in section 3.3.2 and equation (3.7). There is also a radial force of 379.26 N/mm acting outward due to the internal pressure acting on part of the inside edge of the flange. This gives a net radial force of Vo = 1340.955 N/mm inward, applied as an external radial force to the junction. The outward radial force of 379.26 N/mm times the distance (74.68mm) from the junction gives a moment Mo = 28323.14 Nmm/mm anti-clockwise, applied as an external moment to the junction.

The junction results are presented in FIGURE 3.40(e). The highest stress is the hoop membrane plus bending stress SHr = -72.4 N/mm^2 at the inside edge of the flange. Plots of the highest stresses and the flange displacements are shown in FIGURES 3.40(f) to (i).

For the bolting-up condition the input data set and default free displacements are shown in FIGURE 3.40(j). There is no pressure on the flange or hub. The only loads are the flange design bolt load W = 7613922 N total [Correction reference to W_{M1} removed] and its reaction at the gasket. These loads are applied as a point load W1 = 2687.797 N/mm at a radius of 450.85 mm and as a point load W2 = -3637.752 N/mm [Corrected was W1] at a radius of 333.116 mm.

The junction results for the bolting-up condition are presented in FIGURE 3.40(k). The highest stress is the hoop membrane plus bending stress SHr = -148.2 N/mm^2 at the inside edge of the flange. Plots of the highest stresses and the displacement of the flange are shown in FIGURES 3.40(l) to (o).

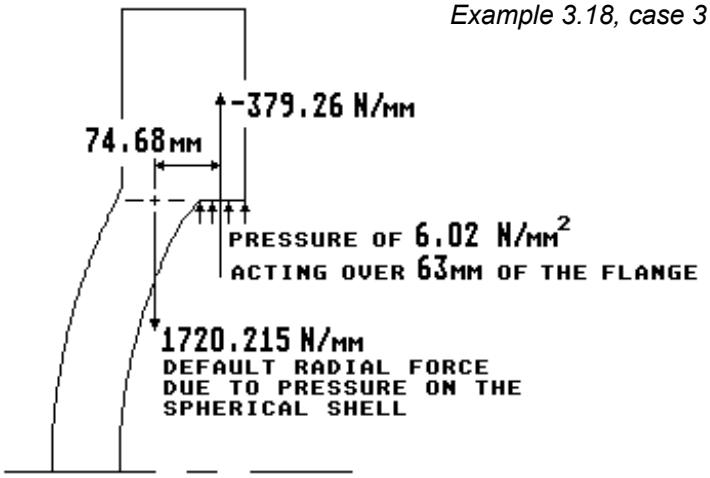

FIGURE 3.40(d) Radial forces acting at the junction

JUNCTION RESULTS
DISCONTINUITY FORCES & MOMENTS
Spherical Domed Flange
Operating Condition

Mj 1 = -41363.86 Nmm/mm clockwise
Vj 1 = -115.046 N/mm outward

Mj 2 = -69687 Nmm/mm anti-clockwise
Vj 2 = 1456.002 N/mm inward

RESULTS COMPONENT No. 1
Spherical Domed Flange
Operating Condition
OMEGA= 0 degrees
Y= -6.324355E-03 mm
THETA= -9.768842E-04 radians
V= 54.13932 N/mm
N1= 2051.088 N/mm
N2= 333.8928 N/mm
M1= -41363.86 Nmm/mm
M2= -30968.99 Nmm/mm
STRESSES N/mm2
SV= .7104897
SL= 26.91717
SH= 4.381796
SBL=+or- 42.74275
SBH=+or- 32.00136
SLo= 69.65991
SLi= -15.82558
SHo= 36.38316
SHi= -27.61956

FIGURE 3.40(e) Junction and flange results for example 3.18 case 3 operating condition

RESULTS COMPONENT No. 2
Spherical Domed Flange
Operating Condition
radius X= 520.7 mm
YL= .221749 mm
Y= -3.178507E-02 mm
THETA= -9.782006E-04 radians
V= -6.103516E-05 N/mm
N1= 0 N/mm
N2= -1517.931 N/mm
M1= 2.734375E-02 Nmm/mm
M2= -75974.57 Nmm/mm
STRESSES N/mm2
SV= -4.369016E-07
SL= 0
SH= -10.86565
SBL=+or- 8.406525E-06
SBH=+or- 23.35752
SLI= -8.406525E-06
SLr= 8.406525E-06
SHI= 12.49187
SHr= -34.22317

RESULTS COMPONENT No. 2
Spherical Domed Flange
Operating Condition
radius X= 304.8 mm
YL= 0 mm
Y= -4.180674E-02 mm
THETA= -9.768844E-04 radians
V= -.4684143 N/mm
N1= 1456.002 N/mm
N2= -2973.933 N/mm
M1= -122571.9 Nmm/mm
M2= -166386.9 Nmm/mm
STRESSES N/mm2
SV= -3.353002E-03
SL= 10.42235
SH= -21.28799
SBL=+or- 37.68334
SBH=+or- 51.15375
SLI= 48.10568
SLr= -27.26099
SHI= 29.86575
SHr= -72.44173

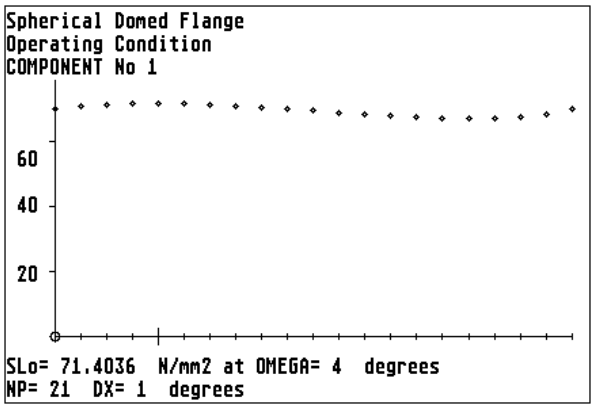

FIGURE 3.40(f) Meridional stress along the outside surface of the spherical shell from the junction with the flange.

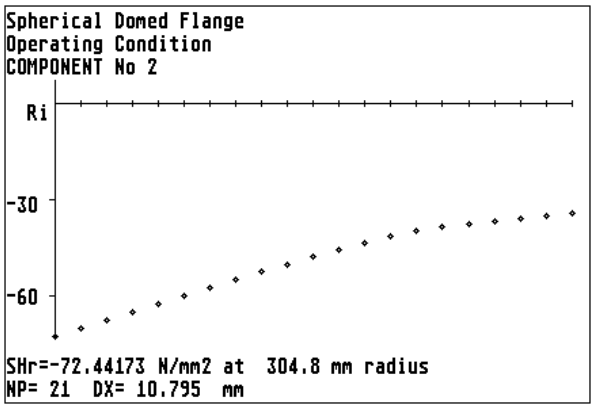

FIGURE 3.40(g) Hoop stress along the right surface of the flange from the junction radius.

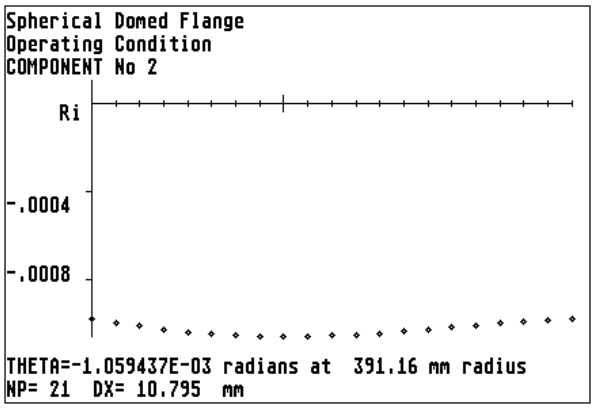

FIGURE 3.40(h) Rotation of the flange from the junction radius.

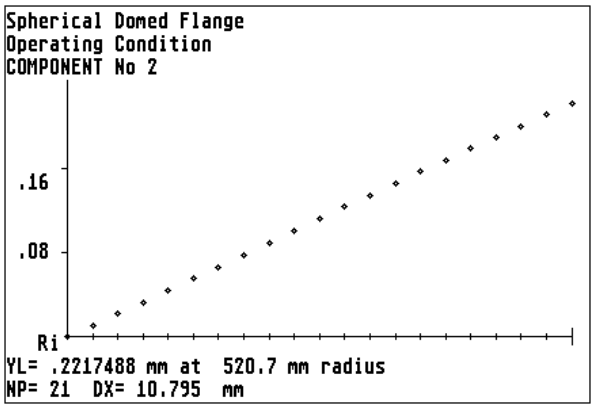

FIGURE 3.40(i) Transverse deflection of the flange from the junction radius.

INPUT DATA, PROGRAM AJAP1

Spherical Domed Flange

Bolting-up Condition

COMPONENT No. 1
SPHERICAL SHELL, JUNCTION AT RIGHT END
Rs= 647.7 mm
T= 76.2 mm
PHI= 28.07249 degrees
E= 200000 N/mm2
PR= .3
BETA= 3.747574

COMPONENT No. 2
FLAT PLATE, JUNCTION AT I.D.
JUNCTION POSITION,
JP= -.52
OFFSET= -36.322 mm
Ro= 520.7 mm
Ri= 304.8 mm
T= 139.7 mm
E= 200000 N/mm2
PR= .3
D= 4.993403E+10 Nmm
W 1 = 2687.797 N/mm
Rw= 450.85 mm
W 2 = -3637.752 N/mm
Rw= 333.116 mm

FREE DISPLACEMENTS AT JUNCTION
COMPONENT No. 1
Yf= 0 mm
THf= 0 radians

COMPONENT No. 2
Yf= .2302226 mm outward
THf= -6.338378E-03 radians clockwise

FIGURE 3.40(j) Input data set for example 3.18 case 3 bolting-up condition

JUNCTION RESULTS
DISCONTINUITY FORCES & MOMENTS
Spherical Domed Flange
Bolting-up Condition

Mj 1 = -189310.4 Nmm/mm clockwise
Vj 1 = -2856.834 N/mm outward

Mj 2 = -189310.3 Nmm/mm anti-clockwise
Vj 2 = 2856.835 N/mm inward

RESULTS COMPONENT No. 1
Spherical Domed Flange
Bolting-up Condition
OMEGA= 0 degrees
Y= -1.005173E-02 mm
THETA= -1.733232E-03 radians
V= 1344.393 N/mm
N1= 2520.735 N/mm
N2= 253.6348 N/mm
M1= -189310.4 Nmm/mm
M2= -93792.79 Nmm/mm
STRESSES N/mm2
SV= 17.64295
SL= 33.08052
SH= 3.32854
SBL=+or- 195.6212
SBH=+or- 96.91942
SLo= 228.7017
SLi= -162.5407
SHo= 100.248
SHi= -93.59088

RESULTS COMPONENT No. 2
Spherical Domed Flange
Bolting-up condition
radius X= 520.7 mm
YL= .41582 mm
Y= -5.550555E-02 mm
THETA= -1.863554E-03 radians
V= 0 N/mm
N1= 0 N/mm
N2= -2978.346 N/mm
M1= 0 Nmm/mm
M2= -162626.9 Nmm/mm
STRESSES N/mm2
SV= 0
SL= 0
SH= -21.31959
SBL=+or- 0
SBH=+or- 49.99779
SLl= 0
SLr= 0
SHl= 28.67821
SHr= -71.31738

RESULTS COMPONENT No. 2
Spherical Domed Flange
Bolting-up Condition
radius X= 304.8 mm
YL= 0 mm
Y= -7.3006116E-02 mm
THETA= -1.733231E-03 radians
V= 0 N/mm
N1= 2856.835 N/mm
N2= -5835.181 N/mm
M1= -293076.2 Nmm/mm
M2= -346315.1 Nmm/mm
STRESSES N/mm2
SV= 0
SL= 20.44978
SH= -41.76937
SBL=+or- 90.10295
SBH=+or- 106.4706
SLl= 110.5527
SLr= -69.65317
SHl= 64.70126
SHr= -148.24

FIGURE 3.40(k) Junction and flange results for example 3.18 case 3 bolting-up condition

Example 3.18, case 3 spherical domed flange

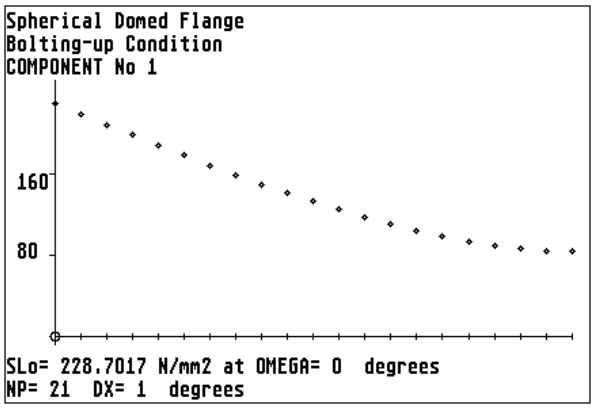

FIGURE 3.40(l) Meridional stress along the outside surface of the spherical shell from the junction with the flange.

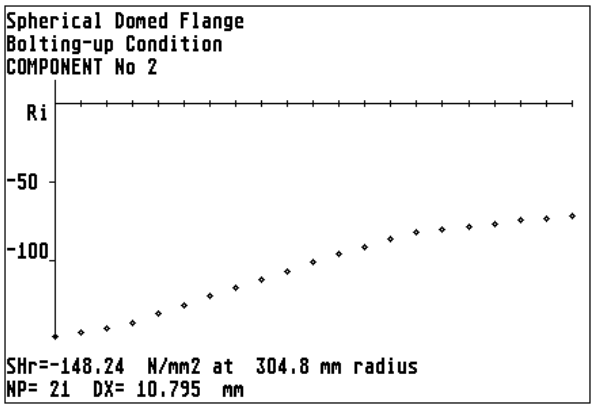

FIGURE 3.40(m) Hoop stress along the right surface of the flange from the junction radius.

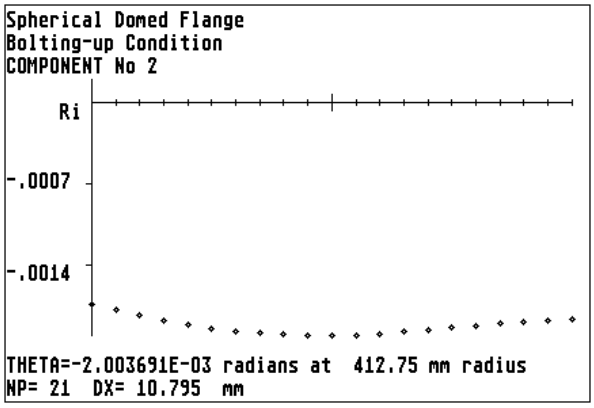

FIGURE 3.40(n) Rotation of the flange from the junction radius.

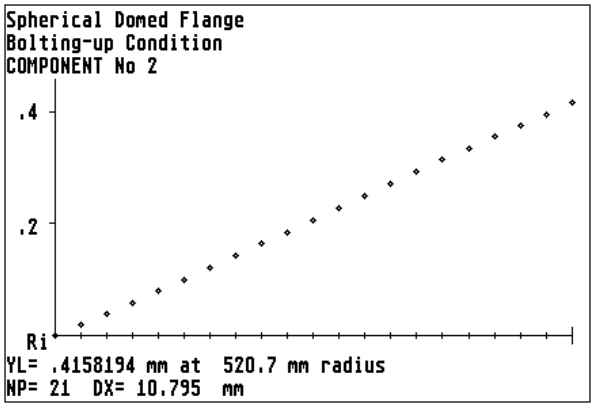

FIGURE 3.40(o) Transverse deflection of the flange from the junction radius.

The position of the junction of the shell and flange has an important influence on the stressing and behaviour of this type of flange. TABLE 3.18 shows the results for different positions of the junction. Inspection of the results show that the stress levels for the operating condition are significantly higher as the shell junction position is moved from the left (negative) side of the flange, towards the centre and right of the flange centre line. The reason for this behaviour is due to the flange bolt load W_{M1} tending to produce a *clockwise* moment to the flange, but the radial force Vo from the shell tends to produce an *anti-clockwise* moment when the junction position is to the *left* of the flange centre line. If the junction position is moved to the *right* of the flange centre line the moment produced by Vo will be *clockwise* and will add to the flange moment due to the bolt load.

	Operating condition	Bolting up condition
Junction Position, JP	0	0
Junction Offset, mm	0	0
Hub stress, N/mm^2	SLo = 93.9	SLo = 257.8
Flange radial stress	SLI = 34.0	SLI = 87.7
Flange hoop stress	SHr = -103.1	SHr = -187.6
Flange rotation, radians	θ = -0.00181	θ = -0.00296
Flange deflection, mm	YL = 0.374	YL = 0.621
Junction Position, JP	+0.52	+0.52
Junction Offset, mm	36.322	36.322
Hub stress, N/mm^2	SHi = -124.3	SHi = -233.0
Flange radial stress	SLI = 12.2	SLI = 60.6
Flange hoop stress	SHr = -115.3	SHr = -194.1
Flange rotation, radians	θ = -0.00261	θ = -0.0038
Flange deflection, mm	YL = 0.521	YL = 0.794

TABLE 3.18 "AJAP1" results for different junction positions, example 3.18 case 3, spherical domed flange

Case 4 Studded Connection. The basic form of a studded connection consists of a shell connected to the outside edge of a flat head (the flange). FIGURE 3.41(a) shows a spherical shell fitted with a studded connection suitable for connecting to a 24" class 900 flange. The position of the junction of the shell and flange is offset by 36.322 mm to the left (negative) of the plate centre line.

A geometry plot is shown in FIGURES 3.41(b). The spherical shell is component No.1 and the flange (component No. 2) is simulated by a flat plate. In cases where the flange is compact, the compact ring could be used to simulate the flange in place of the plate.

The spherical shell, the left surface and inside edge of the flange are subjected to an internal pressure of 6.02 N/mm^2. The flange [Corrected was flange face] is subjected to four transverse loads as follows.

(1) A bolt load W_{M1} = 2836888 N total. This load is applied as a point load W1 = 1001.45 N/mm at a radius of 450.85 mm. Positive acting to the right.

(2) A Hydrostatic end force from the shell H_D = 5127687N total, due to the pressure acting over the outside [Corrected was inside] diameter of the flange. This load is applied as a point load W2 = -1567.307 N/mm at a radius of 520.7 mm. Negative acting to the left.

(3) A gasket reaction load H_G = 739318.7 N total. This load is applied as a point load W3 = -353.229 N/mm at a radius of 333.116 mm. Negative acting to the left. H_G is calculated on the basis of a spiral wound gasket with a gasket factor = 3 and minimum seating stress = 69 N/mm^2.

(4) A Hydrostatic end force H_T = 341441.8 N total, due to the pressure acting on the flange face between the inside of the flange and the gasket reaction diameter. This load is applied as a point load W4 = -170.374 N/mm [Corrected was W2] at a radius of 318.958 mm. Negative acting to the left.

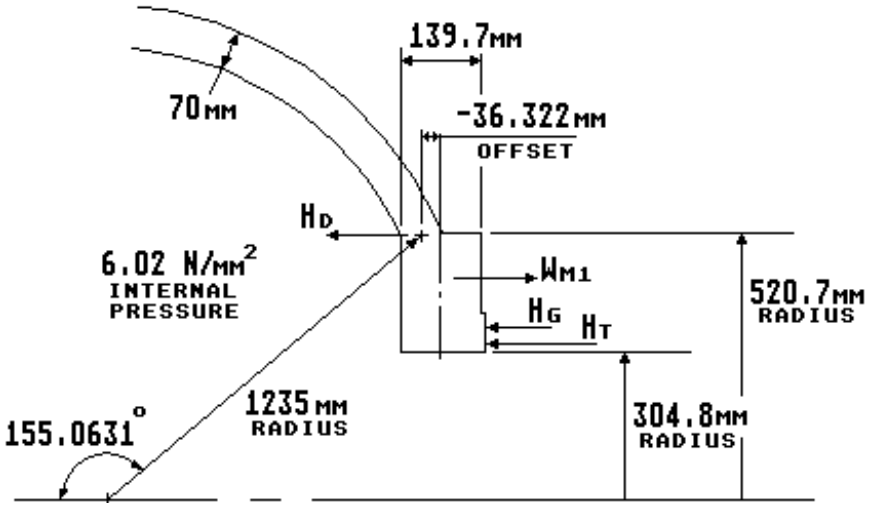

FIGURE 3.41(a) Studded connection in a spherical shell

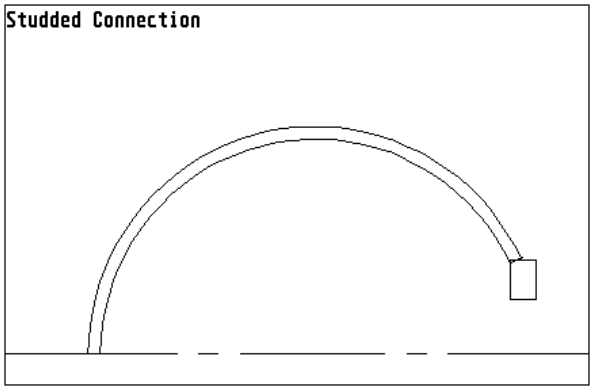

FIGURE 3.41(b) Geometry plot for example 3.18 case 4

Example 3.18, case 4 studded connection

The input data set and default free displacements are given in FIGURE 3.41(c) for the operating condition, i.e. internal pressure plus the flange loads as discussed above. As before, no assumptions are made as regard to points of zero radial deflection and no allowance is made for the effect of the bolt holes in reducing the stiffness of the flange.

Inspection of the input data set shows that an applied junction force Vo has been applied. This force is the default radial force due to the internal pressure acting on the spherical shell, as discussed in section 3.3.2 and equation (3.7). The default moment is zero (the small non-zero value is due to rounding).

The junction results are presented in FIGURE 3.41(d). The highest stress is the hoop membrane plus bending stress SHI = 80.6 N/mm^{2}at the inside edge of the flange. Plots of the highest stresses and the flange displacements are shown in FIGURES 3.41(e) to (h).

For the bolting-up condition the input data set and default free displacements are shown in FIGURE 3.41(i). There is no pressure on the flange or hub. The only loads are the flange design bolt load W = 7613922 N total [Correction reference to W_{M1} removed] and its reaction at the gasket. These loads are applied as a point load W1 = 2687.797 N/mm at a radius of 450.85 mm and as a point load W2 = -3637.752 N/mm [Corrected was W1] at a radius of 333.116 mm.

The junction results for the bolting-up condition are presented in FIGURE 3.41(j). The highest stress is the meridional membrane plus bending stress SLi = -163.17 N/mm^2 in the shell at the junction with the flange. The highest stress in the flange is the hoop membrane plus bending stress SHr = -163.05 N/mm^2 at the inside edge of the flange. Plots of the highest stresses and the displacement of the flange are shown in FIGURES 3.41(k) to (n).

INPUT DATA, PROGRAM AJAP1

Studded Connection
Operating Condition

COMPONENT No. 1
SPHERICAL SHELL, JUNCTION AT RIGHT END
Rs= 1235 mm
T= 70 mm
PHI= 155.0631 degrees
E= 178000 N/mm2
PR= .3
BETA= 5.399147
P= 6.02 N/mm2
Fp= 1567.308 N/mm
Fo= 3717.35 N/mm

COMPONENT No. 2
FLAT PLATE, JUNCTION AT O.D.
JUNCTION POSITION, JP= -.52
OFFSET= -36.322 mm
Ro= 520.7 mm
Ri= 304.8 mm
T= 139.7 mm
E= 178000 N/mm2
PR= .3
D= 4.444128E+10 Nmm
P= 6.02 N/mm2
qo= 0 N/mm2
qi= 6.02 N/mm2
W 1 = 1001.45 N/mm
Rw= 450.85 mm
W 2 = -1567.307 N/mm
Rw= 520.7 mm
W 3 = -353.229 N/mm
Rw= 333.116 mm
W 4 = -170.374 N/mm
Rw= 318.958 mm

APPLIED JUNCTION MOMENT & FORCE
Mo= -.1913217 Nmm/mm anti-clockwise
Vo= -3370.792 N/mm outward

FREE DISPLACEMENTS AT JUNCTION
COMPONENT No. 1
Yf= .108743 mm outward
THf= 0 radians

COMPONENT No. 2
Yf= -6.098225E-02 mm inward
THf= 2.184392E-03 radians anti-clockwise

FIGURE 3.41(c) Input data set for example 3.18 case 4 operating condition

JUNCTION RESULTS
DISCONTINUITY FORCES & MOMENTS
Studded Connection
Operating Condition

Mj 1 = -13315.54 Nmm/mm clockwise
Vj 1 = -237.8794 N/mm outward

Mj 2 = -13315.72 Nmm/mm anti-clockwise
Vj 2 = -3132.912 N/mm outward

RESULTS COMPONENT No. 1
Studded Connection
Operating Condition
OMEGA= 0 degrees
Y= .1352127 mm
THETA= -6.99072E-05 radians
V= 100.2946 N/mm
N1= 3501.648 N/mm
N2= 4286.042 N/mm
M1= -13315.54 Nmm/mm
M2= -3375.27 Nmm/mm
STRESSES N/mm2
SV= 1.43278
SL= 50.02354
SH= 61.22917
SBL=+or- 16.30474
SBH=+or- 4.132984
SLo= 66.32828
SLi= 33.7188
SHo= 65.36215
SHi= 57.09619

RESULTS COMPONENT No. 2
Studded Connection
Operating Condition
radius X= 520.7 mm
YL= 1.201406E-07 mm
Y= .1326735 mm
THETA= -6.990751E-05 radians
V= -1567.033 N/mm
N1= 3132.912 N/mm
N2= 7275.844 N/mm
M1= -100477.9 Nmm/mm
M2= -35572.94 Nmm/mm
STRESSES N/mm2
SV= -11.21713
SL= 22.426
SH= 52.08192
SBL=+or- 30.8908
SBH=+or- 10.9365
SLl= 53.31681
SLr= -8.4648
SHl= 63.01842
SHr= 41.14543

RESULTS COMPONENT No. 2
Studded Connection
Operating Condition
radius X= 304.8 mm
YL= -8.051619E-04 mm
Y= .1409853 mm
THETA= -3.288209E-06 radians
V= 0 N/mm
N1= -840.9939 N/mm
N2= 11249.75 N/mm
M1= 0 Nmm/mm
M2= -436.2872 Nmm/mm
STRESSES N/mm2
SV= 0
SL= -6.02
SH= 80.52792
SBL=+or- 0
SBH=+or- .1341315
SLl= -6.02
SLr= -6.02
SHl= 80.66205
SHr= 80.39378

FIGURE 3.41(d) Junction and flange results for example 3.18 case 4 operating condition

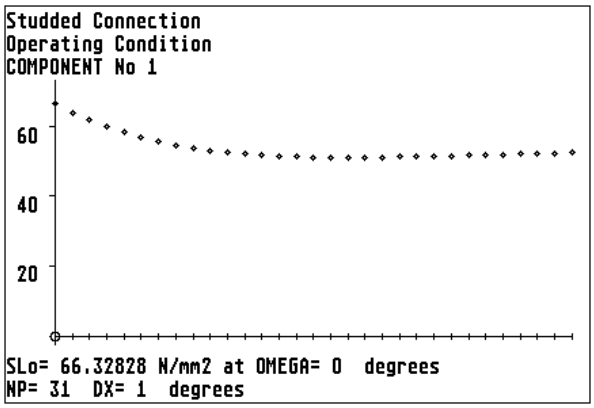

FIGURE 3.41(e) Meridional stress along the outside surface of the spherical shell from the junction with the flange.

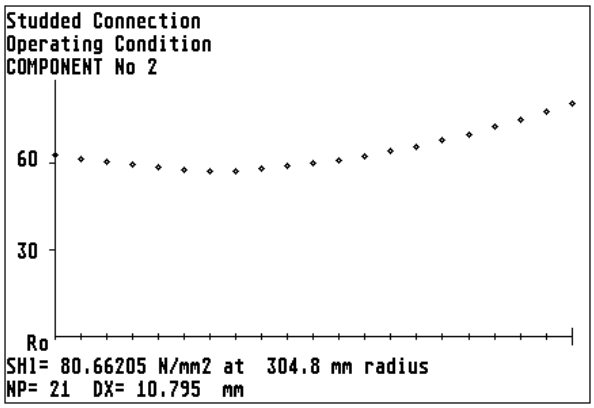

FIGURE 3.41(f) Hoop stress along the left surface of the flange from the junction radius.

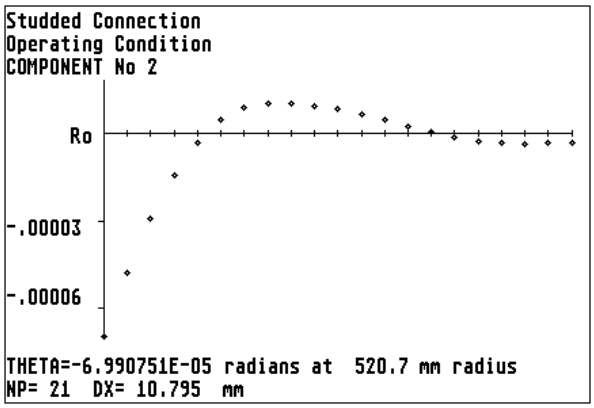

FIGURE 3.41(g) Rotation of the flange from the junction radius.

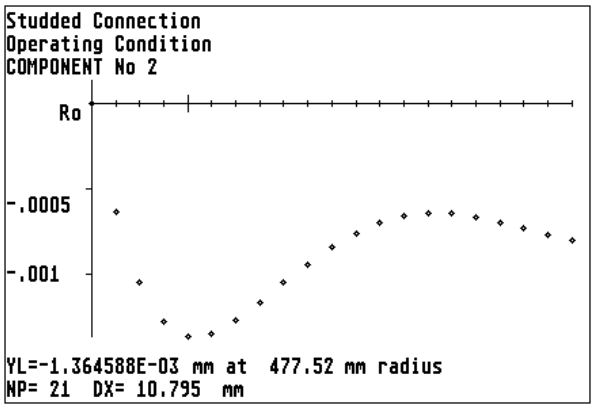

FIGURE 3.41(h) Transverse deflection of the flange from the junction radius.

INPUT DATA, PROGRAM AJAP1

Studded Connection
Bolting-up Condition

COMPONENT No. 1
SPHERICAL SHELL, JUNCTION AT RIGHT END
Rs= 1235 mm
T= 70 mm
PHI= 155.0631 degrees
E= 200000 N/mm2
PR= .3
BETA= 5.399147

COMPONENT No. 2
FLAT PLATE, JUNCTION AT O.D.
JUNCTION POSITION, JP= -.52
OFFSET= -36.322 mm
Ro= 520.7 mm
Ri= 304.8 mm
T= 139.7 mm
E= 200000 N/mm2
PR= .3
D= 4.993403E+10 Nmm
W 1 = 2687.797 N/mm
Rw= 450.85 mm
W 2 = -3637.752 N/mm
Rw= 333.116 mm

FREE DISPLACEMENTS AT JUNCTION
COMPONENT No. 1
Yf= 0 mm
THf= 0 radians

COMPONENT No. 2
Yf= .1948596 mm outward
THf= -5.364782E-03 radians clockwise

FIGURE 3.41(i) Input data set for example 3.18 case 4 bolting-up condition

JUNCTION RESULTS
DISCONTINUITY FORCES & MOMENTS
Studded Connection
Bolting-up Condition

Mj 1 = -120365.7 Nmm/mm clockwise
Vj 1 = -1218.671 N/mm outward

Mj 2 = -120365.7 Nmm/mm anti-clockwise
Vj 2 = 1218.671 N/mm inward

RESULTS COMPONENT No. 1
Studded Connection
Bolting-up Condition
OMEGA= 0 degrees
Y= 3.588228E-02 mm
THETA= -2.077475E-03 radians
V= 513.8155 N/mm
N1= -1105.058 N/mm
N2= 633.2456 N/mm
M1= -120365.7 Nmm/mm
M2= -15427.86 Nmm/mm
STRESSES N/mm2
SV= 7.340221
SL= -15.78654
SH= 9.046366
SBL=+or- 147.3866
SBH=+or- 18.89126
SLo= 131.6
SLi= -163.1731
SHo= 27.93763
SHi= -9.844894

RESULTS COMPONENT No. 2
Studded Connection
Bolting-up condition
radius X= 520.7 mm
YL= 2.682209E-07 mm
Y= -3.957573E-02 mm
THETA= -2.077473E-03 radians
V= 0 N/mm
N1= -1218.671 N/mm
N2= -2489.177 N/mm
M1= 164630.3 Nmm/mm
M2= -131905.9 Nmm/mm
STRESSES N/mm2
SV= 0
SL= -8.723487
SH= -17.81802
SBL=+or- 50.61371
SBH=+or- 40.55297
SLI= -59.3372
SLr= 41.89022
SHI= 22.73495
SHr= -58.37099

RESULTS COMPONENT No. 2
Studded Connection
Bolting-up Condition
radius X= 304.8 mm
YL= -.559855 mm
Y= -4.044926E-02 mm
THETA= -2.97851E-03 radians
V= 0 N/mm
N1= 0 N/mm
N2= -3707.848 N/mm
M1= 0 Nmm/mm
M2= -444040.1 Nmm/mm
STRESSES N/mm2
SV= 0
SL= 0
SH= -26.54151
SBL=+or- 0
SBH=+or- 136.5151
SLI= 0
SLr= 0
SHI= 109.9736
SHr= -163.0566

FIGURE 3.41(j) Junction results for example 3.18 case 4 bolting-up condition

As with the spherical domed flange discussed in case 3, the position of the junction of the shell and flange has an important influence on the stressing and behaviour of the studded connection. TABLE 3.19 shows the results for different positions of the junction. Inspection of the results show that the stress levels for the operating condition are significantly higher as the shell junction position is moved from the left (negative) side of the flange, towards the centre and right of the flange centre line. The reason for this behaviour is due to the pressure on the flange left surface and the bolt load W_{M1} tending to produce an *anti-clockwise* moment to the flange, but the radial force Vo from the shell tends to produce a *clockwise* moment when the junction position is to the *left* of the flange centre line. If the junction position is moved to the *right* of the flange centre line the moment produced by Vo will be *anti-clockwise* and will add to the flange moment due to the bolt load.

It is also seen by inspection of the results, FIGURES 3.41(d) and (j) and TABLE 3.19, that there is a change in sign of the stresses and displacements between the operating and bolting-up conditions. This behaviour is similar to that discussed previously for the reversed flange case 2.

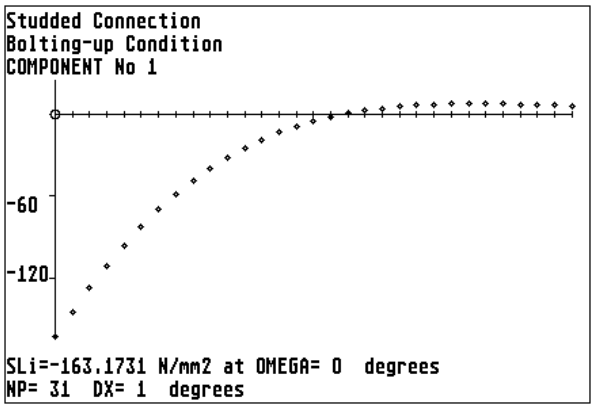

FIGURE 3.41(k) Meridional stress along the inside surface of the spherical shell from the junction with the flange.

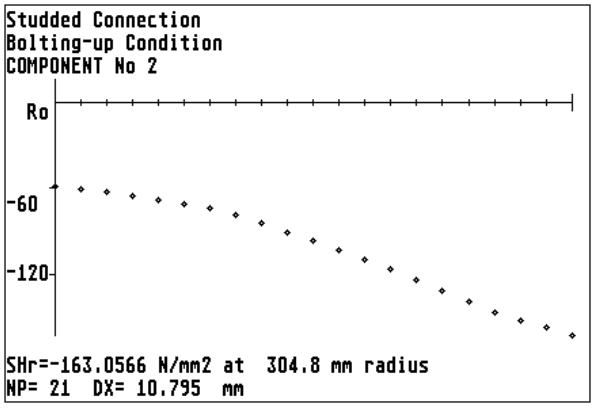

FIGURE 3.41(l) Hoop stress along the right surface of the flange from the junction radius.

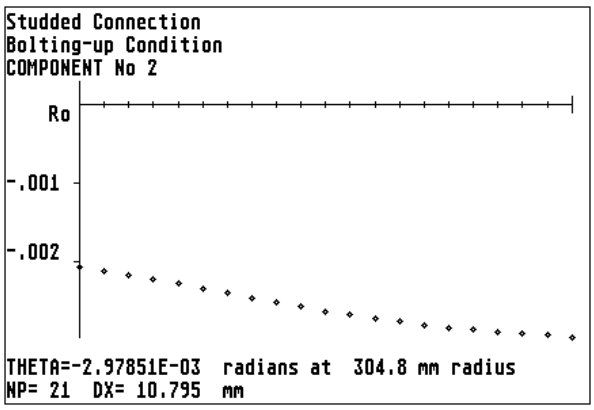

FIGURE 3.41(m) Rotation of the flange from the junction radius.

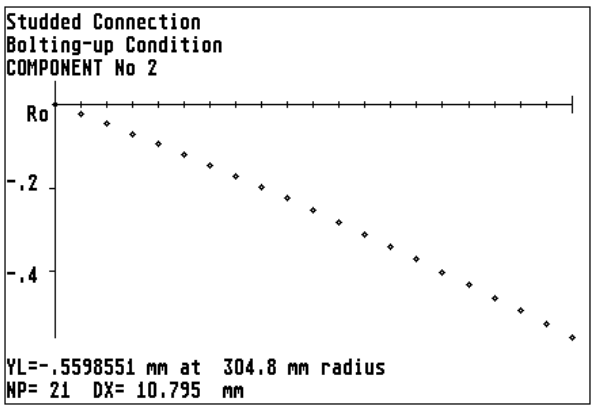

FIGURE 3.41(n) Transverse deflection of the flange from the junction radius.

	Operating condition	Bolting-up condition
Junction Position, JP	0	0
Junction Offset, mm	0	0
Hub stress, N/mm^2	SLi = 106.0	SLi = -169.2
Flange radial stress	SLl = 38.0	SLl = -60.7
Flange hoop stress	SHr = 144.5	SHr = -190.9
Flange rotation, radians	θ = 0.00135	θ = -0.00371
Flange deflection, mm	YL = 0.281	YL = -0.714
Junction Position, JP	+0.52	+0.52
Junction Offset, mm	36.322	36.322
Hub stress, N/mm^2	SLi = 154.9	SHi = -233.0
Flange radial stress	SLr = 53.1	SLl = -49.9
Flange hoop stress	SHr = 218.0	SHr = -201.1
Flange rotation, radians	θ = 0.00322	θ = -0.00425
Flange deflection, mm	YL = 0.672	YL = -0.826

TABLE 3.19 "AJAP1" results for different junction positions, example 3.18 case 4, studded connection

Case 5 Conventional Taper Hub Flange. Many conventional flanges are manufactured with tapered hubs. In "AJAP1" it is possible to model the taper hub by the compact ring. However the resulting analysis is not strictly representative of the real taper hub as the compact ring only has two degrees of freedom and most taper hubs are relatively long. FIGURE 3.42(a) shows a 24" Class 900 taper hub flange. These particular flanges feature a flange and bolting corresponding to the dimensions given in BS1560 (ref. 30).

A geometry plot is shown in FIGURE 3.42(b). The cylindrical shell is component No.1 and the flange is simulated by two flat plates (components 2 and 3) connected at the mean junction radius with the ring. The compact ring simulating the taper hub is component No. 4.

The cylindrical shell, ring and the inside edge of the flange (component 3) are subjected to the internal pressure of 6.02 N/mm^2. The flange [Corrected was flange face] is subjected to the four transverse loads required by the pressure vessel codes BS5500 and ASME SECTION VIII. The basis for the use of these loads is discussed in detail in references (31) and (32).

(1) A bolt load W_{M1} = 2836888 N total. This load is applied as a point load W1 = 1001.45 N/mm at a radius of 450.85 mm to component No.2. Positive acting to the right.

(2) A Hydrostatic end force from the shell H_D = 1336582N total, due to the pressure acting over the inside diameter of the shell. This load is applied as a point load W2 = -664.336 N/mm at the junction radius of 320.205 mm to component No.2. Negative acting to the left. Note that the difference in the value of this load and F_P for the shell is simply due to "AJAP1" calculating the end load based on mean radius. For most cases the difference is not significant.

(3) A gasket reaction load H_G = 739318.7 N total. This load is applied as a point load W3 = -353.229 N/mm at a radius of 333.116 mm to component No.2. Negative acting to the left. H_G is calculated on the basis of a spiral wound gasket with a gasket factor = 3 and minimum seating stress = 69 N/mm^2. Note in some cases this load may act at a smaller radius than the junction radius. In these cases the load would be applied as a point load W2 to component No.3.

(4) A Hydrostatic end force H_T = 760987.6 N total due to the pressure acting on the flange face between the inside diameter and the gasket reaction diameter. This load is applied as a point load W1 = -404.373 N/mm at a radius of 299.513 mm to component No.3. Negative acting to the left.

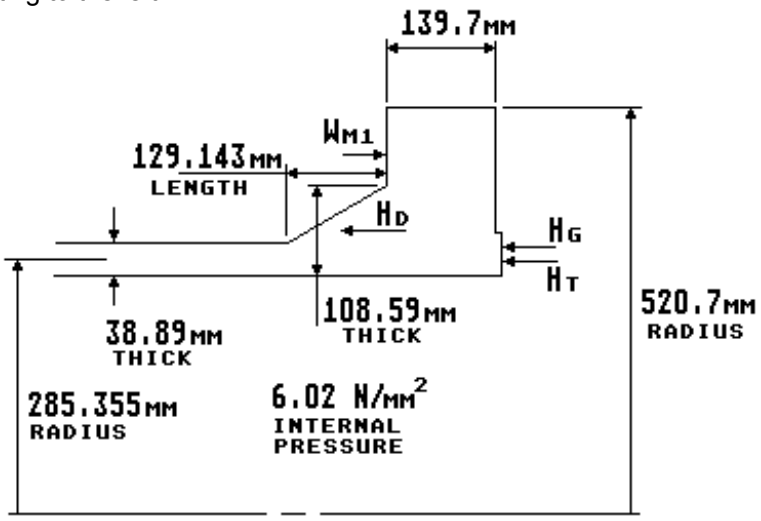

FIGURE 3.42(a) 24 inch class 900 taper hub flange

The pressure loads acting on the compact ring are a radial force Vr = -676.636 N/mm and a moment Mr = 6882.946 Nmm/mm. These loads are calculated by equations (3.31) and (3.32). The input data set and default free displacements are given in FIGURE 3.42(c) for the operating condition, i.e. internal pressure plus the flange loads as discussed above. No assumptions are made as regard to points of zero radial deflection and no allowance is made for the effect of the bolt holes in reducing the stiffness of the flange.

The default moment Mo is the moment produced by the hydrostatic end load F_P on the cylinder (component 1) acting about the ring centroid.

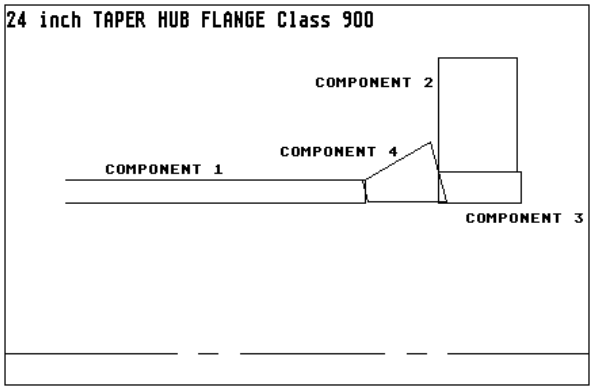

FIGURE 3.42(b) Geometry plot for example 3.18 case 5

INPUT DATA, PROGRAM AJAP1

24 inch TAPER HUB Class 900
Operating Condition

COMPONENT No. 1
CYLINDER, JUNCTION AT RIGHT END
R= 285.355 mm
T= 38.89 mm
E= 178000 N/mm2
PR= .3
BETA= 1.220195E-02 /mm
D= 9.587628E+08 Nmm
P= 6.02 N/mm2
Fp= 858.9186 N/mm
Fo= 858.9186 N/mm

COMPONENT No. 2
FLAT PLATE, JUNCTION AT I.D.
JUNCTION POSITION, LEFT SURFACE
JP= -1
OFFSET= -69.85 mm
Ro= 520.7 mm
Ri= 320.205 mm
T= 139.7 mm
E= 178000 N/mm2
PR= .3
D= 4.444128E+10 Nmm
W 1 = 1001.45 N/mm
Rw= 450.85 mm
W 2 = -664.336 N/mm
Rw= 320.205 mm
W 3 = -353.229 N/mm
Rw= 333.116 mm

COMPONENT No. 3
FLAT PLATE, JUNCTION AT O.D.
JUNCTION POSITION, LEFT SURFACE
JP= -1
OFFSET= -73.05 mm
Ro= 320.205 mm
Ri= 265.91 mm
T= 146.1 mm
E= 178000 N/mm2
PR= .3
D= 5.083327E+10 Nmm
qo= 0 N/mm2
qi= 6.02 N/mm2
W 1 = -404.373 N/mm
Rw= 299.513 mm

COMPONENT No. 4
COMPACT RING AT JUNCTION
Rl= 285.355 mm
Tl= 38.89 mm
Rr= 320.205 mm
Tr= 108.59 mm
L= 129.143 mm
Rc= 305.5251 mm
AREA= 9863.653 mm2
Ina/C= 163629.6 mm3
C= -79.80993 mm
Lx 1 = -74.74381 mm
Lx 2 = -79.80993 mm
Lx 3 = -10.32115 mm
Lx 4 = 40.2534 mm
Lx 5 = 54.3992 mm
Lx 6 = 68.545 mm
Lx 7 = 10.32115 mm
Lx 8 = -69.67768 mm
Lx 9 = 0 mm
CONNECTION 1 , 5 , 5 ,
E= 178000 N/mm2
PR= .3
Mr= 6882.946 Nmm/mm
Vr= -676.636 N/mm

APPLIED JUNCTION MOMENT & FORCE
Mo= 17324.37 Nmm/mm clockwise
Vo= 0 N/mm

FIGURE 3.42(c) Input data set for example 3.18 case 5 operating condition

The junction results are presented in FIGURE 3.42(d). The results for the taper hub are given in FIGURE 3.42(e). The highest stress is the meridional membrane plus bending stress at the outside of the small end of the taper hub, SL2 = 103.5 N/mm^2.

The input data set and results for the bolting-up condition are listed in FIGURES 3.42(f) and (g). The results for the taper hub are given in FIGURE 3.42(e). There is no pressure on the flange or hub. The only loads are the flange design bolt load W = 7613922 N total [Correction reference to W_{M1} removed] and its reaction at the gasket. These loads are applied as a point load W1 = 2687.797 N/mm at a radius of 450.85 mm to component No. 2 and as a point load W2 = -3637.752 N/mm [Corrected was W1] at a radius of 333.116 mm to component No. 2.

The results show that for the bolting-up condition the highest stress is the meridional bending plus membrane stress at the outside of the small end of the taper hub, SL2 = 178.1 N/mm^2.

JUNCTION RESULTS
DISCONTINUITY FORCES & MOMENTS
24 inch TAPER HUB Class 900
Operating Condition

Mj 1 = -20132.72 Nmm/mm clockwise
Vj 1 = -358.7391 N/mm outward

Mj 2 = -138412.3 Nmm/mm anti-clockwise
Vj 2 = -7.517151 N/mm outward

Mj 3 = 62116.71 Nmm/mm clockwise
Vj 3 = 779.4493 N/mm inward

at centroid
Mj 4 = 4681.27 Nmm/mm clockwise
Vj 4 = -413.1927 N/mm outward

RESULTS COMPONENT No. 1
24 inch TAPER HUB Class 900
Operating Condition
X= 0 mm
Y= 9.265141E-02 mm
THETA= -4.643774E-04 radians
V= 358.7391 N/mm
N1= 858.9186 N/mm
N2= 2505.304 N/mm
M1= -20132.72 Nmm/mm
M2= -6039.817 Nmm/mm
STRESSES N/mm2
SV= 9.224456
SL= 22.08585
SH= 64.42026
SBL=+or- 79.86894
SBH=+or- 23.96068
SLo= 101.9548
SLi= -57.78309
SHo= 88.38094
SHi= 40.45958

RESULTS COMPONENT No. 2
24 inch TAPER HUB Class 900
Operating Condition
radius X= 320.205 mm
YL= 0 mm
Y= 2.435706E-04 mm
THETA= -4.64378E-04 radians
V= 378.2384 N/mm
N1= -7.517151 N/mm
N2= 16.66015 N/mm
M1= -137887.2 Nmm/mm
M2= -100016.6 Nmm/mm
STRESSES N/mm2
SV= 2.707505
SL= -5.380924E-02
SH= .1192567
SBL=+or- 42.39186
SBH=+or- 30.74898
SLI= 42.33805
SLr= -42.44567
SHI= 30.86824
SHr= -30.62972

RESULTS COMPONENT No. 3
24 inch TAPER HUB Class 900
Operating Condition
radius X= 320.205 mm
YL= -1.829903E-09 mm
Y= -1.242463E-03 mm
THETA= -4.643778E-04 radians
V= 378.242 N/mm
N1= -779.4493 N/mm
N2= -334.7442 N/mm
M1= -5177.938 Nmm/mm
M2= -68639.53 Nmm/mm
STRESSES N/mm2
SV= 2.588925
SL= -5.335039
SH= -2.291199
SBL=+or- 1.455485
SBH=+or- 19.29412
SLI= -3.879555
SLr= -6.790524
SHI= 17.00292
SHr= -21.58532

FIGURE 3.42(d) Junction results for example 3.18 case 5 operating condition

RESULTS COMPONENT No. 4	RESULTS COMPONENT No. 4
24 inch TAPER HUB Class 900	24 inch TAPER HUB Class 900
Operating Condition	Bolting-up Condition
Y= 5.794208E-02 mm	Y= 4.165574E-02 mm
THETA= -4.643775E-04 radians	THETA= -5.985365E-04 radians
V= 1089.829 N/mm	V= 880.3371 N/mm
M= 11564.22 Nmm/mm	M= 16747.32 Nmm/mm
STRESSES N/mm2	STRESSES N/mm2
SH= 33.75726	SH= 27.2683
SBH= 21.50242	SBH= 31.27018
SV 1 = -3.151724	SV 1 = -21.5562
SL 1 = 23.7264	SL 1 = 5.817063
SH 1 = 61.09697	SH 1 = 58.29865
SL 2(on face 1)= 103.5953	SL 2(on face 1)= 178.1817
SL 2(on face 3)= 0	SL 2(on face 3)= 0
SH 2 = 86.42828	SH 2 = 111.993
SV 3 = 0	SV 3 = 0
SL 3 = 0	SL 3 = 0
SH 3 = 36.54963	SH 3 = 31.31221
SL 4(on face 3)= 0	SL 4(on face 3)= 0
SL 4(on face 5)= 40.67342	SL 4(on face 5)= 116.2504
SH 4 = 35.06881	SH 4 = 46.37181
SV 5 = 6.86319	SV 5 = 15.54705
SL 5 = 1.852037	SL 5 = 4.19546
SH 5 = 19.59528	SH 5 = 7.212885
SL 6(on face 5)= -36.96935	SL 6(on face 5)= -107.8595
SL 6(on face 7)= 0	SL 6(on face 7)= 0
SH 6 = 4.121746	SH 6 = -31.94603
SV 7 = 0	SV 7 = 0
SL 7 = 0	SL 7 = 0
SH 7 = 30.9649	SH 7 = 23.22439
SL 8(on face 7)= 0	SL 8(on face 7)= 0
SL 8(on face 1)= -56.14254	SL 8(on face 1)= -166.5476
SH 8 = 35.76566	SH 8 = 4.604307
SH 9 = 33.75726	SH 9 = 27.2683

FIGURE 3.42(e) Results for the taper hub (compact ring) for both operating and bolting-up condition

TABLE 3.20 summarises the results for several BS1560, Class 900, taper hub flanges compared with BS5500 analysis. These results are based on an operating condition of 6.02 N/mm^2 at 450°C and a bolting-up condition at ambient temperature. Assumed materials were A105 carbon steel for the flange and BS4882 grade B7A bolts [Corrected was B7].

By inspection of these results it is seen that "AJAP1" tends to significantly overestimate the taper hub stresses compared to the BS5500 analysis. It is recommended that for taper hub flanges the analysis of BS5500 or ASME SECTION VIII be used. For large diameter flanges the MURRAY and STUART analysis (ref. 33) is recommended.

Loading	4" BS5500	4" AJAP1	8" BS5500	8" AJAP1
Operating condition	Sh = 48.1 Sr = 49.8 St = 35.5	SL2 = 70.6 SLI = 51.7 SHr = -26.8	Sh = 44.7 Sr = 58.9 St = 32.6	SL2 = 91.7 SLI = 54.5 SHr = -31.9
Bolt-up condition	Sh = 137.1 Sr = 141.7 St = 101.1	SL4 = 201.0 SLI = 166.3 SHr = -81.7	Sh = 114.6 Sr = 151.1 St = 83.7	SL2 = 186.9 SLI = 161.0 SHr = -85.3
Loading	16" BS5500	16" AJAP1	24" BS5500	24" AJAP1
Operating condition	Sh = 46.6 Sr = 64.0 St = 31.0	SL2 = 103.1 SLI = 56.4 SHr = -33.4	Sh = 40.4 Sr = 47.1 St = 30.4	SL2 =103.5 SLr = -42.4 SHI = 30.8
Bolt-up condition	Sh = 102.4 Sr = 140.5 St= 68.2	SL2 = 162.7 SLI = 141.5 SHr = -79.1	Sh = 96.3 Sr = 112.1 St = 72.4	SL2 = 178.1 SLI = 119.7 SHr = -77.6

TABLE 3.20 Comparison of highest stresses (N/mm^2) for taper hub flanges

INPUT DATA, PROGRAM AJAP1

24 inch TAPER HUB Class 900
Bolting-up Condition

COMPONENT No. 1
CYLINDER, JUNCTION AT RIGHT END
R= 285.355 mm
T= 38.89 mm
E= 200000 N/mm2
PR= .3
BETA= 1.220195E-02 /mm
D= 1.077262E+09 Nmm

COMPONENT No. 2
FLAT PLATE, JUNCTION AT I.D.
JUNCTION POSITION, LEFT SURFACE
JP= -1
OFFSET= -69.85 mm
Ro= 520.7 mm
Ri= 320.205 mm
T= 139.7 mm
E= 200000 N/mm2
PR= .3
D= 4.993403E+10 Nmm
W 1 = 2687.797 N/mm
Rw= 450.85 mm
W 2 = -3637.752 N/mm
Rw= 333.116 mm

COMPONENT No. 3
FLAT PLATE, JUNCTION AT O.D.
JUNCTION POSITION, LEFT SURFACE
JP= -1
OFFSET= -73.05 mm
Ro= 320.205 mm
Ri= 265.91 mm
T= 146.1 mm
E= 200000 N/mm2
PR= .3
D= 5.711604E+10 Nmm

COMPONENT No. 4
COMPACT RING AT JUNCTION
Rl= 285.355 mm
Tl= 38.89 mm
Rr= 320.205 mm
Tr= 108.59 mm
L= 129.143 mm
Rc= 305.5251 mm
AREA= 9863.653 mm2
Ina/C= 163629.6 mm3
C= -79.80993 mm
Lx 1 = -74.74381 mm
Lx 2 = -79.80993 mm
Lx 3 = -10.32115 mm
Lx 4 = 40.2534 mm
Lx 5 = 54.3992 mm
Lx 6 = 68.545 mm
Lx 7 = 10.32115 mm
Lx 8 = -69.67768 mm
Lx 9 = 0 mm
CONNECTION 1 , 5 , 5 ,
E= 200000 N/mm2
PR= .3

FIGURE 3.42(f) Input data set for example 3.18 case 5 bolting-up condition

JUNCTION RESULTS
DISCONTINUITY FORCES & MOMENTS
24 inch TAPER HUB Class 900
Bolting-up Condition

Mj 1 = -43448.3 Nmm/mm clockwise
Vj 1 = -868.3084 N/mm outward

Mj 2 = -283983.8 Nmm/mm anti-clockwise
Vj 2 = 1134.341 N/mm inward

Mj 3 = 63762.42 Nmm/mm clockwise
Vj 3 = 614.3036 N/mm inward

at centroid
Mj 4 = 16747.32 Nmm/mm clockwise
Vj 4 = -880.3371 N/mm outward

RESULTS COMPONENT No. 1
24 inch TAPER HUB Class 900
Bolting-up Condition
X= 0 mm
Y= 8.639259E-02 mm
THETA= -5.985361E-04 radians
V= 868.3084 N/mm
N1= 0 N/mm
N2= 2354.827 N/mm
M1= -43448.3 Nmm/mm
M2= -13034.49 Nmm/mm
STRESSES N/mm2
SV= 22.32729
SL= 0
SH= 60.55097
SBL=+or- 172.3646
SBH=+or- 51.70948
SLo= 172.3646
SLi= -172.3646
SHo= 112.2604
SHi= 8.841572

RESULTS COMPONENT No. 2
24 inch TAPER HUB Class 900
Bolting-up Condition
radius X= 320.205 mm
YL= 0 mm
Y= -3.271187E-02 mm
THETA= -5.98534E-04 radians
V= 0 N/mm
N1= 1134.341 N/mm
N2= -2514.025 N/mm
M1= -363217.5 Nmm/mm
M2= -193902.6 Nmm/mm
STRESSES N/mm2
SV= 0
SL= 8.119838
SH= -17.99588
SBL=+or- 111.6671
SBH=+or- 59.61315
SLi= 119.7869
SLr= -103.5472
SHi= 41.61726
SHr= -77.60903

RESULTS COMPONENT No. 3
24 inch TAPER HUB Class 900
Bolting-up Condition
radius X= 320.205 mm
YL= 3.72529E-09 mm
Y= -3.462717E-02 mm
THETA= -5.985357E-04 radians
V= 0 N/mm
N1= -614.3036 N/mm
N2= -3344.162 N/mm
M1= -18887.53 Nmm/mm
M2= -102820.4 Nmm/mm
STRESSES N/mm2
SV= 0
SL= -4.204679
SH= -22.88954
SBL=+or- 5.309162
SBH=+or- 28.90215
SLi= 1.104483
SLr= -9.513841
SHi= 6.01261
SHr= -51.79168

FIGURE 3.42(g) Junction results for example 3.18 case 5 bolting-up condition

4.0 ASSESSMENT OF STRESSES

In previous chapters the method of analysis has been presented and we have seen, by example, what results can be obtained from the program. Once the results are obtained and checked, it is necessary to assess the stresses in the structure to see that they are within acceptable limits. This assessment of stresses is an essential part of the safety requirements for a structure such as a pressure vessel that has been "Designed by Analysis". There may also be additional criteria to be met, such as: (1) Deformation limits for functioning requirements, (2) Prevention of instability (buckling) and (3) Prevention of vibrations. These additional criteria require specialist study and are not discussed in detail here.

For pressure vessels the stress criteria to be satisfied by an assessment are specified in pressure vessel codes such as BS5500 and ASME SECTION VIII division 2. It requires experience and specialist knowledge to assess a vessel to these codes. While it is outside the scope of this book to give a comprehensive discussion on the subject of assessment, it was considered that a brief discussion with guidance notes and a worked example would be useful so that the main principles involved could be understood. The following discussion is based on BS5500 appendix A and C with additional notes to cover some differences with ASME SECTION VIII division 2, appendix 4 and 5 rules. The discussion is limited to an elastic analysis and non-creep conditions. Further background on stress criteria is contained in references (34) and (35). But note that with the passage of time some of the details in these references are out of date and reference to the latest edition of the code is essential. Also note that the fatigue analysis rules in appendix C of BS5500 are likely to be replaced eventually by the alternative fatigue rules in BS5500 enquiry case 79.

4.1 STRESS CATEGORIES

The rules for *general application* (except buckling) require the stresses to be grouped into five *stress categories*. Note that the term category used here has no connection with the construction categories used in the main text of BS5500.

The five stress categories to be satisfied are as follows:

(1) General primary membrane stress category, f_M
(2) Local primary membrane stress category, f_L
(3) Primary membrane plus primary bending stress category f_B, $f_M + f_B$ or $f_L + f_B$
(4) Primary plus secondary stress category, $f_M + f_B + f_G$ or $f_L + f_B + f_G$
(5) Peak stress category, $f_M + f_B + f_G + f_P$ or $f_L + f_B + f_G + f_P$

The terms f_M, f_L, f_B, f_G, and f_P (P_M, P_L, P_B, Q and F in ASME) are *stress intensities*. These stress intensities are discussed in detail in section 4.3.

Categories (1) to (4) are applicable to a stress assessment. Category (5) is additionally required for a fatigue assessment.

Categories (1), (2) and (3) are concerned only with pressure and mechanical loads. The purpose is to ensure that there is no catastrophic failure in a single application of load. It is normal practice to check the vessel for *design conditions*, i.e. design pressure and design mechanical loads. The design mechanical loads may include: weight, wind loading, earthquake loads and pipe forces and moments, FIGURE 4.1. BS5500 appendix B provides rules for combined loading in addition to internal pressure.

Stress category (1) excludes any discontinuities. Category (2) includes gross discontinuities but not local discontinuities, i.e. no geometric stress concentration factors are required. Category (3) requires the primary bending stress to be combined with the primary membrane stress from category (1) or (2). The primary bending stress should exclude any discontinuities.

Category (4) is concerned with mechanical and thermal loads, FIGURES 4.1 and 4.2, and requires the *operating conditions* to be known throughout the service life of the vessel. The purpose of this stress category is to ensure that the vessel will shakedown to elastic conditions after a few operating cycles. Failure is not expected in a single application of load. Incremental collapse will be avoided and elastic assumptions in the fatigue analysis will be valid. GRAY and SPENCE have a brief discussion on shakedown and incremental collapse in reference (20). Category (4) actually requires the *stress range* to be obtained rather than just the absolute magnitude of a stress at a particular point in time. If the vessel has a complex operating history then great care has to be taken with the stress sign so that the maximum stress range is obtained. Gross discontinuities are included but not local discontinuities.

Stress category (5) is applicable to a fatigue analysis. The total stress range must be obtained for all *operating conditions*. Both the gross and local discontinuities must be included and since elastic assumptions are made in the fatigue analysis, it is essential to show that the vessel will shakedown by satisfying stress category (4). Failure is not expected in a single application of load but the allowable stress amplitude (half the stress range) for a specified number of cycles is found from a *design fatigue curve* such

as that given in BS5500 appendix C figure C.2.1 for steels and aluminium alloys. A separate curve is given for bolting materials.

Alternatively the number of cycles to failure for a stress amplitude can be obtained. When the operating history is complex with more than one stress cycle the cumulative damage has to be estimated using MINER's rule. Both BS5500 and ASME SECTION VIII division 2 have simplified procedures which if satisfied may avoid the need for a fatigue analysis.

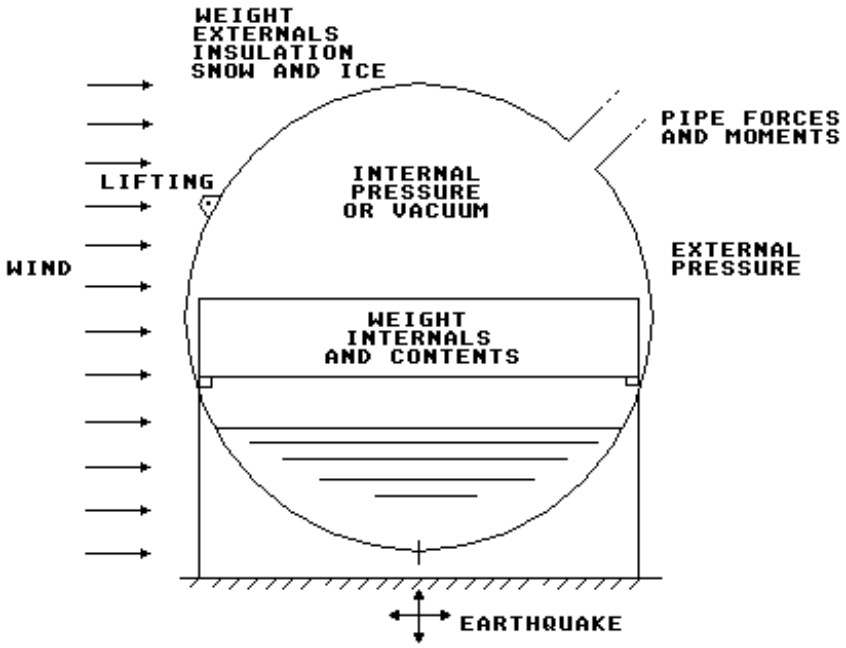

FIGURE 4.1 Some mechanical loads applicable to pressure vessels

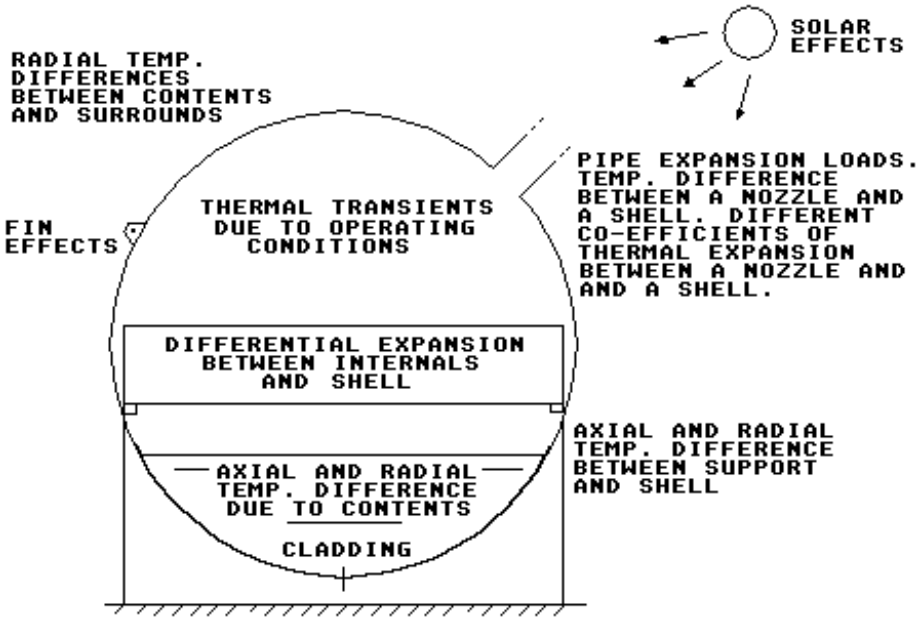

FIGURE 4.2 Some thermal effects applicable to pressure vessels

4.2 STRESS COMPONENTS

The stress intensities f_M, f_L, f_B, f_G, and f_P are *not* single values but are sets of six stress components, i.e. three normal stresses and three shear stresses acting at a point, FIGURE 4.3. When combining the stresses into the categories, the combining must be done at the stress component level and the sign of the stress must be taken into account i.e. +ve tensile, -ve compression. The principal stresses for the combined loading are calculated and the stress intensity (discussed in section 4.3) obtained for the point under consideration.

At the stress component stage it is necessary to have a clear definition of the stress directions in a conventional co-ordinate system like that shown in FIGURE 4.3.

As discussed previously, in section 1.3, for axisymmetric structures it is convenient for reasons of symmetry to define the stress directions in terms of the hoop, transverse and meridional directions. The co-ordinate system shown in FIGURE 4.3 is not always convenient and a local co-ordinate system is more suitable. Unfortunately there is no universally agreed convention for local co-ordinates. BS5500 appendix A does not provide any guidance but does put the Z direction as the meridional stress in appendix B. Hence for the purposes of this text the rather arbitrary choice of local stress directions become:

f_X is the hoop direction
f_Y is the transverse direction
f_Z is the meridional direction

For the shear stresses the rules of complementary shear apply, i.e. $f_{XZ} = f_{ZX}$, $f_{YX} = f_{XY}$, $f_{ZY} = f_{YZ}$, the first subscript letter refers to the plane on which the stress acts while the second subscript refers to the direction. In some textbooks this order of the subscripts is reversed.

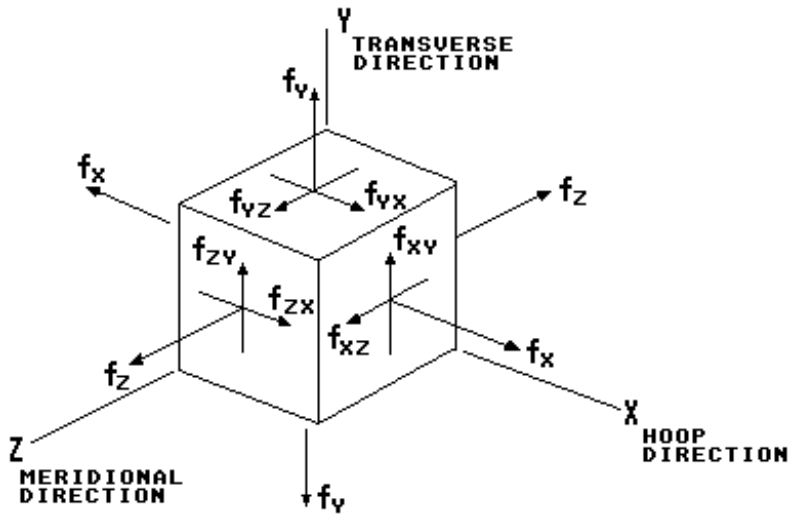

Normal (direct) stresses f_X, f_Y, f_Z
Shear stresses f_{XZ}, f_{YX}, f_{ZY}

FIGURE 4.3 Stresses acting at a point

4.3 STRESS INTENSITY

The stress analysis is based on the "TRESCA" (or maximum shear stress) failure criterion. The application of this criterion actually involves calculating a term called the *stress intensity* which is defined as: twice the maximum shear stress, i.e. the algebraic difference between the largest and smallest principal stresses at a point. By convention we write the principal stress differences as equation (4.1).

$$f_{12} = f_1 - f_2$$

$$f_{23} = f_2 - f_3 \qquad (4.1)$$

$$f_{31} = f_3 - f_1$$

The terms f_1, f_2, and f_3 are the three principal stresses at a point and f_{12}, f_{23} and f_{31} are the three stress differences. The stress intensity is the largest *absolute* value of the three stress differences.

The calculation of the principal stresses are essential for the evaluation of the stress intensity. In a three dimensional co-ordinate system the three principal stresses f_N are given by the roots of equation (4.2).

$$f_N^3 - (f_X + f_Y + f_Z)f_N^2 + (f_Xf_Y + f_Yf_Z + f_Xf_Z - f_{YX}^2 - f_{XZ}^2 - f_{ZY}^2)f_N - (f_Xf_Yf_Z + 2f_{YX}f_{XZ}f_{ZY} - f_Xf_{ZY}^2 - f_Yf_{XZ}^2 - f_Zf_{YX}^2) = 0 \qquad (4.2)$$

For a thin shell axisymmetric structure with axisymmetric loading and no twisting moments it is not necessary to solve equation (4.2) as the shear stresses in directions f_{XZ} and f_{YX} are zero and f_X in the hoop direction is a principal stress f_1. The two remaining principal stresses can be calculated by the well known MOHR's circle equations (4.3).

$$f_2 = 0.5[f_Y + f_Z + \{(f_Y - f_Z)^2 + 4* f_{ZY}^2\}^{1/2}]$$
$$f_3 = 0.5[f_Y + f_Z - \{(f_Y - f_Z)^2 + 4* f_{ZY}^2\}^{1/2}] \qquad (4.3)$$

4.4 PRIMARY, SECONDARY and PEAK STRESSES

The symbols f_M, f_L, f_B, f_G, and f_P mentioned in section 4.1, are actually stress intensities defined as follows:

General primary membrane stress intensity, f_M
Local primary membrane stress intensity, f_L
Primary bending stress intensity, f_B
Secondary stress intensity, f_G
Peak stress intensity, f_P

The code assessment requires that a particular stress be classified as one of the above stress intensities. It requires experience to correctly classify a stress and is one of the major difficulties in applying the "Design by Analysis" rules. The codes recognise this and provide a table of typical cases (e.g. refer to TABLE A.3. of BS5500) as a guide to the analyst. The following examples briefly describe the most common cases likely to be found in the practical assessment of pressure vessels. In general the classification of a stress is dependent upon four considerations:

(1) What *type of component* is being considered, e.g. cylindrical shell, flat end, nozzle, etc.

(2) The *location of the stress* in the component, e.g. remote from discontinuities or at a discontinuity.

(3) The *origin of the stress*, e.g. internal pressure, external mechanical load, axial thermal gradient, temperature difference across the thickness, etc.

(4) The *type of stress*, e.g. general membrane, local membrane, bending across full section, bending across the thickness, stress concentration.

4.4.1 Primary Stresses, f_M, f_L, f_B.

Primary stresses are produced only by mechanical loads. The stress is not self-limiting and must satisfy the laws of equilibrium of external and internal forces and moments. Primary stresses if they exceed the yield strength would result in failure or severe distortion of the structure. The primary stresses can be "general" or "local".

Examples of *general* primary stress are:

(1) With reference to FIGURE 4.4(a). The membrane stress f_M in a shell or nozzle due to pressure, distributed load or an external force or moment. The external forces and moments include design mechanical loads such as weight, wind load, earthquake loads and pipework mechanical loads. In some cases it is necessary to include the stresses due to pipework expansion loads as a primary stress. This is usually the case when there is significant *elastic follow-up*. References (36) and (45) discuss this aspect in detail. The membrane stress is calculated as the average across the *full* section A - A. Note that for a moment across the *full* section the bending stress at the mean radius is considered a membrane stress as shown in FIGURE 4.5(a). Note also that ASME SECTION VIII division 2 has additional rules for nozzle sections, this is discussed in more detail in section 4.4.4 later.

(2) With reference to FIGURE 4.4(b). The membrane stress f_M in the crown or centre region of a dished (domed) or flat head (end) due to pressure. The stress is calculated as the *average across the thickness* of the section(s) A - A.

(3) With reference to FIGURE 4.4(b). The bending stress f_B in the crown or centre region of a dished, conical or flat end due to pressure. The stress is calculated as the *linear gradient across the thickness* of the section(s) A - A, i.e. for a moment across the wall thickness this stress is considered a bending stress as shown in FIGURE 4.5(b).

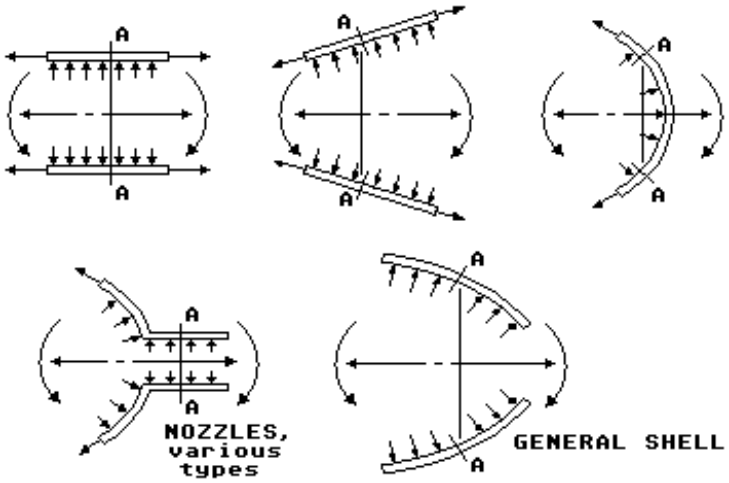

FIGURE 4.4(a) Some examples of vessel components and locations where the classification of general primary membrane stress applies

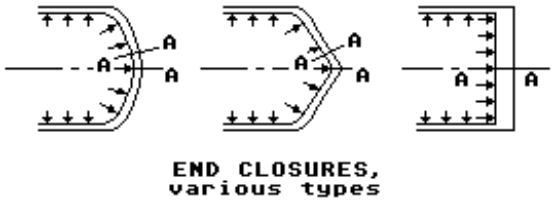

FIGURE 4.4(b) Some examples of vessel components and locations where the classification of general primary membrane stress and primary bending stress apply

Examples of *local* primary membrane stress f_L are:

(4) With reference to FIGURE 4.4(c). The membrane stress at a *gross* structural discontinuity such as: the junction with a head or flange or nozzle or support attachment. The stress is due to pressure, distributed load, external force or moment and is calculated as the *average across the thickness* of the section(s) A - A at (or close to) the junction. The local membrane stress includes the general primary membrane stress in addition to the membrane stress due to the discontinuity. For nozzle sections ASME SECTION VIII has additional rules, refer to section 4.4.4 below.

Both codes have warnings that buckling (wrinkling) and excessive deformation may occur in the knuckle region of dished ends when the vessel has a large diameter to thickness ratio. GALLETLY discusses this aspect in some detail in reference (17).

Both codes provide guidance on the extent of the local primary membrane stress. FIGURE 4.6 shows the limitations required by BS5500 in order that the primary membrane stress be considered as local. The rules are *not* identical with ASME SECTION VIII, e.g. BS5500 limits the distance over which the stress intensity exceeds 1.1*f* to *half* that required by ASME SECTION VIII. Where *f* is the material design strength value discussed in section 4.5.

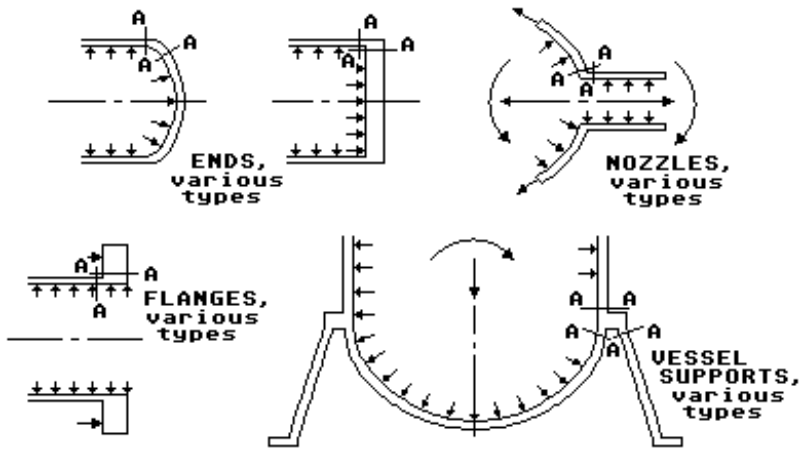

FIGURE 4.4(c) Some examples of vessel components and locations where the classification of local primary membrane stress and secondary bending stress apply

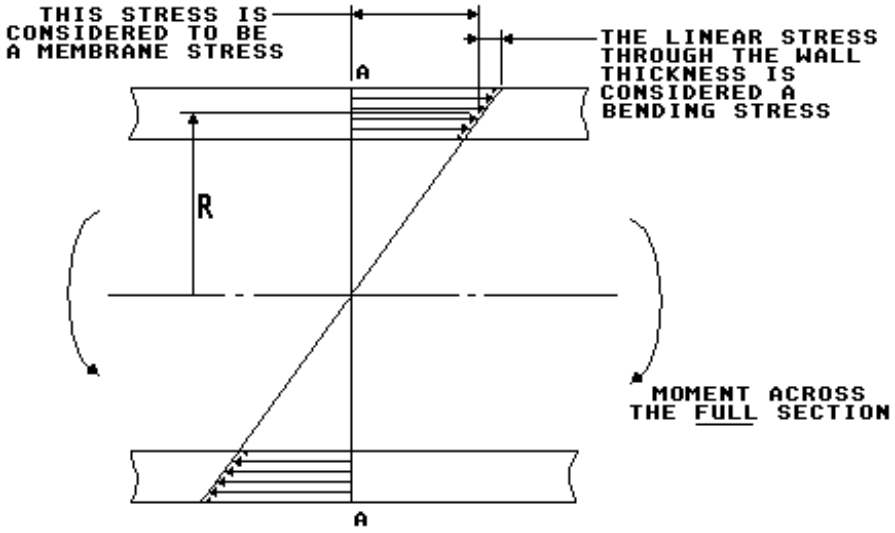

FIGURE 4.5(a) Distribution of stress for a moment applied across a *full* section

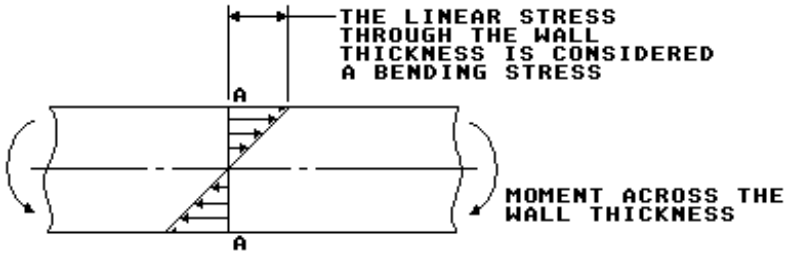

FIGURE 4.5(b) Distribution of stress for a moment applied across the wall thickness

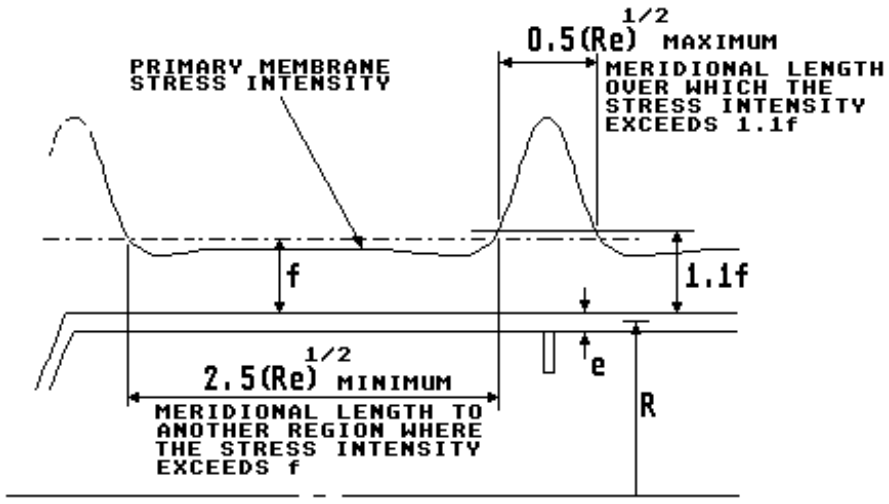

FIGURE 4.6, BS5500 rules for the extent of the limits on local primary membrane stress

4.4.2 Secondary Stresses, f_G

Secondary stresses are produced by mechanical or thermal loads. These stresses are due to the constraint of adjacent parts of the structure or by the self-constraint of the structure. The stress is self-limiting and failure from a single application of load is not expected but some distortion of the structure may occur.

Examples of secondary stresses are:

(1) With reference to FIGURE 4.4(c). The bending stress at a *gross* structural discontinuity such as: the junction with a head or flange or nozzle or support attachment. The stress is due to pressure, distributed load, external force or moment and is calculated as the *linear gradient across the thickness* of the section(s) A - A at (or close to) the junction. For nozzle sections ASME SECTION VIII has additional rules, refer to section 4.4.4 below. The ASME SECTION VIII code also has an additional requirement for flat ends subject to pressure, if the bending moment at the edge (i.e. the junction with the shell) is required to limit the bending stress at the centre region, then the edge bending is to be classified as primary bending rather than secondary. Although this rule is given for flat ends it would appear to have a more general application for vessel components in the form of flat plates or rings subjected to mechanical loads, e.g. flanges and integral supports.

(2) With reference to FIGURE 4.7. The membrane and bending stresses produced by a *general thermal stress*, such as:

(a) the temperature difference ($T_2 – T_1$) between one component and another.
(b) the *linear* bending stress due to a thermal gradient ($T_2 – T_1$) across the thickness of a shell or plate. Note that ASME SECTION VIII has an additional requirement to consider the possibility of a *thermal stress ratchet*. Rules are given in subparagraph 5-130 to assess this requirement.
(c) the stress due to an axial thermal gradient ($T_2 – T_1$).
(d) the stresses due to different co-efficients of thermal expansion between components subjected to a temperature change ΔT, e.g. between an austenitic stainless steel nozzle and a ferritic steel shell.

4.4.3 Peak Stresses, f_P

The peak stress is the additional stress over and above the primary plus secondary stresses. Peak stresses do not cause any significant distortion of the structure but may be a source of fatigue failure or brittle fracture.

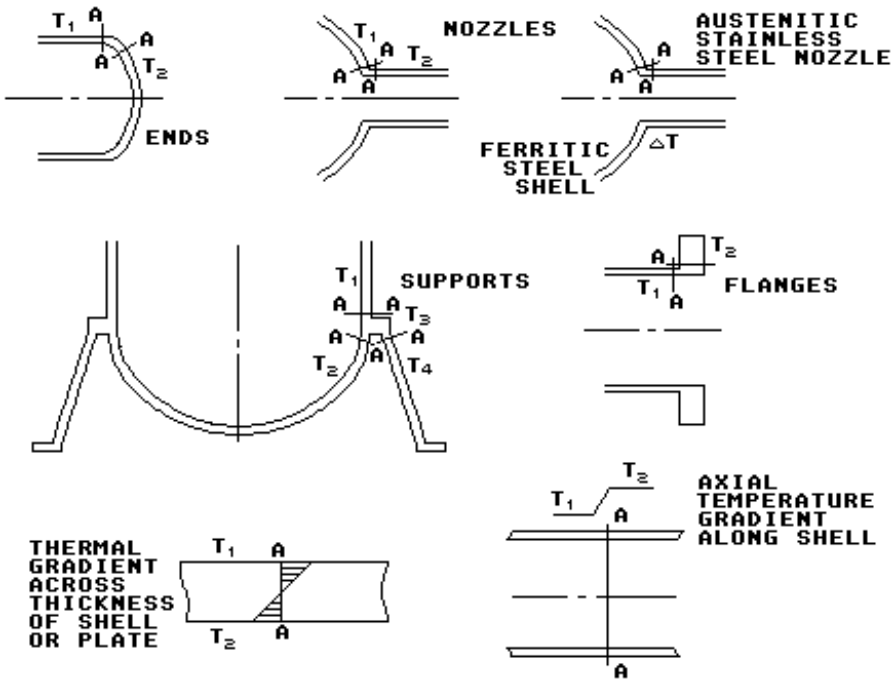

FIGURE 4.7 Some examples of vessel components and locations where the classification of secondary stress applies due to the effect of a *general* thermal stress

Examples of peak stresses are:

(1) With reference to FIGURE 4.8(a). The stress, due to *any* loading, at a *local* structural discontinuity such as a geometric stress concentration (notch) K_t.
Refer to section 1.3.2 for a further discussion.

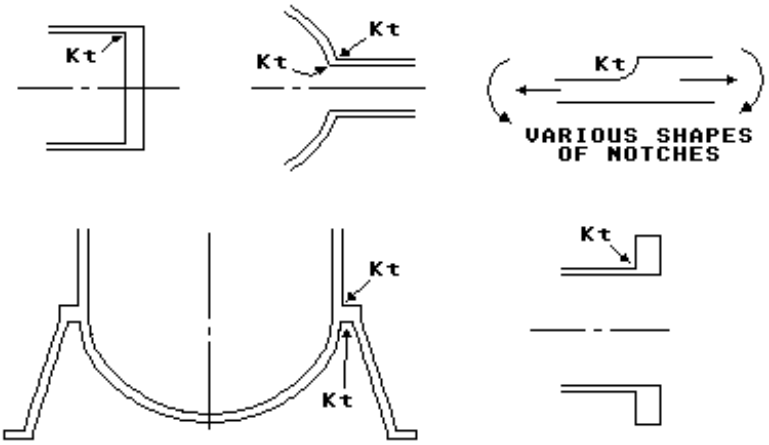

FIGURE 4.8(a) Some examples of vessel components and locations where the classification of peak stress applies due to geometric stress concentrations

(2) With reference to FIGURE 4.8(b). A *local thermal stress* such as that produced by:

(a) the *non-linear* stress due to a thermal gradient ($T_2 - T_1$) across the thickness of a shell or plate. Note that ASME SECTION VIII division 2 has an additional requirement to consider the possibility of a *thermal stress ratchet*. Refer to section 4.5.1(6) for a brief discussion.
(b) a small hot spot in the wall of a shell or plate.
(c) the surface stress in the wall of a shell or plate when subjected to a sudden temperature change (thermal shock), ΔT.
(d) the stress in a cladding material with a different co-efficient of thermal expansion to the base material when subjected to a temperature change ΔT, e.g. between an austenitic stainless steel cladding and a ferritic steel shell or plate.

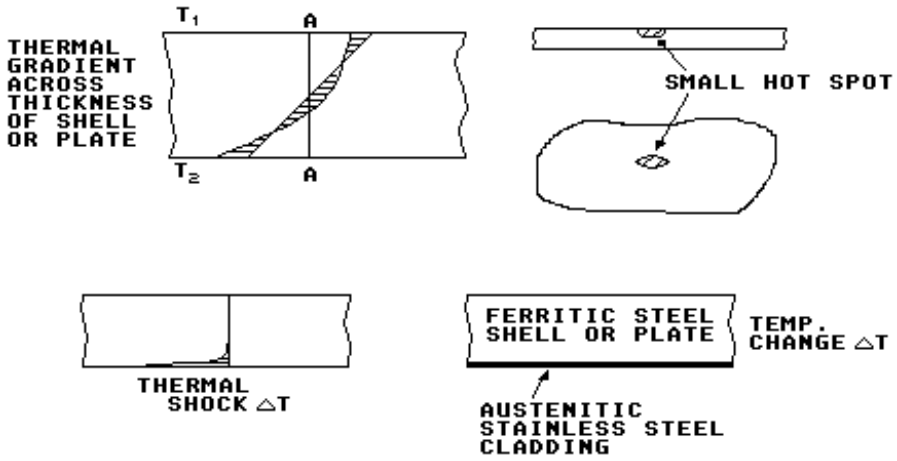

FIGURE 4.8(b) Some examples of vessel components and locations where the classification of peak stress applies due to the effect of *local* thermal stress

4.4.4 Nozzle Neck Classification

The ASME SECTION VIII division 2 code has additional requirements applicable to *nozzle piping transitions* in subparagraph 4.138. With reference to FIGURE 4.9 the rules are applicable to the nozzle *neck*, regardless of whither the nozzle neck is reinforced or not. The rules do *not* affect the vessel stress classification.

The rules demand a different stress classification requirement for the external loads and moments due to the *restrained free end displacements* of the attached pipe, depending on whether the section A - A being considered is within the limits of the reinforcement or not.

The restrained free end displacements include the pipe expansion stresses as a result of the relative thermal expansion movements of the piping and the vessel. *Within* the limits of reinforcement along the nozzle (defined in subparagraph AD-540.2) the stresses due to the restrained free end displacements are *included* as primary general membrane stresses P_M. *Outside* the limits of reinforcement the stresses due to the restrained free end displacements are *excluded* from the primary stress categories P_M and $P_M + P_B$ but are *included* in the primary plus secondary stress category $P_M + P_B + Q$.

A well designed piping system requires to be properly supported and have sufficient *flexibility* so that the pipe connections to the vessel (usually anchors) do not put excessive loads on the vessel. This is one of the main reasons why it is essential for high temperature piping systems to be designed to met the rules for flexibility provided in piping codes such as BS806 or ASME B31.1, references (38) and (39).

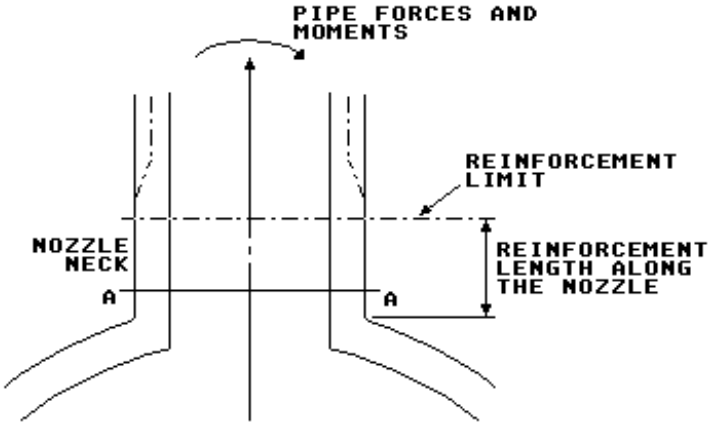

FIGURE 4.9 Nozzle neck subjected to piping forces and moments

4.4.5 Perforated Tubesheets

Both BS5500 and ASME SECTION VIII division 2 consider the classification of stress in the ligament of a perforated end or shell. The ASME code article 4-9 provides additional simplified analysis based on an equivalent solid plate with modified elastic constants. The basis of the method is discussed by O'DONNELL and LANGER in reference 37.

The detailed stress analysis of tubesheets is particularly difficult due to the close spacing of the tube holes and the combined mechanical and thermal loads applied to heat exchangers. There are also additional difficulties at the junction with the unperforated rim and for the inevitable misdrilled hole resulting in a thin ligament.

The classification depends on whether the tube holes are drilled in a typical uniform pattern (like a regular square or triangular pattern) or are an isolated or atypical ligament. The rules for isolated or atypical ligament are included to allow for the possibility of a misdrilled hole. The rules consider the effect of membrane, bending and peak stresses in the ligament between the tube holes, refer to FIGURE 4.10.

If we consider a tubesheet subjected to pressure and thermal loads the stress classification is as follows:

(1) *For ligaments in a uniform pattern* the primary membrane stress f_M is the average stress across the cross section of the ligament between the tube holes. The primary bending stress f_B is averaged through the width of the ligament and is a linear gradient through the thickness of the plate or shell. The additional stress due to the stress concentration factor due to the hole pattern is considered a peak stress, f_P.

(2) *For an isolated or atypical ligament* the membrane stress is considered a secondary stress f_G. The bending stress and the additional stress due to the stress concentration factor of the holes are considered a peak stress f_P. [Additional note, BS5500:1994 Amendment No. 1 now considers the bending stress to be secondary f_G]

(3) In the case of thermal stresses averaged through the cross section of the ligament these would be considered to be secondary stresses f_G as would thermal stresses averaged through the ligament width but linear gradient through the thickness of the plate or shell.

(4) Any non-linear thermal stresses would be considered as peak stresses f_P. This includes any thermal stresses due to a thermal shock (thermal "skin effect") on the surface of the plate or shell.

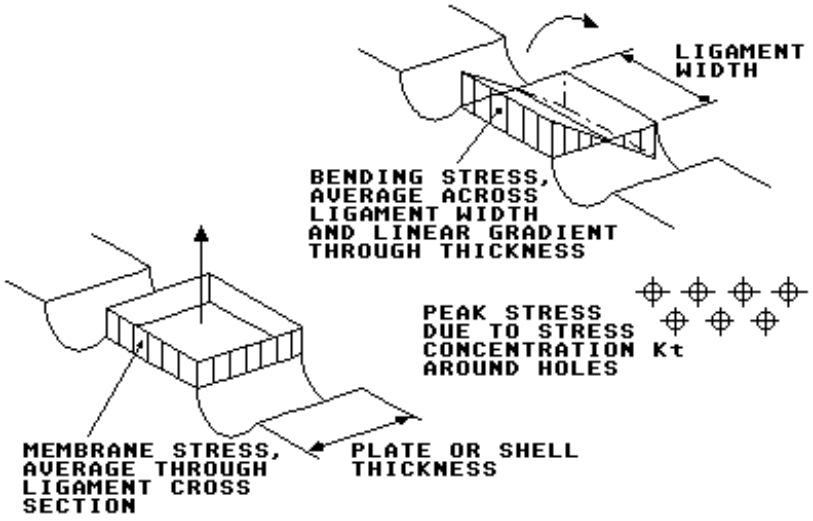

FIGURE 4.10 Stresses in the ligament of a tubesheet

4.5 STRESS LIMITS

The code puts stress limits on each of the five stress categories. Categories (1) to (4) have limits based on the material *design strength value f* (Sm in ASME VIII) as follows:

(1) General primary membrane stress category, $f_M <= f$
(2) Local primary membrane stress category, $f_L <= 1.5f$
(3) Primary membrane plus primary bending stress category, f_B, $f_M + f_B$ or $f_L + f_B <= 1.5f$
(4) Primary plus secondary stress category, $f_M + f_B + f_G$ or $f_L + f_B + f_G <= 3f$

For the peak stress category the fatigue analysis has limits governed by the *design fatigue curve*, discussed later.

Assessment of stresses

The design strength value *f* is obtained from tables in the code (table 2.3 in BS5500) and is material and temperature dependent. In some cases the strength is also dependent upon the material thickness. For materials that are suitable for operation in the creep range the strength is also dependent upon time.

For carbon, carbon manganese and low alloy steels the basic requirement is to limit the design strength value to the lesser of: $^2/_3$ of yield strength or tensile strength/2.35 (tensile strength/3 for ASME VIII division 2). For austenitic stainless steels the factors of safety are different and in the case of ASME VIII division 2 could in some cases allow the design strength value to be as high as 90% of yield strength at temperature. The reason for this is that these stainless steels have high strain hardening properties which after a few stress cycles will tend to increase the yield strength. Working so close to the yield strength does mean that deformations are increased and it may be necessary to use lower stress limits in some cases due to functioning requirements, e.g. bolted gasketed flanges may leak if the flange is not stiff enough.

It is important *not* to use values greater than that quoted in the code tables as the design strength value is one of the fundamental parameters controlling the safety of the vessel. For example, if the basic design strength value is put at $^2/_3$ times the material yield strength Sy then the limits on the stress categories can be summarised:

(1) $f_M <= 2*Sy/3$

(2) $f_L <= Sy$

(3) $f_B, f_M + f_B$ or $f_L + f_B <= Sy$

(4) $f_M + f_B + f_G$ or $f_L + f_B + f_G <= 2*Sy$

Meeting the first three stress categories should ensure that no gross yielding of the structure will occur under mechanical loading. Meeting category (4) will mean that some yielding and hence plastic deformation is expected. However, provided that the range of stress under mechanical and thermal loading is less than twice the yield strength, after a few load cycles the structure should shakedown to elastic cycling between +Sy and -Sy. If category (4) limit is not satisfied then plastic cycling would occur and rapid failure by fatigue could be expected. If the loading was even more severe then incremental collapse could also occur.

Only certain materials are suitable for the manufacture of a pressure vessel. References (40), (41) and (51) discuss many aspects of the material selection and welding of pressure vessels and boilers. The use of a wrong material can be catastrophic. Where design strength values are not given then the material is generally not suitable or not normally used at higher temperatures. It is essential to read and take account of any notes associated with the materials in table 2.3 of BS5500. These notes have important information relating to stress analysis and the use and limitations of certain materials.

The derivation of the design strength values is given in appendix K of BS5500. The strength is based on material properties obtained from tensile tests, i.e. tensile strength, yield strength and stress to rupture together with applied "Factors of Safety". In some cases past experience governs rather than strict adherence to a set of rules.

It is often the case that client will specify materials that are not British Standard materials. The code writing committee recognise this and have provided enquiry cases giving design strengths for several acceptable ASTM and other materials. In other cases BS5500 clauses 2.1.2 and 2.3.2 have requirements to be complied with, before a material can be considered acceptable for use in the manufacture of a pressure boundary part. The amount of information required to enable a full range of design strengths to be derived using BS5500 appendix K rules can be significant. This is best seen by an example.

With reference to TABLE 4.1. This table shows how the design strength is derived for a typical ferritic steel using appendix K rules for a material with specified elevated temperature values. The following information is required: the minimum tensile strength at room temperature R_M, the minimum yield strength at room temperature R_E, the minimum proof stress at temperature $R_{E(T)}$, and the mean stress to rupture at time *t*, S_{Rt}.

Inspection of TABLE 4.1 shows that the design strength is controlled by different material properties dependent upon the temperature, refer to the underlined values. In this particular example at temperatures up to 50°C the strength is controlled by the minimum tensile strength at room temperature. At temperatures of 150°C and up to 410°C the strength is controlled by the 0.2% proof stress at temperature. Beyond 410°C the strength is controlled by the mean stress to rupture.

Temp.°C	50	100	150	200	300	400	410	420	430	440	450	460	470
R_M N/mm^2	450												
R_M /2.35	191		191	191	191	191	191	191	191	191	191	191	191
R_E	300												
R_E /1.5	200												
$R_{E(T)}$	300		250	230	195	170	168	166	164	162	160	157	153
$R_{E(T)}$ /1.5	200		167	153	130	113	112	111	109	108	107	105	102
f_E	191	179+	167	153	130	113	112	111	109	108	107	105	102
S_{Rt} for 100000HRS						180	156	135	115	100	80	70	60
S_{Rt} /1.3						138	120	104	88	77	61	54	46
f_F						138	120	104	88	77	61	54	46
f	191	179	167	153	130	113	112	104	88	77	61	54	46

+ values of f_E between 50 and 150°C obtained by linear interpolation

TABLE 4.1 Design strength values, f for a typical ferritic steel
(not to be used for design purposes use the code tables)

The value of design strength to be used in the stress analysis is to be based on the *highest* metal temperature of the point under consideration, except in the case of primary plus secondary stress category if the secondary stress is due only to a temperature transient. In such a case the design strength is based on the average value of f for the highest and lowest temperature of the metal during the temperature cycle. If part or all of the secondary stress is due to mechanical loads then the design strength must be based on the highest metal temperature. Note that ASME SECTION VIII division 2 has similar rules but will allow the average value of design strength to be used regardless of whether the secondary stress is due to mechanical loads or thermal transient.

Design Fatigue Curves. The peak stress category $f_M + f_B + f_G + f_P$ or $f_L + f_B + f_G + f_P$ is limited by fatigue considerations. FIGURE 4.11 shows a typical design fatigue curve. The equation of the curve has the form given in equation (4.4). The curve has a *fatigue limit* at a specified number of cycles when the stress amplitude is so low that the life can be considered as infinite.

$$N*S_A^{\,m} = A \qquad (4.4)$$

where N is the number of cycles to failure
S_A is the allowable stress amplitude (half the stress range)
m is the exponent index
A is a constant

The BS5500 figure C.2.1 has values of m = 3.5 and A = $1.1\text{x}10^{12}$ the fatigue limit is approximately 34 N/mm^2 at $5\text{x}10^6$ cycles.

Therefore the *allowable* number of cycles for a given stress amplitude S becomes equation (4.5).

$$\text{allowable, } N = 1.1\text{x}10^{12}/S^{3.5} \qquad (4.5)$$

The curve is plotted on a log - log scale and there are factors of safety included in the curve. The curve has a safety factor of about 15 on life and 2.2 on stress. The corresponding values for ASME SECTION VIII division 2 fatigue curves are 20 on life and 2 on stress. It is necessary to have these safety factors as there is considerable scatter in the test data used to construct the curve. The BS5500 curve is based on test specimens containing flush ground butt welds and this is one of the reasons why the BS5500 curve is lower than the ASME curve.

The curve has a specified Young's modulus. The reason for this is because the curve is derived from *strain controlled* test data and is simply converted to units of stress by multiplying the strain range by Young's modulus at ambient temperature and dividing by 2, refer to equation (4.6).

$$S = \text{strain range}*E/2 \qquad (4.6)$$

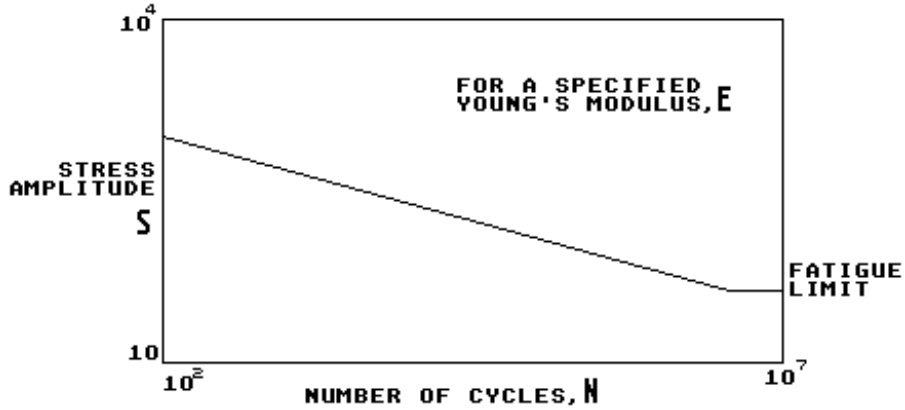

FIGURE 4.11 A typical design fatigue curve

At high strain ranges the stresses are pseudo-elastic stresses, but provided the structure will shakedown it is permissible to use elastic stresses to predict the fatigue life from the curve.

The values of Young's modulus tend to reduce at higher temperatures. This would have the effect of *lowering* the curve and results in reduced life for a given stress amplitude or alternatively a reduced allowable stress amplitude for a given life.

In practice the curve is not usually lowered but the alternating stress intensity, obtained from a stress analysis, is corrected by increasing the amplitude by the ratio of the Young's modulus used to construct the curve divided by the actual Young's modulus at temperature, equation (4.7). Note that in BS5500 appendix C the design fatigue curve is applicable for steels and aluminium alloys for temperatures up to and including 375 and 100°C respectively. The curve is plotted for *steel* at room temperature, E = 206000 N/mm^2, but the curve is also used for aluminium alloys. The correction to the alternating stress intensity must be made for the lower Young's modulus for these aluminium alloys before applying the figure C.2.1 curve.

$$S_{ALT}(\text{corrected}) = S_{ALT} * E_C / E_A \qquad (4.7)$$

where S_{ALT} is the alternating stress intensity, i.e. half the stress range.
E_C is the value of Young's modulus used to plot the design fatigue curve.
E_A is the actual value of Young's modulus.

The alternating stress intensity is half the stress range therefore equation (4.7) can be simply written as equation (4.8).

$$S_{ALT} = 0.5 * f_R * E_C / E_A \qquad (4.8)$$

where f_R is the total stress range of the peak stress category, ($f_M + f_B + f_G + f_P$) or ($f_L + f_B + f_G + f_P$).

Equation (4.8) can be substituted in (4.5) to give the *allowable* number of cycles for a given total stress range obtained from a stress analysis f_R , equation (4.9).

$$\text{allowable } N = 1.1 \times 10^{12} / (0.5 * f_R * E_C / E_A)^{3.5} \qquad (4.9)$$

Alternatively re-arranging equation (4.9) gives the *allowable* range of stress intensity for a given number of cycles N, equation (4.10).

$$\text{allowable } f_R = \{1.1 \times 10^{12} / [(0.5 * E_C / E_A)^{3.5} N]\}^{1/3.5} \qquad (4.10)$$

4.5.1 Special Stress Limits

(1) *Buckling*. The five stress categories discussed in section 4.1 will *not* predict failure by buckling. In cases where significant compression stresses are present, BS5500 clause A.3.5 puts a limit on the longitudinal compressive general membrane stress. The most obvious cases of buckling occur in vessels subjected to external pressure. However it is possible for local hoop compression stresses to occur under internal pressure. Example 3.5 shows that hoop compression stresses are present in the spherical end cap near the junction with the cylinder. It is known that buckling can occur in torispherical ends when subjected to internal pressure. GALLETLY discusses this aspect in detail in reference (17).

Finite Element programs are also available to predict elastic buckling (ROSS ref. 18), but for elastic-plastic buckling a more sophisticated program such as BOSOR5 (ref. 19) is required.

(2) *Pure Shear Stress and Bearing Stress*. In cases of protruding ledges, bearing areas etc., it is usual to apply special stress limits. BS5500 criteria for limited application has limits specified in clause A.3.3.3.

(3) *Bolting*. Special study is required when analysing bolt service stresses. Special design strength values, stress limits and design fatigue curves apply to bolting, refer to BS5500 table 3.8.1.4 and clause C.3. Note that bolts are not normally welded. The calculation of the actual service stresses in bolts requires consideration of the assembly preload, pressure, applied external forces and moments and differential thermal expansion. The stiffness of the bolts, the gasket and the connected members all have an important influence on the evaluation of the service stresses.

(4) *Wind and Earthquake Loads*. A 20% increase in the stress limits (except limits on compressive stresses) is allowed when wind and earthquake loads are considered. These loads need not be considered to act simultaneously. ASME SECTION VIII division 2, table AD-150.1 also allows a 20% increase in the stress limits when considering wave action on ocean going ships, etc.

(5) *Simplified Elastic-Plastic Analysis*. In cases where the limit on primary plus secondary stress category is exceeded the ASME SECTION VIII division 2 code has rules for a simplified elastic-plastic analysis in subparagraph 4-136.7. These rules may allow a justification to be made in cases where the limit is satisfied when the thermal bending stresses (due to axial and through thickness thermal gradients) are excluded.

(6) *Thermal Stress Ratchet*. In cases where shakedown cannot be shown to occur it is possible for a structure to fail by *incremental collapse* due to ratcheting. The phenomenon results from the combination of a steady sustained load and a cyclic thermal load. The deformations increase each cycle and are particularly serious for items such as nonintegral connections (screwed plugs, breach lock and shear ring closures, etc.) which could disengage if the deformations become too large. ASME SECTION VIII division 2, subparagraphs 5-130 and 5-140 have rules for limiting the ratcheting in shells and nonintegral connections. MILLER provides a discussion on thermal ratcheting in reference (43).

(7) *Creep*. As the temperature increases there comes a point where the deformations of a loaded structure become dependent upon stress, temperature and time. For British Standard pressure vessel materials the point at which the design strength becomes governed by creep considerations is given by the *italic* values in table 2.3 of BS5500.

If the structure is subjected to a load controlled stress, it will continue to deform (creep) over a period of time until the material fails by stress rupture or the structure becomes unstable by buckling.

Alternatively if the structure is subjected to a strain controlled stress, the stress will reduce (*stress relaxation*) over a period of time until the structure may no longer function correctly or if it is a bolted flange, leakage may become excessive unless it is seal welded.

The detailed stress analysis and assessment of a structure operating the creep range is a time consuming exercise and is particularly difficult when conditions of fatigue or buckling are present. The ASME code case N-47 (ref. 44) and the Nuclear Electric R5 procedure (ref. 46) are currently the most comprehensive set of rules for the assessment of vessels operating in the creep range. The background to the ASME N-47 rules is discussed in reference (45). But note that there have been detailed changes and additions to the rules since reference (45) was written.

(8) *Test Conditions*. BS5500 clause 5.8.5.2 puts a limit on the general membrane stress of 90% of the minimum specified yield or proof stress. ASME SECTION VIII division 2 has additional limits specified in subparagraph AD-151.

(9) *Fracture Assessment*. The stress assessment discussed above relate to defect free structures. All structures contain defects especially welded structures. Defects that are outside the defect acceptance levels specified by the applicable code require to be repaired or assessed to a recognised procedure.

BS5500 appendix U recommends the use of BSI published document PD6493 (ref. 47). The 1991 edition now incorporates the CEGB two criteria, R6 method (ref. 48) failure assessment diagrams.

Other acceptable methods in use are ASME SECTION XI (ref. 49 and 50) and for elevated temperatures the R5 procedure (ref. 46) is the most comprehensive available. It is not intended to consider any of these procedures in this text as they require specialist study. Note that regardless of which procedure is used, it is essential to have a stress analysis carried out and it is necessary to consider the effects of residual stresses at welded joints.

4.6 ASSESSMENT EXAMPLE

In this section an example will be worked through in detail using "AJAP1" to calculate the stresses and BS5500 appendix A for the stress assessment. The example chosen is the cylinder with a flat end closure as shown in Example 3.5, FIGURE 3.21(c).

The input data set and results for internal pressure are given in FIGURE 3.21(f) and (g). The assessment will cover the following three cases: (1) Design Condition, (2) Operating Condition and (3) Fatigue Life.

4.6.1 Design Condition

The design internal pressure is 0.5 N/mm^{2}g and the design temperature is 200°C. The material is a carbon steel with a design strength value f = 150 N/mm^2 at 200°C.

To assess the design condition it is necessary to show that the primary stress intensities are acceptable by satisfying the following stress categories.

General primary membrane stress category, f_M <= f
Local primary membrane stress category, f_L <= 1.5f
Primary membrane plus primary bending stress category, $f_M + f_B$ or $f_L + f_B$ <= 1.5f

For the cylinder flat end closure we need to consider the stresses in at least four sections as shown in FIGURE 4.12.

(1) General primary membrane stress intensity f_M at section A - A

(2) Local primary membrane stress intensity f_L at section B - B in the cylinder at (or near) to the junction.

(3) Local primary membrane stress f_L at the junction in the flat end section C - C.

(4) Primary membrane f_M or f_L and primary membrane plus primary bending stress $f_M + f_B$ or $f_L + f_B$ at the centre of the flat end section C - C.

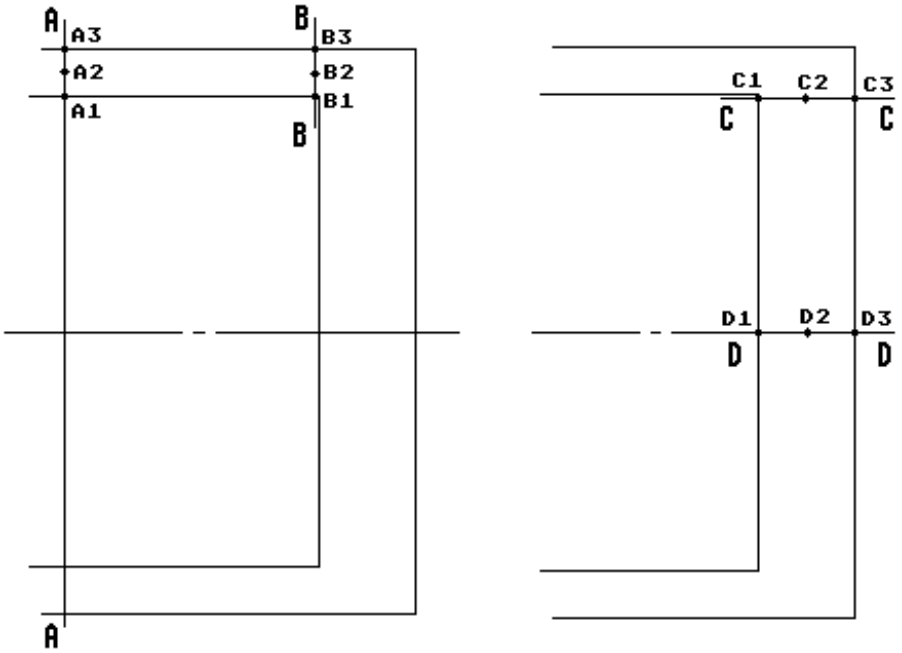

FIGURE 4.12 Sections considered in the assessment

Section A - A, point A2 on the mean radius. The purpose of this assessment is to check the general primary membrane stress intensity f_M *remote* from the junction discontinuity. Note that the bending stress across the thickness of a thin shell due to pressure is small and is usually neglected. The section is taken across the *full* section and the average stresses across the thickness obtained. In this case the geometry and loading are axisymmetric therefore it does not matter where the section orientation, in the circumferential direction, is taken. If there had been a moment applied across the full section (as shown in FIGURE 4.5(a)) it would have been necessary to take account of the circumferential position of the section to obtain the highest stresses.

The six component stresses due to internal pressure can be calculated by hand from simple theory or by running "AJAP1".

f_X = hoop membrane stress = SH = P*R/T = 0.5*500/15 = 16.67 N/mm^2
Note that in some text the inside radius is used.

f_Y = average transverse normal stress through the thickness. For thin shells this is half the pressure difference across the thickness as shown in FIGURE 4.13. In some text this stress is ignored.
= -P/2 = -0.5/2 = -0.25 N/mm^2 (note that P is always substituted with a positive sign in this expression).

f_Z = meridional membrane stress = SL = SH/2 = 8.33 N/mm^2

$f_{XZ} = f_{YX} = f_{ZY}$ = SV = zero (since the loading and geometry are axisymmetric and the section is remote from any discontinuity)

Therefore the three principal stresses can be written:

$$f_1 = f_X = 16.67 \text{ N/mm}^2$$

$$f_2 = f_Y = -0.25 \text{ N/mm}^2$$

$$f_3 = f_Z = 8.33 \text{ N/mm}^2$$

Note that in some text the principal stresses are put in the order $f_1 > f_2 > f_3$ in such a case f_1 = 16.67, f_2 = 8.33 and f_3 = -0.25 N/mm^2, the largest stress difference would then be $f_1 - f_3$.

The three stress differences (equation 4.1) are:

$$f_{12} = 16.67 - (-0.25) = 16.92 \text{ N/mm}^2$$

$$f_{23} = -0.25 - 8.33 = -8.58 \text{ N/mm}^2$$

$$f_{31} = 8.33 - 16.67 = -8.34 \text{ N/mm}^2$$

The stress intensity is largest absolute stress difference, in this case = f_{12} = 16.92 N/mm^2. The allowable stress limit is f =150 N/mm^2 therefore section A - A point A2 is satisfactory.

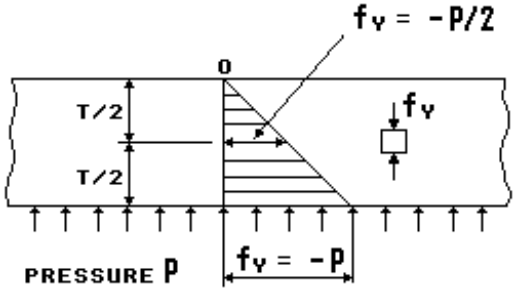

FIGURE 4.13 Distribution of the transverse normal stress across the thickness of a thin shell or plate due to pressure

Section B - B, point B2 on the mean radius. The purpose of this assessment is to check the local primary membrane stress intensity f_L at the junction discontinuity. Section B - B has the same thickness and loading as section A - A and will pass the general primary membrane limit, but since the section is at the junction with the flat end we can expect discontinuity stresses to be present at the junction in addition to the general membrane stresses. The stresses are found direct from "AJAP1". The results (for component 1 at X = 0) are given in FIGURE 3.21(g): SV= -10.7, SL= 8.33 and SH= -15.01 N/mm^2.

Assessment example

The six component stresses are:

$$f_X = SH = -15.01 \text{ N/mm}^2$$

$$f_Y = -P/2 = -0.25 \text{ N/mm}^2$$

$$f_Z = SL = 8.33 \text{ N/mm}^2$$

f_{ZY} = maximum shear stress, assuming a parabolic shear distribution, refer to FIGURE 1.16
= 1.5*SV = 1.5*(-10.7) = -16.05 N/mm^2

$f_{YX} = f_{XZ} = 0$

The three principal stresses become:

$$f_1 = f_X = -15.01 \text{ N/mm}^2 \text{ (hoop stress)}$$

The other principal stresses are calculated from the well known MOHR's circle equations (4.3):

$$f_2 = 0.5[f_Y + f_Z + \{(f_Y - f_Z)^2 + 4* f_{ZY}^2\}^{1/2}] = 20.65 \text{ N/mm}^2$$

$$f_3 = 0.5[f_Y + f_Z - \{(f_Y - f_Z)^2 + 4* f_{ZY}^2\}^{1/2}] = -12.57 \text{ N/mm}^2$$

The stress differences (equation 4.1) are:

$$f_{12} = -15.01 - 20.65 = -35.66 \text{ N/mm}^2$$

$$f_{23} = 20.65 - (-12.57) = 33.22 \text{ N/mm}^2$$

$$f_{31} = -12.57 - (-15.02) = 2.45 \text{ N/mm}^2$$

The stress intensity is 35.66 N/mm^2. The allowable stress limit is 1.5*f = 225 N/mm^2. Therefore section B - B point B2 at the junction is satisfactory.

It is tempting to consider the local primary membrane stress as having been satisfied. However, a plot of the hoop stress along the cylinder FIGURE 3.21(i) shows that the hoop stress is a maximum at 40mm from the junction. An assessment is therefore required at this position. The "AJAP1" results for X = 40mm are given in FIGURE 3.21(g).

The six component stresses are:

$$f_X = SH = -37.13 \text{ N/mm}^2$$

$$f_Y = -P/2 = -0.25 \text{ N/mm}^2$$

$$f_Z = SL = 8.33 \text{ N/mm}^2$$

f_{ZY} = maximum shear stress, assuming a parabolic shear distribution, refer to FIGURE 1.16
= 1.5*SV = 1.5*(-6.88) = -10.32 N/mm^2

$f_{YX} = f_{XZ} = 0$

The three principal stresses become:

$$f_1 = f_X = -37.13 \text{ N/mm}^2 \text{ (hoop stress)}$$

$$f_2 = 0.5[f_Y + f_Z + \{(f_Y - f_Z)^2 + 4* f_{ZY}^2\}^{1/2}] = 15.21 \text{ N/mm}^2$$

$$f_3 = 0.5[f_Y + f_Z - \{(f_Y - f_Z)^2 + 4* f_{ZY}^2\}^{1/2}] = -7.13 \text{ N/mm}^2$$

and the stress differences (equation 4.1) are:

$$f_{12} = -37.13 - 15.21 = -52.34 \text{ N/mm}^2$$

$$f_{23} = 15.21 - (-7.13) = 22.34 \text{ N/mm}^2$$

$$f_{31} = -7.13 - (-37.13) = 30.0 \text{ N/mm}^2$$

The stress intensity is 52.34 N/mm^2. The allowable stress limit is 1.5*f = 225 N/mm^2. Therefore section B - B point B2 is satisfactory.

Section C - C, point C2. The purpose of this assessment is to check the local primary membrane stress intensity at the junction discontinuity.

Only the membrane stress is checked as the bending stress is considered to be secondary except in a particular case as follows. ASME Section VIII division 2 requires the bending stress at the junction to be primary if the bending moment has been used to reduce the stress at the centre of the flat end to acceptable limits. BS5500 makes no such restriction so the bending stress will be considered as secondary at the junction. From FIGURE 3.21(g) for component 2 at radius X = 500mm, the six component stresses are:

$$f_X = SH = 5.35 \text{ N/mm}^2$$

$$f_Y = -P/2 = -0.25 \text{ N/mm}^2$$

$$f_Z = SL = 5.35 \text{ N/mm}^2$$

$$f_{ZY} = 1.5*SV = 1.5*(-4.17) = -6.25 \text{ N/mm}^2$$

$$f_{YX} = f_{XZ} = 0$$

The principal stresses become:

$$f_1 = f_X = 5.35 \text{ N/mm}^2$$

$$f_2 = 0.5[f_Y + f_Z + \{(f_Y - f_Z)^2 + 4* f_{ZY}^2\}^{1/2}] = 9.4 \text{ N/mm}^2$$

$$f_3 = 0.5[f_Y + f_Z - \{(f_Y - f_Z)^2 + 4* f_{ZY}^2\}^{1/2}] = -4.3 \text{ N/mm}^2$$

The stress differences are:

$$f_{12} = 5.35 – 9.4 = -4.05 \text{ N/mm}^2$$

$$f_{23} = 9.4 - (-4.3) = 13.7 \text{ N/mm}^2$$

$$f_{31} = -4.33 - 5.35 = -9.65 \text{ N/mm}^2$$

The stress intensity is 13.7 N/mm^2. The allowable stress limit is 1.5*f = 225 N/mm^2. Therefore section C - C point C2 is satisfactory.

Section D - D, at the centre of the flat end. The assessment of points D1, D2 and D3 will illustrate several aspects and difficulties of the assessment procedure that are not at all clear from a straight reading of the code rules.

Point D2 at the mid thickness of the flat end. The purpose of this assessment is to check the primary membrane stress intensity f_M or f_L at the centre region of the flat end. The stresses direct from "AJAP1" (for component 2 at radius X = 0) are shown in FIGURE 3.21(g). The results show that there are membrane stresses SL= 5.35 and SH= 5.35 N/mm^2. These stresses are a result of the shear force due to the discontinuity loads at the junction with the cylinder, i.e. Vj2/T = 160.5591/30 = 5.35 N/mm^2. These membrane stresses apply over the *whole* end plate so it is appropriate to consider these as local primary membrane stresses rather than secondary stresses.

Assessment example

The six component stresses are:

$$f_X = SH = 5.35 \text{ N/mm}^2$$

$$f_Y = -P/2 = -0.25 \text{ N/mm}^2$$

$$f_Z = SL = 5.35 \text{ N/mm}^2$$

$$f_{ZY} = SV = 0$$

$$f_{YX} = f_{XZ} = 0$$

as all the shear stresses are zero the three principal stresses are:

$$f_1 = f_X = 5.35 \text{ N/mm}^2$$

$$f_2 = f_Y = -0.25 \text{ N/mm}^2$$

$$f_3 = f_Z = 5.35 \text{ N/mm}^2$$

and the stress differences (equation 4.1) are:

$$f_{12} = 5.35 - (-0.25) = 5.6 \text{ N/mm}^2$$

$$f_{23} = -0.25 - 5.35 = -5.6 \text{ N/mm}^2$$

$$f_{31} = 5.35 - 5.35 = 0 \text{ N/mm}^2$$

Therefore the stress intensity is 5.6 N/mm^2. The allowable stress limit is 1.5f = 225 N/mm^2. Therefore point D2 is satisfactory.

The general membrane stress intensity in the flat end is that due to f_Y = -P/2 = -0.25 N/mm^2 only, and easily satisfies the stress limit of f = 150 N/mm^2. Had the pressure been *external* there would have been an additional general membrane stresses f_X = SH= -P and f_Z = SL= -P across the whole plate to be considered.

Section D - D, points D1 and D3 on the plate surface. The purpose of this assessment is to check the primary membrane plus primary bending stress intensity $f_M + f_B$ at the centre of the flat end. Like the previous result the assessment is not as straight forward as it first appears. The results obtained direct from "AJAP1" (component 2 at radius X = 0) given in FIGURE 3.21(g), are actually the combination of primary plus secondary stresses, i.e. $f_L + f_B + f_G$ stresses. The term f_L is the local primary membrane stress discussed above and the f_G stress is the secondary bending stress at the centre of the end due to the discontinuity moment Mj2 at the outside edge of the plate.

If it is required that the bending stresses, due to the discontinuity moment at the junction, are to be considered as secondary we must check the centre of the flat end for $f_M + f_B$ stresses only. The only safe way is to proceed as follows.

"AJAP1" is run for the case of a flat plate, *simply supported* at the outside edge, and subjected to a design pressure of 0.5 N/mm^2. The results are shown in FIGURE 4.14.

There are no hoop or meridional membrane stresses in the plate. The highest stresses are the hoop and meridional bending stresses at the centre of the plate. These stresses are primary bending stresses.

For point D1 at the *left* surface, the six stress components are:

$$f_X = SHl = -171.87 \text{ N/mm}^2$$

f_Y = the normal stress acting on the left (inside) surface = -P = -0.5 N/mm^2

$$f_Z = SLl = -171.87 \text{ N/mm}^2$$

All three shear stresses are assumed zero on the surface.

```
INPUT DATA, PROGRAM AJAP1

FLAT END ONLY
Internal Design Pressure
FLAT PLATE, support at O.D.
Ro= 500 mm
Ri= 0 mm
T= 30 mm
E= 200000 N/mm2
PR= .3
D= 4.945055E+08 Nmm
P= .5 N/mm2

RESULTS COMPONENT No. 1
FLAT END ONLY
Internal Design Pressure
radius X= 500 mm
YL= -2.384186E-07 mm
Y= 0 mm
THETA= 1.215278E-02 radians
V= -125 N/mm
N1= 0 N/mm
N2= 0 N/mm
M1= 0 Nmm/mm
M2= 10937.5 Nmm/mm
STRESSES N/mm2
SV= -4.166667
SL= 0
SH= 0
SBL=+or-  0
SBH=+or-  72.91666
SLl= 0
SLr= 0
SHl= -72.91666
SHr= 72.91666

RESULTS COMPONENT No. 1
FLAT END ONLY
Internal Design Pressure
radius X= 0 mm
YL= 4.025608 mm
Y= 0 mm
THETA= 0 radians
V= 0 N/mm
N1= 0 N/mm
N2= 0 N/mm
M1= 25781.25 Nmm/mm
M2= 25781.25 Nmm/mm
STRESSES N/mm2
SV= 0
SL= 0
SH= 0
SBL=+or-  171.875
SBH=+or-  171.875
SLl= -171.875
SLr= 171.875
SHl= -171.875
SHr= 171.875
```

FIGURE 4.14 Input data set and results for a simply supported flat plate subjected to a uniform pressure across the thickness

The principal stresses become:

$$f_1 = f_X = -171.87 \text{ N/mm}^2$$

$$f_2 = f_Y = -0.5 \text{ N/mm}^2$$

$$f_3 = f_Z = -171.87 \text{ N/mm}^2$$

The stress differences become:

$$f_{12} = -171.87 - (-0.5) = -171.37 \text{ N/mm}^2$$

$$f_{23} = -0.5 - (-171.87) = -171.37 \text{ N/mm}^2$$

$$f_{31} = -171.87 - (-171.87) = 0 \text{ N/mm}^2$$

The stress intensity is 171.37 N/mm^2. The allowable stress limit is $1.5*f$ = 225 N/mm^2. Therefore section D - D, point D1 is satisfactory.

Assessment example

For point D3 at the *right* surface, the six stress components are:

f_X = SHr = 171.87 N/mm^2

f_Y = 0 (no pressure on the right (outside) surface)

f_Z = SLr = 171.87 N/mm^2

All three shear stresses are assumed zero on the surface.

The principal stresses become:

$f_1 = f_X$ = 171.87 N/mm^2

$f_2 = f_Y$ = 0 N/mm^2

$f_3 = f_Z$ = 171.87 N/mm^2

The stress differences become:

f_{12} = 171.87 - 0 = 171.87 N/mm^2

f_{23} = 0 - 171.87 = -171.87 N/mm^2

f_{31} = 171.87 - 171.87 = 0 N/mm^2

The stress intensity is 171.87 N/mm^2. The allowable stress limit is 1.5**f* = 225 N/mm^2. Therefore section D - D point D3 is satisfactory.

Therefore it is concluded that this flat end has sufficient strength so that the discontinuity moment at the edge is *not* required to maintain the bending stress at the centre within limits.

4.6.2 Operating Condition

To assess the operating condition we must show that primary membrane plus primary bending plus secondary stress range is less than 3**f*. The design strength *f* is based on the highest operating temperature as the secondary stress f_G is due to a mechanical load. For an operating temperature of 200°C, *f* = 150 N/mm^2. Therefore the stress limit to be satisfied is 3**f* = 450 N/mm^2.

The operating pressure cycle is shown diagrammatically in FIGURE 4.15, i.e. zero to a maximum pressure of 0.475 N/mm^{2}g and back to zero with a full vacuum during the cooldown from an operating temperature of 200°C.

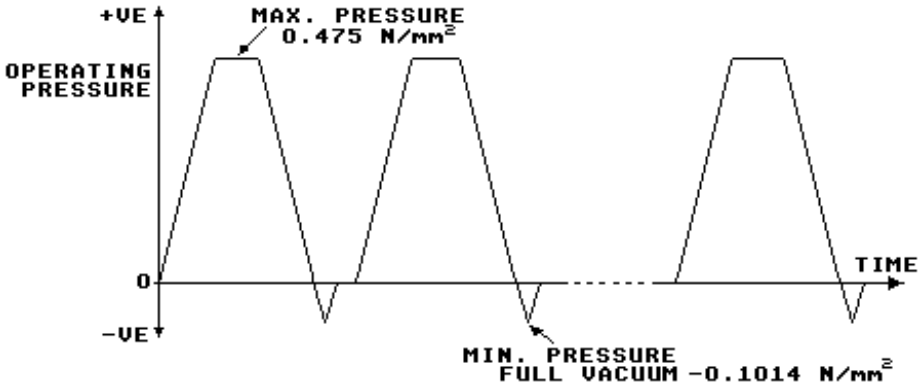

FIGURE 4.15 Operating pressure cycles for the assessment example

The stress range will be governed by the extreme range of the operating pressures, i.e. the full pressure range of 0.475 - (-0.1014) = 0.5764 N/mm^2 must be considered. The "AJAP1" results for the extreme operating pressures are shown in FIGURES 4.16 and 4.17 respectively.

From the results for design pressure given previously in Example 3.5, the plots of the maximum stresses, FIGURES 3.21(h), (j) and (k), show that the overall highest stress occurs at the inside surface of the cylinder at the junction with the end. Therefore section B - B point B1 will be checked first.

The method of calculating the stress intensity range will be based on the general assumption that the principal stress direction changes during the stress cycle. The method used is that described in ASME SECTION VIII, division 2, subparagraph 5-110.3. This method is known to give consistent results in cases where the direction of the principal stresses do not change (ref. 52).

INPUT DATA, PROGRAM AJAP1

CYLINDER WITH FLAT END CLOSURE
Operating Pressure

COMPONENT No. 1
CYLINDER, JUNCTION AT RIGHT END
R= 500 mm
T= 15 mm
E= 200000 N/mm2
PR= .3
BETA= .0148426 /mm
D= 6.181319E+07 Nmm
P= .475 N/mm2
Fp= 118.75 N/mm
Fo= 118.75 N/mm

COMPONENT No. 2
FLAT PLATE, JUNCTION AT O.D.
JUNCTION POSITION, LEFT SURFACE
JP= -1
OFFSET= -15 mm
Ro= 500 mm
Ri= 0 mm
T= 30 mm
E= 200000 N/mm2
PR= .3
D= 4.945055E+08 Nmm
P= .475 N/mm2

RESULTS COMPONENT No. 1
CYLINDER WITH FLAT END CLOSURE
Operating Pressure
X= 0 mm
Y= -4.160318E-02 mm
THETA= 3.366718E-03 radians
V= -152.531 N/mm
N1= 118.75 N/mm
N2= -213.9941 N/mm
M1= 8227.141 Nmm/mm
M2= 2468.142 Nmm/mm
STRESSES N/mm2
SV= -10.16873
SL= 7.916667
SH= -14.26627
SBL=+or- 219.3904
SBH=+or- 65.81713
SLo= -211.4738
SLi= 227.3071
SHo= -80.0834
SHi= 51.55085

RESULTS COMPONENT No. 2
CYLINDER WITH FLAT END CLOSURE
Operating Pressure
radius X= 500 mm
YL= -1.788139E-07 mm
Y= 8.897627E-03 mm
THETA= 3.36672E-03 radians
V= -118.75 N/mm
N1= 152.5308 N/mm
N2= 152.5308 N/mm
M1= -10515.11 Nmm/mm
M2= -124.4851 Nmm/mm
STRESSES N/mm2
SV= -3.958333
SL= 5.084359
SH= 5.084359
SBL=+or- 70.10073
SBH=+or- .8299008
SLi= 75.18509
SLr= -65.01638
SHi= 5.91426
SHr= 4.254458

RESULTS COMPONENT No. 2
CYLINDER WITH FLAT END CLOSURE
Operating Pressure
radius X= 0 mm
YL= 1.779723 mm
Y= 0 mm
THETA= 0 radians
V= 0 N/mm
N1= 152.5308 N/mm
N2= 152.5308 N/mm
M1= 13977.08 Nmm/mm
M2= 13977.08 Nmm/mm
STRESSES N/mm2
SV= 0
SL= 5.084359
SH= 5.084359
SBL=+or- 93.18052
SBH=+or- 93.18052
SLi= -88.09616
SLr= 98.26488
SHi= -88.09616
SHr= 98.26488

FIGURE 4.16 Results for the maximum operating pressure condition

INPUT DATA, PROGRAM AJAP1

CYLINDER WITH FLAT END CLOSURE
Vacuum

COMPONENT No. 1
CYLINDER, JUNCTION AT RIGHT END
R= 500 mm
T= 15 mm
E= 200000 N/mm2
PR= .3
BETA= .0148426 /mm
D= 6.181319E+07 Nmm
P= -.1014 N/mm2
Fp= -25.35 N/mm
Fo= -25.35 N/mm

COMPONENT No. 2
FLAT PLATE, JUNCTION AT O.D.
JUNCTION POSITION, LEFT SURFACE
JP= -1
OFFSET= -15 mm
Ro= 500 mm
Ri= 0 mm
T= 30 mm
E= 200000 N/mm2
PR= .3
D= 4.945055E+08 Nmm
P= -.1014 N/mm2
qo= .1014 N/mm2
qi= 0 N/mm2

RESULTS COMPONENT No. 1
CYLINDER WITH FLAT END CLOSURE
Vacuum
X= 0 mm
Y= 8.732902E-03 mm
THETA= -7.203594E-04 radians
V= 32.48652 N/mm
N1= -25.35 N/mm
N2= 44.79241 N/mm
M1= -1755.274 Nmm/mm
M2= -526.5823 Nmm/mm
STRESSES N/mm2
SV= 2.165768
SL= -1.69
SH= 2.986161
SBL=+or- 46.80732
SBH=+or- 14.0422
SLo= 45.11732
SLi= -48.49732
SHo= 17.02836
SHi= -11.05604

RESULTS COMPONENT No. 2
CYLINDER WITH FLAT END CLOSURE
Vacuum
radius X= 500 mm
YL= -1.490116E-08 mm
Y= -2.072495E-03 mm
THETA= -7.203599E-04 radians
V= 25.35 N/mm
N1= -35.52848 N/mm
N2= -35.52848 N/mm
M1= 2242.573 Nmm/mm
M2= 24.44806 Nmm/mm
STRESSES N/mm2
SV= .845
SL= -1.184283
SH= -1.184283
SBL=+or- 14.95049
SBH=+or- .1629871
SLl= -16.13477
SLr= 13.7662
SHl= -1.34727
SHr= -1.021296

RESULTS COMPONENT No. 2
CYLINDER WITH FLAT END CLOSURE
Vacuum
radius X= 0 mm
YL= -.3803374 mm
Y= 0 mm
THETA= 0 radians
V= 0 N/mm
N1= -35.52848 N/mm
N2= -35.52848 N/mm
M1= -2985.865 Nmm/mm
M2= -2985.865 Nmm/mm
STRESSES N/mm2
SV= 0
SL= -1.184283
SH= -1.184283
SBL=+or- 19.90576
SBH=+or- 19.90576
SLl= 18.72148
SLr= -21.09005
SHl= 18.72148
SHr= -21.09005

FIGURE 4.17 Results for vacuum condition

Section B - B, point B1 at the *inside* surface of component 1 at X = 0

For the extreme positive pressure of 0.475 N/mm^2 the membrane plus bending stresses from FIGURE 4.16 are:

f_X = SHi = 51.55 N/mm^2

f_Y = -P = -0.475 N/mm^2 (normal stress due to max. pressure on the inside surface)

f_Z = SLi = 227.3 N/mm^2

All shear stresses are assumed zero on the surface.

For the extreme negative pressure of -0.1014 N/mm^2 the membrane plus bending stresses from FIGURE 4.17 are:

f_X = SHi = -11.05 N/mm^2

f_Y = 0 (no normal stress on the inside surface due to vacuum)

f_Z = SLi = -48.49 N/mm^2

All shear stresses are assumed zero on the surface.

The stress *range* is obtained by choosing one of the extremes (say the vacuum condition) and subtracting algebraically the component stresses for the vacuum condition from the maximum operating pressure condition.

f_X = SHi = 51.55 - (-11.05) = 62.6 N/mm^2

f_Y = -0.475 - 0 = -0.475 N/mm^2

f_Z = SLi = 227.3 - (-48.49) = 275.79 N/mm^2

As there are no shear stresses on the surface the principal stresses become:

$f_1 = f_X$ = 62.6 N/mm^2

$f_2 = f_Y$ = -0.475 N/mm^2

$f_3 = f_Z$ = 275.79 N/mm^2

The stress differences are:

f_{12} = 62.6 - (-0.475) = 63.07 N/mm^2

f_{23} = -0.475 - 275.79 = -276.26 N/mm^2

f_{31} = 275.79 – 62.6 = 213.19 N/mm^2

The stress intensity range for point B1 is 276.26 N/mm^2. The limit is 3*f* = 450 N/mm^2 therefore satisfactory.

Section B - B, point B3 at the *outside* surface of component 1 at X = 0

For the extreme positive pressure of 0.475 N/mm^2 the membrane plus bending stresses from FIGURE 4.16 are:

f_X = SHo = -80.08 N/mm^2

f_Y = 0 (zero pressure on outside)

f_Z = SLo = -211.47 N/mm^2

All shear stresses are assumed zero on the surface.

Assessment example, Section B - B, point B3

For the extreme negative pressure of -0.1014 N/mm^2 the membrane plus bending stresses from FIGURE 4.17 are:

f_X = SHo = 17.02 N/mm^2

f_Y = -0.1014 (external pressure outside)

f_Z = SLo = 45.11 N/mm^2

All shear stresses are assumed zero on the surface.

The stress *range* is obtained by subtracting algebraically the component stresses for the vacuum condition from the maximum operating pressure condition.

f_X = SHo = -80.08 – 17.02 = -97.1 N/mm^2

f_Y = 0 - (-0.1014) = 0.1014 N/mm^2

f_Z = SLo = -211.47 – 45.11 = -256.58 N/mm^2

As there are no shear stresses on the surface the principal stresses become:

$f_1 = f_X$ = -97.1 N/mm^2

$f_2 = f_Y$ = 0.1014 N/mm^2

$f_3 = f_Z$ = -256.58 N/mm^2

Stress differences are:

f_{12} = -97.1 - 0.1014 = -97.2 N/mm^2

f_{23} = 0.1014 - (-256.58) = 256.68 N/mm^2

f_{31} = -256.58 - (-97.1) = -159.48 N/mm^2

The stress intensity range for point B3 is 256.68 N/mm^2. The limit is 3*f* = 450 N/mm^2, therefore satisfactory.

TABLE 4.1 summarises the above steps and for completeness includes the assessment for the surface stresses at sections C - C and D - D.

4.6.3 Fatigue Assessment

An estimate of the fatigue life of the cylinder to flat end junction will now be made using BS5500 appendix C rules. It is likely that these rules will be replaced by the alternative rules presented in BS5500 enquiry case 79 at some time in the future. If the reader finds that this change has taken place then the following section can be ignored. Appendix 1 shows an example of the use of the enquiry case 79 rules.

An estimate of the allowable number of cycles (fatigue life) can be made from a *design fatigue curve* such as FIGURE C.2.1 in BS5500. Section 4.5 discusses the use of this design fatigue curve and shows that for a single cycle type the allowable number of cycles is given by the equation (4.9).

$$\text{allowable N} = 1.1\text{x}10^{12}/(0.5*f_R*E_C/E_A)^{3.5}$$

where E_C is the value of Young's modulus for the curve = 206000 N/mm^2

E_A is the actual value of Young's modulus = 200000 N/mm^2

f_R is the total stress range of the peak stress category = ($f_M + f_B + f_G + f_P$) or ($f_L + f_B + f_G + f_P$).

The stress ranges for the operating condition have been obtained in section 4.6.2. Table 4.1 summarises the stress intensity range for the most critical points in the vessel. The worst primary plus secondary stress intensity range is at the junction, section B - B point B1, $f_L + f_B + f_G$ = 276.26 N/mm^2. This stress represents a full range cycle and since the shakedown limit is satisfied, elastic assumptions can be used in the fatigue assessment.

Section B - B point B1	max. operating	vacuum	stress range	principal stresses	stress differences	stress intensity	stress limit
f_X =	51.55	-11.05	62.6	f_1 = 62.6	f_{12} = 63.07		
f_Y =	-0.47	0.0	-0.47	f_2 = -0.47	f_{23} = -276.26	276.26	450
f_Z =	227.3	-48.49	275.79	f_3 = 275.79	f_{31} = 213.19		
f_{XZ} =	0.0	0.0	0.0				
f_{YX} =	0.0	0.0	0.0				
f_{ZY} =	0.0	0.0	0.0				

Section B - B point B3	max. operating	vacuum	stress range	principal stresses	stress differences	stress intensity	stress limit
f_X =	-80.08	17.02	-97.1	f_1 = -97.1	f_{12} = -97.2		
f_Y =	0.0	-0.10	0.10	f_2 = 0.10	f_{23} = 256.68	256.68	450
f_Z =	-211.47	45.11	-256.58	f_3 = -256.58	f_{31} = -159.48		
f_{XZ} =	0.0	0.0	0.0	[Corrected was f_{ZY}]			
f_{YX} =	0.0	0.0	0.0				
f_{ZY} =	0.0	0.0	0.0				

Section C - C point C1	max. operating	vacuum	stress range	principal stresses	stress differences	stress intensity	stress limit
f_X =	5.91	-1.34	7.25	f_1 = 7.25	f_{12} = 7.25		
f_Y =	-0.47	0.0	-0.47	f_2 = -0.47	f_{23} = -91.78	91.78	450
f_Z =	75.18	-16.13	91.31	f_3 = 91.31	f_{31} = 84.06		
f_{XZ} =	0.0	0.0	0.0				
f_{YX} =	0.0	0.0	0.0				
f_{ZY} =	0.0	0.0	0.0				

Section C - C point C3	max. operating	vacuum	stress range	principal stresses	stress differences	stress intensity	stress limit
f_X =	4.25	-1.02	5.27	f_1 = 5.27	f_{12} = 5.27		
f_Y =	0.0	-0.10	0.10	f_2 = 0.10	f_{23} = 78.87		
f_Z =	-65.01	13.76	-78.77	f_3 = -78.77	f_{31} = -84.04	84.04	450
f_{XZ} =	0.0	0.0	0.0	[Corrected was f_{ZY}]			
f_{YX} =	0.0	0.0	0.0				
f_{ZY} =	0.0	0.0	0.0				

Section D - D point D1	max. operating	vacuum	stress range	principal stresses	stress differences	stress intensity	stress limit
f_X =	-88.09	18.72	-106.81	f_1 = -106.81	f_{12} = -106.34	106.34	450
f_Y =	-0.47	0.0	-0.47	f_2 = -0.47	f_{23} = 106.34		
f_Z =	-88.09	18.72	-106.81	f_3 = -106.81	f_{31} = 0.0		
f_{XZ} =	0.0	0.0	0.0				
f_{YX} =	0.0	0.0	0.0				
f_{ZY} =	0.0	0.0	0.0				

Section D - D point D3	max. operating	vacuum	stress range	principal stresses	stress differences	stress intensity	stress limit
f_X =	98.26	-21.09	119.35	f_1 = 119.35	f_{12} = 119.25	119.25	450
f_Y =	0.0	-0.10	0.10	f_2 = 0.10	f_{23} = -119.25		
f_Z =	98.26	-21.09	119.35	f_3 = 119.35	f_{31} = 0.0		
f_{XZ} =	0.0	0.0	0.0	[Corrected was f_{ZY}]			
f_{YX} =	0.0	0.0	0.0				
f_{ZY} =	0.0	0.0	0.0				

TABLE 4.1 Summary of primary plus secondary stress assessment, N/mm^2

Assessment example

For a fatigue assessment it is essential to include the peak stress due to the local structural discontinuity at the junction. Therefore it is necessary to consider in detail the geometry connecting the cylinder to the flat end. The shape and weld profile at the connection has an important influence on the fatigue life. This can best be seen by considering two different connection geometries as shown in FIGURE 4.18(a) and (b).

(1) *Assessment of an as-welded corner joint*. FIGURE 4.18(a) shows an as welded corner joint. This consists of a butt weld on the outside and a 45° fillet weld on the inside. BS5500 clause C.2.3.3 considers that a stress concentration factor of at least 2.5 should be used for as-welded butt or fillet welds. So we put $K_t = 2.5$ for the junction. Note that ASME SECTION VIII division 2 recommends a factor of 4 for fillet welds. One reason for the different factors is that the BS5500 design fatigue curve for vessels is based on specimens containing ground flush butt welds whereas the ASME curve is based on specimens without welds.

The peak stress can be calculated from equation (4.11).

$$f_P = (K_t - 1)(f_L + f_B + f_G) \qquad (4.11)$$

Where K_t is the stress concentration factor or fatigue strength reduction factor due to the local structural discontinuity (notch).

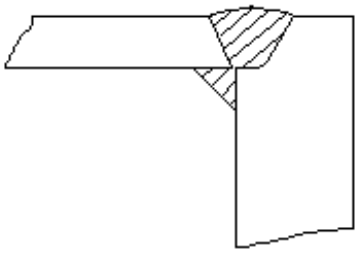

FIGURE 4.18(a) As welded corner joint.

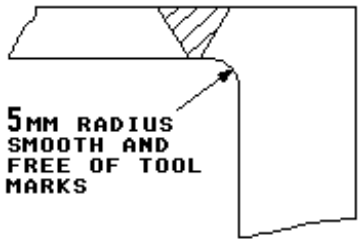

FIGURE 4.18(b) Dressed smooth butt weld joint.

The total stress intensity range, including the peak stress, becomes equation (4.12).

$$f_R = (f_L + f_B + f_G) + (K_t - 1)(f_L + f_B + f_G)$$

$$= K_t*(f_L + f_B + f_G) \qquad (4.12)$$

Hence equation (4.9) can be written as equation (4.13).

$$\text{allowable } N = 1.1\text{x}10^{12}/(0.5*K_t*(f_L + f_B + f_G)*E_C/E_A)^{3.5} \qquad (4.13)$$

Check the amplitude of the alternating stress intensity, equation (4.14).

$$S_{ALT} = 0.5*K_t*(f_L + f_B + f_G)*E_C/E_A \qquad (4.14)$$

$$= 0.5*2.5*276.26*206000/200000 = 355.68 \text{ N/mm}^2$$

S_{ALT} is > the fatigue limit of 34 N/mm^2. Therefore the fatigue life of point B1 is not infinite. The allowable number of cycles from equation (4.13) becomes:

$$\text{allowable } N = 1.1\text{x}10^{12}/(0.5*2.5*276.26*206000/200000)^{3.5} = 1296 \text{ cycles}$$

Therefore 1296 full range cycles are allowed for the junction with a weld detail like that shown in FIGURE 4.18(a).

(2) *Assessment of a dressed smooth butt weld*. If we now consider FIGURE 4.18(b) which shows a dressed smooth butt weld and fillet radius at the inside corner, the dressed smooth butt weld can be assumed to have a K_t = 1. The fillet radius therefore controls the stress concentration at the inside corner. A K_t for the fillet radius can be estimated, from PETERSON (ref. 16), assuming a flat bar with a shoulder fillet as shown in FIGURES 4.19(a) and (b).

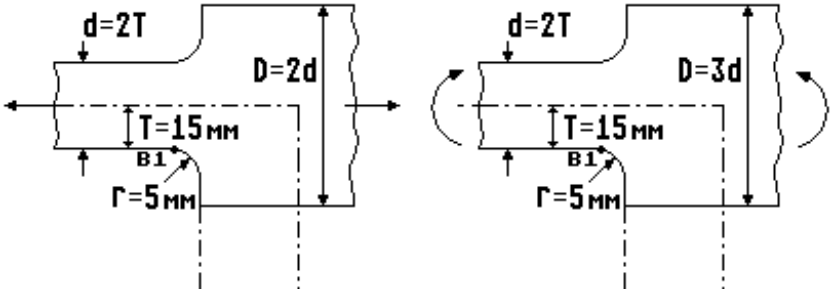

r/d=0.17 K_t = 2.05 r/d=0.17 K_t = 1.6

FIGURE 4.19(a) Tension and bending assumed applicable to section B - B

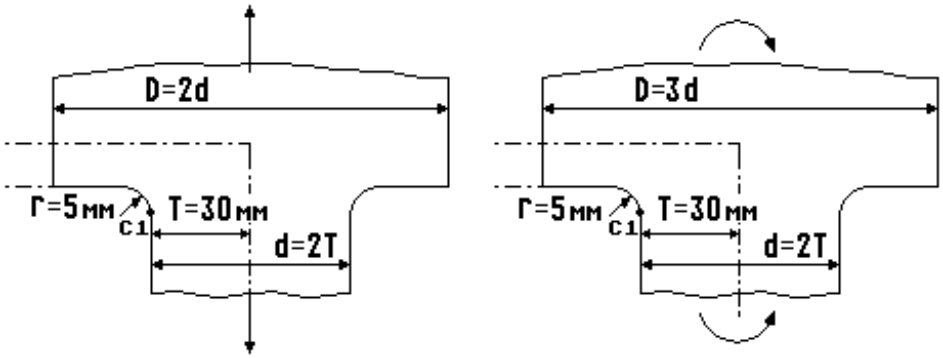

r/d=0.083 K_t = 2.6 r/d=0.083 K_t = 2.07

FIGURE 4.19(b) Tension and bending assumed applicable to section C - C

FIGURE 4.19 Stepped flat bar with shoulder fillets

For *section B - B point B1*, K_t = 2.05 in tension and 1.6 in bending. A value of K_t = 2.05 will be applied to the point as a whole. Note that had stress concentration factors been available in X, Y and Z directions, it would be permissible to obtain the total stress range by applying the applicable factors to the component stresses.

Check the amplitude of the alternating stress intensity, equation (4.14).

$$S_{ALT} = 0.5*K_t*(f_L + f_B + f_G)*E_C/E_A \qquad (4.14)$$

$$= 0.5*2.05*276.26*206000/200000 = 291.66 \text{ N/mm}^2$$

S_{ALT} is > the fatigue limit of 34 N/mm^2. Therefore the fatigue life of point B1 is not infinite. The allowable number of cycles from equation (4.13) becomes:

$$\text{allowable N} = 1.1x10^{12}/(0.5*2.05*276.26*206000/200000)^{3.5} = 2596 \text{ cycles}$$

Point C1 on the flat end must also be checked as it has a higher stress concentration factor from PETERSON reference (16).

For *section C - C point C1*, K_t = 2.6 in tension and 2.07 in bending, a value of K_t = 2.6 will be applied to the point as a whole.

Assessment example

Check the amplitude of the alternating stress intensity, equation (4.14).

$$S_{ALT} = 0.5*K_t*(f_L + f_B + f_G)*E_C/E_A \qquad (4.14)$$

$$= 0.5*2.6*91.78*206000/200000 = 122.89 \text{ N/mm}^2$$

S_{ALT} is > the fatigue limit of 34 N/mm^2. Therefore the fatigue life of point C1 is not infinite. The allowable number of cycles from equation (4.13) becomes:

$$\text{allowable N} = 1.1x10^{12}/(0.5*2.6*91.78*206000/200000)^{3.5} = 53461 \text{ cycles}$$

Therefore point B1 controls the fatigue life. A total of 2596 full range cycles are allowed for the junction with a weld detail like that shown in FIGURE 4.18(b). It is seen that a 18% reduction in stress, by dressing the weld and introducing a fillet radius, has brought about a 2 times increase in the fatigue life.

In the above example the cycles calculated represent the allowable cycles for the same repetition of the extreme pressure range from vacuum to maximum operating pressure and back to vacuum. In practice it is usual for a vessel to be loaded in a more random manner and it is to be expected that the various cycle types to have different extremes and different repetitions. Where there is more than one cycle type the codes use MINER's linear damage rule to calculate usage factors for each cycle and sum these to obtain a cumulative usage factor which must be <=1. The method is well established. However, it is necessary to consider the super-position of cycles that result in a total stress range greater than that of the individual cycles. This can best be seen by an example.

If one type of stress cycle gives 100 cycles of stress range from zero to say 300 N/mm^2 and a second type of stress cycle gives 7000 cycles from say -150 to 250 N/mm^2 the cycles to be considered are as follows.

It is necessary to superimpose 100 cycles from zero to -150 N/mm^2 from the second stress cycle together with the 100 cycles from zero to 300 N/mm^2 from the first stress cycle to obtain the maximum alternating stress amplitude.

Hence we have: Cycle Type 1, $n_1 = 100$, $S_{ALT1} = [300 - (-150)]/2 = 225$ N/mm^2

The next maximum stress range is from -150 to 250 N/mm^2 for the second stress cycle but only for 6900 cycles as we have superimposed 100 cycles from zero to -150 N/mm^2 to cycle type 1 above.

Hence we have: Cycle Type 2, $n_2 = 6900$, $S_{ALT2} = [250 - (-150)]/2 = 200$ N/mm^2

Finally we must include the 100 cycles from zero to 250 N/mm^2 that were not included in cycle type 1 when the -150 N/mm^2 was superimposed.

Hence we have: Cycle Type 3, $n_3 = 100$, $S_{ALT3} = [250 - 0]/2 = 125$ N/mm^2

The maximum alternating stress intensity is therefore 225 N/mm^2. The allowable number of cycles, if this was the only cycle type, is:

$$N_1 = 1.1x10^{12}/225^{3.5} = 6438 \text{ cycles}$$

As there are 7100 cycles in total this result is unacceptable. The rules for cumulative usage must be used to justify the cycles as follows.

The cumulative usage factor U is given by equation (4.15).

$$U = U_1 + U_2 + U_3 + ... U_n <= 1 \qquad (4.15)$$

where U_n is the ratio n_n/N_n for each cycle type

n_n is the *specified* number of cycles for the cycle type

N_n is the *allowable* number of cycles from the design fatigue curve for the cycle type

therefore: for cycle type 1, $n_1 = 100$, $N_1 = 6438$ and $U_1 = n_1/N_1 = 0.015$
for cycle type 2, $n_2 = 6900$, $N_2 = 9722$ and $U_2 = n_2/N_2 = 0.709$
for cycle type 3, $n_3 = 100$, $N_3 = 50374$ and $U_3 = n_3/N_3 = 0.002$

$$U = U_1 + U_2 + U_3 = \underline{0.726}$$

The cumulative usage factor U is < 1 therefore the number of cycles are acceptable.

In general the determination of the cycle types to give the worst cumulative damage is often much more difficult than the above simple example would indicate. A complete detailed fatigue analysis and assessment is a time consuming exercise and additional difficulties can be experienced in obtaining the alternating stress intensity, especially if the direction of the principal stresses are changing throughout the cycle. R. HOUSTON provides a discussion on fatigue damage in reference (22) and shows by comparison that significant differences can be obtained, in the calculation of the usage factor, depending on which code (BS5500 or ASME) is used for the assessment.

REFERENCES

(1) A.E.H. LOVE, The Small Free Vibrations and Deformation of a Thin Elastic Shell. Philosophical Transactions of the Royal Society, 1888, 179A, 491-546.
(2) M. HETÉNYI, Beams on Elastic Foundation. University of Mitchigan Press. 1946.
(3) G.W. WATTS and W.R. BURROWS, The Basic Elastic Theory of Vessel Heads Under Internal Pressure. ASME Journal of Applied Mechanics, paper No.47 A-153, March 1949.
(4) W. FLÜGGE, Stresses in Shells, 2nd. edition. Published by Springer-Verlag, 1990.
(5) N.A. WEIL and J.J. MURPHY, Design and Analysis of Welded Pressure Vessel Skirt Supports. ASME, journal of engineering for industry, February 1960.
(6) M.B. BICKELL and C. RUIZ, Pressure Vessel Design and Analysis. Published by MacMillan 1967.
(7) S.S. GILL, The Stress Analysis of Pressure Vessels and Pressure Vessel Components. Published Pergamon press 1970.
(8) E.H. BAKER, L. KOVALEVSKY and F.L. RISH, Structural Analysis of Shells. Published by McGraw-Hill 1972.
(9) J.F. HARVEY, Theory and Design of Modern Pressure Vessels. Published by Van Nostrand Reinhold 1974
(10) American Society of Mechanical Engineers, Boiler and Pressure Vessel Code, SECTION VIII, Division 2, Appendix 4 and 5, 1992 edition up to and including 1993 addenda.
(11) W.C. YOUNG, Roark's Formulas for Stress and Strain, 6th. edition. Published by McGraw-Hill 1989.
(12) M. HETÉNYI, Spherical Shells subjected to Axial Symmetrical Bending, Vol. 5. International Association for Bridge and Structural Engineers, 1938.
(13) S. TIMOSHENKO, Theory of Plates and Shells, 2nd edition. Published by McGraw-Hill, 1959.
(14) British Standards Institution, BS5500:1994, Specification for Unfired Fusion Welded Pressure Vessels.
(15) P. POLAK, Designing for Strength. Published MacMillan Press 1982.
(16) R.E. PETERSON, Stress Concentration Factors. Published by J. Wiley & Sons 1974.
(17) G.D. GALLETLY, Design Equations for Preventing Buckling in Fabricated Torispherical Shells Subjected to Internal Pressure. Proceedings of I.Mech.E. Vol. 200, No. A2, 1986.
(18) C.T.F. ROSS, Finite Element Programs for Axisymmetric Problems in Engineering. Published by Ellis Horwood 1984.
(19) D. BUSHNEL, BOSOR5 - A Computer Program for Buckling of Elastic-Plastic Complex Shells of Revolution Including Large Deflections and Creep. Lockheed Missiles Space Co., Sunnyvale California.
(20) T.G.F. GRAY and J. SPENCE, Rational Welding Design. Second edition Butterworths 1982.
(21) J.P. DEN HARTOG, Advanced Strength of Materials. Published by McGraw-Hill 1952.
(22) R. HOUSTON, British Standards Institution Boiler and Pressure Vessel Design Criteria. Pressure Vessel Codes and Standards, Developments in Pressure Vessel Technology 5, edited by R.W.NICHOLS. Published by Elsevier Applied Science 1987.
(23) C.R. CALLADINE, The Theory of Thin Shell Structures 1888-1988, Love Centenary Lecture, I.Mech.E. Proceedings 1988, Volume 202, No.42.
(24) C.R. CALLADINE, Theory of Shell Structures, Cambridge University Press 1983.
(25) British Standards Institution PD6550:1989, Explanatory Supplement to BS5500:1988 'Specification for Unfired Fusion Welded Pressure Vessels', Section three 'Design'. Part 1 Domed ends(heads), Part 2 Openings and branch connections, Part 3 Vessels under external pressure, Part 4 Heat exchanger tubesheets.
(26) C.E. TURNER, Introduction to Plate and Shell Theory. Published Longmans 1965.
(27) A.E.H. LOVE, A Treatise on the Mathematical Theory of Elasticity. First edition (two volumes) 1892/93, second edition 1906, third edition 1920, fourth edition 1927 (Cambridge University Press).
(28) C.E. TAYLOR, Simplification of the Analysis of Stress in Conical Shells, University of Illinois, TAM Report 385, April 1974
(29) F.A. LECKIE and R.K. PENNY, Solutions for the stresses at nozzles in pressure vessels. Stress concentration factors for the stresses at nozzles intersections in pressure vessels. Welding Research Council Bulletin No. 90, 1963.
(30) BS1560: Section 3.1: 1989. Circular flanges for pipes, valves and fittings (Class designated), Section 3.1 Specification for steel flanges.
(31) E.O. WATERS, D.B. WESSTROM, D.B. ROSSHEIM, F.S.G. WILLIAMS, Formulas for Stresses in Bolted Flanged Connections. ASME Transactions, 1937.
(32) Modern Flange Design, Gulf and Western Manufacturing Company, Energy Products Group, Bulletin 502.
(33) N.W. MURRAY and D.G. STUART, Behaviour of Large Taper Hub Flanges, Paper 9, Symposium on pressure vessel research towards better design, I.Mech.E., 1961.
(34) Criteria of the ASME boiler and pressure vessel code for design by analysis in Sections III and VIII, division 2. ASME 1969.
(35) British Standards Institution, PD6433, Guide to the application of Stress Analysis to Design, 1969.

(36) R.L. ROCHE, Practical procedures for stress classification Design Codes and Structural Mechanics, edited by R.L. ROCHE and J.R. FARR. Published by Elsevier Applied Science 1989.
(37) W.J. O'DONNELL and B.F. LANGER, Design of Perforated Plates, ASME Pressure Vessels and Piping, Design and Analysis, Volume 2, Components and Structural Dynamics.
(38) BS806 Specification for Design & Construction of Ferrous Piping for and in connection with Land Boilers.
(39) ASME B31.1 Power Piping.
(40) J.F. LANCASTER, Chapter 5, Material Selection, Pressure Vessel Engineering Technology, edited by R.W. NICHOLS, Elsevier Publishing 1971.
(41) L.M. WYATT, Materials of Construction for Power Plant. Applied Science Publishers 1976.
(42) S.J. MADDOX, Fatigue of Welded Structures, 2nd edition. Abington Publishing 1991.
(43) D.R. MILLER, Thermal stress Ratchet Mechanism in Pressure Vessels, ASME Transactions, Vol. 81, Ser. D, No. 2, 1959.
(44) ASME Code Cases: Nuclear Components, Case N-47, Class 1 Components in Elevated Temperature Service, Section III, Division 1.
(45) Criteria for the Design of Elevated Temperature Class 1 Components in Section III, Division 1, of the ASME Boiler and Pressure Vessel Code, May 1976.
(46) Nuclear Electric, Assessment Procedure R5, An Assessment Procedure for the High Temperature Response of Structures, Issue 1, October 1990.
(47) British Standards Institution, PD6493:1991, Guidance on Methods for Assessing the Acceptability of Flaws in Fusion Welded Structures.
(48) CEGB Document R/H/R6-Rev. 3, Assessment of the Integrity of Structures Containing Defects, May 1986.
(49) ASME Boiler and Pressure Vessel Code, Section XI, Rules for the Inservice Inspection of Nuclear Power Plant Components, Appendix A.
(50) Electrical Power Research Institute (EPRI), NP-719-SR, Flaw Evaluation Procedures ASME Section XI.
(51) R.G. BAKER, The Welding of Pressure Vessel Steels, Climax Molybdenum Co. Ltd.
(52) F.S. KELLEY, A General Fatigue Evaluation Method (Elastic Stress or Plastic Strain with Constant or Varying Principal Direction), ASME Journal of Pressure Vessel Technology, Vol. 102, August 1980.
(53) Pressure Vessel Design, Concepts and principals, Edited by J. SPENCE and A.S. TOOTH, Published by E & F N Spon 1994.
(54) Private communication, C.E. TAYLOR, 23rd June 1994.
(55) C.E. TAYLOR and E. WENK, Analysis of Stresses in the Conical Elements of Shell Structures, Proceedings of the Second U.S National Congress of Applied Mechanics, 1954.

APPENDIX 1 Fatigue Assessment to BS5500 Enquiry Case 5500/79

A1.1 As from May 1988 it has been possible to assess pressure vessels that are subjected to cyclic loading using the rules provided in BS5500 enquiry case 79 as an alternative to the rules contained in BS5500 appendix C.

The rules of enquiry case (EC) 5500/79 are a departure from the traditional appendix C rules in that they have their origin in the bridge code BS5400: Part 10: "Code of Practice for Fatigue", modified where necessary to suit pressure vessels. The background to the rules are discussed in detail by MADDOX in reference (42). This reference is essential reading for a full understanding of the basis of the rules. His chapter on fatigue in reference (53) is also recommended reading. It is intended to assess the worked example given in section 4.6 for a cylinder with flat end closure using the rules of EC 5500/79.

A1.2 The rules of EC 5500/79 differ in many aspects from the appendix C rules. The main differences that affect the assessment can be summarised as follows:

(1) There are seven fatigue design curves, lettered C, D, E, F, F2, G and W. The highest curve C is for unwelded material but the other six curves relate to weld details. A typical curve is shown in FIGURE A1.1. It is necessary to classify the weld detail to the appropriate curve from a table of given examples. The table of examples cover (a) seam welds (b) branch connections and (c) attachments. Unclassified details are treated (with some exceptions) as class G, or class W for load carrying weld metal. It is usual to refer to MADDOX (ref. 42) for additional details.

(2) The curves are based on a Young's modulus of 209000 N/mm^2 rather than 206000 N/mm^2.

(3) A thickness correction is necessary for some weld details when the plate thickness is over 22 mm.

(4) More than one classification may apply to a particular weld detail as there are several ways a weld detail may fail.

(5) The primary plus secondary stress category is used in the assessment but note that direct stress is used rather than stress intensity.

(6) The curves already take account of the peak stress due to the weld detail. The implication here is that the stress to be used should include the gross structural discontinuity but *not* the local stress concentration factor associated with the weld. Some care is required when applying this rule. R. HOUSTON (ref. 22) found that a wide range of fatigue damage could be obtained due to the method of calculating the stresses and the amount of local stress concentration factor contained in the fatigue curves. If the weld detail used does not match the classification examples it may be necessary to include some local stress concentration as will be seen by example in section A1.6.2.

(7) The curves use stress range regardless of mean stress and do not have a fatigue limit.

(8) Rules are given for the deviation from design shape.

(9) The "rainflow" or "reservoir" methods are recommended for cycle counting.

(10) Austenitic stainless steels are applicable up to and including 430°C (the temperature limits for ferritic steels and aluminium alloys are unchanged at 375 and 100°C respectively).

A1.3 The rules provide a "screening" equation which if satisfied will avoid the need for a fatigue analysis. In addition there is a simplified assessment procedure provided. MADDOX in reference (53) provides background details for these simplified procedures. For the example of the cylinder to flat end junction (discussed in section 4.6) the *detailed* assessment rules of clause 3 will be used as this will illustrate several difficulties associated with the application of the rules of EC 5500/79.

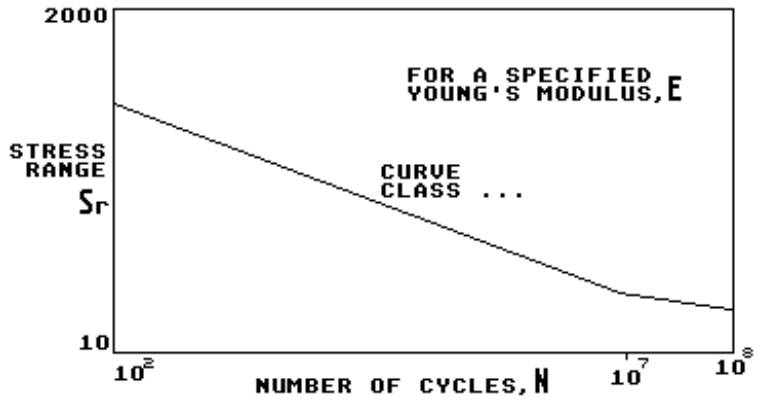

FIGURE A1.1 A typical design fatigue curve. Note that there is no fatigue limit

A1.4 The design fatigue curves have the form given by equation (A1.1):

$$S_R{}^m N = A \qquad \text{(A1.1)}$$

where S_R is the stress range
N is the number of cycles to failure
m is an index and A is a constant

Rearranging equation (A1.1) and correcting for Young's modulus, as discussed previously in section 4.5, the allowable number of cycles for a given stress range is given by equation (A1.2). A lower Young's modulus reduces the number of cycles for a given stress range.

$$\text{allowable, } N = A/(S_R * E_C/E_A)^m \qquad \text{(A1.2)}$$

where E_C is the Young's modulus for the fatigue curve = 209000 N/mm^2
E_A is Young's modulus at maximum operating temperature.

If the allowable stress range for a given number of cycles is required, rearranging equation (A1.2) gives equation (A1.3):

$$\text{allowable, } S_R = (A/N)^{1/m} E_A / E_C \qquad \text{(A1.3)}$$

With *some* weld details it is necessary to correct for thickness when the plate thickness is >22 mm. Additional details are given in MADDOX (ref. 42). The correction reduces the number of cycles for a given stress range. The allowable cycles to failure becomes equation (A1.4).

$$\text{allowable, } N = A*(22/e)^{m/4}/(S_R * E_C/E_A)^m \qquad \text{(A1.4)}$$

where e is the plate thickness in mm

Rearranging equation (A1.4) gives the allowable stress range for a given number of cycles, equation (A1.5):

$$\text{allowable, } S_R = [A*(22/e)^{m/4}/N]^{1/m} E_A / E_C \qquad \text{(A1.5)}$$

A1.5 It is necessary to show that the structure will shakedown by satisfying the primary plus secondary stress category ($f_M + f_B + f_G$) or ($f_L + f_B + f_G$). The stress analysis carried out for Example 3.5 in section 4.6.2 shows that the vessel will shakedown to elastic cycling. The results given in TABLE 4.1 are valid as they include the gross structural discontinuity but not the local discontinuity, but note that *direct* stress must be used in the EC 5500/79 assessment rather than stress intensity.

The direct stresses are the three principal stresses f_1, f_2, and f_3 given in TABLE 4.1. The stress range S_R is the numerically greatest of the three principal stresses. TABLE A1.1 summarises the results from TABLE 4.1. Note that clause 3.3.2 of EC 5500/79 considers that the through thickness stress can be ignored for the assessment of a welded joint. In TABLE A1.1 (and TABLE 4.1) the through thickness stress is represented by the f_Y and f_2 stresses.

Section B - B point B1	component stress	principal	S_R
max. operating vacuum	difference	stresses	
f_X = 51.55 -11.05	62.6	f_1 = 62.6	
f_Y = -0.47 0.0	-0.47	f_2 = -0.47	
f_Z = 227.3 -48.49	275.79	f_3 = 275.79	275.79
f_{XZ} = 0.0 0.0	0.0		
f_{YX} = 0.0 0.0	0.0		
f_{ZY} = 0.0 0.0	0.0		
Section B - B point B3	component stress	principal	S_R
max. operating vacuum	difference	stresses	
f_X = -80.08 17.02	-97.1	f_1 = -97.1	
f_Y = 0.0 -0.10	0.10	f_2 = 0.10	
f_Z = -211.47 45.11	-256.58	f_3 = -256.58	256.58
f_{XZ} = 0.0 0.0	0.0		
f_{YX} = 0.0 0.0	0.0		
f_{ZY} = 0.0 0.0	0.0		
Section C - C point C1	component stress	principal	S_R
max. operating vacuum	difference	stresses	
f_X = 5.91 -1.34	7.25	f_1 = 7.25	
f_Y = -0.47 0.0	-0.47	f_2 = -0.47	
f_Z = 75.18 -16.13	91.31	f_3 = 91.31	91.31
f_{XZ} = 0.0 0.0	0.0		
f_{YX} = 0.0 0.0	0.0		
f_{ZY} = 0.0 0.0	0.0		
Section C - C point C3	component stress	principal	S_R
max. operating vacuum	difference	stresses	
f_X = 4.25 -1.02	5.27	f_1 = 5.27	
f_Y = 0.0 -0.10	0.10	f_2 = 0.10	
f_Z = -65.01 13.76	-78.77	f_3 = -78.77	78.77
f_{XZ} = 0.0 0.0	0.0		
f_{YX} = 0.0 0.0	0.0		
f_{ZY} = 0.0 0.0	0.0		
Section D - D point D1	component stress	principal	S_R
max. operating vacuum	difference	stresses	
f_X = -88.09 18.72	-106.81	f_1 = -106.81	106.81
f_Y = -0.47 0.0	-0.47	f_2 = -0.47	
f_Z = -88.09 18.72	-106.81	f_3 = -106.81	106.81
f_{XZ} = 0.0 0.0	0.0		
f_{YX} = 0.0 0.0	0.0		
f_{ZY} = 0.0 0.0	0.0		
Section D - D point D3	component stress	principal	S_R
max. operating vacuum	difference	stresses	
f_X = 98.26 -21.09	119.35	f_1 = 119.35	119.35
f_Y = 0.0 -0.10	0.10	f_2 = 0.10 [Corrected –ve sign removed]	
f_Z = 98.26 -21.09	119.35	f_3 = 119.35	119.35
f_{XZ} = 0.0 0.0	0.0		
f_{YX} = 0.0 0.0	0.0		
f_{ZY} = 0.0 0.0	0.0		

TABLE A1.1 Summary of stress range S_R in N/mm^2 for example 3.5

A1.6 The weld details connecting the cylinder to the end are shown in FIGURE 4.18. The weld detail examples given in EC 5500/79 do not specifically cover cylinder to flat end junctions. The fatigue life is estimated as follows

A1.6.1 Considering FIGURE 4.18(a) detail first. This detail is a full penetration corner weld, as welded and proved free of significant defects. Since the detail is *unclassified* then clause 3.4.4 of EC 5500/79 applies and requires the detail to be treated as class W as the weld is load carrying. This classification is conservative for the following reasons:

(1) Cracking could be expected from the weld toes into the shell or end as shown in FIGURE A1.2(a). This would suggest no higher than class F would be permitted based on branch type connections.

(2) Cracking could also be expected from the butt weld on the outside as shown in FIGURE A1.2(b). Based on a seam weld if the overfill profile angle θ is < 150° then no higher than class E is permitted. If the overfill angle θ is >= 150° then class D is permitted.

(3) Cracking could also occur in the hoop direction due to the weld metal being stressed along its length as shown in FIGURE A1.2(c). Based on a branch type connection no higher than class F would be permitted. However, this classification appears to be for a partial penetration detail. MADDOX reference (42) suggests that class D would be applicable for a full penetration detail.

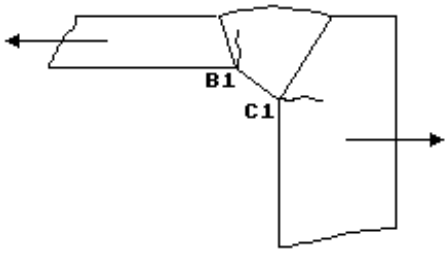

FIGURE A1.2(a) Class F

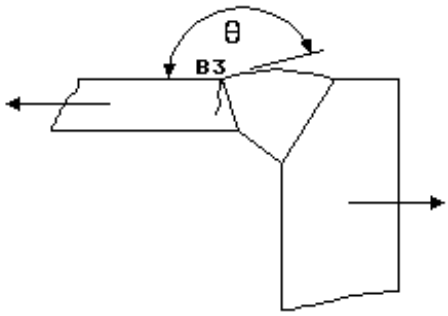

FIGURE A1.2(b) Class E if θ < 150°
Class D if θ >=150°

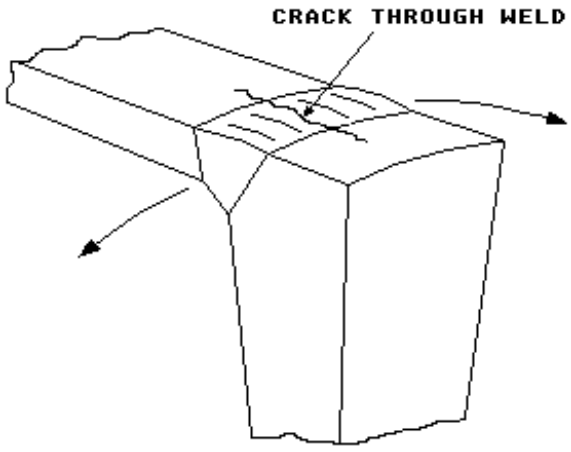

FIGURE A1.2(c) Class D

FIGURE A1.2 Classification at a corner weld

For the class W curve the index m = 3 and constant A = 1.58×10^{11}. The actual Young's modulus for the material is 200000 N/mm^2 at 200°C. From TABLE A1.1 the highest stress range is 275.79 N/mm^2 at point B1. The fatigue life is estimated from equation (A1.2).

allowable N = $1.58 \times 10^{11}/(275.79*209000/200000)^3$ = 6600 cycles

Check that N is < 10^7 cycles (if N is > 10^7 cycles then a different constant and index is applicable and N must be re-calculated).

Point C1 must also be checked. Although the stress range is much lower than point B1 the thickness of the end is 30 mm. Therefore, based on a branch type connection, the correction for thickness is assumed to apply to the end. The fatigue life is calculated from equation (A1.4).

allowable N = $1.58 \times 10^{11}(22/30)^{3/4}/(91.31*209000/200000)^3$ = 144121 cycles

Check that N is < 10^7 cycles.

Therefore in summary: if a class W weld detail applies to the junction, shown in FIGURE 4.18(a), the fatigue life is governed by point B1 with 6600 cycles. This compares with 1296 cycles using BS5500 appendix C rules.

A1.6.2 If we now consider the detail in FIGURE 4.18(b). This is a full penetration butt weld, dressed flush and proved free from significant defects by non-destructive testing. The corner radius is smooth and free of tool marks. There will be a local stress concentration factor (notch) due to the corner radius and stress concentration factors K_t of 2.05 for point B1 and 2.6 for point C1 have been estimated as discussed in section 4.6.3.(2). Some allowance must be made for the local discontinuity in this case, as the classification examples for seam welds do *not* include any local stress concentration factor for a fillet radius adjacent to the weld detail. The classification for the butt weld can be justified as follows.

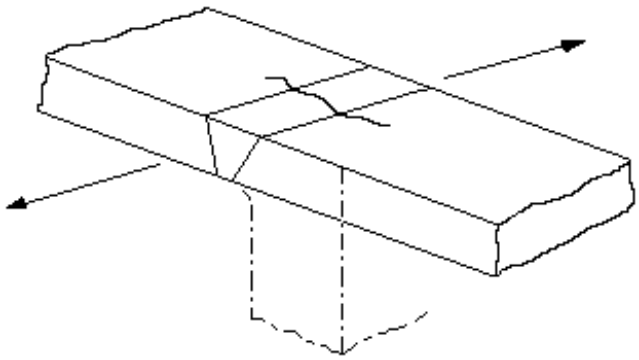

FIGURE A1.3(a) For stresses acting essentially along the weld.
Class D plus local stress concentration factor.

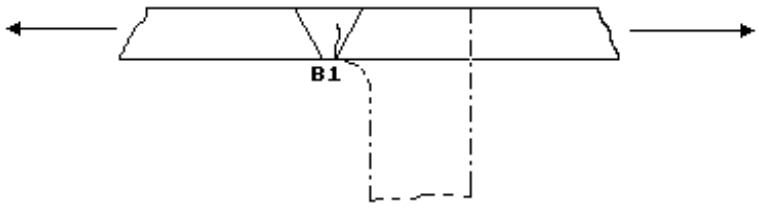

FIGURE A1.3(b) For stresses acting essentially normal to the weld.
Class E plus local stress concentration factor.

FIGURE A1.3 Classification at a butt weld adjacent to a local structural discontinuity

(1) For stresses acting essentially along the weld, i.e. in the hoop direction shown in FIGURE A1.3(a). Based on a seam weld a class D detail is considered applicable.

(2) For stresses acting essentially normal to the weld, i.e. in the meridional direction shown in FIGURE A1.3(b). A class E detail is considered applicable based on a single sided weld where full penetration can be assured. Note that EC 5500/79 does not recommend this joint type for fatigue applications when subjected to this form of stressing unless full weld penetration can be assured.

Note that in practice it is sometimes necessary to have a closing weld on a vessel without being able to get clear access to the root of the weld for inspection. The fatigue life is critically dependent on the root condition hence every effort should be made to avoid a vessel closing weld that cannot be inspected. In the case of circular section tubes with single sided welds where full penetration can be assured, MADDOX (ref. 42) suggests that a class F2 detail is applicable.

The allowable number of cycles can be obtained by introducing the stress concentration factor K_t into equation (A1.2) to form equation (A1.6):

$$\text{allowable, } N = A/(K_t * S_R * E_C/E_A)^m \qquad \text{(A1.6)}$$

By inspection of the results listed a TABLE A1.1 it is seen that the highest stress is the principal stress f_3 = 275.79 N/mm^2 at point B1. This stress is due to the meridional stress f_Z, i.e. this stress is normal to the circumferential weld. Therefore the class E curve will control the fatigue life of this weld detail.

Note that in general it is possible to have a situation with these rules where a *point* with a *lower* stress range and a *lower* weld class could be more critical than *another* point with a *higher* stress range and *higher* weld class. If any doubt exists the only safe way to proceed is to check both points for their applicable stress range and weld class to obtain the lowest number of cycles to failure. We have seen that it is possible to have a different weld classification in different directions of stress at the *same* point. Consequently it is possible for a *direction* with a *lower* stress range and a *lower* weld class to be more critical than another direction (at the same point) with a *higher* stress range and *higher* weld class. Again if any doubt exists the only safe way is to check both directions to obtain the lowest number of cycles to failure.

For the class E curve the index m = 3 and constant A = 1.04x10^{12}. The fatigue life from equation (A1.6) becomes:

$$\text{allowable, } N = 1.04\text{x}10^{12}/(2.05*275.79*209000/200000)^3 = 5042 \text{ cycles}$$

Check that N is < 10^7 cycles.

Since the stress concentration factor K_t = 2.6 for point C1 is higher than point B1, point C1 must also be checked as it could be more critical than point B1. Point C1 is not at a weld so class C curve could apply, however it is good practice to use the class D curve on the basis that a weld repair may be required anywhere. The thickness correction will also be applied on the basis that the weld repair could be required at the corner junction. Equation (A1.6) becomes equation (A1.7).

$$\text{allowable, } N = A*(22/e)^{m/4}/(K_t * S_R * E_C/E_A)^m \qquad \text{(A1.7)}$$

For the class D curve the constant A = 1.52x10^{12} and index m = 3. The fatigue life from equation (A1.7) becomes.

$$\text{allowable } N = 1.52\text{x}10^{12}(22/30)^{3/4}/(2.6*91.31*209000/200000)^3 = 78885 \text{ cycles}$$

Check that N is < 10^7 cycles.

Therefore in summary: if a class E weld detail applies to the junction, shown in FIGURE 4.18(b), the fatigue life is governed by point B1 with 5042 cycles. This compares with 2596 cycles using BS5500 appendix C rules.

In conclusion it would appear that there is potential for increased fatigue life based on EC 5500/79 rules compared to appendix C rules. The most controversial aspect however is that EC 5500/79 rules predict a lower fatigue life for the butt weld detail FIGURE 4.18(b) compared to the corner joint detail FIGURE 4.18(a). This tends to confirm R. HOUSTON's predictions in reference (22) regarding how sensitive the fatigue analysis is to slight changes in the method of calculating the stresses.

A1.7 When more than one cycle type is applicable, MINER's linear damage rule is used to assess the cumulative usage factor as discussed previously in section 4.6.3. The "rainflow" or "reservoir" methods are recommended for cycle counting. MADDOX has examples in the use of these methods of cycle counting in reference (42). Both methods give the same result if used in the form required by the reservoir method.

A1.8 Rules are given for deviation from the design shape when pressure stresses are being considered. The rules include: offset misalignment, ovality, angular misalignment and local peaking. The rules apply even if the allowable assembly tolerances of BS5500 are met.

A1.9 Rules are given whereby the classification of *some* weld details can be improved by: (1) Detailed stress analysis, including strain measurements on prototype or actual vessels. Applicable published data obtained for geometrically similar vessels is also acceptable. (2) Weld toe dressing is acceptable for some details. The method of dressing should conform to the rules specified in clause 4 of EC 5500/79.

A1.10 Separate rules and design fatigue curves are given for bolting (which should not be welded). The rules and curves are essentially the same as that given in appendix C of BS5500 except that the curves are plotted for stress range, rather than stress amplitude, and Young's modulus is 209000 N/mm^2 rather than 206000 N/mm^2. A stress concentration factor or strength reduction factor must be included when calculating the peak stress range. For high strength steel bolts a fatigue strength reduction factor of at least 4 should be used.

A1.11 The discussion above is for defect free structures. Enquiry case 5500/79 provides rules for the fatigue assessment of welds containing defects. These rules apply even for defects that meet the acceptance criteria of table 5.7 of BS5500.

APPENDIX 2 Strain Energy Considerations

A2.1 A facility has been included in the program to plot the ratio of strain energy variation along the shell from the junction. Such a plot can sometimes provide a useful picture of the way the shell resists the applied loading by a combination of membrane (stretching) and bending actions.

A2.2 It is convenient to calculate the elastic strain energy of the unit surface area of the shell or plate, at a section, in terms of the stress resultants N1, N2, M1 and M2 as follows [line 4790].

The linear elastic strain energy of stretching in terms of the membrane forces is given by equation (A2.1):

$$Um = [(N1 + N2)^2 + 2(1 + \mu)(-N1*N2)]/(2*E*T) \qquad (A2.1)$$

and for the strain energy of bending in terms of the bending moments is given by equation (A2.2):

$$Ub = 6[(M1 + M2)^2 + 2(1 + \mu)(-M1*M2)]/(E*T^3) \qquad (A2.2)$$

Note that since the loading considered is axisymmetric, no effects of twisting moments or In-Plane shear forces are included.

The total strain energy at a section is given by the summation of the strain energy terms, equation (A2.3).

$$Ut = Um + Ub \qquad (A2.3)$$

The program allows the strain energy terms Um, Ub and Ut to be plotted. It is also convenient to plot the energy terms Um and Ub as ratios of the total strain energy Ut as given by equations (A2.4) and (A2.5).

$$RATIOm = Um/Ut \qquad (A2.4)$$

$$RATIOb = Ub/Ut \qquad (A2.5)$$

A plot of these ratios along the shell will give an indication of how the shell is resisting the loading by stretching and bending. The effect is best seen by an example.

A2.3 The cylinder with a flat end closure, discussed previously in Example 3.5, will be used to show how the strain energy varies along the cylinder and flat end when subjected to internal pressure. Plots of the strain energy and strain energy ratios along the cylinder (component 1) and the flat end (component 2) are shown in FIGURES A2.1 to A2.10.

Inspection of FIGURES A2.1 to A2.3 for the strain energy in the cylinder shows that close to the junction the energy is dominated by bending effects, but by 80 mm from the junction the bending strain energy has reduced to almost zero. The plots of the energy ratio, FIGURES A2.4 and A2.5, show that at the junction and for a short distance away from the junction the cylinder resists the loading by a combination of membrane and bending actions, after which the loading is resisted almost entirely by membrane action.

For the flat end, inspection of FIGURES A2.6 to A2.10, show that the plate, as expected, resists the pressure loading almost entirely by bending action.

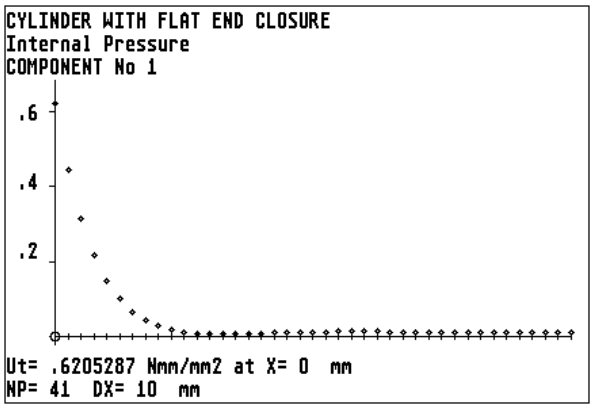

FIGURE A2.1 Total strain energy along the cylinder from the junction.

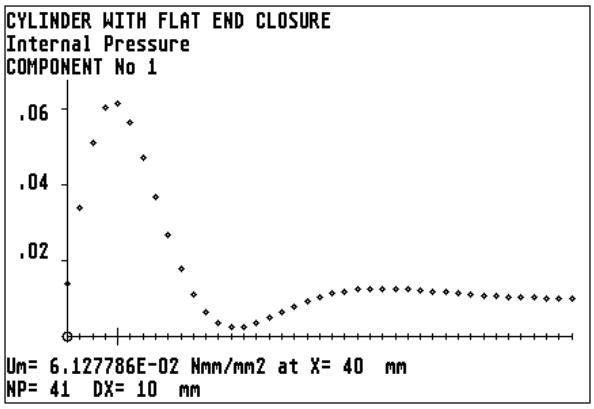

FIGURE A2.2 Membrane strain energy along the cylinder from the junction.

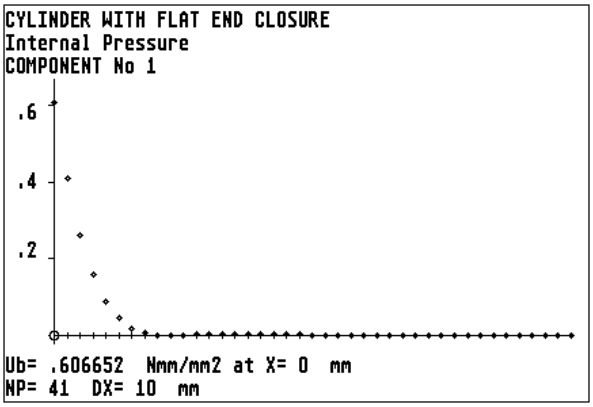

FIGURE A2.3 Bending strain energy along the cylinder from the junction.

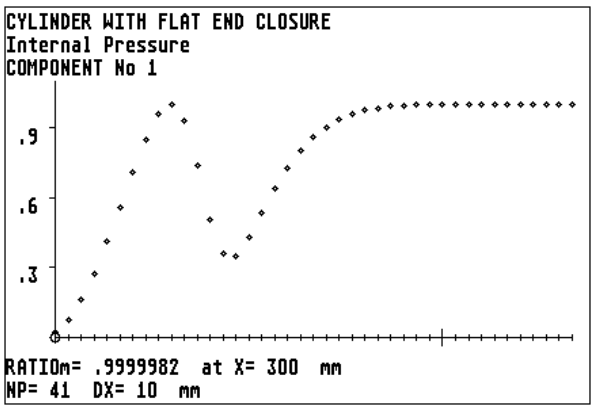

FIGURE A2.4 Membrane strain energy ratio along the cylinder from the junction.

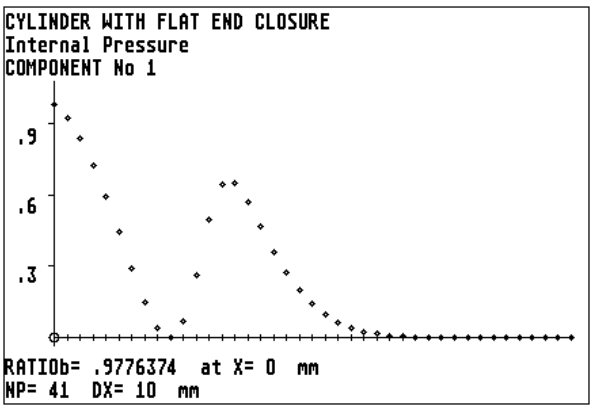

FIGURE A2.5 Bending strain energy ratio along the cylinder from the junction.

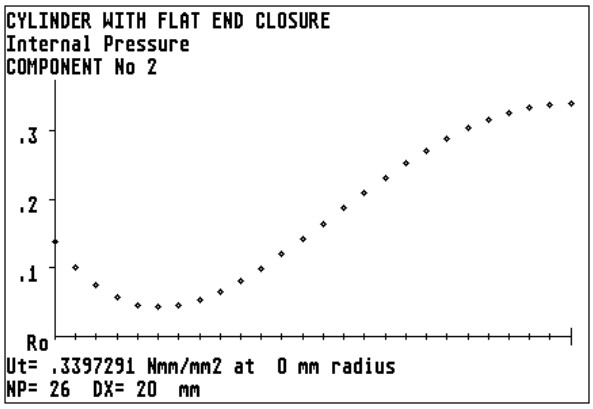

FIGURE A2.6 Total strain energy along the flat end from the junction.

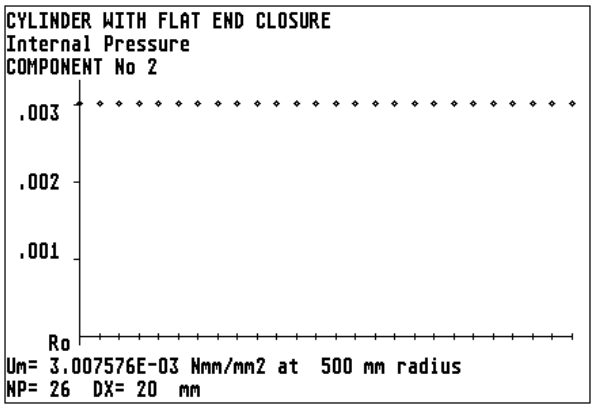

FIGURE A2.7 Membrane strain energy along the flat end from the junction.

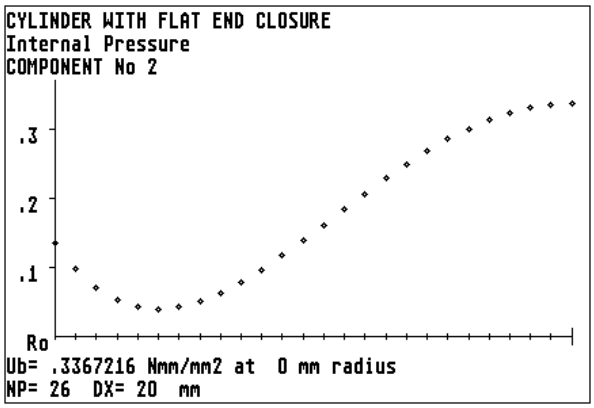

FIGURE A2.8 Bending strain energy along the flat end from the junction.

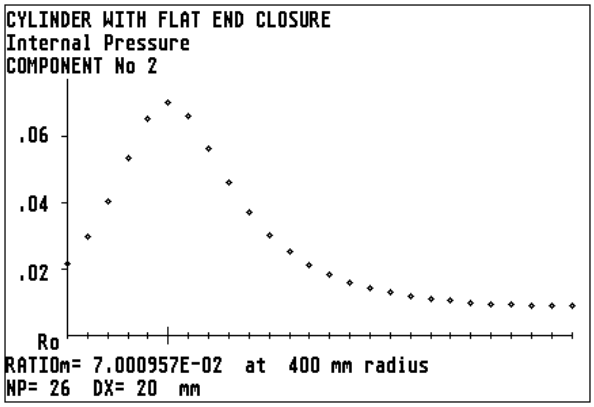

FIGURE A2.9 Membrane strain energy ratio in the flat end from the junction to the centre.

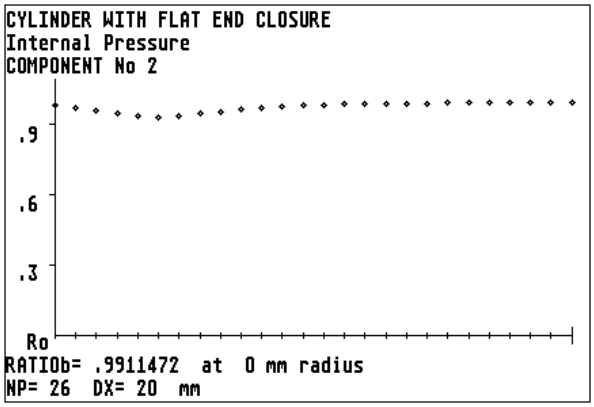

FIGURE A2.10 Bending strain energy ratio in the flat end from the junction to the centre.

APPENDIX 3 List of Program Input Error Traps

Line 540 checks that the number of components N is not less than 1
Line 870 checks that the compact ring is the last component.
Line 880 checks that the component type number is within range for a junction analysis, i.e. within 1 to 11 inclusive.
Line 970 checks that the component type number is within range for a single component, i.e. within 1 to 7 inclusive.
Line 1120 checks that the component radius is > 0.
Line 1130 checks that the inside radius of the flat plate is not greater than or equal to the outside radius.
Line 1140 checks that the inside radius is not zero if there is a junction at the inside radius.
Line 1150 checks that the component thickness is > 0.
Line 1160 checks that the angle ϕ is > 0.
Line 1170 checks that angle ϕ is < 180 degrees for spherical shells.
Line 1180 checks that angle ϕ is < 90 degrees for cones.
Line 1190 checks that the junction position for flat plates is not outside the plate surface.
Lines 1220 to 1224 check the geometry of the compact ring.
Line 1340 checks that the compact ring connection point numbers are within range, i.e. within 1 to 9 inclusive.
Line 1410 checks that Young's modulus is > 0
Line 1420 checks that Poisson's ratio is within range, i.e. $0 =< \mu < 0.5$
If $\mu = 0$ then μ defaults to 1E-6 at line 1425.
Line 1440 checks that the mass density is not less than zero.
Line 1600 checks that the number of point loads applied to a flat plate is within range, i.e. within 0 to 12 inclusive. The maximum value of 12 can be altered by changing the value of MPL at line 520.
Line 1620 and 1636 checks that the radius of the point load is within the plate surface and is not zero.
Line 1730 checks that the centrifugal loading in revolutions per second is not less than zero.
Line 2620 checks that the menu option called for is within range, i.e. within 0 to 4 inclusive.
Line 2710 checks that the menu option called for is within range, i.e. within 0 to 10 inclusive.
Line 2750 checks that the component number of the component being altered is within range, i.e. within 1 to N inclusive.
Line 3500 checks that the component number of the free displacement being altered is within range, i.e. within 1 to N inclusive.
Line 3770 checks that the component number of the stiffness coefficient being altered is within range, i.e. within 1 to N inclusive.
Line 3780 checks that the coefficient number being altered is within range, i.e. within 1 to 4 inclusive.
Line 4260 checks that the menu option asked for is within range, i.e. within 0 to 3 inclusive.
Line 4370 checks that the component number for the result output is within range, i.e. within 1 to N inclusive.
Line 4420 checks that distance (or angle) specified from the junction is not less than zero.
Line 4430 checks that spherical shell angle specified is < angle ϕ.
Line 4440 checks that the distance specified along the cone is not too long.
Line 4450 checks that the radius specified is within the dimensions of the flat plate.
Line 7700 checks that the component number in the result plot is within range, i.e. within 1 to N inclusive.
Line 7730 checks that the parameter to be plotted matches the program library in subroutine lines 8160 to 8370.
Line 7740 checks that the number of points to be plotted is > 1
Line 7750 checks that the distance between points plotted is > 0
Line 7760 checks that the angle between points plotted is > 0
Line 20040 checks that the printer type is not < 1

APPENDIX 4 Program Verification

All reasonable precautions have been taken to ensure that the program is correct and free from bugs. The following approach has been used to verify the program.

A4.1 The program is written in BASIC and is uncompiled. The program can be listed, using the standard LIST or LLIST commands in BASIC, and the code studied. The coding has been kept simple and the use of special commands has been avoided wherever possible.

A4.2 The equations used in the program are based on simple theory, well known relationships or specified references. Only simple component geometries that can be easily checked have been considered.

A4.3 Many test examples have been run (more than 70 to date) and compared with well known text book or technical paper solutions. In some cases where there was no known solution, a comparison was made with thin walled tapered conical shell elements.

A4.4 Each program was compared with several multi-component test examples to check for numerical consistency.

A4.5 Finally the test examples in *A4.3* were cross checked using a PC compatible system and an Atari ST system, i.e. results from two different computers and two different BASIC programs were cross checked against each other. Both these versions of BASIC work to a single precision internal accuracy of seven digits. The results are virtually identical apart from minor differences due to rounding.

If in spite of all the above checks an error or bug is discovered then the author would like to know about it.

APPENDIX 5 Conical Shell Notation

The analysis of long conical shells is based on the work by Professor Charles E. Taylor in reference (28). Readers who wish to study the solution in greater detail will need to obtain a copy of reference (28). Copies of this reference can be obtained from the University of Illinois, Illinois Research and Reference Center, 128 Library, 1408 W. Gregory Drive, Urbana, Illinois 61801, USA.

The symbols used in the program closely follow reference (28) with some adaptation necessary to suit the BASIC programming. In some cases the sign convention is also different. This appendix therefore summarises and cross references the symbols so the readers can easily identify the applicable variables and equations used in reference (28). Two typographical errors in reference (28) have been corrected (ref. 54).

TAYLOR notation (ref. 28)	Equivalent notation in "AJAP1" (lines 5240-5880)
R mean radius of a point on the cone.	RX = (Z $\pm$ X)*SIN(PHI)
R_1 mean radius at the cone large end.	R = Z*SIN(PHI)
R_2 mean radius at the cone small end.	R = Z*SIN(PHI)
h thickness.	T
α half apex angle.	PHI | +ve large end -ve small end
xi cone parameter, $\xi = 2*\text{lambda}*(x)^{1/2}$	XI |
xi_1 cone parameter at the cone large end.	XIA
xi_2 cone parameter at the cone small end.	-XIA
lambda, $\lambda = [12(1 - nu^2)/(h^2\tan^2\alpha)]^{1/4}$	LAMBDA
$x = R/\sin\alpha$ distance along the cone from the apex.	Z - X for large end Z + X for small end
$x_1 = R_1/\sin\alpha$ distance from apex to cone large end.	Z = R/SIN(PHI)
$x_2 = R_2/\sin\alpha$ distance from apex to cone small end.	Z = R/SIN(PHI)
$y = x_1 - x$ distance from cone edge to a point x.	X
nu, ν = Poisson's ratio.	PR
l, m, s, t series terms.	L1, M, S, F
l_1, m_1, s_1, t_1 series terms at the edge.	LA, MA, SA, FA
$\phi_1 = l_1(s_1 - t_1) + m_1(s_1 + t_1) + 2*nu*2^{1/2}(l_1^2 + m_1^2)/xi_1$	PHI1
$\phi_2 = l_1(s - t) + m_1(s + t) + 2*nu*2^{1/2}(l_1 l + m_1 m)/xi$	PHI2
$\phi_3 = l_1(s + t) - m_1(s - t) + 2*nu*2^{1/2}(l_1 m - m_1 l)/xi$	PHI3
$\phi_4 = (s_1 t - t_1 s) + nu*2^{1/2}[l_1(s + t) - m_1(s - t)]/xi_1$ $+ nu*2^{1/2}[-l(s_1 + t_1) + m(s_1 - t_1)]/xi$ $+ 4*nu^2(l_1 m - m_1 l)/(xi_1*xi)$	PHI4
$\phi_5 = (s_1 s + t_1 t) + nu*2^{1/2}[l_1(s - t) + m_1(s + t)]/xi_1$ $+ nu*2^{1/2}[l(s_1 - t_1) + m(s_1 + t_1)]/xi$ $+ 4*nu^2(l_1 l + m_1 m)/(xi_1*xi)$	PHI5
$\phi_6 = m_1 l - l_1 m$	PHI6

TAYLOR notation (ref. 28)	Equivalent notation in "AJAP1" (lines 5240-5880)
$\phi_7 = l_1l + m_1m$	PHI7
$\phi_8 = l(s_1 - t_1) + m(s_1 + t_1) + 2*nu*2^{1/2}(l_1l + m_1m)/xi_1$	PHI8
$\phi_9 = l(s_1 + t_1) - m(s_1 - t_1) + 2*nu*2^{1/2}(m_1l - l_1m)/xi_1$	PHI9
$\phi_{10} = l_1(s - t) + m_1(s + t) + 2*2^{1/2}(l_1l + m_1m)/(nu*xi)$	PHI10
$\phi_{11} = l_1(s + t) - m_1(s - t) + 2*2^{1/2}(l_1m - m_1l)/(nu*xi)$	PHI11
$\phi_{12} = s_1t - t_1s + nu*2^{1/2}[l_1(s + t) - m_1(s - t)]/xi_1$ $+ 2^{1/2}[-l(s_1 + t_1) + m(s_1 - t_1)]/(nu*xi)$ $+ 4*(l_1m - m_1l)/(xi_1*xi)$	PHI12
$\phi_{13} = s_1s + t_1t + nu*2^{1/2}[l_1(s - t) + m_1(s + t)]/xi_1$ $+ 2^{1/2}[l(s_1 - t_1) + m(s_1 + t_1)]/(nu*xi)$ $+ 4*(l_1l + m_1m)/(xi_1*xi)$	PHI13
$\phi_{14} = l_1(s + t) - m_1(s - t)$	PHI14
$\phi_{15} = l_1(s - t) + m_1(s + t)$	PHI15
$\phi_{16} = s_1s + t_1t + nu*2^{1/2}[l_1(s - t) + m_1(s + t)]/xi_1$	PHI16
$\phi_{17} = s_1t - t_1s + nu*2^{1/2}[l_1(s + t) - m_1(s - t)]/xi_1$	PHI17
$U^2 = [12(1 - nu^2)]^{1/2}$	U2
$\beta y \approx (xi_1 - xi)/(2)^{1/2}$ the length parameter	LP=|XIA - XI|/C2 $C2 = 2^{1/2}$
$\beta = [3(1 - nu^2)\cos^2\alpha/(h^2R^2)]^{1/4}$	
$\beta_1 = \beta$ calculated at the cone edge where $R = R_1$	BETAA
$\theta = \cos[(xi_1 - xi)/2^{1/2}]*e^{(xi - xi_1)/2^{1/2}}$	MU
zeta, $\zeta = \sin[(xi_1 - xi)/2^{1/2}]*e^{(xi - xi_1)/2^{1/2}}$	ZETA
M_1 meridional moment per unit circumference at the cone edge.	-MJ
H_1 radial force per unit circumference at the cone edge.	-VJ
Q_1 shear force per unit circumference at the cone edge = $H_1\cos\alpha$.	-VJ*COS(PHI)
N_1 meridional force per unit circumference at the cone edge = $H_1\sin\alpha$.	-VJ*SIN(PHI)
M_X meridional moment per unit circumference at distance x along the cone from the apex.	-M1
$M\phi$ hoop moment per unit circumference at distance x along the cone from the apex.	-M2
N_X meridional force per unit circumference at distance x along the cone from the apex. = $Q_X\tan\alpha$	N1

Appendix 5

TAYLOR notation (ref. 28)	Equivalent notation in "AJAP1" (lines 5240-5880)
$N\phi$ hoop force per unit circumference at distance x along the cone from the apex.	N2
Q_X shear force per unit circumference at distance x along the cone from the apex. = $N_X/\tan\alpha$	V=N1/TAN(PHI)
$M'_X/M_1 = (xi_1/xi)^{3/2}(\phi_2\theta + \phi_3 zeta)/\phi_1$	M1/MJ
$M''_X/Q_1/\beta_1 = (xi_1/xi)^{3/2}(\phi_4\theta - \phi_5 zeta)/\phi_1$ *Note that β_1 above has its subscript missing in reference 28.*	-M1*BETAA/[VJ*COS(PHI)]
$Q'_X/(2\beta_1 M_1) = (xi_1/xi)^{5/2}(\phi_6\theta + \phi_7 zeta)/\phi_1$	-N1/[MJ*2*BETAA*TAN(PHI)]
$Q''_X/Q_1 = (xi_1/xi)^{5/2}(\phi_8\theta - \phi_9 zeta)/\phi_1$	N1/[VJ*SIN(PHI)]
$M'\phi/(M_1 nu) = (xi_1/xi)^{3/2}(\phi_{10}\theta + \phi_{11} zeta)/\phi_1$	M2/(MJ*PR)
$M''\phi/(Q_1 nu/\beta_1) = (xi_1/xi)^{3/2}(\phi_{12}\theta - \phi_{13} zeta)/\phi_1$	-M2*BETAA/[VJ*COS(PHI)*PR]
$N'\phi/(M_1 U^2/h) = (xi_1/xi)^{3/2}(-\phi_{14}\theta + \phi_{15} zeta)/\phi_1$ *Note in reference 28 the right hand side of the above equation is given as:* $= (xi_1/xi)^{3/2}(-\theta/\phi_{14} + \phi_{15} zeta)/\phi_1$	-N2*T/(MJ*U2)
$N''\phi/(Q_1 U^2/(h\beta_1)) = (xi_1/xi)^{3/2}(\phi_{16}\theta + \phi_{17} zeta)/\phi_1$	N2*T*BETAA/[VJ*COS(PHI)*U2]

Equations for displacements are not given in reference (28) but can be obtained by substituting the forces and moments (stress resultants) into equations (A5.1) and (A5.2) as follows ("AJAP1" notation):

Radial deflection (+ve outward) [line 5760] = Y = RX*(N2 - PR*N1)/(E*T) (A5.1)

Rotation of a tangent to the meridian (+ve anti-clockwise) [line 5780] =

TH = -12*(M2 - PR*M1)*RX/[E*T^{3}SIN(PHI)] radians (A5.2)

The stiffness coefficients (loads per unit displacement at the edge of the cone) required for the junction analysis are obtained by substituting the stress resultants in terms of VJ and MJ in equations (A5.1) and (A5.2) and rearranging to become equations (A5.3) [lines 5410-5430]:

Radial force per unit radial deflection = VJ/Y = K(1,i) =

STIF1 = E*T*PHI1/[R*(U2*PHI16*COS(PHI)/(T*BETAA) - PR*PHI8*SIN(PHI))]

Meridional moment per unit radial deflection = MJ/Y = K(2,i) =

STIF2 = E*T^{2}PHI1/(R*U2*PHI14) (A5.3)

Radial force per radian = VJ/TH = K(3,i) =

STIF3 = E*T^{2}PHI1/(R*U2*PHI9)

Meridional moment per radian = MJ/TH = K(4,i) =

STIF4 = E*T^{3}XIA*SIN(PHI)*PHI1/(2*C2*U4*R*PHI7)

INDEX

About the author, a quick summary....

Andrew C. Whyte was born in Kelvinside, Glasgow 1945

EDUCATION	Knightswood Primary School, Glasgow. Queen Victoria School, Dunblane. Stow College of Engineering, Glasgow. University of Strathclyde, Glasgow.
ACADEMIC QUALIFICATIONS	M.Sc, B.Sc(Hons), HNC, ONC all in mechanical engineering.
PROFESSIONAL QUALIFICATIONS	Chartered Engineer Corporate Member of the Institution of Mechanical Engineers.
CAREER EXPERIENCE	5 Year engineering apprenticeship with British Polar Engines, Govan, Glasgow. Design draughtsman with British Polar Engines responsible for design and drawing of diesel engine components. 8 Years with Weir Pumps Ltd., Cathcart, Glasgow as a design engineer responsible for the mechanical design and stress analysis of various centrifugal and axial flow pumps. Present employment 16 years as a senior design engineer with Babcock Energy Ltd., of Renfrew. He is responsible for all mechanical design aspects of pressure vessels, piping, boilers and other structural work including detailed stress and thermal analysis and assessment to all the major pressure vessel codes, i.e. BS5500, ASME SECTION VIII, ASME SECTION III and ASME Code Case N-47.
OTHERS	Has served a short time on BSI committee for BS5500 Saddle Supports sub group SSWP8. Published technical paper: Design Criteria for Boilers and Pressure Vessels in the United Kingdom, ASME PVP VOL.97, 1984.
HOME INTERESTS	Include: photography, hillwalking and computer aided design.

About this book:

This book presents a classical discontinuity analysis complete with BASIC computer programs suitable for running on an IBM PC compatible or Atari ST computer. A general method of analysing multishell axisymmetric junctions is given together with the stiffness coefficients for several common types of component used to form axisymmetric junctions including: cylinders, cones, spherical shells, flat plates and compact ring.

The stress analysis of each component type is discussed and the means to calculate the discontinuity stresses and deformations by use of the computer program provided is fully explained. A feature of the program is its ability to present the stress results in easy graphical form. The program will calculate the stresses and deformations both at and away from the junction, as well as analysing single components. It is possible to analyse many geometries under a combination of loads including: pressure, temperature, applied external forces and moments and centrifugal loading.

The book illustrates the use of the program through examples and highlights many aspects of stress analysis likely to be encountered in solving practical problems. Examples are given of: vessel ends, nozzles, supports and attachments, stiffeners, thermal sleeves, bolted flanges, tubesheets, etc. An example of "Design by Analysis" and the assessment procedure used by pressure vessel codes is given.

The book will be of use to engineers and stress analysts in the pressure vessel, boiler, civil engineering and aircraft industries as well as students and research engineers who require an understanding of discontinuity analysis and a means of analysing the stresses on a microcomputer.

The author is a Chartered Engineer and graduate of the University of Strathclyde, Glasgow. He has worked in industry for over thirty years and is particularly interested in the development of design methods and the use of computers for solving practical analytical problems.

To run "AJAP1" you will need the following:

An IBM PC, XT or AT compatible computer (DOS 2.0 or higher) with BASICA or GW BASIC or QBasic.

or

An Atari ST computer with ST BASIC (enhanced version) or FirST BASIC. FirST BASIC users will require at least 1M byte of RAM.
